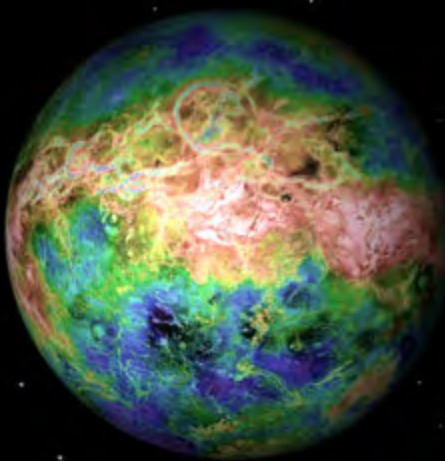
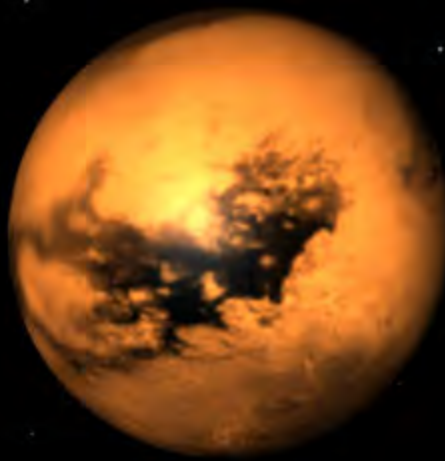
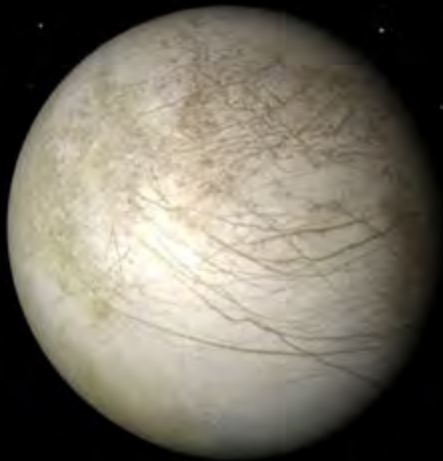




Extreme Environments Technologies for Future Space Science Missions



JPL D-32832

EXTREME ENVIRONMENT TECHNOLOGIES FOR FUTURE SPACE SCIENCE MISSIONS

NASA–Jet Propulsion Laboratory

Elizabeth Kolawa, *Lead Author*

Tibor Balint	Ram Manvi
Gaj Birur	Mohammad Mojarradi
Gary Bolotin	Alina Moussessian
Eric Brandon	Jagdish Patel
Linda Del Castillo	Michael Pauken
Henry Garrett	Craig Peterson
Jeffery Hall	Rao Surampudi
Michael Johnson	Harald Schone
Jack Jones	Jay Whitacre
Insoo Jun	

NASA–Ames Research Center

Ed Martinez Raj Venkopathy
Bernard Laub

NASA–Glenn Research Center

Phil Neudeck

Original Issue: September 19, 2007



Note: this page is left blank intentionally

Foreword

In 2003, the NRC Decadal Survey for Solar System Exploration recommended that “NASA commit to significant new investments in advanced technology so that future high-priority flight missions can succeed.” The NRC report identified the need for a number of technologies for tolerating extreme planetary environments that would be needed to implement the program of high-priority missions, identified by the Decadal Survey team. The purpose of this report, which is the culmination of a series of studies that were set in motion by the Decadal Survey, is to assess the state of the relevant technologies and to formulate roadmaps to enable the Solar System Exploration Program.

This assessment was initiated and originally sponsored jointly with NASA’s Aerospace Research Directorate. When Code R, which was the Office of Aerospace Technology, responsible for the Aerospace Technology Enterprise, was incorporated into the Exploration Systems Missions Directorate (ESMD) shortly after the initiation of the study, the Planetary Science Division continued with the task. Information gathered in this study played a key role in formulating the Capability Roadmaps developed for NASA in the fall of 2004, and the technology plans included in the Planetary Science Division’s 2006 Solar System Exploration Roadmap. The Science Mission Directorate (SMD) Science Plan published in May 2007 identifies technologies for extreme environments as a high-priority systems technology needed to enable exploration of the outer solar system and Venus.

There has been progress, but also significant setbacks, in addressing these technology needs. One serious setback was the dissolution of the Aerospace Technology program, which had planned to initiate a program of technologies for extreme environments. When its funding was folded into the Exploration Systems Missions Directorate, this plan was abandoned. However, some work funded by ESMD on components for operation at cold temperatures is also relevant to the needs of the Planetary Science mission set. SMD is also sponsoring technology development for high-temperature electronics, high-temperature motors, advanced pressure vessels, and thermal control systems as part of NASA’s Small Business Innovative Research (SBIR) Program for Robotic Exploration of the solar system.

At this time, however, there is no program within SMD that directly supports development of the needed technologies by NASA centers, universities, and industries not qualifying for the SBIR program. This report should play an important role in documenting the need for new technology investments and in supporting the formulation of a coherent program to address extreme environment technology needs.

James A. Cutts
Chief Technologist, Solar System Exploration Programs Directorate and
Manager, NASA Planetary Program Support Task

Acknowledgments

This work was conducted as part of the Planetary Program Support task that JPL carries out for NASA's Planetary Science Division. The support of Dr James Green and Mr Dave Lavery in carrying out this work is gratefully acknowledged.

This research was carried out at the Jet Propulsion Laboratory, California Institute of Technology, under a contract with the National Aeronautics and Space Administration.

Reference herein to any specific commercial product, process or service by trade name, trademark, manufacturer, or otherwise, does not constitute or imply its endorsement by the United States Government or the Jet Propulsion Laboratory, California Institute of Technology.

Other Reports in This Series

POWER TECHNOLOGY

- Advanced Radioisotope Power Systems Report, Report No. JPL D-20757 6/01, March 2001
- Solar Cell and Array Technology for Future Space Missions, Report No. JPL D-24454, Rev.A., December 2003
- Energy Storage Technology for Future Space Science Missions, Report No. JPL D-30268, Rev.A., November 2004

PLANETARY PROTECTION TECHNOLOGY

- Planetary Protection and Contamination Control Technologies for Future Space Science Missions, Report No. JPL D-31974, June 2005

In Preparation

- Guidance, Navigation, and Control Systems for Future Space Science Missions

Contents

Foreword	1
Acknowledgments	2
Other Reports in This Series	2
Executive Summary	1
1 Study Overview	18
1.1 Introduction	18
1.2 Definition of Extreme Environments	20
1.2.1 Coupling of Extreme Environments	20
1.2.2 Extreme Environments and Mission Stage	22
1.2.3 Exploiting Extreme Environments	22
2 State-of-Practice of Extreme Environments Exploration	24
2.1 Deep Space: Hypervelocity Impacts	24
2.1.1 Stardust, CONTOUR, and Deep Impact	24
2.1.2 Cassini	29
2.2 High Temperatures and Pressures	31
2.2.1 Venus: Soviet RKA missions	31
2.2.2 Venus: United States NASA Missions	48
2.2.3 Venus: Lessons Learned	57
2.2.4 Jupiter Atmosphere: Galileo Probe	57
2.3 Cold Temperatures	61
2.3.1 Titan: Cassini–Huygens Probe	61
2.3.2 The Moon	69
2.3.3 Mars	74
2.4 High Radiation	79
2.4.1 Galileo	81
3 Mission Impact of Extreme Environment Technologies	88
3.1 NASA planning activities	88
3.2 Overview of Science Missions Directorate Missions	88
3.2.1 Mars Exploration Program	89
3.2.2 Exploration of the Solar System	90
3.3 Mission Impact of Technology Development for EEs	93
3.3.1 Mission Set	93
3.3.2 High Temperature and High Pressure	97
3.3.3 Low Temperatures	102
3.3.4 Low Temperatures and High Radiation	107
3.3.5 Thermal Cycling	111

4 Emerging Capabilities in Technologies for EEs	114
4.1 Systems Architectures for Missions to Extreme Environments	114
4.1.1 Environmental Isolation	114
4.1.2 Environmental Tolerance	114
4.1.3 Hybrid Systems	115
4.2 Protection Systems	116
4.2.1 Hypervelocity Entry	116
4.2.2 Hypervelocity Impact Protection	128
4.2.3 Radiation Shielding	133
4.2.4 Pressure and Thermal Control Technologies	140
4.3 Component Hardening	160
4.3.1 High-Temperature Electronics	160
4.3.2 Low-Temperature Electronics	169
4.3.3 Radiation Tolerant Electronics	177
4.3.4 High-Temperature Energy Storage	191
4.3.5 Low-Temperature Energy Storage Devices	205
4.4 Robotics	215
4.4.1 High-Temperature Mechanisms	215
4.4.2 Low-Temperature Mechanisms	218
4.4.3 High-Temperature Aerial Mobility	219
4.4.4 Low-Temperature Aerial Mobility	223
5 Roadmaps	229
5.1 Roadmaps for Protection Systems	230
5.1.1 Hypervelocity Entry	230
5.1.2 Hypervelocity Particle Impacts	231
5.1.3 Radiation Shielding	234
5.1.4 Pressure Vessel and Thermal Control Technologies	236
5.2 Roadmaps for Component Hardening	238
5.2.1 High-Temperature Electronics	238
5.2.2 Low-Temperature Electronics	240
5.2.3 High-Temperature Energy Storage	243
5.2.4 Low-Temperature Energy Storage	245
5.3 Roadmaps for Robotics	248
5.3.1 High-Temperature Mechanisms	249
5.3.2 Low-Temperature Mechanisms	250
5.3.3 High-Temperature Mobility	251
5.3.4 Low-Temperature Aerial Mobility	253
6 Resources and Background Information	255
Acronyms and Abbreviations	257

References**261**

List of Figures

2.1	Stardust Whipple shield.	25
2.2	CONTOUR spacecraft with protective blanket rolled back.	26
2.3	Close-up of protective blanket mounted on CONTOUR spacecraft.	26
2.4	Impactor copper shielding on Deep Impact.	29
2.5	A schematic of the protective multilayer insulation protecting Cassini.	30
2.6	The Venera 1 spacecraft.	33
2.7	The Venera 3 architecture.	35
2.8	The Venera 7 descent module.	38
2.9	Internal layout of the Venera 8 descent module.	39
2.10	The Venera 9 gamma ray densitometer.	40
2.11	The Venera 11 descent module.	43
2.12	The Venera 13 spacecraft.	44
2.13	The Venera 13 and Venera 14 sample collection system.	45
2.14	The Vega spacecraft (front and back).	46
2.15	Diagram of the atmospheric structure of Venus (T: turquoise; p: dark blue).	49
2.16	The Pioneer Orbiter and Multiprobe Bus.	49
2.17	Schematic of the Pioneer Large Probe pressure vessel and deceleration module.	51
2.18	Internal layout of the Pioneer Large Probe pressure vessel.	52
2.19	The main features of the Pioneer Small Probes.	54
2.20	Internal layout of the pressure vessel of the Pioneer Small Probe.	56
2.21	Main structural elements of the Galileo Probe.	58
2.22	Convective and radiative heat fluxes experienced by various missions.	61
2.23	Heat shield ablation of the Galileo Probe.	62
2.24	Main elements of the Huygens Probe.	63
2.25	Location of the scientific instruments in the Huygens Probe.	64
2.26	Installation of the multilayer insulation (MLI) blanket on the Huygens Probe (Courtesy of ESA).	65
2.27	One of the Lunar Surveyor spacecraft.	70
2.28	One of the Lunar Surveyor Spacecraft.	73
2.29	The Sojourner rover from Mars Pathfinder.	76
2.30	Mars Polar Lander Flight System, showing lander thermal enclosure.	77
2.31	Mars Polar Lander spacecraft, with both DS-2 aeroshells mounted in place.	77
2.32	Deep Space 2 architecture with thermal protection and probe.	78
2.33	Location of the warm electronics box (WEB) in the Mars Exploration Rover.	79
2.34	Implementation of the MER warm electronics box (WEB).	80
2.35	Radiation spectra at Earth and at Jupiter.	80
2.36	Schematic of the Solid-State Imaging system on Galileo, including tantalum radiation shielding.	82
2.37	Schematic of the Extreme Ultraviolet Spectrometer on Galileo, including radiation shielding.	82
3.1	NASA's 2006 Solar System Exploration Roadmap.	92

List of Tables

1.1	“Workshop on Extreme Environments” plenary panel members and affiliations.	19
1.2	“Workshop on Extreme Environments” participants and affiliations.	19
1.3	Extreme environments in the Solar System.	21
2.1	The Venera 1 probe, the Zond impactor, and the Venera 2 and 3 missions.	32
2.2	Descent times for the Venera probes 4, 5, and 6.	36
2.3	Descent and surface survival times for Venera landers 7, 8, 9, and 10.	37
2.4	Descent and survival times for Venera landers 11, 12, 13, and 14.	42
2.5	Descent and survival times for the Vega 1 and Vega 2 missions.	47
2.6	Descent and survival times for the NASA Pioneer Venus mission (1974 launch)	50
2.7	Anomalies experienced by the Pioneer Venus Probes at and below 12.5 km altitude.	55
2.8	Survival times for robotic landed missions to the Moon.	69
2.9	Survival times for past landed missions to Mars.	74
2.10	Radiation-induced failure modes in the avionics and communications systems on the Galileo orbiter.	83
2.11	Radiation-induced failure modes in elements of the Attitude Control System on the Galileo orbiter.	84
2.12	Radiation-induced failure modes in imaging instruments on the Galileo orbiter.	85
2.13	Radiation-induced failure modes in particle, dust, and magnetic field detectors on the Galileo orbiter.	86
3.1	Mars mission classes and estimated cost caps.	90
3.2	Proposed Design Reference Mission set for Mars exploration.	90
3.3	Solar System Exploration mission classes and estimated cost caps.	91
3.4	SSE DRM set for ongoing and proposed missions to primitive bodies and inner planets (without the Moon).	93
3.5	SSE DRM set for ongoing and proposed missions to giant planets and large moons.	94
3.6	Extreme environments affecting planned missions.	95
3.7	Planned DRMs to extreme environments until 2035.	96
3.8	Symbol codes for mission impact analysis.	97
3.9	Impact of technology development on missions to Venus.	99
3.10	Estimated entry velocity at the outer planets.	102
3.11	Impact of technology development on probe missions to the outer planets.	103
3.12	Impact of technology development for missions to low-temperature environments.	107
3.13	Impact of technology development for missions to Europa, a low-temperature, high-radiation environment.	110
3.14	Diurnal cycles of targets experiencing thermal cycling.	111

3.15 Impact of technology development for missions to the thermal cycling environments of the Moon and Mars.	112
4.1 TPS materials with flight heritage or under development.	122
4.2 TPS materials used on past and planned Mars and sample return missions.	122
4.3 Particle environments and associated representative velocities of hypervelocity impacts.	129
4.4 Radiation-shielding materials and atomic weights.	138
4.5 Candidate materials for pressure vessel shell structure.	145
4.6 Thermal storage of water- and lithium-based passive cooling.	152
4.7 Estimated material thermal properties at 92 bars in order of increasing melting temperature.	152
4.8 Theoretical and empirical limits for high-temperature materials.	162
4.9 Characteristics of high-temperature materials.	162
4.10 High-temperature behavior of die attach materials.	165
4.11 Maximum temperatures and limiting properties for select bondpad-wire metallurgical combinations.	167
4.12 Theoretical and empirical limits for low temperature electronics.	171
4.13 Temperature variations of silicon device parameters.	174
4.14 System impact of CMOS and SiGe technologies.	176
4.15 Measured parameters for a single NAND logic gate manufactured with commercial, RHBD, and rad-hard processes (adapted from R. Lacoé, the Aerospace Corporation).	180
4.16 Memory characteristics of nonvolatile memory available currently or in the near future.	181
4.17 Radiation tolerance characteristics of radiation-tolerant, nonvolatile memory available currently or in the near future.	181
4.18 Radiation-tolerant SRAM memory available currently or in the near future.	183
4.19 Radiation-tolerant commercial and radiation-hardened space processors available currently or in the near future.	184
4.20 ADCs available currently or in the near future.	185
4.21 Specifications for ADCs available currently or in the near future.	186
4.22 Radiation-tolerant and radiation-hardened FPGAs available currently or in the near future.	187
4.23 A model radiation hard PPC750 implementation using customizable gate arrays or standard ASICs.	188
4.24 State-of-the-art high-temperature secondary batteries.	196
4.25 State-of-the-art intermediate-temperature (50–250 °C) batteries.	198
4.26 Anode candidates for solid electrolyte batteries.	200
4.27 Cathode candidates for solid electrolyte batteries.	201
4.28 Electrolyte candidates for high-temperature batteries.	201
4.29 Characterization of the atmospheres of Earth and Titan.	223
5.1 Performance metrics for hypervelocity entry protection.	230
5.2 Development timeline for hypervelocity entry protection.	231

5.3	Performance metrics for hypervelocity particle impact protection.	232
5.4	Development timeline for hypervelocity particle impact protection.	233
5.5	Performance metrics for radiation shielding technologies.	234
5.6	Development timeline for radiation shielding technologies.	235
5.7	Performance metrics for pressure vessel and thermal control systems.	236
5.8	Development timeline for pressure vessel and thermal control technologies. .	238
5.9	Performance metrics for high temperature electronics technologies.	239
5.10	Development timeline for high temperature electronics technologies.	241
5.11	Performance metrics for low-temperature electronics technologies.	242
5.12	Development timeline for low-temperature electronics technologies.	244
5.13	Performance metrics for high-temperature energy storage.	244
5.14	Development timeline for high-temperature energy storage.	246
5.15	Performance metrics for low-temperature energy storage.	246
5.16	Development timelines for low-temperature energy storage.	248
5.17	Performance metrics for high-temperature mechanisms.	249
5.18	Development timeline for high-temperature mechanisms.	250
5.19	Performance metrics for low-temperature mechanisms.	250
5.20	Development timeline for low-temperature mechanisms.	251
5.21	Performance metrics for high-temperature aerial mobility.	252
5.22	Development timelines for high-temperature aerial mobility.	253
5.23	Performance metrics for low-temperature aerial mobility.	254
5.24	Development timelines for low-temperature aerial mobility.	254

Note: this page is left blank intentionally

Executive Summary

The Planetary Science Division of the Science Mission Directorate, National Aeronautics and Space Administration (NASA), supports a technology planning effort at JPL, whose goal is to identify the technologies needed for future missions. More specifically, it attempts to determine those technologies where a NASA investment can have the greatest impact on future missions. This report on technologies for extreme environments is the culmination of a multiyear study. Interim results from this effort have already been incorporated into NASA strategic planning through the 2006 Solar System Exploration Roadmap and the 2007 SMD Science Plan. This report is expected to support the formulation of a NASA technology program, specifically focused on extreme environment technologies, and to guide the selection of the technologies that comprise that program.

A number of planned or potential planetary science missions have elements that must survive and operate in extreme environments. Environments are defined here as “extreme” if they involve exposure to extremes in pressures, temperatures, ionizing radiation, chemical and/or physical corrosion, and the impact of hypervelocity particles. In addition, certain missions would induce extremes in heat flux or deceleration, leading to their inclusion as missions in need of technologies for extreme environments.

In 2003, the NRC Decadal Survey for Solar System Exploration identified the need for mission-specific extreme environment technologies needed to implement the missions that it recommended for implementation in the decade 2002–2013, as well as more ambitious technology developments for missions in the subsequent decade. Technologies needed during the first decade of the plan included:

- Radiation-hard electronics for missions to the intense radiation environments of the Jupiter system;
- Entry probe technology that could enable entry into the Jupiter environment and for operation down to 100 bars pressure depth;
- Technologies for (short-duration) survival, operation, and sample acquisition on the surface of Venus; and
- Drilling, sample manipulation, and storage at cryogenic temperatures for comet missions.

For the subsequent decade, the NRC report identified the need for technology for aerial vehicles for the exploration of Venus, Mars, and Titan; and long-lived high-temperature and high-pressure systems for operation on and near the surface of Venus.

An initial step for this study was the “*Workshop on Extreme Environments Technologies for Space Exploration*,” hosted at JPL in late 2003. It included representatives of the aerospace, oil drilling, automotive, energy, and electronics industries, as well as leading university research faculty members. This workshop provided an important reference point

for developing solutions to the technology needs identified by the Decadal Survey. In 2004, this information was incorporated in the Capability Roadmaps developed for the agency under the direction of Administrator Sean O’Keefe, and when the Planetary Program Support task began its support of the development of a Strategic Roadmap for Solar System Exploration early the following year, the work on extreme environments was embodied in the technology plan laid out in the 2006 Solar System Exploration Roadmap published in September 2006.

The present report begins with an assessment of the current state of practice in the pertinent technologies, then examines the missions to see where advances in technology would have the greatest impact and continues with a review of the emerging technologies that have not yet been used in space, but have the potential for enabling and enhancing missions. The report concludes with a set of technology roadmaps to guide the agency’s future investment plans.

E.1 STATE OF PRACTICE OF EXTREME ENVIRONMENT EXPLORATION

Planetary exploration presents a variety of extreme environments to the mission architect and technologist (Table E.1). During more than 40 years of planetary exploration, a variety of architectural approaches and technological solutions have been used to cope with these extreme environments.

E.1.1 Hypervelocity impact environments

These environments are ubiquitous in Earth orbit and interplanetary space, but for planetary missions the greatest challenges have occurred in the exploration of active comets, where the density of coma particles far exceeds the space ambient, and in crossing Saturn’s ring plane. Three NASA Discovery-class missions to active comets — Stardust, CONTOUR, and Deep Impact — were all equipped with shielding to cope with the environment. Stardust and CONTOUR used multilayer Whipple shields composed of a multilayer Nextel “bumper” to disrupt particles and included a Kevlar backup layer. The Deep Impact mission, which consisted of two spacecraft, employed the most complex approach to protection because of the need to observe the comet throughout the comet encounter.

The Flagship-class Cassini mission protected vulnerable parts of its vital propulsion system from the low-level, but still mission-threatening, ambient micrometeoroids flux during its long cruise phase by exploiting the particle disruptive properties of multilayer insulation (MLI). Especially vulnerable components such as the rocket nozzles are protected with a retractable cover that is withdrawn when the engines are operated. For the much more intense, but highly directional fluxes experienced in crossing the narrow ring plane, the spacecraft must be oriented in the least vulnerable attitude.

Table E.1: Extreme Environments Experienced by Past & Future SSE Missions.

Target and Mission Type	Extreme Environment					Missions	
	Hypervelocity Impact	Hypervelocity Entry	High Temperatures	High Pressures	Low Temperatures	Ionizing Radiation	
<i>Past Missions</i>							<i>Future Missions</i>
Mercury							
Flyby/Orbiter		○		○		Mariner 10 (f/b), Messenger (orb.)	
Moon							
Landers/SR		○				Surveyor	NF-SPABSR
Rovers			○		○	Lunakhod	Exploration Program
Venus							
Flybys/Orbiters	○					Venera, Magellan	Discovery Program
Probes/Landers	○	○	●	●		Venera / VEGA / Pioneer	NF-VISE, F-VGN
Mobile Vehicles	○	○	●	●			F-VME, F-VSSR
Mars							
Flybys/Orbiters	○					Mariner, Viking, MGS, MRO, Odyssey	MSO
Probes/Landers		○			○	Viking, Pathfinder	S-Phoenix
Mobile Vehicles		○			○	Sojourner, MER	MSL, AFL
Asteroids							
Flybys/Orbiters	○				○	NM-DS1, NEAR	D-DAWN
Landers/SR	○				○	NEAR, Hayabusa	Discovery Program
Comets							
Fast Flyby/SR	●					Deep Impact, Stardust	Discovery Program
Rendezvous/SR	○	○			○		NF-CSSR
Jupiter							
Flybys/Orbiters	○					○	NF-Juno, F-JSO
Probes	○	●	●	●	●	Galileo Probe	NF-JDEP
Satellite Orbiter	○					●	F-EE
Satellite Lander	○				●	●	F-EAL
Saturn							
Flyby/Orbiters	○					○	Cassini
Saturn Probes	○	●	●	○	○	○	NF-SP
Ring mission	●					○	
Moon Orbiter	○	○			○		F-TE
Moon In Situ	○	○		●	○	Huygens (Titan)	F-TL/B
Uranus/Neptune							
Flyby Orbiters	○	●				○	Voyager
Probes		●	●	○	○	○	F-NP
Satellite Landers				●	○		F-TL
Pluto							
Flyby	○			●	○		NF-NH
Convention: Small Impact: ○; Medium Impact: ●; High Impact: ●							
F — Flagship Class; NF — New Frontiers Class; D — Discovery Class; S — Mars Scout Class; EE — Europa Explorer; SPABSR — South Pole-Aitken Basin Sample Return; VISE — Venus In Situ Explorer; VGN — Venus Geophysical Network; CSSR — Comet Surface Sample Return; SP — Saturn Flyby with Shallow Probes; TL — Triton Lander; TE — Titan / Enceladus Exp.; VME — Venus Mobile Exp.; EAL — Europa Astrobiology Lander; NH — New Horizons; JSO — Jupiter System Observer; JDEP — Jupiter Deep Entry Probes; AFL — Astrobiology Field Laboratory; NP — Neptune Probe; TL/B — Titan Lander / Balloon; VSSR — Venus Surface Sample Return; NTE — Neptune-Triton Exp.; MER — Mars Exploration Rover; MSO — Mars Science Observer; MSL — Mars Science Laboratory							

E.1.2 Hypervelocity entry environments

Entry environments experienced in planetary missions range from the comparatively benign environments at Mars and Titan, to the more severe environments at Venus and Earth (required for sample return), to the most severe environments at the giant outer planets. The Galileo entry probe to Jupiter entered the atmosphere of Jupiter at more than 47 km/s, more than four times the entry velocity of the Pioneer Venus probes. The Galileo probe used a deceleration module of a similar design to the Pioneer Venus probes and its ablative heat shields were protected with dense carbon phenolic material. Sensors in the heat shield indicated that more than half the mass of the heat shield and almost one quarter of the mass of the entire probe was ablated during entry. In terms of future missions to Jupiter and other outer planets, there is a concern that it will be difficult to replicate the carbon phenolic technology and to validate it, because NASA’s hydrogen arc jet facility is no longer operational and would be very costly to refurbish.

E.1.3 High-pressure and high-temperature environments

These environments have been experienced by the Soviet and U.S. missions to the deep atmosphere and surface of Venus. The Soviets sent their first probe into Venus before the severity of the surface conditions was known, but by the time of the last mission they had developed the technology for surviving, making measurements in the surface environment, and acquiring samples within the constraints of a mission limited to two hours of surface time. They also appear to have developed methods for coping with the corrosive aspects of the environment — not only for sulfuric acid in the upper atmosphere (using Teflon-coated VEGA balloons), but also carbon dioxide in a supercritical state in the lower atmosphere.

Pioneer Venus, NASA’s only mission to the deep atmosphere of Venus, was purely an atmospheric probe not designed or equipped for surface observations. Unlike the Soviet probes, Pioneer Venus probes were only tested in a nitrogen environment at the temperature and pressure conditions of the Venus surface. A number of spacecraft anomalies experienced by both the Pioneer and the early Soviet spacecraft as they descended into to the surface of Venus may be attributable to the transition to supercritical CO₂.

E.1.4 Cold-temperature environments

Severe cold-temperature environments are inherent to exploration of the outer solar system and are experienced in the inner solar system during the exploration of airless bodies (Moon, Mercury, asteroids) and Mars, a body with a thin atmosphere and extreme diurnal temperature changes. Short-duration missions, such as the Huygens probe to Titan, have coped with environments as cold as 90K. The Mars Exploration Rover (MER) mission, a multiyear mission, experiences diurnal temperature cycles with lows near 170K and protects electronic components that will not function over this range in a warm electronics box (WEB). The MER rovers used a lithium-ion battery with an advanced electrolyte, permitting operation down to -40°C.

E.1.5 Severe radiation environments

While ionizing radiation environments are ubiquitous in space, the focus of this report is on the most severe environments, which are encountered in the Jupiter radiation belts. In its multiyear mission, the Galileo orbiter not only provided the most complete characterization of this environment, but was exposed to a much higher cumulative dose of 600 krads — higher than any other planetary spacecraft — before the mission was ended by sending the spacecraft to impact Jupiter. To cope with the Jovian environment, Galileo employed extensive use of shielding, radiation-tolerant electronic parts, and operational methods for recovering from radiation damage. The extensive base of experience from Galileo on the nature of the Jovian environment, its effects on spacecraft components, and methods of mitigating these effects is being applied to the Juno (Jupiter Orbiter) mission currently in formulation and to other missions that are in the study phase.

E.2 MISSION IMPACT OF EE TECHNOLOGIES

The mission set used to evaluate developments in extreme environment technologies is based on the recommendations of the NRC Decadal Survey of 2003. In 2005, NASA's Planetary Science division assembled a set of Design Reference Missions, based on the NRC Decadal Survey recommendations, which were used to formulate a three-decade strategy in the 2006 Solar System Strategic Roadmap. Inputs from this study on the technology readiness were used in determining the sequence of missions in the Roadmap. The first decade of Roadmap missions has been adopted in the SMD Science Plan, published in March 2007. The extreme environments that would be experienced by these future missions are depicted in Table E.1.

E.2.1 Hypervelocity impact

All long-duration missions in the solar system are subject to a hypervelocity impact hazard, but among the roadmapped missions a return to the Saturn system would likely involve the most difficult challenges. Cassini's ability to penetrate Saturn's rings and to conduct a close-up reconnaissance of the plumes of Enceladus is limited by the design of the spacecraft. Advances in shield technology might enable more aggressive sampling of the icy plumes in a future mission to Enceladus.

E.2.2 Hypervelocity entry

Although the Decadal Survey in 2003 recommended development of entry probe technology that could enable entry into Jupiter's atmosphere, NASA selected a mission in 2006 that probes the Jupiter atmosphere with remote sensing and therefore did not require entry probe technology. In 2006, the Solar System Exploration Roadmap recommended a Saturn entry probe mission for which the entry velocity (~ 26 km/sec) is much smaller than for Jupiter (~ 47 km/sec) and correspondingly less technically challenging. While probe missions to Uranus or Neptune may be even less technically challenging than for Saturn, orbital missions to these distant targets would require aerocapture technology. Aerocapture requires

extended hypervelocity sustained flight through the atmosphere, placing new demands on the performance of the thermal protection system and requiring other new technologies as well, in connection with guidance, navigation and control, and thermal management.

E.2.3 High temperatures and high pressures

Prior landed missions to Venus have been limited to surface lifetimes of two hours. The Venus In Situ Explorer (VISE) mission, which would investigate surface chemistry at one location on Venus, would be enhanced by passive technologies (advanced pressure vessels, insulation, phase-change materials) that extend Venus surface mission lifetime. These technologies would also be applicable to deep probe missions to Jupiter, Saturn, and other outer planets. Missions such as the Venus Mobile Explorer (VME), which would be planned to operate at the surface of Venus for several months, would also require surface power generation, active cooling technologies, and high-temperature electronics to achieve the long-lifetime objectives. Sample acquisition mechanisms would necessarily be exposed to the environment and advances in components would have major advantages.

E.2.4 Low temperatures

While all missions to the outer solar system are exposed to cold temperatures, in situ missions present the greatest challenges because of their power constraints and thermal control complexities. Low-temperature batteries and low-temperature electronics can enable extended operations on cold targets. For mobile vehicles with motors and actuators exposed to the surface environment, cold electronics can greatly simplify cabling.

Repetitive changes in environmental conditions can cause even more stress on engineering systems than stable extreme conditions. Slowly rotating bodies such as the Moon and Mercury experienced extreme temperature excursions between night and day and electronics and components must be designed to tolerate the resulting cyclical stresses.

E.2.5 Ionizing radiation

The highest priority mission recommended by the Decadal Survey is Europa Explorer (EE) — a mission to orbit the Jovian satellite Europa. A typical mission profile of two years in Jupiter orbit followed by a 90-day mission in Europa orbit would involve radiation doses to the spacecraft five to ten times that experienced by the Galileo mission. The Europa Astrobiology Lander (EAL), conceived as a follow-on mission to EE, may experience lower dose rates than the orbiter due to Europa's self-shielding. However, lander missions are much more mass constrained than orbiters, so it is possible that the requirements on the components might be even more demanding.

E.3 EMERGING TECHNOLOGIES FOR EXTREME ENVIRONMENTS

In formulating technology roadmaps to handle the extreme environments of these future planetary missions, it is important to understand not only what has been done previously in planetary missions, but also to consider emerging technologies not previously used in space. The emerging technologies have been categorized into three general areas:

- **Environmental protection technologies**, providing partial or complete isolation from the extreme environments;
- **Environmental tolerance for exposed components**, comprising those technologies for which it is practical to develop tolerance to relatively harsh conditions, such as electronics, where temperature and/or radiation tolerance can be included by design; and
- **Robotics in extreme environments**, encompassing technologies like mobility or sample acquisition, which provide capabilities to operate in extreme environments in order to achieve mission science objectives.

The impact of these new technologies on the Roadmap missions, shown in Table E.2, represents an assessment of the potential for further advances in the technologies and their enabling or enhancing effect on the missions. Technology roadmaps have been developed synchronizing the technology development to address these requirements with the milestones of the proposed missions.

Table E.2: Impact of Advanced Technology Development on Roadmap Missions.

Technology Areas	Discovery				New Frontiers				Flagship (Small/Large)								
	SB	Moon	Venus	Mercury	NH	Juno	SPABSR	VISE	CSSR	SP	C-H	EE	TE	VME	EAL	NTE	CCSR*
Specific Technologies																	
Protection & Component Hardening																	
▷ High Temperature			●		⊕	⊕		●			⊕			●			●
▷ High Pressure			●		⊕	⊕		●			⊕			●			●
▷ Low Temperature	●	●	●	⊕	⊕	⊕	●	●	⊕		●	●	●	●	●	●	●
▷ Ionizing Radiation				⊕	⊕				⊕	●		●	●				
▷ Hypervelocity Impact			●	●	⊕	⊕		●	●	●	⊕	●	●	●	●	●	●
▷ Hypervelocity Entry			●		⊕	⊕	●	●	●	●	⊕		●	●	●	●	●
Robotics																	
▷ High-T Aerial Mobility			●		⊕	⊕				⊕		●					●
▷ Low-T Aerial Mobility					⊕	⊕				⊕	●						
▷ High-T Mechanisms			●		⊕	⊕		●		⊕		●					●
▷ Low-T Mechanisms	●	●	●	⊕	⊕	⊕	●	●	⊕	⊕	●	●	●	●	●	●	●
Convention: ● Medium; ● High; ⊕ Ongoing Mission or Project																	
SB — small bodies; NH — New Horizons; SPABSR — South Pole–Aitken Basin Sample Return; VISE — Venus In Situ Explorer; CSSR — Comet Surface Sample Return; SP — Saturn Flyby with Shallow Probes; C-H — Cassini–Huygens; EE — Europa Explorer; TE — Titan / Enceladus Exp.; VME — Venus Mobile Exp.; EAL — Europa Astrobiology Lander; NTE — Neptune–Triton Explorer; CCSR — Cryogenic Comet Surface Sample Return; VSSR — Venus Surface Sample Return * — beyond the 5 proposed Flagship missions in the 2006 SSE Roadmap																	

E.3.1 Protection systems

Protection systems are applicable to each of the five environments considered. However, the potential of emerging technologies in each area varies, as discussed below.

E.3.1.1 Hypervelocity particle impact

The Foam Core Shield (FCS), designed to shield propellant tanks, also provides a combination of thermal control and hypervelocity impact protection that represents a significant improvement over the use of MLI. Some of the work on penetration codes that has been focused on the space station can be relevant to solar system exploration. Otherwise, there has been limited NASA research specifically focused on the challenges faced in solar system exploration.

Future investments: To meet the needs of Roadmap missions, NASA should consider the following investments in protective systems for hypervelocity particle impacts:

1. New environmental models for meteoroids (data and new models outside/inside 1 AU), cometary, planetary ring, and debris models above 2000 km for the outer planets;
2. Standardized, validated empirical cratering and penetration models and validated hydrocodes capable of modeling complex shielding geometries for impacts of 5–40 km/s;
3. Techniques for rapidly and cheaply testing new shielding configurations for particle masses up to 1 mg and for velocities up to 40 km/s;
4. Shielding technologies for light shielding designs for 1 mg particles impacting at 5 to 40 km/s; and
5. Standardized methodology for evaluating the efficiency and reliability of complex shielding schemes.

In addition to preventing spacecraft damage or destruction, accurate environmental impact models, along with valid ground test capabilities, would permit potentially significant savings in mass and mission complexity and possibly increase performance.

E.3.1.2 Hypervelocity entry

Most developments in thermal protection systems in the last two decade have been targeted at improving the payload fractions. New ablative and reusable materials have been developed and evaluated through arc jet testing. A proposed testing of a number of these materials under the New Millennium program is now on hold. The aeroshell for the Mars Science Laboratory is being instrumented in order to characterize the entry conditions and entry shell performance.

Future investments: To meet the needs of Roadmap missions, NASA should consider the following investments in thermal protection systems (TPS) for hypervelocity entry:

1. **Thermal protection systems** — The emphasis here must be on dense ablative materials for the environments of the outer planets. Jupiter probes deployed at higher latitudes, such as those envisioned in the Jupiter Flyby with Deep Probes, would require TPS mass fractions exceeding 70% with conventional materials. Venus missions requiring entry and sample return missions would also benefit from lowered mass fractions of thermal protection systems. The testing of these materials for the outer planets would require major facility investments.
2. **Sensors for aeroshell** — Pressure and temperature sensors are commercially available, but development is needed for measurements of heat flux and recession rates.
3. **Physics-based models** — Although the environment around bodies under benign entry conditions is well understood, extreme environments associated with Jupiter and Saturn probes and a Neptune aerocapture mission are not well demonstrated by the Galileo probe heat shield behavior. The model development must include a strong emphasis on validation.

E.3.1.3 High temperatures and pressures

This area has the broadest potential for progress of any of the protection technologies considered in this report. For protection from high pressure, high buckling strength beryllium and titanium matrix materials can enable much lighter pressure vessels than those used previously. Their creep resistance also permits longer-duration missions in the elevated temperature environment at the surface of Venus or for an outer planet deep probe.

For protection from elevated temperatures, a number of different approaches show potential. New insulating materials and architectures for employing those insulating materials have been identified. Phase-change materials offer a mixed prognosis. While there is only limited potential for advances in using the liquid–solid phase transition beyond those achieved with lithium nitrate (195 kJ/kg), a water lithium system exploiting the water–vapor transition with venting to the Venus environment may permit up to 700 kJ/kg. However, these essentially passive or one-shot approaches can only prolong surface operations from hours to perhaps days on the surface. For months of operation, a heat pump or refrigerator powered by a radioisotopic power system will be needed. In order to handle the substantial temperature differentials, efficient mechanical systems will be required.

Future investments: To meet the needs of Roadmap missions, NASA should consider the following investments in technologies for high pressure–temperature environments:

1. A pressure vessel with a mass savings of 50–60% compared to a standard monolithic titanium shell;
2. A thermal energy storage system with twice the specific energy capacity of the current state of the art;

3. A thermal energy storage system integrated with the pressure vessel with a tenfold improvement in storage capacity relative to the current phase-change material (PCM) module technology; and
4. A scaleable powered refrigeration/cooling system capable of providing a temperature lift of $\sim 400^{\circ}\text{C}$, while removing 80 W for a system mass of 60 kg (including a radioisotope power system (RPS)), giving an effective cooling density of about 5 kJ/kg.

E.3.1.4 Cold temperatures

Protection against cold-temperature environments involves extension of the WEB technologies used on the Mars Exploration Rovers. In addition to this purely passive solution, radioisotope heater units (RHUs) may be used to avoid demands on scarce electrical power. For those missions using RPSs, waste heat from the RPS can provide further protection against the cold environment. Protection from cold environments is not as challenging as protection and isolation from high temperatures.

E.3.1.5 Ionizing radiation

Protection from ionizing radiation environments may include shielding by the target body under investigation, shielding by spacecraft systems, such as propellant tanks, as well as dedicated shielding for sensitive components. Recent work has indicated that self-shielding by both Europa and Ganymede is significant and should be accounted for in the design of both orbital and landed missions. There has been a great deal of work on the development of radiation codes, but high-fidelity codes for predicting radiation effects in spacecraft and tests of the effectiveness of different shielding materials are lacking.

Future investments: To meet the needs of future planetary missions, NASA should consider the following investments in ionizing radiation protection technology:

1. Establish magnetically trapped charged particle population models, including completing a Jovian model with the remaining Galileo data; revising the Saturn model with Cassini data; developing models for Neptune and Uranus; and modeling the solar charged particle environments near Venus and Mercury;
2. Develop shielding effectiveness and spacecraft modeling, including multilayer shielding design guidelines and CAD interface evaluation and development with NOVICE or ITS5;
3. Conduct ground testing of shielding materials, electron testing of single-layer and multilayer material shielding, and proton testing of single-layer and multilayer material shielding; and
4. Validate radiation transport codes and evaluate charged particle adjoint Monte Carlo codes, beginning with ITS5 by comparing outputs of other codes (NOVICE, MCNPX, GEANT4, and ITS5) with ground test results.

The benefits to missions are the reduction in shielding mass required to protect the spacecraft electronics and dielectric materials, as well as increased spacecraft lifetime in severe radiation environments.

E.3.2. Component hardening

Developing components that can tolerate extreme environments is a complementary approach to protecting the components of a system from the environment. Component hardening is particularly relevant for dealing with environments with extreme temperatures and ionizing radiation effects where complete protection may not be practical for meeting mission objectives.

E.3.2.1 High-temperature electronics

NASA has not implemented a mission to a high-temperature solar system environment since the Pioneer Venus and Galileo probes, and neither was equipped with electronic components to tolerate elevated temperatures. However, developments within NASA and the commercial drivers of deep subsurface access have resulted in significant progress on components tolerant of high-temperature environments.

Large-bandgap semiconductors, such as silicon carbide (SiC) and gallium nitride (GaN), as well as vacuum tube active components, have the potential for operating at 500°C, but so far this potential has only been validated for SiC. A SiC transistor designed and packaged for high temperature has demonstrated 1000 hrs of operation at 500°C. In addition to the active devices, passive components (resistors and capacitors) have been demonstrated and progress has been made on development of thermally compatible substrates. A key challenge is the development of interconnects that can survive extended exposure to these temperatures.

In Venus surface missions, high-power electronic and telecommunications systems act as internal heat sources. Placing these systems outside the thermally protected vessel may reduce internal heating and extend the life of the mission. Small-scale integrated SiC, and GaN high-temperature technologies and heterogeneous high-temperature packaging can support this need and provide components for power conversion, electronic drives for actuators, and sensor amplifiers.

Another architectural approach is the use of devices that operate at an intermediate temperature of 300°C, such as commercially available silicon-on-insulator (SOI) devices. Electronics operating at medium temperatures can reduce the difference between the outside environment and inside the thermally protected system, significantly reducing the associated power requirements for cooling. High-temperature batteries have also demonstrated significant progress and can enable and/or enhance future missions to high-temperature environments.

Future investments: To meet the needs of Roadmap missions, NASA should consider the following investments in high-temperature electronics:

1. High-temperature, long-life (500 hrs) SiC, GaN, and vacuum tube active components;
2. Small-scale, high-temperature (500°C) SiC, GaN, and microvacuum device-based integration technology;
3. High-temperature passive components and packaging technology;
4. Device characterization and modeling capability that results in the tools that enable extreme environment electronic design;
5. High-temperature integrated systems;
6. Medium-temperature (300°C) LSI-scale ultra-low-power SOI CMOS;
7. Integrated medium-temperature electronic systems, such as solid-state recorder, flight microcomputer, and actuator/sensor controller.

E.3.2.2 Low-temperature electronics

Developments in cold temperature electronics are currently being sponsored to support the needs of the Mars Science Laboratory and future lunar robotic missions. Commercial development of silicon germanium (SiGe) components is showing a great deal of promise.

Future investments: To meet the needs of Roadmap missions, NASA should consider the following investments in low-temperature electronics:

1. Design methodology for making reliable, ultra-low-power, wide-range low-temperature and low-temperature VLSI class digital and mixed-signal ASICs;
2. Low-temperature and wide-range low-temperature radiation-tolerant, VLSI class, ultra-low-power, long-life Si and silicon-germanium (SiGe)-based electronic components for sensor and avionics systems;
3. Wide-range low-temperature passive components and high-density packaging technology;
4. Research and modeling tools that produce the models that enable low-temperature and wide-range low-temperature radiation-tolerant electronic design;
5. Low-temperature integrated systems, such as solid-state recorder, flight microcomputer, and actuator/sensor controller.

Avionics systems, components (such as sensors, transmitters), and in situ systems (using wheels, drills, and other actuators) that can directly work at cold temperatures (down to -230°C) will enable the elimination of the warm electronics box and the implementation of distributed architectures that will enable the development of ultra-low-power, efficient

and reliable systems.

E.3.2.3 Radiation-tolerant electronics

At present the space industry relies on three distinct sources for radiation-tolerant components:

1. **Commercial components:** These are components that are determined to be — perhaps serendipitously — radiation tolerant;
2. **Radiation hard by process (RHPB):** These are components manufactured with radiation hardened material processes at specialized foundries;
3. **Radiation hard by design (RDBD):** These are components built on commercial lines with commercial materials and processes but designed to tolerate high radiation doses.

In addition to the DoD developments, NASA has carried out focused investments in rad-hard technology aimed specifically at missions to the Jupiter system under the X-2000 program in the late 1990s, and as part of the Prometheus program between 2002 and 2004. As a result, many components are now available rated at a 1 Mrad total integrated dose and a broader range of components to 300 krads.

One major gap in the technology has been dense nonvolatile memory (NVM). High-density solid-state recorders (SSRs) used for Earth orbital missions use commercial flash memory devices, which are inherently rad soft. Even massive vaults may not provide the level of shielding needed for operation in the Jupiter system. However, recent progress on chalcogenide random access memory (CRAM) and magnetoresistive memory (MRAM), for which the memory elements are rad hard, may provide a solution.

Future investments: Since this assessment is being superseded by a more comprehensive study conducted in 2007 under the aegis of the Europa Flagship mission study, no specific recommendations are made here. However, NASA will need to initiate a significant effort in this area to evaluate and characterize the options for avionics systems in a methodical fashion. Electro optical components for science instruments will require particular attention since the ability to successfully execute the scientific measurements is inherent to the success of the proposed missions.

E.3.2.4 High-temperature energy storage

Primary batteries that release their electrical charge by thermal activation are in routine use on NASA and DoD programs. In the 1970s and 1980s, there was active research on high-temperature rechargeable batteries that operated at 300°C to 600°C because of the prospects of achieving high energy densities. Progress in lithium-ion technology removed that impetus, but still provided a foundation for several technologies that could be applied in a Venus surface mission, such as the DoE Sandia all solid-state battery developed for

oil drilling applications. Longer-range possibilities include a primary battery concept from JPL using a calcium (Ca) metal anode, nickel-fluoride (NiF_2) cathode, and fluoride-ion based solid-state electrolyte. Not having to cool the batteries will significantly lower the thermal load in a space mission, and if the battery can be moved outside the temperature-controlled housing, the size of the enclosure can be reduced.

Future investments: To meet the needs of Roadmap missions, NASA should consider the following investments in high-temperature energy storage:

1. Characterize the performance and stability of existing primary batteries at high temperatures (500°C) and if a promising candidate is found, select it for advanced development;
2. Develop an intermediate-temperature secondary battery (250°C) based on current lithium ion technology; and
3. Select the most successful components and create a flight-qualifiable primary and secondary battery for the 250 – 500°C performance range.

E.3.2.5 Low-temperature energy storage

Storing energy at low temperatures using devices based on chemical energy is challenging since the chemical reactions needed to release electrical energy slow down at low temperatures. There is potential for reducing the operating temperature from the -40°C achieved in the batteries on the MER mission to perhaps -100°C . Other chemistries with potential for low-temperature operation are lithium-sulfur and lithium-copper chloride. For energy storage at lower temperatures than -100°C , other approaches such as flywheels and superconducting magnetic storage would need to be pursued. However, it is not clear that these approaches would be practical or the needs of Roadmap missions would warrant the investment.

Future investments: To meet the needs of Roadmap missions, NASA should consider the following investments in low-temperature energy storage:

1. Identify electrolytes that have good lithium conductivity at low temperatures;
2. Improve lithium electrode/electrolyte interfacial properties for enhanced charge transfer;
3. Demonstrate technology feasibility with experimental cells at appropriate rates of charge and discharge.

These technologies enable effective operation of rovers/probes/landers in cold environments through mass and volume savings associated with the heavy thermal system that is needed with state-of-practice batteries and corresponding cost savings.

E.3.3 Robotic systems

Robotic systems are essential for in situ mission goals to be met and enable the collection and direct examination of samples. Technologies here include the mechanical systems required for in situ sample acquisition and analysis, as well as aerial mobility systems on Venus or Titan, where atmospheric conditions provide the opportunity for broad survey operations.

E.3.3.1 High-temperature mechanisms

Motors and actuators are required for a variety of functions, such as opening and closing valves, deploying landing gear, and operating robotic arms and antenna gimbals. Motors are also required for operating drills, and the acquisition of unweathered samples from at least 20 cm below the surface layer of Venus is required for the VISE mission. For VME, motors and actuators will be also needed for the mobility systems and will require reliable operations for at least hundreds of hours.

Standard actuators based on ferromagnetic or ferroelectric materials face an intrinsic challenge at high temperatures since at the Curie temperature the phase transition causes them to lose their actuation capability. In response to this need, NASA has sponsored the industry development of a switched reluctance motor, which operates without permanent magnets and it has been successfully tested at 460°C. No other motors are currently known that could operate under Venus conditions for any significant period of time.

Future investments: To meet the needs of Roadmap missions, NASA should consider the following investments in high-temperature mechanisms:

1. Develop a sample acquisition system operable at 500°C;
2. Develop mechanisms associated with aerial mobility; and
3. Provide for extended operations for tens of hours.

E.3.3.2 Low-temperature mechanisms

Cold-temperature mechanisms are needed to provide many of the same functions identified for the hot mechanisms discussed above. Low-temperature motors and actuators are needed for the Titan Explorer, for rovers associated with the Lunar Aitken Basin mission, and for the Europa Astrobiology Lander. The motors are needed for sample acquisition systems, mobility systems, robotic arms, and other applications.

Current operation of gears bearings and lubricants at -130°C is limited to 1,000,000 cycles, and drive and position sensors are also limited to operation at -130°C.

Future investments: To meet the needs of Roadmap missions, NASA should consider the following investments in low-temperature mechanisms:

1. An integrated wheel/ballute motor, with appropriate lubrication, capable of operation down to -180°C and 50,000 revolutions;

2. A low-temperature robotic arm for sample acquisition; and
3. Integration with technologies hardened to 1000 krad of radiation.

E.3.3.3 High-temperature mobility

High-temperature mobility systems are needed for future missions to the surface and lower atmosphere of Venus. For a Venus Surface Sample Return (VSSR) mission, it is necessary to raise samples from the surface to altitudes of 50 to 60 km. Efforts to develop a single stage polymer balloon for this application have been unsuccessful, however a two stage balloon with a metal bellows first stage appears practical. The metal bellows approach has been tested at Venus temperatures. The metal bellows technology also appears to be applicable to the proposed VME mission and would easily permit operations over an altitude range of 10 km.

Future investments: To meet the needs of Roadmap missions, NASA should consider the following investments in high-temperature mobility systems:

1. Large-diameter bellows balloon design, fabrication, and testing;
2. Deployment and inflation design, fabrication, and testing;
3. System integration and testing.

E.3.3.4 Low-temperature mobility

Low-temperature mobility systems would primarily needed for the Titan Explorer mission. There has been significant progress over the last several years in aerial mobility systems. Balloon envelope materials have been developed that can tolerate Titan temperatures and various architectures for controlled mobility have been investigated. A thermal Montgolfière balloon capable of multiyear operation looks particularly attractive, although it has not yet been demonstrated in a relevant environment. Autonomous control systems capable of responding to unpredictable conditions in the environment have also been evaluated.

Future investments: To meet the needs of Roadmap missions, NASA should consider investments in low-temperature mobility to mature the technology to the point that it could be adopted for the Titan Explorer mission. This technology has several sub-components including cryogenic balloon materials, balloon fabrication, aerial deployment and inflation, aerobot autonomy, and surface sample acquisition and handling. The technology needs are currently being updated in a NASA sponsored flagship class mission study in order to define the technology needs for a Titan Explorer mission.

E.4. SUMMARY ASSESSMENT

Most targets of interest present multiple environmental challenges, requiring the development of technologies designed for multiple environmental extremes. In general, there may be several architectural approaches for coping with these environments, some involving protection, others environmental tolerance or a combination of both. Systems analyses and

architectural trades will be needed to develop specific performance targets for the different technologies and to establish priorities in the technology investment program.

1 Study Overview

In nearly all of the future planned Solar System Exploration in situ missions, the proposed spacecraft or probes are exposed to local environments much harsher than those typically encountered on Earth, in near-Earth environments, and in free space. Not surprisingly, there has been very little industrial investment directly focused on the development of technologies able to function in these environments. The result is state-of-practice mission designs that rely on massive and inefficient environmental protection systems keeping sensitive technologies in an Earth-like environment, even though it has been possible to leverage existing technology development, particularly in electronics. These technologies and others are needed to reduce risk on scientifically meaningful missions to more challenging targets.

1.1 Introduction

The charter of this study was to assess the potential advances in technologies required for extreme environments that will enable, and/or enhance, future (2010 – 2020) space science missions of NASA and will define developmental roadmaps for those technologies that will result in a major impact on the cost and efficiency of future in situ missions. This work was sponsored by NASA through the Solar System Exploration Division and the Aerospace Research Directorate (known at the time as Code R). The study was conducted prior to the reorganization of the Code R program as the Exploration Systems Mission Directorate (ESMD); at the time of the study, Code R's ECT (Enabling Cross-cutting Technology) program charter was to address basic technology needs across NASA.

This study focuses on the technology needs of Solar System Exploration missions. It did not encompass missions of the Office of Exploration in the early definition phase, although many would clearly benefit from these technologies.

The specific objectives of the study were as follows:

- Assess the capabilities of current state-of-practice in technologies for extreme environments and their potential for future improvement.
- Understand the mission needs in both science and engineering and determine the impact of development of technologies for extreme environments.
- Formulate technology development plans to fill any gaps remaining between development programs and mission needs.

The study was led by the Jet Propulsion Laboratory and conducted by an assessment team drawn from NASA Centers, other agencies, and universities with relevant experience in extreme environment technology. Because key input was sought from industrial partners working in relevant fields, an initial step of the assessment team was to sponsor the “Workshop on Extreme Environments Technologies for Space Exploration,” hosted at JPL in May, 2003. This workshop included representatives of the aerospace, oil drilling, automotive, en-

ergy, and electronics industries, as well as leading university research faculty members.

The plenary panel members at the workshop were drawn from the science and engineering community in order to articulate the mission plans and describe the technology needs. These plenary panel members are listed in Table 1.1.

Table 1.1: “Workshop on Extreme Environments” plenary panel members and affiliations.

J. Hall (JPL)	T. Morgan (NASA HQ)
G. Briggs (ARC)	D. Senske (JPL)
G. Birur (JPL)	D. Crisp (JPL)
C. Peterson (JPL)	S. Smrekar (JPL)
M. Mojarradi (JPL)	V. Kerzhanovich (JPL)
K. Bugga (JPL)	A. Ingersoll (Caltech)

In addition, the workshop speakers were drawn broadly from a number of places, including non-NASA government agencies, academia, and industry. These speakers are listed in Table 1.2.

Table 1.2: “Workshop on Extreme Environments” participants and affiliations.

C. Moore (NASA HQ, Code R)	T. Lynch (Boeing)
T. Morgan (NASA HQ, Code S)	C. Joshi (Energen Inc.)
R. Patterson (NASA, Glenn)	M. Stapelbroek (DRS Sensors & Targeting Systems)
R. Kirschman (Consulting physicist)	M. Hennessy (MTECH)
S. Cristoloveanu (ENSERG, France)	B. Ohme (Honeywell)
J. Cressler (Georgia Tech.)	J. Suhling (Auburn Univ.)
B. Blalock (Univ. of Tennessee)	R. Estes (Baker-Hughes)
L. Nguyen (Inphi)	R. Norman (Sandia Nat. Labs.)
S. Courts (Lakeshore Cryotronics)	C. Britton (ORNL)
J. Weisend (Stanford Univ.)	N. Ericson (ORNL)
G. Harman (NIST)	K. Nechev (Saft America Inc.)
P. McCluskey (University of Maryland)	R. Yazami (CNRS France and Caltech)
S. D'Agostino (JPL)	D. Krut (Spectrolab)
B. Blaes (JPL)	S. Balagopalan (Ceramatec)
J. Cooper (Purdue U.)	C. Schlaikjer (Wilson Greatbatch)
A. Agarwal (Cree)	R. Manvi (California State University, Los Angeles)
L. Sadwick (Innosys Inc.)	J. Zou (Advanced Cooling Technologies)

An assessment team was assembled throughout NASA to synthesize the results of this workshop and other related workshops and conferences to analyze the existing gaps and possible technology development paths.

1.2 Definition of Extreme Environments

For the purposes of this report, a mission environment is defined as “extreme” if one or more of the following criteria are met:

Heat flux at atmospheric entry: Heat fluxes exceeding 1 kW/cm^2

Hypervelocity impact: Higher than 20 km/sec

Low temperature: Lower than $-55^\circ C$

High temperature: Exceeding $+125^\circ C$

Thermal cycling: Cycling between temperature extremes outside of the military standard range of $-55^\circ C$ to $+125^\circ C$

High pressures: Exceeding 20 bars

High radiation: Total ionizing dose (TID) exceeding 300 $krad$ (Si)

Additional extremes include deceleration (g-loading) exceeding 100g, acidic environments, and dusty environments. While these present significant technology challenges, they are discussed in this report as they impact solutions to operation in the extreme environments representing this report’s focus.

A summary of targets of interest and the relevant extreme environments are shown in Table 1.3. Targets are organized by extremes in temperature; however, it is evident that missions often encounter multiple extremes simultaneously.

While this report will organize the technologies and associated missions by temperature, the coupling of extreme environments will be noted and included in technology development planning.

1.2.1 Coupling of Extreme Environments

Table 1.3 shows that not only do multiple targets have extremes in temperature, pressure, or radiation, but that they often present these challenges in parallel. An adequate technical solution for coping with one or the other of these environments may not work when they are presented simultaneously. For example, at Venus and Jupiter, high temperatures are typically coupled with high pressures, requiring technical developments that integrate solutions for both extreme conditions. Europa’s surface couples low temperatures and high radiation levels, requiring radiation-hard electronics that also function at low temperatures, even though low temperatures may accelerate radiation damage in electronics. Therefore, while the technology roadmaps described here are organized by extremes in temperatures,

Table 1.3: Extreme environments in the Solar System.

Target	Radiation (krad/day)	Heat flux at atm. entry (kW/cm ²)	Deceleration (g)	Pressure (bar)	Low temperatures (°C)	High temperatures (°C)	Rotational Period (Earth days)	Chemical corrosion	Physical corrosion
High temperatures									
Venus		2.5	300	92		482	243	Sulfuric acid clouds	
Jupiter (upper atmosphere)		30	228	22		230	0.4		
Low temperatures									
Lunar permanently shadowed regions					-230				Dust
Comet (nucleus)		0.5 [†]			-270				
Titan	0.01	15	1.5	-178		16	<i>CH</i> ₄		
Enceladus (equator)					-193				
Enceladus (south pole)					-188				
Low temperatures and high radiation									
Europa (orbit)	40								
Europa (surface)	20				-180		3.6		
Europa (sub-surface)	0.3 at 10cm				~0 at 5km				
Thermal cycling									
Moon					-233	+197	27		Dust
Mars		0.05–0.1		0.007	-143	+27	1		Dust

[†]Applies to any Earth return mission, including sample return from comets.

additional development may be needed in order to satisfy all the mission requirements simultaneously. This integration is described and provided for in the roadmaps.

1.2.2 Extreme Environments and Mission Stage

Although extreme environments are typically discussed for each target independently, an important consideration is the timing of the encounter with the extreme environment. This varies with the target. Examples include the following:

- *Venus*: The temperature and pressure increase steadily during descent until extremes are reached at the surface.
- *Jupiter*: Extreme temperatures and pressures increase during the descent phase into the atmosphere.
- *Europa*: High radiation is experienced as the spacecraft enters the Jovian radiation environment, with a substantial fraction received just prior to entering orbit. The exact radiation levels depend upon the mission architecture.

Therefore, determining the technology needs requires understanding the planned mission architecture. For example, for Europa missions, the radiation tolerance required of the electronics depends strongly on the mission target (orbit, surface, or subsurface) and mission duration. On the other hand, while Venus and Jupiter present similar environmental conditions, the challenges for mission designers differ substantially. Highest temperatures and pressures on Venus are experienced at the surface, while at Jupiter they vary with the depth of the descending probe. Therefore, although success of missions to Venus depends on the capability of the spacecraft to survive in the ambient environment, the major challenge for probe missions to Jupiter is the thermal protection during descent and the probe's ability to communicate with the orbiter. The links between technologies for environmental extremes and mission architectures will be further described.

1.2.3 Exploiting Extreme Environments

While extreme environments generally present a challenge, certain environments may be exploited for specific missions. Mission architectures may then be designed to take advantage of these properties. Two targets presenting opportunities are the following:

- Venus atmosphere.
 - The dense atmosphere may provide buoyancy for certain balloon designs.
 - High temperatures may be needed for some battery chemistries.
 - Carbon dioxide can be utilized in novel energy-production technologies.
- Titan atmosphere.

- The composition and density suggest that altitude control may be possible with a simple design.
- Atmospheric methane may be used to produce hydrogen needed for refilling balloons.

Concepts like these are currently under study.

2 State-of-Practice of Extreme Environments Exploration

During the past 40 years, NASA, the Soviet Union Space Agency, and the European Space Agency (ESA) have sent landers to the Moon, Mars, and Venus, as well as atmospheric probes to Jupiter, Venus, and Titan. Generally, all of these missions were designed to minimize the exposure of subsystems to the ambient environment by protecting the payload, avionics, navigation, power, and telecom subsystems from the environment using elaborate thermal-control, and pressure control. Past experiences with missions to extreme environments are summarized below.

2.1 Deep Space: Hypervelocity Impacts

Hypervelocity impacts refer to particles and debris impacting spacecraft, posing risk of damage to critical subsystems. Past missions strongly affected by this risk were Stardust, Comet Nucleus Tour (or CONTOUR), and Deep Impact, all of which were designed to sample cometary matter in situ, that is, in an environment of heavy dust and debris. The other mission taking extra precautions was Cassini, subject to debris-rich environments in Saturn's ring plane. Mitigation strategies follow.

2.1.1 Stardust, CONTOUR, and Deep Impact

Stardust, CONTOUR, and Deep Impact were all designed for in situ collection of cometary samples.

Stardust

Stardust, a Discovery-class sample return mission, launched on February 7, 1999, and returned on January 15, 2006. The mission's primary objective was to fly by the comet P/Wild 2 to collect samples of dust and volatiles from the coma of the comet, then to return these samples to Earth for detailed study. In addition, Stardust returned a number of images of the Wild 2 nucleus and performed some in situ analysis.

Stardust was protected during the high-speed encounter with particles in the cometary coma by Whipple shields shadowing the spacecraft. The Whipple shield is designed to act as a bumper shield to protect the spacecraft during high-speed encounters with particles in the cometary coma. The bumper shields are composite panels that disrupt particles as they hit. Nextel blankets of ceramic cloth further dissipated the energy in the plasma field produced by the hypervelocity impact and explosion of the incoming particles. Three blankets are used in the main body shield, with two used in the solar array shields. The composite catcher absorbs the plasma pressure and the surviving debris without damage or penetration. The five-part Whipple shield was tested to survive primary particles up to 1 cm in diameter for the shield protecting the spacecraft main body. Nylon spheres were used to simulate the maximum density coma "rocks." The Stardust flight system mass at launch was 385 kg. The Stardust spacecraft Whipple shield is shown in Figure 2.1. During passage through the coma of Wild 2, the sensors on the first layer of Nextel were activated

Figure 2.1: Stardust Whipple shield.



seven times. From the pre-launch testing this indicates that particles of about 3 mm size hit the Whipple shield.

CONTOUR

The CONTOUR spacecraft, a Discovery-class mission, launched on July 3, 2002. Unfortunately, CONTOUR is presumed lost after numerous attempts at contact. On August 15, 2003, the spacecraft was scheduled to ignite its solid-rocket engine to take CONTOUR out of Earth orbit and put it on a heliocentric trajectory. However, following the scheduled firing time, no further contact was made with the craft. An investigation board concluded that the most likely cause of the mishap was structural failure of the spacecraft due to plume heating during the solid-rocket motor burn. Alternate possible but less likely causes determined were catastrophic failure of the solid-rocket motor, collision with space debris, and loss of dynamic control of the spacecraft.

This loss was unrelated to CONTOUR’s goal of performing close flybys of two comet nuclei to perform spectra mapping and nucleus imaging. A key part of CONTOUR’s design was a 25-cm-thick dust shield at the bottom to protect against high-speed dust and grit. There were five layers of Nextel fabric and a backup layer of Kevlar. Figures 2.2 and 2.3 show the installation of this blanket.

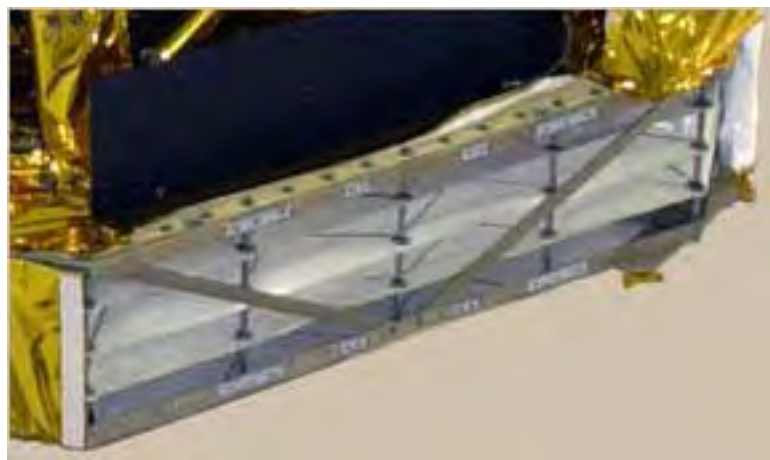
Deep Impact

Deep Impact, a Discovery-class mission, launched on January 12, 2005. The goals of the

Figure 2.2: CONTOUR spacecraft with protective blanket rolled back.



Figure 2.3: Close-up of protective blanket mounted on CONTOUR spacecraft.



Deep Impact mission were to rendezvous with comet 9P/Tempel 1 and launch a projectile into the comet nucleus. Observations were made of the ejecta and the newly observed surface to improve scientific understanding of the evolution of cometary nuclei, particularly their approach to dormancy, by comparing the interior and the surface.

On July 4, 2005, the Deep Impact mission delivered a 370 kg impactor at 10 km/sec to the surface of comet Tempel 1. The separate flyby spacecraft studied the properties of the debris ejected from the comet's nucleus in order to characterize the interior structure of comets. To accomplish this mission, the impactor had to survive the blizzard of particles surrounding the comet (the coma) to its point of impact with the comet's nucleus. After imaging the crater formation on the surface of the comet, the flyby spacecraft also needed to survive a journey through the coma to send data back to Earth.

Structural protection of critical components and systems from hundreds of expected hypervelocity impacts was critical to the success of this mission. The spacecraft was designed and built by Ball Aerospace and the University of Denver Center for Space Systems Survivability designed the shields for both flyby and impactor.

The design cometary dust models describing estimated numbers and sizes of particles were formulated based on observations from the 1986 rendezvous of the Giotto spacecraft with Comet Halley, and were modified to include ground-based observations of Tempel 1. These results were increased a factor of two for safety before estimating impact frequencies on the impactor and flyby spacecraft.

Relative to the flyby spacecraft, the impactor spacecraft experienced 50 times the particle flux because it had to fly into the heart of the comet nucleus and survive long enough to accurately steer into a sunlit section of the surface to improve the image quality. The flyby, after imaging the first 800 sec of the crater formation in Tempel 1, rotated into a “shield mode” and flew within 500 km of the centerline of the coma streaming away from the comet. The coma flux impacted the spacecraft at the spacecraft–comet relative velocity of 10.2 km/sec at an oblique angle of approximately 25°. The impactor collided with the comet with an impact energy of about 19 GJ. Material from the nucleus was ejected into space and the impactor and much of the ejecta was vaporized.

The hypervelocity impact shields for both flyby and impactor were composed of multiple sheets of material forming a Whipple shield. The first shield, called the bumper, was designed to break the particle into a debris cloud containing thousands of melted and vaporized fragments. The debris cloud dissipated the incident energy sufficiently for the subsequent shield (or shields) to further dissipate or stop the fragments.

The hypervelocity impact shields were critical for both impactor and flyby spacecraft because a failed shield on the impactor could potentially lead to steering errors, resulting in missing the comet. Since a large portion of the 370 kg impactor was the impact mass, a

large portion of it could be allocated to accommodate the shielding. The main challenge for the shield arose from the science requirements; in order to facilitate the science instruments' differentiating between the impactor materials and the ejected crater debris, the shield was constructed from copper instead of traditionally used aluminum.

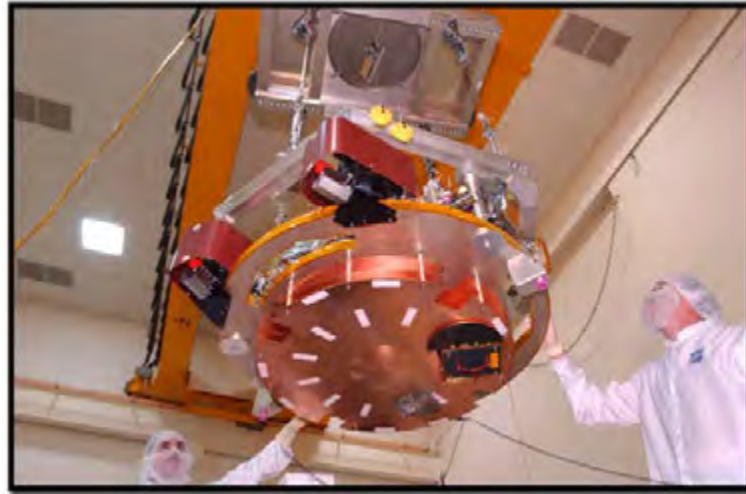
The flyby shield design presented different challenges. The original protection requirement for the flyby was to prevent penetration of a 0.1g dust particle over the entire spacecraft. However, mass resources for structural protection of the flyby were extremely limited; only 23 kg of the spacecraft total mass (516 kg) were allotted to shielding because of launch weight restrictions. Further complications arose because the spacecraft rotated as it entered and passed through the first part of the coma in order to image the impact; it rotated again upon exiting the coma. This rotation caused six of the seven sides of the flyby spacecraft body to be exposed to coma flux.

Consequently, the shielding design approach for the Deep Impact flyby differed significantly from that of NASA's CONTOUR (or Comet Nucleus Tour) and Stardust. Because neither rotated during their passage through the comet's coma, a single large shield protected the front surface; the Deep Impact shield was fabricated from ceramic cloth material developed for the International Space Station.

To save mass, only those components critical to imaging and data collection and transmission were protected in the flyby shielding, resulting in a distributed shielding system. The main shield consisted of dual sheets of aluminum separated by a 4 inch void; the void allowed for fabric inserts to be added up to a few months preceding launch if late observations indicated a worsening comet environment. External cables were wrapped in Aracon, a Kevlar-based material, in order to protect them from smaller coma particles. Whipple shielding was added in front of the batteries, primary and secondary telescope lenses, critical external electronics, and thrusters. To save mass, most shields were integrated with the flyby structure. In addition, several of the flyby spacecraft's side walls were constructed of thickened honeycomb sheets that also acted as shields.

In order to optimize the shield design, location, and mass, the University of Denver modified NASA's BUMPER code and its own SpaceSurv code, originally designed for the meteoroid and orbital debris environment of the International Space Station, to include the new directional, diameter, and density distributions of the coma flux. Using these tools, the University of Denver/Ball Aerospace team identified the "hot spots" in the design requiring additional shielding. These included optics, propulsion elements, batteries, and the communication subsystem. Shielding mass was allocated to the most critical elements first, and other, less critical elements were protected through redundancy and separation. This approach of using modeling to identify the most vulnerable elements and providing extra shielding proved to be successful. The copper shielding is shown in Figure 2.4.

Figure 2.4: Impactor copper shielding on Deep Impact.



2.1.2 Cassini

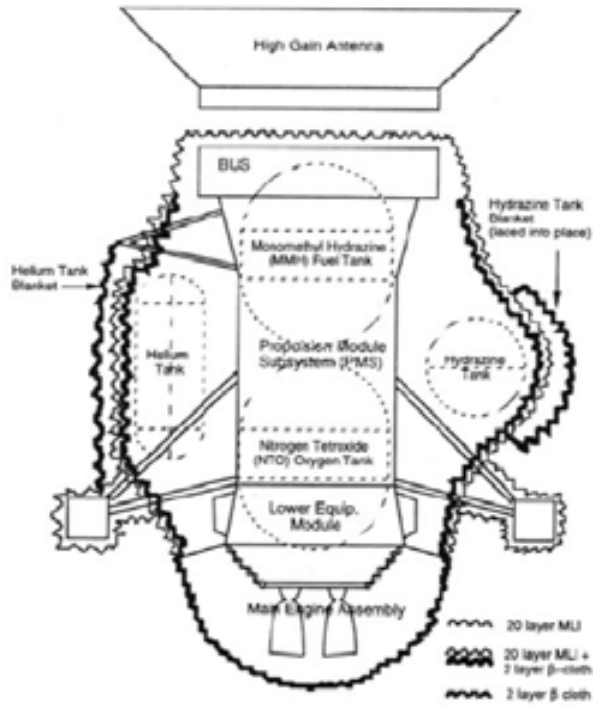
Launched on October 15, 1997, Cassini is the largest interplanetary spacecraft ever constructed by NASA. It measures 6.8 m in length with a 4 m high-gain antenna and at launch, the spacecraft had a mass of 5655 kg, of which 3132 kg were propellant. Cassini neared the end of its four-year prime mission at the time of publication of this report. The Cassini Orbiter's mission consisted of delivering the ESA Huygens probe to Titan, and then remaining in orbit around Saturn for detailed geophysical studies of the planet, its rings, and satellites, particularly Titan.

Early studies showed that Cassini was expected to have a higher risk of damage from ring particles (micrometeoroids) because of potential damage as it crossed the Saturn ring plane. Cassini was expected to face extra challenges from its extended duration and trajectory through the outer Solar System passing through cometary debris.

In general, meteoroid protection is often provided by placement of multilayer insulation (MLI) blankets on critical areas of the spacecraft, such as propellant and helium tanks. MLI blankets are composed of layers of a Kapton polyamide or mylar; gold foil on one side and silver on the other provides very effective thermal insulation and thermal radiation transfer. As a projectile shield, the blanket works to break up the projectile before it strikes an exterior wall, disperse the fragments, and reduce the velocity of the fragments below that of the original projectile. An MLI layer density approximating that of tissue paper is sufficient to stop most strikes due to the very small mass of the typical micrometeoroid.

Specification of MLI blankets for meteoroid protection is not generally practiced because

Figure 2.5: A schematic of the protective multilayer insulation protecting Cassini.



MLI blankets are optimized for thermal control rather than shielding. However, on Cassini, MLI layers were used specifically to shield certain components of the rocket nozzles, as shown in Figure 2.5.

Because further analysis showed that the highest risk of catastrophic damage was borne by the main engines, a retractable cover was mounted below the main engine assembly (MEA) to protect it from damage. The thin disilicide refractory ceramic coating on the inside of the engines is especially vulnerable to micrometeoroid damage: it could lead to burn-through and engine loss. This cover can be extended and retracted at least 25 times; in addition, a pyrotechnic ejection mechanism is in place to jettison the cover if a mechanical problem interferes with engine operation. The cover remains closed during cruise when the main engines are not used.

The mission plan for Cassini provides guidelines for the maximum cover open time allowed prior to its encounter with Saturn. Furthermore, while Cassini crosses Saturn's ring plane, the antenna is oriented forward to serve as additional shielding. The guidelines are designed to keep the probable risk of engine nozzle loss to less than 3%.

2.2 High Temperatures and Pressures

Although high temperatures and pressures are experienced at both Venus and Jupiter, these targets differ because on Venus, the temperature and pressure increase steadily during descent until extremes are reached at the surface, while at Jupiter, temperatures and pressures increase without limit during the descent phase into the atmosphere.

Many missions have opened the doors of exploration of the atmosphere and surface of Venus, while only NASA's Galileo mission has investigated the atmosphere of Jupiter. Surface missions to Venus face particular challenges because they need to operate in extremely high temperature and pressure environments (487°C and 92 bar pressure). Atmospheric probes or balloon missions operating at higher altitudes (about 50 km above the surface) have to be protected from deteriorating interactions with corrosive sulfuric acid clouds.

In 1961 the Soviet space program initiated an extensive program of Venus exploration that included atmospheric probes, landers, orbiters, and balloon missions. This program produced many successful missions after years of study to determine how to survive and conduct experiments in the Venus environment. In the late seventies, NASA conducted a multiprobe mission aimed at understanding the atmosphere, Pioneer Venus. The lessons learned from the entire series of missions will be discussed here, as will the single investigation of the Jupiter planetary environment.

2.2.1 Venus: Soviet RKA missions

The Soviet Venus exploration program extended over more than two decades from the first attempt to send a spacecraft to Venus to the program's closure. At the program's inception, scientists underestimated the atmospheric and surface conditions, making the initial missions underprepared for the challenges of conducting scientific investigations. While later missions benefited from returned science and were designed with increased capabilities to deal with the severe environmental conditions, in some cases spacecraft design was unable to keep pace with the rapidly increasing science understanding and missions were launched with only partially effective protection systems.

Venera 1, Zond 1, Venera 2, and Venera 3

The Soviet program began with the Venera 1 probe. After 1961, the Soviet RKA developed a new spacecraft architecture consisting of an orbital module connected to a descent probe or lander for in situ missions, or to an instrument module for orbital or flyby missions. This architecture was implemented in all Venus missions from Zond 1 up to Venera 8. After the initial attempt with Venera 1, the Zond 1 impactor and the Venera 2 probe soon followed. The next step was the Venera 3 probe, the first man-made object to land on another planet. The characteristics of these first missions are summarized in Table 2.1.

Even though it had no provision for surviving entry, Venera 1 was the first spacecraft targeted at Venus. It was designed to take measurements on the way to Venus, impact the

Table 2.1: The Venera 1 probe, the Zond impactor, and the Venera 2 and 3 missions.

Mission (Launch date)	Mission architecture	Mass (kg)	Thermal control	Pressure control	Comments
Venera 1 (1961)	Impactor	N/A	Circulating fans, motorized shutters	Spacecraft sealed and pressurized with nitrogen	Failure of both sun sensor and thermal shutters
Zond 1 (1964)	Probe and main bus	N/A	Entry capsule designed to withstand 60–80°C	2–5 bar	Loss of pressure in navigation system sealed “dome”
Venera 2 (1965)	Flyby (main bus only)	N/A	Thermal radiator, tubes with liquid coolant		Failure of the communication system—overheating
Venera 3 [†] (1965)	Probe and main bus	~340	Entry capsule designed to withstand 60–80°C [‡]	2–5 bar	Entered the Venus atmosphere

[†] First spacecraft to actually land on another planet.

[‡] These capsules were designed to withstand surface pressures of 5 bars and had a thermal radiator and ammonia cooling system to withstand temperatures of 60–80°C.

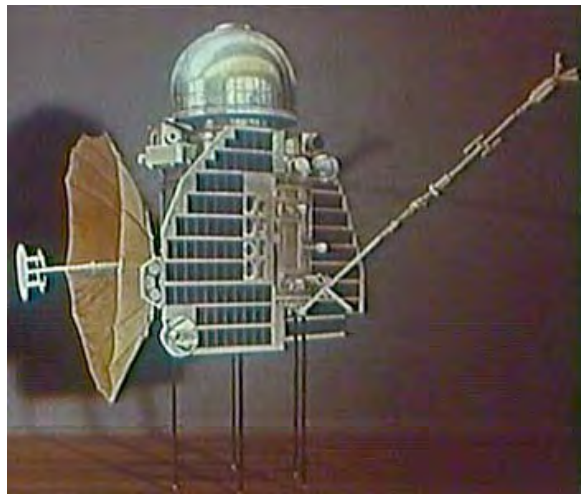
planet and deposit a pennant on the surface. Venera 1, shown in Figure 2.6, did not carry a landing capsule. The cylindrical body of the spacecraft (~1 m diameter by 2 m tall) weighed approximately 643 kg and contained a radio, a tape recorder, a program timing unit, and silver-zinc batteries charged by solar cells.

The spacecraft cylinder was sealed and filled with nitrogen to 1.2 atm, circulated by fans to evenly distribute heat inside the spacecraft body. The motorized shutters on the back of the spacecraft regulated heat radiation, keeping the temperature around 30°C. Venera 1 carried an elaborate navigation system consisting of solar and star sensors based on photomultiplier tubes, as well as gyroscopes and accelerometers. The spacecraft was able to perform orientation adjustments using microjets powered by compressed nitrogen and trajectory corrections using a vernier engine. The telecommunications system was designed to transmit the data on 8 cm and 32 cm bands with a 1 bit/sec data rate. The spacecraft control system was not limited to vacuum tubes; it also used transistor-based electronics.

The spacecraft conducted three scientific telemetry sessions before it lost contact with Earth. It is believed that when the spacecraft was on the course to Venus, the sun sensor failed

Figure 2.6: The Venera 1 spacecraft.

The communications antenna is on the left and the solar panels face to the right. The cylindrical object with the dome is the spacecraft, which was pressurized to 1.2 bars.



after overheating; the thermal shutters failed as well.

Based on the experience with Venera 1, several design changes in the orbital module were implemented. The guidance and navigation sensors were no longer exposed to the space environment but were kept inside a pressurized and temperature-controlled quartz “dome.” Motorized shutters were replaced with hemispherical thermal control radiators. The radiators were coated with 40 layers of terylene plastic and powdered aluminum to absorb or radiate heat, as needed. The temperature inside the pressurized body of the spacecraft was kept within 20–30°C using heating and coolant lines filled with ditolyl methane or isoctane, respectively, and coupled by heat exchangers with the circulating nitrogen inside the spacecraft. In addition, the whole spacecraft was covered with a blanket of thermal vacuum insulation consisting of layers of metal foil and fiberglass cloth.

The lander capsule, designed specifically for Venus missions, weighed approximately 350 kg and measured about 1 m in diameter. The descent capsules were sterilized before launch to prevent contamination of Venus. The capsule contained a heat shield, transmitter, crystal oscillators, program timing system, solar batteries, science payload, and three-stage parachute system. With minor modifications, this parachute system was used on all later Soviet Venus missions, including the Vega landers.

In 1962 two landers and one flyby mission were sent to Venus by the Soviet RKA. All three of these Soviet missions failed when they were stranded in a parking orbit. In 1964, the Soviet RKA repeated the attempt with two landers. One of the spacecraft was again

stranded in the parking orbit but the second one, Zond 1, was successfully launched toward Venus. Unfortunately, a leak in the navigation system quartz dome caused a discharge in the electronics, leading to mission failure.

Of three missions attempted by the Soviet RKA in 1965, two were successfully launched on a trajectory to Venus: the flyby mission Venera 2, and Venera 3, which included a descent capsule. After 26 successful telecommunication sessions, the communication system overheated and Venera 2 consequently lost contact with Earth as the spacecraft passed Venus at 24,000 km.

Venera 3, shown in Figure 2.7, carried a 340 kg descent module placed on an impact trajectory by the orbiter bus within 800 km from Venus. The design of the descent capsule was based on the knowledge of the Venus environment available to mission architects at that time; the design evolved as more science data were returned. For example, descent capsules designed in the early 1960s included solar cells and an ammonia cooling system. They were built to survive pressures up to 5 bars and temperatures up to approximately 70°C. Interestingly, they were also designed to float in water and included sensors to detect the wave motion. Due to thermal failure, the telemetry data from the capsule were never received, but it is generally accepted that Venera 3 was the first man-made object impacting another planet.

Venera 4, Venera 5, and Venera 6

During the late 1960s, the Soviet RKA continued to improve both the Venus orbiting module and descent capsule. At the time, it was thought that the surface temperature of Venus was approximately 300°C, with an atmosphere consisting mainly of carbon dioxide and nitrogen at about 20 bars. Consequently, the capsule was designed to survive 300°C and 25 bars. The Venera 4, 5, and 6 missions are summarized in Table 2.2.

The thermal design of the orbiting module was modified by using an antenna as a thermal radiator. The 1 m diameter descent capsule of Venera 4 weighed about 380 kg and included two 922 MHz transmitters capable of data transmission at 1 bit/sec. Significant modifications to the heat shield were based on experience with warhead designs; after the development of ablative shields designed to sublimate or burn away, Venera 4 employed a heat shield made of a lightweight, porous phenolic epoxy resin.

Venera 4, launched in 1967, reached Venus and transmitted data on the atmosphere and environment until it reached an attitude of about 26 km after 93 minutes of descent. The reason for failure is not clear. The capsule could have been crushed by pressure or it may simply have run out of power, since battery life was designed for 100 min. One day after Venera 4 arrived at Venus, the American probe Mariner 5 arrived at Venus and conducted radio occultation measurements on the atmospheric pressure.

In 1968, Soviet and American scientists met in Tucson, Arizona, to discuss and compare

Figure 2.7: The Venera 3 architecture.

This picture shows the architecture used in all the Venera missions between Zond 1 and Venera 8. The lander capsule is stacked above the cruise vehicle.



results from both the Venera series and Mariner. This meeting led to a new estimate of 427°C for the surface temperature and an estimate of 75 bars for the pressure, levels that exceeded the design limits of the Venera 4, 5, and 6 spacecraft family.

Venera 5 and Venera 6 were launched in 1969 within a week of one another. Both were equipped with a set of sensors to further characterize the Venus atmospheric temperature, pressure, and composition. Because they were designed to survive 25 bars, they were not expected to deliver any surface data. Although mission designers were aware of the new analysis of the Venus environment, it was too late to significantly redesign the landing capsule without missing the next launch opportunity. However, based on the experience with Venera 4, the parachutes were modified to accelerate the capsule's descent, allowing it to reach greater depths prior to overheating the capsule's electronics.

Both Venera 5 and 6 survived the descent for about 50 min and reached altitudes of approximately 20 km, where the pressure exceeded 27 bars and temperature exceeded 300°C . Their failures were most likely due to crushing of the pressure vessel.

Table 2.2: Descent times for the Venera probes 4, 5, and 6.

Mission (Launch date)	Mission architecture	Mass (kg)	Descent (min)	Thermal control	Pressure control	Comments
Venera 4 (1967)	Probe and main bus	~380	93	Designed [†] for 300°C	Pressure vessel designed to withstand 20 bars	Stopped transmitting at 25 km altitude (battery stopped operating or capsule crushed)
Venera 5 (1969)	Probe and main bus	~380	53	See Venera 4	Pressure vessel designed to withstand 25 bars	Stopped transmitting at 20 km (capsule crushed)
Venera 6 (1969)	Probe and main bus	~380	51	See Venera 4	Pressure vessel designed to withstand 25 bars	Stopped transmitting at 20 km (capsule crushed)

[†] Veneras 4, 5, and 6 were all designed for operation at 300°C, believed at the time to be the temperature of the Venus surface. The thermal control system included ablative heat shields for the descent capsule, internal and external insulation, and a temperature control system with a circulation fan.

Venera 7, Venera 8, Venera 9, and Venera 10

The next series of missions, Veneras 7–10, represented a leap forward for in situ science as the first data were returned from another planet. These spacecraft were designed to sufficiently mitigate the challenging conditions experienced during descent through the Venus atmosphere, as well as on the surface. The descent and survival times of this series are summarized in Table 2.3.

The next landing module, Venera 7, was launched in 1970 with a mass of approximately 500 kg. Shown in Figure 2.8, it was built to withstand a pressure of 150 bars and a temperature of 540°C in order to reach the surface and survive for a brief time. The substantial margins in this design proved adequate to accommodate the actual surface temperatures; although the actual temperatures fell below the design requirements, they still significantly exceeded prior measurements.

Table 2.3: Descent and surface survival times for Venera landers 7, 8, 9, and 10.

Mission (Launch date)	Mission architecture	Mass (kg)	Descent time (min)	Surface time (min)	Thermal control	Pressure control	Comments
Venera 7 [†] (1970)	Lander and main bus	~500	35	23	Designed [‡] for 540°C	Titanium vessel inside capsule, rated to 150 bars	Parachute failure, rough landing, after bouncing landed on the side
Venera 8 (1972)	Lander and main bus	~495	55	50	Designed [‡] for 490°C	Titanium vessel inside capsule, rated to 100 bars	Performed as designed, returned scientific data from all instruments on board
Venera 9 (1975)	Lander and orbiter	660	75	53	See Venera 8	Titanium pressure vessel, rated to 100 bars and integrated with landing gear.	Transmission of data stopped after orbiter went out of radio range
Venera 10 (1975)	Lander and orbiter	660	75	65	See Venera 8	See Venera 9	Transmission of data stopped after orbiter went out of radio range

[†] First spacecraft to transmit data back to Earth from another planet.

[‡] Internal and external thermal insulation, and a circulation fan.

PCM used for heat absorption, with honeycomb composite insulation for feedthroughs.

Capsule pre-cooled to -10°C before separation from main bus.

The descent capsule held a spherical titanium pressure vessel rated to 150 bars, a rating much higher than the hemispherical capsules of Veneras 5 and 6. The thermal control sys-

Figure 2.8: The Venera 7 descent module.



tem of Venera 7 consisted of internal and external insulation layers, as well as a circulating fan designed to evenly distribute gas within the pressure vessel. The capsule was cooled down to -10°C prior to separation from the main bus.

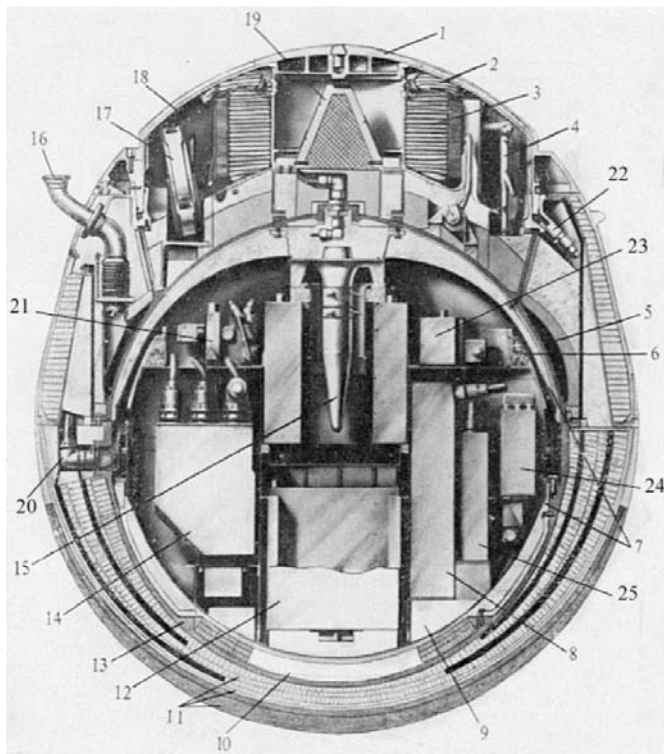
The parachute landing system was also modified in order to achieve both a rapid descent through the atmosphere and a soft landing. Rapid descent was accomplished by keeping the main parachute partially closed with a cord wrapped around its cables. The cord was designed to melt at 200°C and allowed the parachute to fully open for the landing. The parachute was made of a heat-resistant fiber.

The Doppler tracking data for Venera 7 indicated that after release of the parachute, the rate of descent significantly slowed, accelerating again after a few minutes. Just before landing, the descent rate increased to free fall and Venera 7 hit the surface at about 20 m/sec. It is thought that the parachute material deteriorated and the parachute collapsed before landing. After landing, Venera 7 continued to transmit a very weak signal (3% of power) for 23 min. Venera 7 was the first man-made object to transmit data to Earth from the surface of another planet.

By 1972, when Venera 8 was launched, scientists had accurate estimates of pressure and temperature on the surface of Venus. Design improvements based on these analyses included a modified pressure vessel and an improved thermal control system. For the first time, a phase change material (PCM), lithium nitrate trihydrate, was introduced as an efficient heat sink. Another breakthrough was the development of a lightweight honeycomb composite external insulator able to withstand high temperatures and pressures. These new materials resulted in a large mass savings. Although the Venera 8 capsule weighed 495 kg,

it represented a significant improvement in science payload over the 500 kg Venera 7. The internal layout of Venera 8 is shown in Figure 2.9. The Venera 8 descent lasted about 55 min, transmitting scientific data from the surface for approximately 50 min with all the instruments functioning as expected.

*Figure 2.9: Internal layout of the Venera 8 descent module.
The diameter of the module was approximately 1 m.*



1. Cover of parachute housing
2. Drogue parachute
3. Main parachute
4. Altimeter antenna
5. Heat exchanger
6. Heat accumulator
7. Internal thermal insulation
8. Program timing unit
9. Heat accumulator
10. Shock absorbing damper
11. External thermal insulation
12. Radio transmitter
13. Spherical instrument compartment
14. Commutation unit
15. Circulation fan
16. Cooling conduit from bus
17. Ejectable secondary antenna
18. Parachute housing
19. Primary antenna
20. Electrical umbilical
21. Antenna feeder system
22. Explosive bolts of cover
23. Telemetry unit
24. Stabilized quartz oscillator
25. Commutation unit

With Venera 9 and 10, the Soviet space agency introduced a completely redesigned spacecraft, used for all later Venus missions. At 2.4 m and 1,560 kg, the spherical entry capsule was significantly larger and heavier than that of previous missions. The entry capsule contained an 80 cm diameter titanium pressure vessel and housed the 660 kg lander. A 2 m aerodynamic brake to slow descent and a semi-directional antenna were mounted above the vessel. At the bottom of the lander were shock absorbers and a crush pad. The titanium pressure vessel was covered with a few inches of thick layers of composite honeycomb insulation, then with a thin layer of titanium, and finally with a coating of sealant. Inside, the pressure vessel, lined with layers of fiberglass and metal foil, contained large PCM heat absorbers and a circulating fan.

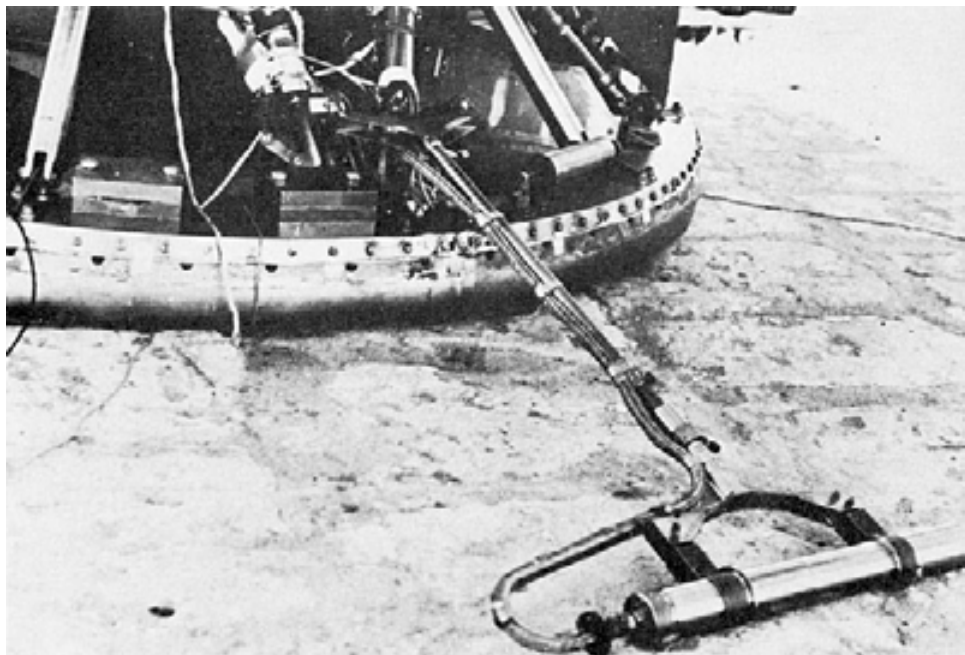
Instruments selected for Venera 9 and 10 were designed to study clouds, the atmosphere,

and the surface. Both Venera 9 and 10 were equipped with halogen lamps for surface operation. For the first time, cycloramic cameras were used for imaging after landing. The two cameras, mounted in front of 1 cm thick cylindrical quartz pressure windows on two opposite sides of the vessel, could each scan a field of view of $180^\circ \times 40^\circ$.

Some of the sensors designed to study clouds and atmosphere during descent, specifically nephelometers and spectrometer sensors, were mounted external to the pressure vessel with their own insulation and PCM for thermal protection. The spectrometer sensors were connected to the spectrometer through fiber optic pipes to view upward and downward. The temperature, pressure, and density sensors were designed to survive and operate in the Venus environment. The platinum temperature sensors were enameled to protect them from chemical corrosion and from the absorption of gas into metal.

A gamma-ray densitometer on Venera 9 was the first instrument designed to operate on the surface of Venus without any thermal protection. The cylindrical densitometer, shown as the “paint roller” in Figure 2.10, was 36.2 cm long and 4 cm in diameter. Three Geiger-tube detectors measured the distribution of reflected gamma rays from a radioactive cesium-137 source in the end of the densitometer. A thick lead shield between the source and the detectors blocked unscattered rays. The device measured atmospheric scattering during descent and was later deployed on the surface to measure the scattering from the denser rock.

Figure 2.10: The Venera 9 gamma ray densitometer.



The instrument comprised two units: the detector portion, consisting of three gas discharge counters located at different distances from the gamma radiation source, and signal processing electronics, located inside the temperature-controlled pressure vessel and connected to the detectors with shielded cables. In this configuration, the unconditioned, low-amplitude electrical signal from detectors had to pass through a series of feedthroughs and cables. Therefore, in addition to the temperature dependence of the detector response, required calibration studies included the transmission properties of the cables and feedthroughs at high temperatures.

Like Venera 8, Venera 9 included a gamma-ray spectrometer within the pressure hull to measure potassium, uranium, and thorium abundances. This sensor consisted of a large sodium iodide crystal scintillator and a photomultiplier tube.¹

Veneras 9 and 10 were launched in 1975 within a few days of one another. Two days before reaching Venus, the descent capsule was separated from a main spacecraft. The two main spacecraft entered the orbit of Venus to serve as communication relays. This mission architecture was desirable since both Veneras had onboard visible cameras and needed to land on the sunlit side of Venus, out of Earth's radio line-of-sight. Since both Veneras carried instruments to study clouds, they were decelerated with braking and parachutes after reaching approximately 65 km altitude. After traversing clouds for about 20 min, the parachutes were jettisoned and the landers fell free for approximately 55 min.

Both Veneras 9 and 10 carried the first mass spectrometers ever used to study planetary atmospheres, but these instruments did not function properly, possibly because of contamination by materials from the cloud layers. Although both landers carried two cameras, each lander transmitted pictures from only one camera due to a failure in removing the camera's protective covers with pyro charges. While halogen lamps were included, natural illumination proved to be sufficient for imaging and the halogen lamps were eliminated from later missions.

Veneras 9 and 10 transmitted data from the surface for 53 and 65 minutes, respectively. The landers' capabilities were not the limiting factors in the surface survival time; instead, each mission terminated when its orbiter exited the communication range.

Venera 11, Venera 12, Venera 13, and Venera 14

The next series of landers, Venera missions 11, 12, 13, and 14, improved upon the successes of the ongoing Soviet Venus exploration program. These missions all descended to the surface in approximately one hour and lasted on the surface for up to two hours. Their characteristics are summarized in Table 2.4.

The Venera 11 and 12 spacecraft were quite similar to Venera 9 and 10, with a few modifi-

¹Both the densitometer and spectrometer were built by Iu. A. Surkov's team.

Table 2.4: Descent and survival times for Venera landers 11, 12, 13, and 14.

Mission (Launch date)	Mission architec- ture [†]	Descent time (min)	Surface time (min)	Thermal control	Pressure control	Comments
Venera 11 (1978)	Lander and flyby	60	95	Same as Venera 9 with an addition of polyurethane foam to the outer insula- tion.	See Venera 9	Communica- tion was lost after orbiter moved out of range [‡]
Venera 12 (1978)	Lander and flyby	60	110	See Venera 11	See Venera 9	See Venera 11
Venera 13 (1978)	Lander and flyby	55	127	See Venera 11	Similar to Venera 9 with an addition of metal teeth ringing to the landing pad	See Venera 11
Venera 14 (1978)	Lander and flyby	55	57	See Venera 11	See Venera 13	See Venera 11

[†] All landers had a mass of 760 kg, although each had a distinctly different science payload.

[‡] Communication with all of these vehicles was lost when they moved out of range.

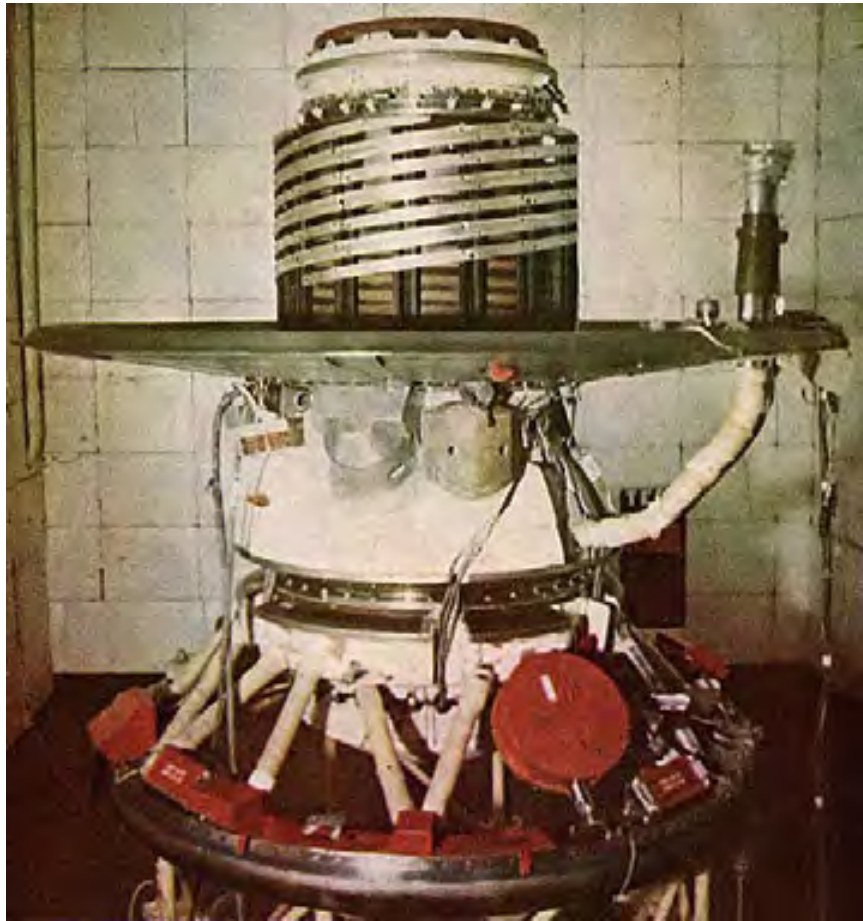
cations and new instruments. The Venera 11 descent module is shown in Figure 2.11.

The outside thermal insulation of the pressure vessel on Venera 11 and 12 was improved by adding high-temperature polyurethane foam. The mass spectrometer had suffered from clogging on Venera 9 and was therefore modified by adding a meter-long intake system with a large opening served by a very fast inlet valve. New science instruments added to Venera 11 and 12 included a radio sensor designed to measure disturbances in electrical properties of the atmosphere (Groza), a gas chromatograph, a soil sampling drill connected to an analysis chamber, a penetrometer, and two color cameras.

Venera 11 and 12 were launched in 1978 within a few days of each other and descended through the clouds and atmosphere to reach the surface in about one hour. Venera 11 transmitted data for about 95 minutes, until the flyby spacecraft used as relays were out of reach.

Figure 2.11: The Venera 11 descent module.

This is the third of a class of larger lander vehicles, beginning with Venera 9 and 10, launched in 1975. The 2 m diameter aerodynamic decelerator slowed the descent speed and eliminated the need for a parachute in the lower atmosphere. Above it, a helical antenna enclosed the parachute compartment. At the bottom of the lander were shock absorbers and crash pads. The inlet for the mass spectrometer was located above the decelerator.



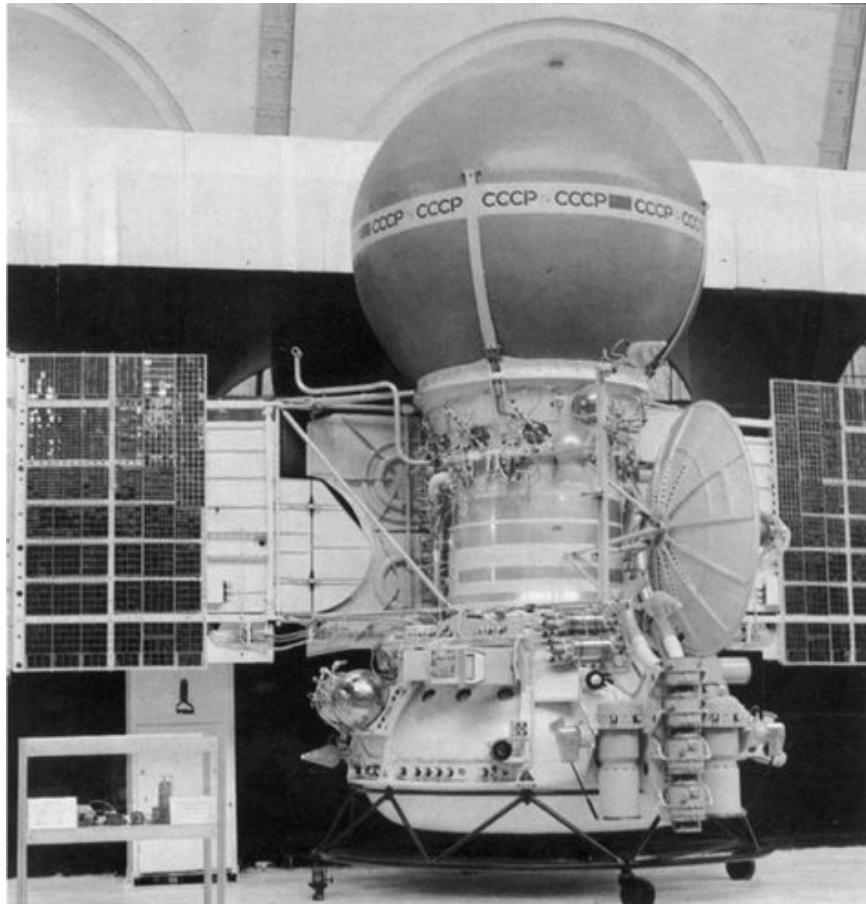
Venera 12 transmitted data for 110 min. Unfortunately, not all the experiments on Venera 11 and 12 succeeded. For instance, the color cameras did not return data; even though the protective caps on the camera windows were modified to avoid problems encountered in Venera 9, the new design caused a bond seal to form between the caps and windows during descent, preventing the ejection of the caps. Additional instruments that did not work due to failed pressure seals included a drill-based sample acquisition system and a penetrometer.

A low-frequency radio sensor, Groza, returned new data indicating the presence of discharges similar to lighting storms, possibly caused by atmospheric phenomena not yet un-

derstood. In addition, Groza registered anomalous readings and unexplained phase shifts in the Doppler radio measurements at the same altitude at which all four NASA Pioneer probes (discussed below) reported problems with both housekeeping and science sensors.

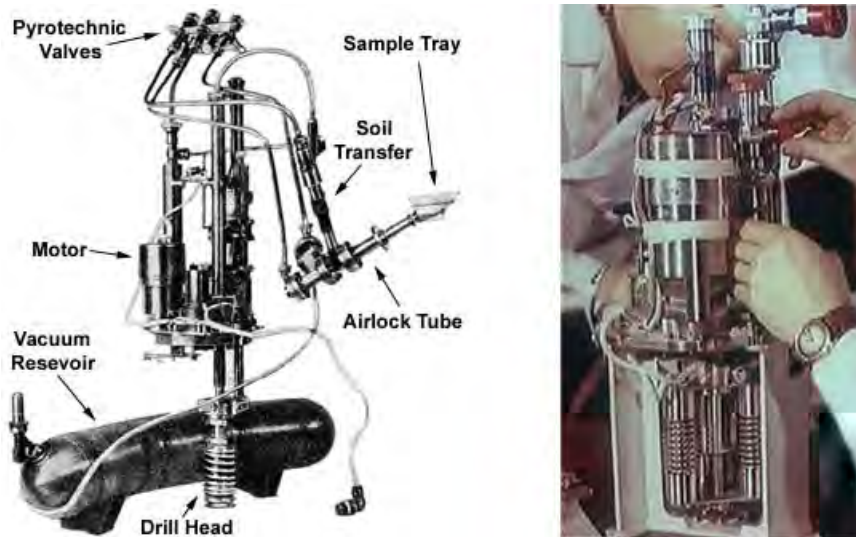
Venera 13, shown in Figure 2.12, was very similar to Venera 12, except for increased battery power and more instruments. Venera 13 included some aerodynamic modifications that increased the lander's stability during free fall. To prevent spinning, damping blades were installed underneath the lander vehicle, and a sleeve just below the aerobrake was installed to reduce the turbulent effect of externally mounted instruments. These changes were implemented due to concerns that spinning and oscillation during descent could have damaged the Venera 11 and 12 landers, resulting in poor science return.

Figure 2.12: The Venera 13 spacecraft.



The Venera 13 and 14 landers featured an improved sample acquisition system, shown in Figure 2.13. Featuring the capability to drill to 30 cm, this system collected the sample,

Figure 2.13: The Venera 13 and Venera 14 sample collection system.



reduced the sample pressure, and ultimately transported it into the lander for analysis. All these operations were conducted in the ambient environment of Venus.

The elements of the sample collection system, including an electrical motor for the drill, were designed to function at 500°C, taking into account the thermal coefficient of expansion of materials to achieve a proper fit at this temperature. The sample was transferred in stages through an elaborate system of tubes opened with pyroelectric charges. Finally, the sample was contained and transferred through an airlock into the X-ray fluorescence analysis chamber that was kept under vacuum. The whole process of collection and analysis took a few minutes per sample. The sample collection and transfer system weighed about 26 kg and consumed 90 W. The system worked reliably on both the Venera 13 and 14 missions and later on the Vega landers. This level of success was achieved by extensive testing conducted under conditions similar to those on the surface of Venus.

Both cameras on the Venera 13 and 14 landers functioned successfully, producing the most accurate pictures of the Venus surface to date. Venera 13 transmitted for 127 min and Venera 14 for 57 min to the relay bus, until the relay moved out of the lander's communication range.

Vega 1 and Vega 2

The last Soviet mission to the surface of Venus, Vega, launched in 1984 with two identical spacecraft containing a lander and a balloon. This mission combined a Venus swingby and a Comet Halley flyby (thus the name Venera–Gallei, or Vega). Two identical spacecraft, Vega 1 and Vega 2, were launched December 15 and 21, 1984, respectively. After carrying

Figure 2.14: The Vega spacecraft (front and back).



Venus entry probes to the vicinity of Venus, the two spacecraft were retargetted using Venus gravity field assistance to intercept Comet Halley in March 1986. The Venus landers and balloons are described in Table 2.5.

The Vega architecture, shown in Figure 2.14, was similar to Venera 14, but it included new instruments focused on measuring the composition and size distribution of cloud particles, as well as on the direct detection of sulfuric acid. The cloud studies instrument suite worked only on Vega 1, malfunctioning on Vega 2. The landers were also equipped with an improved accuracy pressure– and temperature–sensing unit; unfortunately, it did not work on Vega 1.

At about 18 km altitude during the Vega 1 descent, the UV spectrometer measured a sharp absorption peak in coincidence with unexplained electrical impulses in the sensors and avionics and fluctuations in the Doppler tracking. The electrical shock to the spacecraft prematurely initiated the deployment and operation of the sample drill; these events should not have taken place until touchdown. Similar electrical disturbances at altitudes of 12–18 km were observed by Veneras 11, 12, 13, and 14, as well as by the NASA Pioneer probes (discussed below). The Vega 1 lander transmitted data for 57 min but did not acquire a solid sample. The Vega 2 lander successfully conducted soil drill experiments, transmitting data for 20 min. Neither lander carried cameras since they were designed to land on the night side of Venus.

Vegas 1 and 2 carried identical balloons. The 3.4 m balloon probe weighed 21 kg, with

Table 2.5: Descent and survival times for the Vega 1 and Vega 2 missions.

Mission architecture	Mass (kg)	Descent time (min)	Surface time (min)	Thermal control	Pressure control	Comments
Vega 1 (1984)						
Lander	750	60	20 min	See Venera 11	Same as Venera 13, with an addition of damping blades underneath the lander	Loss of contact after 20 min of lander operation at the surface
Balloon	21	N/A	48 hours	Designed to operate at 54–55 km altitude where temperature is about +40°C.	Designed to operate at 0.5–1 bar. Pressure vessel in the gondola was not needed.	Transmission stopped after batteries were exhausted and balloon reached a day side
Vega 2 (1984)						
Lander	750	60	56 min	See Vega 1 lander	See Vega 1 lander	Transmission of data stopped after a flyby bus got out of communication range
Balloon	21	N/A	48 hours	See Vega 1 balloon	See Vega 1 balloon	Transmission stopped after batteries were exhausted and balloon reached a day side

the gondola weighing 6.9 kg. The balloons were designed to deploy and float high in the atmospheric clouds where the temperature was near that of Earth. However, the balloon

materials had to be tolerant of the corrosive effects of concentrated sulfuric acid and other chemical agents present in the clouds, as well as to potential damage from ultraviolet radiation. In addition, the balloon materials and the deployment system had to survive in a folded state for months, exposed to vacuum during the cruise.

The balloon probes were designed to deploy and operate autonomously. Extensive design efforts and experiments, including materials selection, went into the building of the balloon probe. The balloons were built using a coated material similar to Teflon, fluorolon. The tether and straps between gondola compartments were made of kapron, similar to nylon-6. The deployment system included bottles of compressed helium and a 35 m^2 parachute used while filling the balloons with helium. The filling process took about 230 sec and was controlled with barometric sensors.

Both the Vega 1 and Vega 2 balloons operated at the middle of the cloud layer, as shown in Figure 2.15, at altitudes of approximately 53 km and average pressures of 0.5 bar. They stopped transmitting after approximately 48 hrs of operation, after exhausting their batteries. Both balloons traveled about 12,000 km, or one-third of the way around the planet, reaching the day side of Venus, where they probably burst from overheating. An unexplained anomaly was observed with the Vega 2 balloon. It plunged several kilometers down to the 1 bar pressure zone shortly after reaching the daylight of Venus, recovering to a normal altitude just before the final data transmission. Transmission ended for unknown reasons.

2.2.2 Venus: United States NASA Missions

The NASA program of in situ Venus exploration has to date launched only one mission, Pioneer Venus, launched in 1978. Pioneer Venus consisted of one Large Probe with a parachute to prolong its descent and three small probes. These probes were designed to operate deep in the atmosphere but there was no requirement for them to survive a landing on Venus. Ultimately, even though they all experienced a number of anomalies in the lower atmosphere, they all operated until surface impact, with one continuing to send data after impact. The designs of the probes and mission scenarios are summarized in Table 2.6. One Multiprobe Bus, shown in Figure 2.16, carried all probes until they were separated sequentially near Venus to reach different regions. It then entered the atmosphere and obtained atmospheric composition data until burnup.

Pioneer Large Probe

The Pioneer Large Probe consisted of a pressure vessel enclosed in a deceleration module to protect it from aerodynamic heating during atmospheric entry. The large probe major elements are depicted in Figure 2.17.

The deceleration module featured a carbon phenolic conical aeroshell, an aft body covered

Figure 2.15: Diagram of the atmospheric structure of Venus (*T*: turquoise; *p*: dark blue).

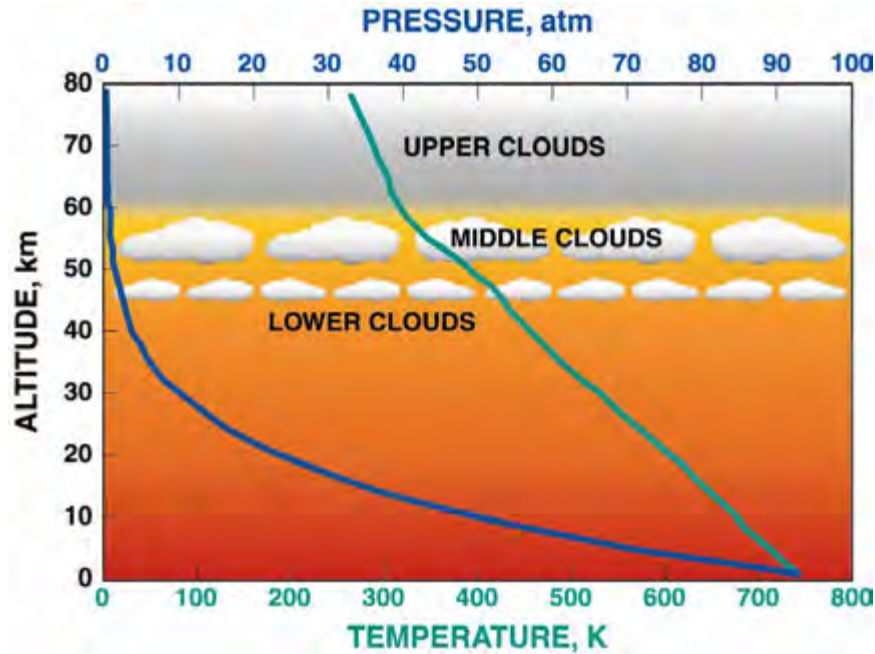


Figure 2.16: The Pioneer Orbiter and Multiprobe Bus.

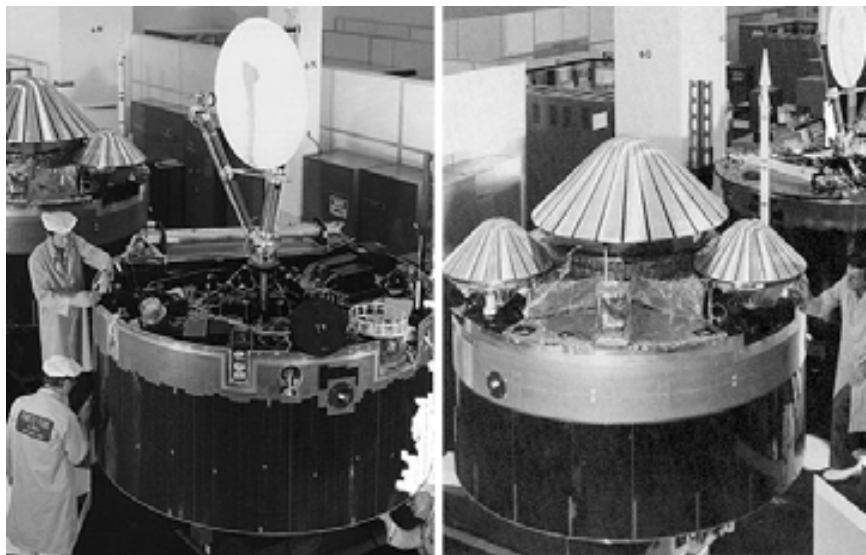


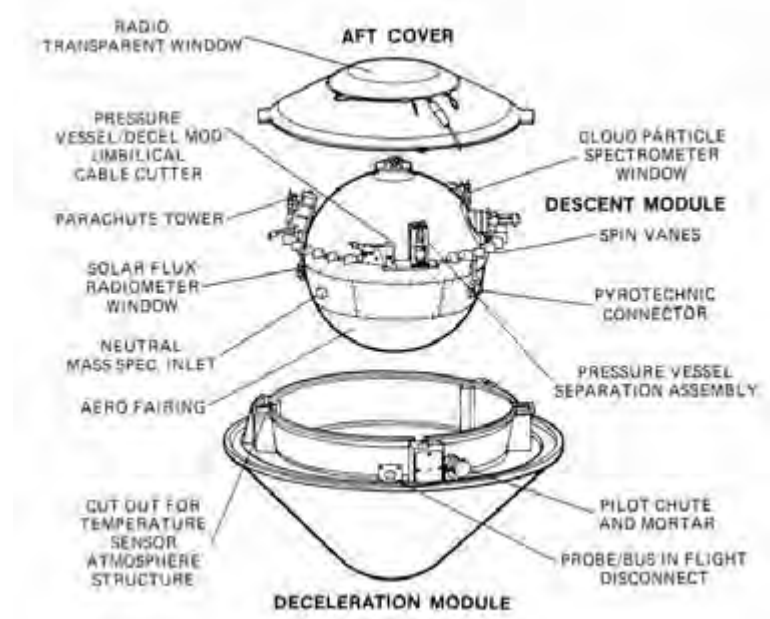
Table 2.6: Descent and survival times for the NASA Pioneer Venus mission (1974 launch)

Mission element	Mass (kg)	Descent (min)	Surface (min)	Thermal control	Pressure control
Pioneer Large Probe	302 [†]	54	None	Vessel lined with 41 layers of metallized Kapton insulation blanket, beryllium heat sink, low emittance coating	Titanium pressure vessel, 78 cm in diameter, filled with nitrogen
Small North Probe	94 [‡]	53	None	Vessel lined with 61 layers of metallized kapton insulation blanket, beryllium heatsink, low emittance coating	Titanium pressure vessel, 47 cm in diameter, filled with xenon
Small Day Probe	94 [‡]	56	67	See North Probe	See North Probe
Small Night Probe	94 [‡]	56	None	See North Probe	See North Probe

[†] Deceleration module mass: 109 kg, and pressure vessel mass: 193 kg

[‡] Deceleration module mass: 33 kg, and pressure vessel mass: 61 kg

Figure 2.17: Schematic of the Pioneer Large Probe pressure vessel and deceleration module.



with a foamed elastomer material, and a solid Teflon radome transparent to radio frequencies. The 78 cm diameter spherical pressure vessel consisted of two dome-shaped titanium sections joined to a midsection element. These three sections were bolted together with an o-ring based seal to prevent the nitrogen gas, pressurized to 100 bars inside the vessel, from leaking out during transit between Earth and Venus.

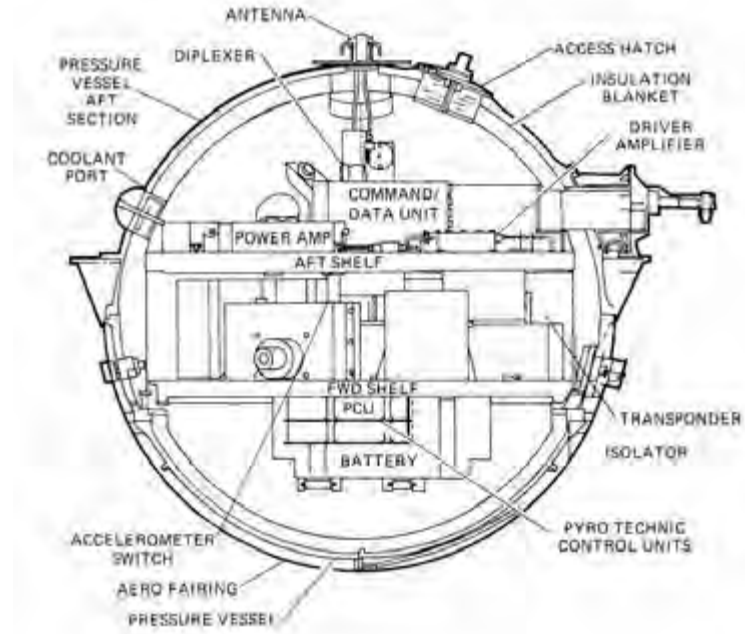
The seal system included graphoil flat gaskets to prevent leakage of Venus atmospheric gases into the probe during descent. With a pressure vessel diameter of 78 cm, the two sealing surfaces totaled nearly 5 m. In order to mitigate the risk of nitrogen leaking out through small fissures, a small pressurized nitrogen tank was flown and used to increase the internal nitrogen pressure by 42 bars prior to the probe separation from the main bus.

For probes operating in dense planetary atmospheres, such as those seen at Venus, Jupiter, or Titan, convection plays a larger role in heat transfer than radiation, requiring a novel design process for thermal control systems. Specifically, convection is harder to model a priori and requires greater use of empirical models and laboratory validation. As a result, the thermal control for the Pioneer Large Probe differed from that used for smaller probes.

The thermal control for the Large Probe included an internally mounted thermal isolation

system, with the mass of the payload and structural elements providing an additional transient heatsink. The inner surface of the pressure vessel was lined with 41 layers of dimpled and flat aluminized Kapton (about 2.5 cm total thickness) that created a convection and radiation barrier. The multilayer Kapton insulation was held in place with thin, spherical titanium retainers. The Kapton was also used to close out all blanket feedthroughs and edges. This system effectively created a 2.5 cm thick gas conduction volume, isolating the hot pressure vessel wall from the payload. In addition, all interior surfaces of the vessel were covered with a low emittance film to create radiative isolation between the payload and the vessel itself. The shelves and equipment were isolated from the pressure vessel walls through the use of 24 titanium (6Al–4V) standoffs and a cylindrical titanium shelf support structure. The internal layout of the Large Probe pressure vessel is shown in Figure 2.18.

Figure 2.18: Internal layout of the Pioneer Large Probe pressure vessel.



Two mounting shelves for equipment served as the main heatsinks for the payload because they were constructed from approximately 37 kg of solid beryllium, chosen for its high thermal capacity (2000 J/kgK). The Pioneer probes used only heatsinks to extend the operational lifetime, unlike the Soviet Venera probes, which used phase change material.

The Large Probe carried seven instruments located inside the pressure vessel, requiring 11 inlets for sensing and nine windows with downward-looking access to the atmosphere. Con-

sequently, it was necessary to extract the pressure vessel from the descent module and heat shield with a mortar-fired pilot parachute that pulled off the aft cover, allowing the main parachute to deploy. After the main parachute stabilized the descent, the explosive bolts separated the aeroshell so that all inlets and windows covered by the aeroshell were exposed to the ambient atmosphere. In order to slow down the descent through the cloud layers, the Large Probe remained attached to the parachute. After traversing the cloud layer, the parachute was released and the pressure vessel was allowed to free-fall to the surface.

The design and implementation of inlets and windows able to withstand increasing temperature and pressure during descent posed a challenge to mission design. At the time of design, it was known that sulfuric acid is a main component of a cloud layer, presenting a concern that the visibility through the sapphire windows would be obscured by the clouds' condensates. An electrical heater was mounted on the perimeter of each window to remove condensates.

The infrared radiometer required a window other than sapphire and ultimately utilized prime and backup windows made of 231 carats natural diamond. Unfortunately, the brazing technique developed for the sapphire windows was inappropriate for the diamond windows because of their hardness. Ultimately, experimental work led to a diamond window seal that used a preloaded system consisting of a graphoil sealing surface with anviloy and inconel alloys.

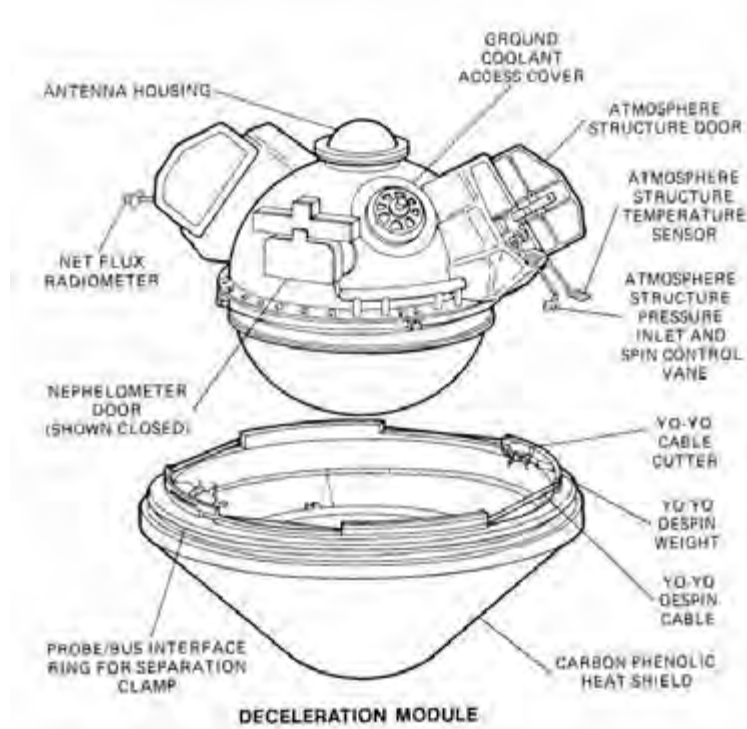
Pioneer Small Probes

The three Pioneer Small Probes were identical, with a design similar to the Large Probe, but with several exceptions. The Small Probe pressure vessels (47 cm in diameter) were assembled from two hemispheres, sealed with a system of o-rings and graphoil seals like the Large Probe. Since the Small Probes' pressure vessels had a higher area-to-volume ratio than the Large Probe, they required 61, rather than 41, layers of thermal blanket insulation. Beryllium shelves were used once again as heat sinks. Xenon replaced nitrogen as the fill gas because of its low thermal conductivity. The atmospheric entry protection for the Small Probes is shown in Figure 2.19.

The deceleration module was attached to the forward end of the pressure vessel and consisted of a 45° half-angle blunt cone covered with a carbon phenolic material. The Small Probe descent sequence was simpler than that of the Large Probe. The three instruments inside the Small Probes' pressure vessels, shown in Figure 2.20, were mounted above the deceleration module. The design of the housing doors for the three instruments presented the biggest challenge. The doors had to be carefully opened at an altitude of 70 km using an actuation mechanism with adequate torque to overcome aerodynamic forces generated by the Probes' descent through the atmosphere.

Two Small Probes (labeled North and South) entered on the nightside, and one Small Probe (labeled Day) entered on the dayside of the planet. Although none of the probes

Figure 2.19: The main features of the Pioneer Small Probes.



were specifically designed to survive landing, the Small Day Probe successfully reached the surface and transmitted from there for over an hour. It returned some basic engineering data before the battery depleted and the transmitter overheated and ceased operating.

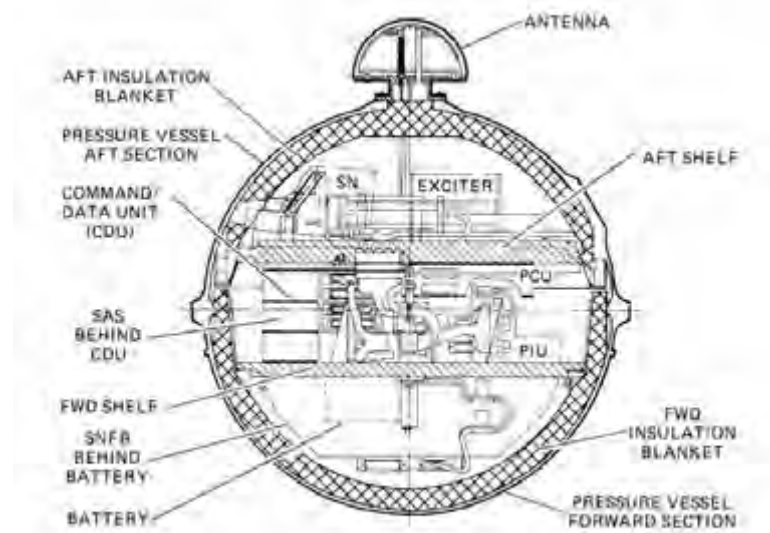
All four Pioneer Probes experienced anomalous behavior at and below 12.5 km altitude. Temperature sensors on all four spacecraft showed a discontinuous drop in temperatures, while net flux radiometers showed a sudden decrease concurrent with a sharp increase in atmospheric temperature. Status signals on boxes from which the temperature sensor and net flux radiometer had been deployed on the Small Probes indicated the sensors had, impossibly, been re-stowed. Large Probe thermocouple wires, cut prior to jettisoning of the heat shield at parachute deployment, indicated signals of a few millivolts. The summary of the observed anomalies is presented in Table 2.7. Because of design and instrument payload differences, many of the Small Probe anomalies were not experienced by the Large Probe and vice versa.

These electrical anomalies resulted in a partial loss of science data below that altitude. Prior to late 1993, the cause of these anomalies had never been explained or understood. In

Table 2.7: Anomalies experienced by the Pioneer Venus Probes at and below 12.5 km altitude.

Anomaly	Probe			
	Large	North	Day	Night
Temperature sensors failed	✓	✓	✓	✓
Changes and spikes in pressure data	✓	✓	✓	✓
Failure of net flux radiometer fluxplate temperature sensors		✓	✓	✓
Abrupt changes and spikes in data from net flux radiometer		✓	✓	✓
Change in the indicated deployment status of the atmosphere structure temperature sensor and net flux radiometer booms		✓	✓	✓
Erratic data from two thermocouples embedded in the heat shield		✓	✓	✓
Erratic data from a thermistor measuring junction temperature of the heat-shield thermocouples		✓	✓	✓
Slight variations of current and voltage levels in the power bus		✓	✓	✓
Slight offsets or jumps in the values for temperatures of the forward and aft shelves and the internal pressure		✓	✓	✓
Abrupt changes in cloud particle size laser alignment monitor	✓	N/A	N/A	N/A
Decrease in the intensity of the beam returned to the cloud-particle-size spectrometer	✓	N/A	N/A	N/A
Steady increase in flux readings of the infrared radiometer	✓	N/A	N/A	N/A
Noise in the data from the infrared radiometer	✓	N/A	N/A	N/A
Spikes in the data monitoring the ion pump current of the mass spectrometer analyzer	✓	N/A	N/A	N/A
Abrupt decrease of current in the power bus	✓	N/A	N/A	N/A
Jumps in the receiver (transponder) static phase error	✓	N/A	N/A	N/A
Spikes in the receiver automatic gain control	✓	N/A	N/A	N/A
Spurious reading from thermocouples that had been dropped from the probe in its heat shield	✓	N/A	N/A	N/A

Figure 2.20: Internal layout of the pressure vessel of the Pioneer Small Probe.



1993, a workshop was held at the NASA Ames Research Center to bring together principal investigators, instrument engineers, spacecraft designers, and other scientists in an attempt to identify the cause of the anomalies. In addition to hardware failures, a number of atmospheric phenomena were considered, including the following:

- Chemical interactions of atmospheric constituents with the probe and sensors, such as residual sulfuric acid from the clouds interacting with the harness or sensor materials, or carbon dioxide oxidation of titanium parts or polymers.
- Probe charging followed by electrical breakdown of the atmosphere, leading to sparks igniting fires on the probe exterior.
- Condensation of conductive vapors on the external sensors in the deep atmosphere, leading to shorted electrical circuits.

Although the last of these phenomena appeared to be the most likely, laboratory tests conducted on the probe harness after the workshop indicated that the principal cause of the anomalies was insulation breakdown of the external harness.

Later, the NASA orbital spacecraft Magellan provided corroborating evidence for altitude-dependent phenomena affecting materials on Venus. The microwave radiometer observed a substantial decrease in radar emissivity and increased conductivity of the planet surface at

elevations around 5 km.

The anomalies experienced by the Venus descent probes point to the need to simulate the Venus environment as accurately as possible. The Pioneer Venus probes were tested in nitrogen at temperatures up to 500°C and pressures up to 100 bars and were never tested under these conditions in a carbon dioxide environment under the assumption that the substitution of carbon dioxide by nitrogen was acceptable. Further research has led to a new understanding of the environment experienced by the Venus descent probes.

2.2.3 Venus: Lessons Learned

The Venus exploration programs conducted by both the United States and the Soviet Union led to a number of interesting observations:

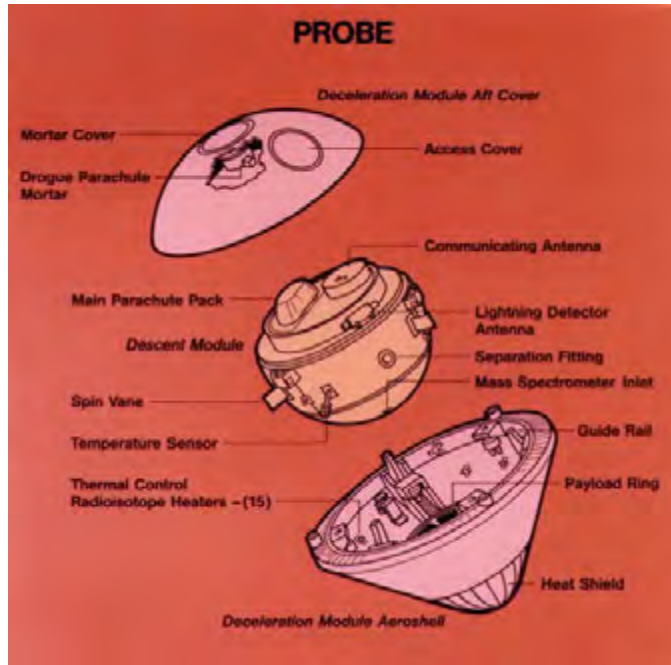
- It is feasible to reach the surface of Venus and conduct scientific measurements in the Venus environment for time periods of the order of an hour or so, subject to limitations from communications relays.
- Certain atmospheric phenomena taking place at 12 km altitude may affect or damage the spacecraft, with serious consequences for mission success and returned science.
- Descent systems for Venus require innovations in both design and materials for survival and operation in the high temperatures and pressures.
- The effects of long exposure to the lower atmosphere of Venus are unknown, requiring added research to determine the chemical and physical interactions with novel materials.
- While some instruments may be exposed to the Venus environment, most must be contained in the temperature- and pressure-controlled vehicle.

2.2.4 Jupiter Atmosphere: Galileo Probe

The original Galileo orbiter, launched in 1989, is discussed more fully below. Its probe, designed to study the atmosphere of Jupiter, separated from the orbiter on July 13, 1995, and entered the atmosphere 155 days later, on December 7, 1995. The total mass of the Galileo Probe was 339 kg, comprising the deceleration module mass of 213 kg and the descent module mass of 126 kg. The Galileo Probe's structural design, shown in Figure 2.21, was based principally on the Pioneer Venus Large and Small Probes.

In particular, the deceleration module of the Galileo Probe was very similar to that of the Pioneer probes. Like the Pioneer Large Probe, the descent module was separated from the deceleration module to accommodate multiple atmospheric instruments. While the Pioneer Venus Large Probe jettisoned its parachute within 17 min of deployment, the Galileo Probe

Figure 2.21: Main structural elements of the Galileo Probe.



included a parachute, which it retained for the duration of its mission.

Descent Module

The thermal and pressure control approach to the Galileo Probe descent module differed significantly from the Pioneer Venus Probes. A thick titanium aerofairing, 0.008 inch thick, surrounded the descent module and consisted of a forward dome and side panels bolted to the probe's structural support. To equalize the internal pressure to the steadily increasing external atmospheric pressure, the descent module used an atmospheric intake through an external vent located on the aft side of the probe. This vented probe design replaced the pressure vessel of the Pioneer Venus design.

This approach, made possible because of the significantly lower pressures and temperatures encountered at Jupiter relative to Venus, resulted in mass savings. It eliminated the pressure vessel and simplified the sample acquisition system and optical windows' designs, which were major problems for Pioneer Venus. The multilayer thermal blanket system, similar to the one developed for the Pioneer Venus Probes, provided thermal protection to the systems and restricted gas flow within the probe.

The descent module, bearing six science instruments, consisted of four distinct parts: the forward compartment, the main science compartment, the communication shelf, and those

parts in direct contact with the Jovian environment. The forward compartment housed the data and command processor (DCP), the subsystem power interface unit (SPIU), and the three battery modules. The DCP and SPIU were mounted directly to the main equipment shelf, made from aluminum honeycomb covered with aluminum face-sheets. Batteries were then mounted on top of the DCP and SPIU. The Galileo Probe was the first to use LiSO₂ batteries, still under development at the time and now used commonly in current spacecraft designs. In order to achieve the high current capacity needed to fire the pyrotechnic initiators that separated the descent module from the deceleration module, the Galileo Probe also flew thermal batteries.

The main science compartment was located on the aftside of the main equipment shelf. The communications shelf was formed by the actual units, including the transmitter, the ultra-stable oscillator, and the excitors, mounted to a titanium ring and supported by titanium honeycomb. To eliminate single-point, catastrophic mission failures, the electrical and electronic subsystems, including the radio frequency link with the Orbiter and receiver on the Orbiter, were dual-string. The fourth part of the descent module consisted of sections requiring direct contact with the Jovian environment, including the four inlet ports, one outlet port, four windows, and a single deployable arm for the nephelometer.

The Galileo Probe survived for 59 minutes and traversed 95 miles of the Jovian atmosphere, where the environmental temperature reached 152°C and the pressure reached 22 bars. The Probe housekeeping temperature was monitored during the mission. One transmitter failed after 49 min, while the second transmitter continued to operate for an additional 10 min, failing at 115°C and concluding the mission.

The Probe experienced two significant anomalies during descent:

- The parachute deployed 53 seconds too late, so that the probe mission started slightly deeper in the atmosphere than planned, thus missing some science data; and
- Sensors indicated that the temperature rise inside the probe exceeded the predictions from ground testing, necessitating the recalibration of some instruments.

The second observed anomaly illustrates a major difficulty with the design of atmospheric probes, where convective heat dominates over radiative heat transfer. Convective heat transfer is more difficult to model and predict than radiative processes since, in addition to gravity, it is influenced by many unpredictable effects, such as turbulent fluctuations in pressure during descent, mechanical agitation and others. This again emphasizes the importance of testing in environmental conditions resembling, as closely as possible, the conditions encountered by the mission.

Heat Shield

The Galileo Probe to Jupiter was the most challenging entry mission undertaken to date by

NASA. The probe, using a 45° blunt cone aeroshell, entered the Jovian atmosphere at approximately 47.4 km/s. The combined convective and radiative peak heat loads, including the effects of blockage from ablation products, have been estimated at 35 kW/cm², with a total integrated heat load of 200 kJ/cm².

The heat shield worked principally by absorbing the energy through an ablation process that allowed the heat to be carried away by the gases coming off the surface. The forward heat shield employed fully dense carbon phenolic ($\rho = 1450 \text{ kg/m}^3$), the best known ablator, while the aft heat shield was made of phenolic nylon. These materials have been used extensively for Earth re-entry vehicles as well as on Pioneer Venus probes; however, on the Galileo Probe they were subjected to conditions not experienced before in flight because of the high entry velocity (48 km/s, four times faster than the Venus Pioneer Probes) caused by Jupiter's massive gravitational field.

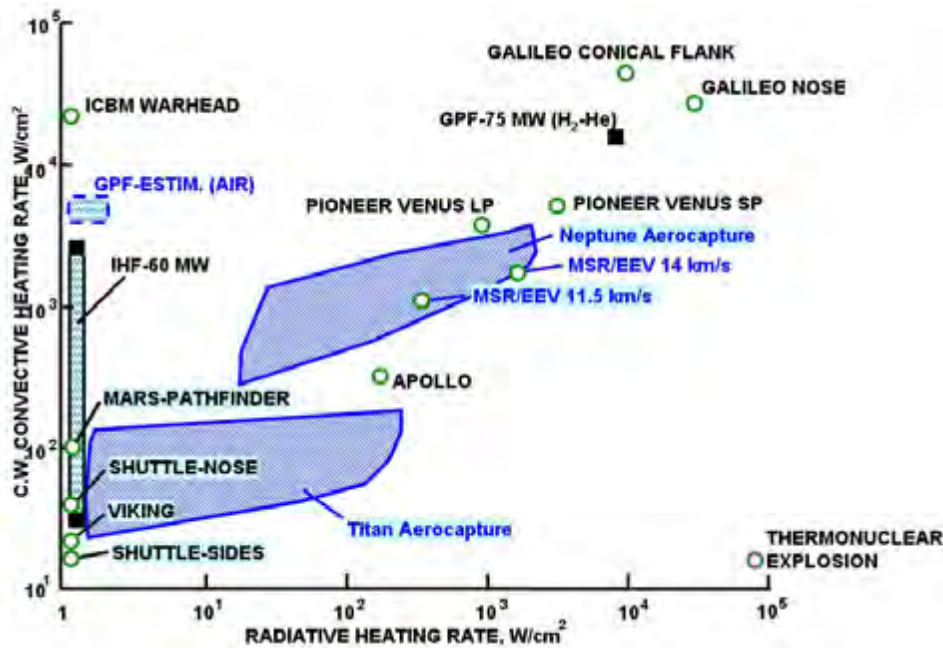
To enable qualification testing of the thermal protection system (TPS), the NASA Ames Research Center developed and built test facilities that included the arc jet Giant Planet Facility (GPF) and a laser test facility to understand the spallation characteristics. The GPF arc jet operated on an H₂-He gas mixture and was capable of producing very high heat fluxes (convective and radiation) on test samples. Figure 2.22 shows the heating environments for many missions, including the Galileo Probe and the Pioneer Venus Probes, as well as the operational environment of the GPF. Arc jet testing was augmented by testing with continuous wave (CW) carbon dioxide (CO₂) lasers, capable of even higher heat fluxes, albeit with small spot sizes on the target.

The Galileo Probe TPS design employed engineering tools developed in the 1970s and was very sophisticated for the time. A handful of teams independently developed and applied their methods for the analysis and evaluation of the design. These models addressed the coupled chemically reacting boundary layer and shock layer in the presence of thermochemical ablation and some spall. But it was also apparent that some of the models could not be validated (e.g., shock layer radiation) due to limitations in existing ground test facilities. Ultimately, design teams converged on a final TPS design and thickness distribution by adding a margin to the conservative side of the many models.

During the high-speed, high-temperature entry phase, mechanical erosion of the forward heat shield reduced its mass from approximately 152 kg to 70 kg. The Analog Resistance Ablation Detector (ARAD) system installed in the forebody TPS returned data describing the actual profile. A schematic of the changed profile is shown in Figure 2.23.

The ablation data demonstrated that stagnation point recession was less than predicted, but that real ablation at the shoulder exceeded the modeled values; in fact, the data suggest that there was almost a burn-through at the shoulder. Current physical models do not accurately describe the Galileo flight recession data, demonstrating significant uncertainty in the models describing coupling of the environment with the ablation physics.

Figure 2.22: Convective and radiative heat fluxes experienced by various missions.
The shaded area shows the test capabilities for the Giant Planet Facility (GPF). Note that conditions experienced by the Galileo Probe are equivalent to that of an ICBM warhead flying through a thermonuclear explosion.



2.3 Cold Temperatures

Only one spacecraft has landed on the surface of an outer planet moon. The European Space Agency was responsible for the design and execution of the Huygens probe, transported to Titan by the NASA Cassini spacecraft. This experience will be described below.

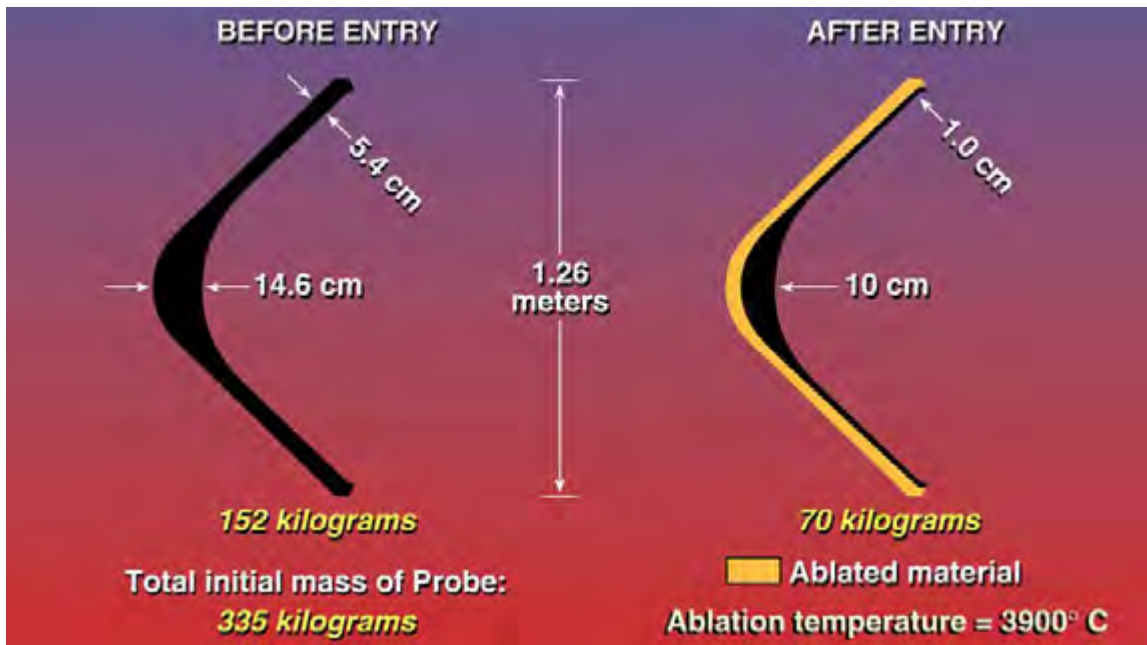
2.3.1 Titan: Cassini–Huygens Probe

NASA's Cassini spacecraft, launched in 1997, carried the Huygens Probe to Saturn's moon, Titan, where it successfully descended through the atmosphere and landed on the surface on January 14, 2005. The entire Huygens mission was designed to be carried out during a 2.5-hour descent through the atmosphere and possibly a few more minutes on the surface.

Architecture

When the Cassini–Huygens spacecraft was launched, the probe was mated onto the side of the orbiter. In this configuration, the orbiter provided the probe with electrical power, command, and data through an umbilical connection. During the seven-year journey to

Figure 2.23: Heat shield ablation of the Galileo Probe.



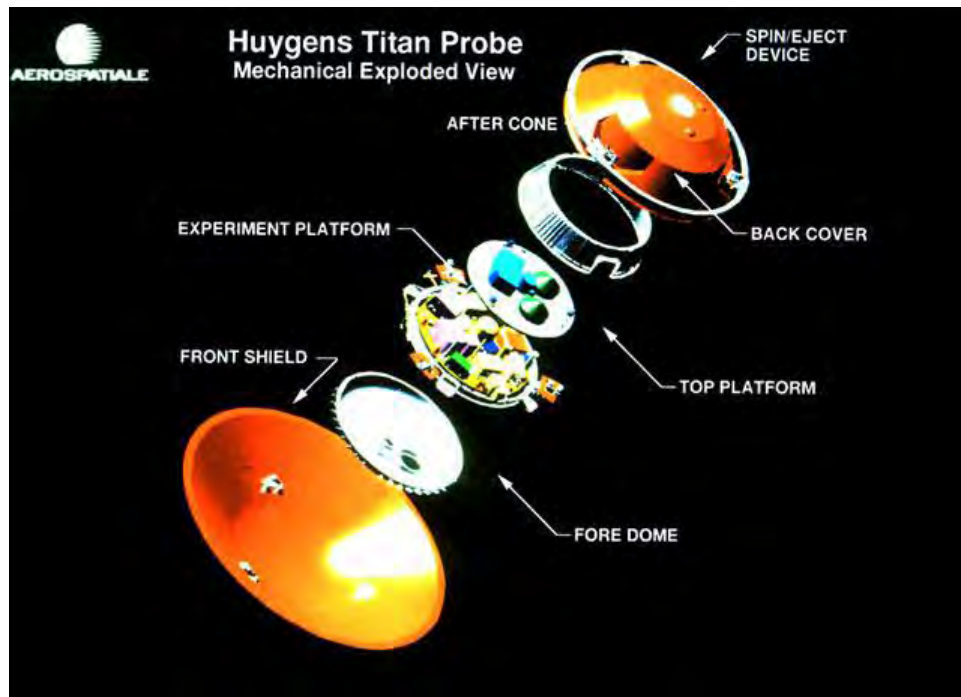
Saturn, the Huygens Probe was subjected to 16 in-flight checkouts to monitor the health of its subsystems and scientific instruments. The first link test in 2000 uncovered a flaw in the design of the Huygens telemetry receiver onboard the orbiter; this flaw would have resulted in the loss of the probe's scientific data during the actual mission at Titan. It was discovered that the Cassini receiver could not accommodate a large Doppler shift in the signal received from Huygens because of inappropriate parameters encoded into the Probe Support Avionics (PSA) firmware. The mission was redesigned to decrease the Doppler shift by increasing Cassini's altitude to 60,000 km at closest approach, rather than 1,200 km, replacing the first two planned orbits with three shorter ones. The Huygens mission was then executed in the third orbit, rather than the first.

Furthermore, the new trajectory allowed early orbiter observations of Titan's upper atmosphere in order to validate the atmospheric engineering model well before the probe release. This activity led to improvements in the knowledge of the structure and the composition of the upper atmosphere; in particular, it provided better constraints on the argon concentration and indicated that methane was not present in sufficient quantity to affect the probe entry.

The probe itself, shown in Figure 2.24, was designed as a descent module cocooned in a shell consisting of a 2.75 m diameter heat shield and a back cover. The heat shield and the back cover protected the enclosed descent module from the radiative and convective heat

fluxes generated during the entry into Titan's methane-rich, nitrogen atmosphere.

Figure 2.24: Main elements of the Huygens Probe.



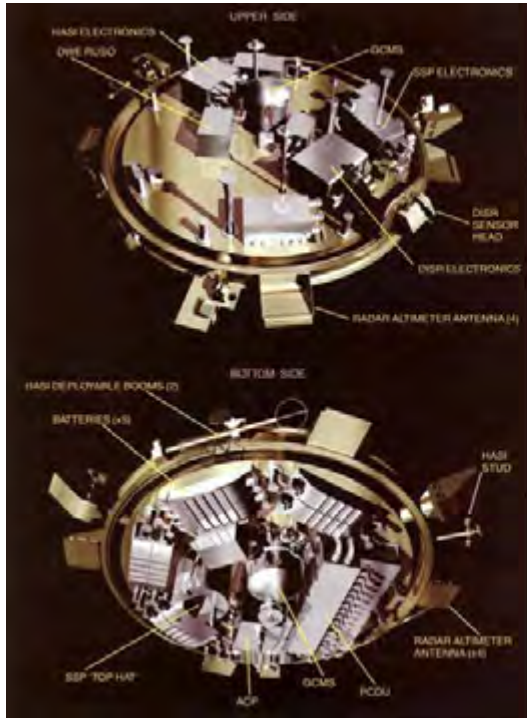
Descent Module

The descent module consisted of an aluminum inner shell containing the scientific instruments and servicing subsystems. The instruments and all the probe electronic equipment were distributed on two platforms: the main platform supporting most of the instruments, and the top platform supporting the container for both the main and the stabilizer chutes, the probe radio transmission antennae, and the mortar that deployed the pilot chute and then removed the back cover.

The inner structure of the descent module was coated with thick foam blankets to minimize convective cooling during the descent. The fore dome of the descent module was instrumented with a set of 36 spin vanes that used the aerodynamic interaction with the gas flow to force the probe to spin. The descent module was gas-tight, except for a single 6 cm² hole to equalize pressure during launch and descent to Titan's surface.

The layout of the descent module is shown in Figure 2.25. The spacecraft's instrument suite included an aerosol collector and pyrolyser, a decent imager/spectral radiometer, a Doppler wind experiment, a gas chromatograph/mass spectrometer, an atmospheric sensor suite, and a surface sensor suite.

Figure 2.25: Location of the scientific instruments in the Huygens Probe. The distributed battery system is shown in the bottom side. (Courtesy of ESA)



Huygens Instrument suite:

Huygens Atmospheric Structure Instrument (HASI):
measured physical and electrical properties of Titan's atmosphere

Gas Chromatograph Mass Spectrometer (GCMS):
identified and measured chemical species abundant in moon's atmosphere

Aerosol Collector and Pyrolyser (ACP):
drew in and analyzed atmospheric aerosol particles

Descent Imager/Spectral Radiometer (DISR):
imaged descent and investigated light levels

Doppler Wind Experiment (DWE):
studied direction and strength of Titan's winds

Surface-Science Package (SSP):
determined physical properties of moon's surface

Thermal Control

Surprisingly, before tolerating the cold temperature of Titan, the spacecraft design called for protection from high temperatures because the mission architecture included two Venus flybys, producing high solar heat. Although the probe, was partially protected by shadow of the high-gain antenna (HGA), when the orbiter, and thus the HGA, was off Sun-point for maneuvers or communication, the probe was protected by multilayer insulation (MLI) that burned off during the later atmospheric entry.

For thermal control, the probe used multiple layers of insulation and about 35 W of radioisotope heater units. Prior to separation, all power to the probe was provided by the Cassini orbiter. However, the probe's thermal subsystem (THSS) maintained all experiments and subsystem units within their allowed temperature ranges during all mission phases. In space, the THSS partially insulated the probe from the orbiter, ensuring only small variations in the probe's internal temperatures, despite the incident solar flux varying from 3800 W/m² (near Venus) to 17 W/m² (approaching Titan after 22 days of the coast phase following orbiter separation).

Probe thermal control was achieved by:

- MLI covering all external surfaces, except for the small “thermal window” of the Front Shield,
- 35 radioisotope heater units (RHUs) continuously providing about 1 W each even when the probe is dormant, and
- A white-painted 0.17 m² thin aluminum sheet on the front shield’s forward face acting as a controlled heat leak (about 8 W during cruise) to reduce the sensitivity of thermal performances to MLI efficiency.

The installation of the MLI layer is shown below in Figure 2.26. The MLI was burned and torn away during entry, leaving temperature control to the AQ60 high-temperature tiles on the front shield’s front face, and to Prosial on the front shield’s aft surface and on the back cover.

During the descent phase, thermal control was provided by foam insulation and gas-tight seals, preventing convection cooling by Titan’s cold atmosphere (70K at 45 km altitude) and therefore thermally decoupling the instruments from the cold aluminum shells.

Figure 2.26: Installation of the multilayer insulation (MLI) blanket on the Huygens Probe (Courtesy of ESA).



Thermal Protection System

The 79 kg, 2.7 m diameter, 60° half-angle coni-spherical front shield was designed to decelerate the probe in Titan’s upper atmosphere from about 6 km/s at entry to a velocity

equivalent to Mach 1.5 by 160 km altitude. Tiles of AQ60 ablative material, a felt of silica fibers reinforced by phenolic resin, provided protection against the entry's 1 MW/m² thermal flux. These AQ60 tiles were attached with CAF/730 adhesive to the honeycomb shell forming the front shield supporting structure. Prosial, a suspension of hollow silica spheres in silicon elastomer, was sprayed directly onto the aluminium structure of the front shield rear surfaces. Thermal fluxes at the front surface exceeded those at the rear by a factor of ten. After entry, the front shield was jettisoned.

The back cover protected the descent module during entry, ensured depressurisation during launch, and carried multilayer insulation (MLI) for the cruise and coast phases. Since it did not have to meet stringent aerothermodynamic requirements, it was constructed of a stiffened aluminum shell of minimal mass (11.4 kg) protected by Prosial (5 kg). The back cover included an access door for late access during integration and for forced-air ground cooling of the probe, a break-out patch through which the first drogue parachute was fired, and a labyrinth sealing joint with the front shield, providing a nonstructural thermal and particulate barrier.

Avionics

Huygens comprised the 318 kg probe and the 30 kg probe support equipment (PSE). Although a part of the Huygens system, the PSE remained attached to the Cassini orbiter after separation. It consisted of the avionics equipment that received and processed probe data for the Cassini orbiter solid-state recorders, for later transmission to Earth.

The Probe avionics system was organized in two branches, Channel A and Channel B, operating in active redundancy in handling payload data acquisition and formatting, and in the reception and recording of the data onboard Cassini. This architecture, designed for robustness, featured single-failure tolerance in the transmission of the acquired telemetry (including the science data), and in controlling the pre-entry, entry, and descent activities. Each of the two branches consisted of:

- One Command and Data Management Unit (CDMU) containing the onboard software that collected and formatted the telemetry, housekeeping and science data; autonomously controlled the mission activities according to the programmed timeline; and processed sensor (entry and spin measurement accelerometers, radar altimeters) data to support the probe autonomy and the operation of the science instruments during the entry and descent.
- One S-band (either 2040 or 2098 MHz) 12W RF transmitter, connected to a low-gain helical antenna transmitting the Huygens telemetry to Cassini. The telemetry rate of each branch was 8192 bps. On Channel A, the RF signal frequency was controlled by an ultrastable oscillator that was part of the Doppler Wind Experiment.
- One digital receiver in the PSE, amplifying and coherently demodulating the probe signal, then passing the data to the orbiter's Command and Data System via a MIL

1553 data bus. During the cruise phase, when the probe was attached to the orbiter, the RF signal was passed to the orbiter via the umbilical connection; during mission operations, the probe RF signal was received via the Cassini high-gain antenna, pointed toward the predicted Huygens location on Titan's surface.

Critical functions were implemented with triple redundancy; such functions included the probe wake-up function, performed by three mission timer units; and the deceleration measurement during atmospheric entry, monitored by three central acceleration sensor units. This approach allowed a safe detection of the 10 m/s^2 threshold on the falling edge of the deceleration profile to trigger the parachute sequence deployment and define the mission event time " t_0 ". To further increase the robustness of the mission, these critical functions were backed up by G(gravity)-switches and a software time-out function. Because all entry detection methods performed nominally, G-switches and the software time-out function were not used by the onboard computers to trigger the parachute deployment sequence.

Release from Cassini

The probe separated from the Cassini spacecraft on December 25, 2004, using the spring-loaded separation mechanism, called the spin eject device. This device provided a nominal relative separation velocity of 33 cm/s and a nominal spin of 7.5 rpm (viewed from the orbiter) to provide inertial stability during the ballistic trajectory and atmospheric entry. Following release, the probe had no maneuvering capability and functioned autonomously. After 20 days, Huygens arrived at the at the 1,270 km interface altitude on the predicted trajectory, triggering the sequence to turn on the batteries, the onboard computers, and the sensors and instruments according to the preprogrammed sequence.

Parachutes

The probe was not guaranteed to survive its impact on what was unknown terrain, but included instruments for characterizing any liquid medium in which it landed. Because of large uncertainties in the lateral distances the probe would cover during its descent under parachute, the coordinates of the predicted landing site were uncertain by several hundred kilometers.

Three parachutes controlled the descent of the probe through Titan's atmosphere, requiring knowledge of the aerodynamic conditions for deployment. The probe onboard computers processed the measurements from the accelerometers monitoring the probe's deceleration, autonomously determining the correct instant for parachute deployment.

The probe descended for 2 h 27 min 50 s, within the predicted duration (2 h 15 min \pm 15 min). Initially, the probe followed the nominal chronological sequence, with instrument operations defined by commands in the onboard mission timeline. Later, the onboard computers filtered measurements from two radar altimeters, providing redundancy to exclude erratic measurements at high altitude and provide reliable measured altitude information to the payload instruments. This allowed for optimization of the measurements during the

last part of the descent.

During entry, telemetry could not be transmitted by the probe until its back cover was removed. Ultimately, the probe landed safely with a vertical speed of about 5 m/s and continued thereafter to transmit data for at least another 3 h 14 min, as determined by monitoring the probe's 2.040 GHz carrier signal by the Earth-based radio telescopes. It is thought that the probe continued to function until the batteries were exhausted.

The Huygens landing site was found to have a sponge-like consistency, and data from the Huygens probe indicated that the surface of Titan likely has some liquid methane and heavier hydrocarbons (tholins) in the form of aerosols and/or rain, providing clearly seen river channels. The probe lasted several hours beyond its 2-hour postlanding mission design.

Anomalies

A number of anomalies were encountered during the mission and include the following:

- One of the receivers (channel B) was phase-locked and functioned properly. Channel A had an anomaly that was later identified as resulting from the unfortunate omission of the telecommand to apply power to the ultra-stable oscillator driving the channel A receiver. The loss of data on channel A was largely compensated by the flawless transmission on channel B and the fact that the Doppler Wind Experiment scientific objectives were largely met with data recovered from the Earth-based radio telescope observations.
- The probe arrived at the entry interface with the spin imparted at separation in the anti-clockwise direction. No significant spin modification was observed during the entry. The spin decreased more than expected under the main parachute and unexpectedly changed direction after 10 min. The probe continued spinning in the unexpected direction (clockwise) for the rest of the descent. No explanation was found for this behavior. The postflight verifications made from design documentation do not show evidence for incorrect design or implementation of the spin vanes.
- At the start of the descent, the inner probe temperature was about 7°C warmer than predicted. Two explanations exist for this anomaly:
 1. a lower-than-expected decrease of the inner temperature during the 20 days of coast; or
 2. a temperature increase exceeding predictions during the four-hour preheating.
- The descent was rather smooth under the main parachute, but rougher than anticipated during the first hour under the last parachute.

2.3.2 The Moon

During the 1960s and 1970s, both NASA and the Soviet space agency sponsored extensive lunar landing programs, with many missions surviving for several lunar nights. Survival times for robotic landed missions to the Moon are listed in Table 2.8.

Table 2.8: Survival times for robotic landed missions to the Moon.

Mission	Agency	Launch date	Status	Survival in Lunar days	Thermal management
Lunar Surveyor 1	NASA	1966	Completed	2	Electric heater [†]
Lunar Surveyor 2	NASA	1966	Failed	N/A	N/A
Lunar Surveyor 3	NASA	1967	Completed	1	Electric heater
Lunar Surveyor 4	NASA	1967	Failed	N/A	N/A
Lunar Surveyor 5	NASA	1967	Completed	4	Electric heater
Lunar Surveyor 6	NASA	1966	Completed	1	Electric heater
Lunar Surveyor 7	NASA	1966	Completed	2	Electric heater
Lunokhod 1	Soviet SA	1971	Completed	11	RTG [‡]
Lunokhod 2	Soviet SA	1973	Completed	3	RTG

[†] Two compartments equipped with superinsulating blankets were heated, as described fully in the text. These were similar in concept to the warm electronics box (WEB) architecture described in detail for spacecraft for Mars.

[‡] Polonium-210 radioisotope thermal generator (RTG).

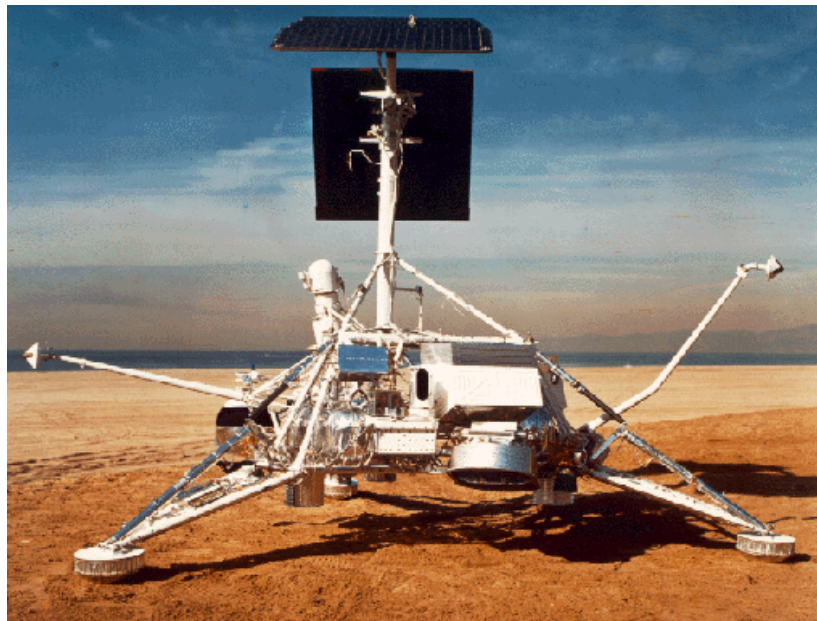
Lunar Surveyors

The NASA Lunar Surveyor missions, operated in 1966–1968, were designed to obtain close-up images of the lunar surface and to determine if the terrain was safe for manned landings. Although the Surveyor 2 and 4 missions failed, the remaining five spacecraft landed successfully and transmitted images from onboard television cameras. Surveyors 3 and 7 also each carried a soil mechanics surface sampler scoop to dig trenches and conduct soil mechanics tests, while Surveyors 5, 6, and 7 had magnets attached to the footpads and an alpha scattering instrument for chemical analysis of the lunar material.

Throughout the series, the Surveyor craft survived 1–4 lunar days. Thermal control was achieved by a combination of white paint, high IR-emittance thermal finish, and a polished aluminum underside. Two thermally controlled compartments, equipped with superinsulating blankets, conductive heat paths, thermal switches and small electric heaters, were mounted on the spacecraft structure. One compartment, held at 5–50°C, housed communications and power supply electronics. The other, held between –20°C and 50°C, housed the command and signal processing components. The TV survey camera was mounted near the top of the tripod and strain gauges, temperature sensors, and other engineering instruments

are incorporated throughout the spacecraft. A picture of the Surveyor spacecraft is shown below in Figure 2.27.

Figure 2.27: One of the Lunar Surveyor spacecraft.



Surveyor 1

Surveyor 1 was launched on May 30, 1966, and landed on June 2, 1966. The first hour on the Moon was spent performing engineering tests. Photography sessions were then initiated throughout the remainder of the lunar day. The television system acquired over 10,000 images prior to nightfall on June 14. The spacecraft also acquired data on the radar reflectivity of the lunar surface, bearing strength of the lunar surface, and spacecraft temperatures for use in the analysis of the lunar surface temperatures. Surveyor 1 was able to withstand the first lunar night and near high noon on its second lunar day, July 7, photos again were returned. After transmitting an additional 1,000 photographs, Surveyor 1's mission was terminated due to a dramatic drop in battery voltage just after sunset on July 13, 1966. Engineering interrogations continued until January 7, 1967. All mission objectives were accomplished.

Surveyor 2

Surveyor 2 was launched on September 20, 1966. During the midcourse maneuver, one vernier engine failed to ignite, resulting in an unbalanced thrust that caused the spacecraft to tumble. Attempts to salvage the mission failed.

Surveyor 3

Surveyor 3 was launched on April 17, 1967, and landed on April 20, 1967. Surveyor 3 was similar in design to Surveyors 1 and 2 but had several changes in the payload. Like the earlier Surveyor craft, Surveyor 3 carried soil mechanics experiments, and devices to measure temperature and radar reflectivity, but the television camera was improved. Furthermore, a surface sampler replaced the approach television camera. Two flat auxiliary mirrors were attached to the frame to provide the camera with a view of the ground beneath the engines and one of the footpads.

Initial photos were received within an hour of landing and the surface sampler was used two days later. Surveyor operated throughout the lunar day until after local sunset on May 3. The lunar sampler was operated for a total of 18 hr, 22 min, digging trenches as deep as 18 cm, and the television camera returned 6,326 pictures, transmitting information on the strength, texture, and structure of lunar material. Images of an eclipse of the Sun by the Earth and related thermal measurements were recorded. The last data were returned on May 4, 1967, and Surveyor 3 failed to come back to life following the first lunar night.

Surveyor 4

The payload of Surveyor 4 included a television camera and auxiliary mirrors, a soil mechanics surface sampler, strain gauges on the spacecraft landing legs, and numerous engineering sensors. Surveyor 4 launched on July 14, 1967. After a flawless flight to the moon, radio signals from the spacecraft ceased during the terminal-descent phase, approximately 2.5 min before touchdown on July 17, 1967. Contact with the spacecraft was never reestablished, and the mission was unsuccessful.

Surveyor 5

Surveyor 5 was launched on September 8, 1967, and touched down on the lunar surface on September 11, 1967. All experiments were performed successfully. Surveyor 5 returned 18,006 television pictures during its first lunar day. The alpha-scattering instrument was deployed and performed the first in situ analysis of an extraterrestrial body, returning 83 hours of data on lunar soil composition during the first lunar day. The spacecraft shut down from September 24 to October 15, 1967, over the first lunar night.

An additional 1048 pictures and 22 hours of alpha-scattering data were received during the second lunar day. On October 18, Surveyor 5 acquired thermal data during a total eclipse of the Sun. Transmissions for the second day were received until November 1, 1967, when shutdown for the second lunar night occurred about 200 hours after sunset. Transmissions were resumed on the third and fourth lunar days, with the final transmission occurring on December 17, 1967. Nearly 20,000 photographs were collected over the first, second, and fourth lunar days.

Surveyor 6

Surveyor 6 was nearly identical to Surveyor 5, with the exception of new polarizing fil-

ters on the TV camera, a different type of glare hood, and 3 auxiliary mirrors instead of 2. Surveyor 6 launched on November 7, 1967, and touched down on the lunar surface on November 10, 1967. On November 17, the vernier engines were fired for 2.5 seconds, causing Surveyor to lift off the lunar surface 3 to 4 meters and land about 2.4 meters west of its original position. This lunar “hop” represented the first powered takeoff from the lunar surface and furnished new information on the effects of firing rocket engines on the Moon, allowed viewing of the original landing site, and provided a baseline for stereoscopic viewing and photogrammetric mapping of the surrounding terrain. The mission transmitted images until a few hours after sunset on November 24, returning a total of 29,952 images. The alpha-scattering experiment acquired 30 hours of data on the surface material.

The spacecraft was placed into hibernation for the lunar night on November 26. Contact with the spacecraft was resumed on December 14 for a short period, but no useful data were returned and the last transmission was received on December 14, 1967.

Surveyor 7

Surveyor 7 was launched on January 7, 1968, and landed on January 10, 1968. Science operations commenced shortly after landing. The TV camera returned 20,993 pictures on the first lunar day. The alpha-scattering instrument failed to deploy fully, but the surface sampler was used to force it to the ground; later, the sampler set the alpha-scattering instrument on a rock and then into a trench it had dug. Approximately 66 hours of alpha-scattering data were obtained during the first lunar day on the three sites. Operations were continued after sunset and included pictures of the Earth, stars, and the solar corona. Operation was terminated on January 26, 80 hours after sunset. Second lunar day operations began on February 12, 1968, and included an additional 45 pictures for a total of 21,038 and 34 hours of alpha-scattering data from inside the trench. Operations were terminated on February 21. The lunar surface sampler operated flawlessly for a total of 36 hours, 21 minutes, digging trenches and moving and manipulating four rocks.

Lunokhod Rovers

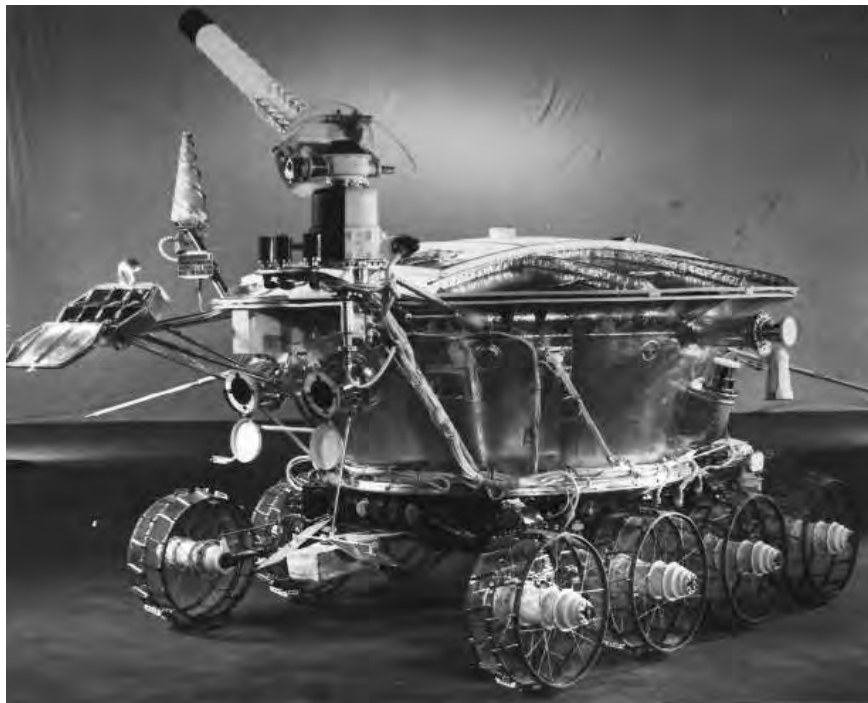
The most long-lived lunar missions were the Soviet Lunokod 1 and 2 rovers, flown in 1971 and 1973; these survived 11 and 4 lunar days and covered 10 and 37 km, respectively. These rovers used polonium-210 radioisotopic heat sources for nighttime thermal management, and a solar/battery hybrid power system for daytime activities. The lander-rover systems had a total mass of 1814 kg, approximately half of which was the 840 kg rovers. These rovers moved at speeds up to 2 km/hr, with instruments including a soil mechanics tester, solar X-ray experiment, an astrophotometer to measure visible and UV light levels, a magnetometer deployed in front of the rover on the end of a 2.5 m boom, a radiometer, a photodetector for laser detection experiments, and a laser corner-reflector.

Lunokhod 1

As shown in Figure 2.28, Lunokhod 1 was a lunar vehicle formed of a tub-like compartment with a large convex lid on eight independently powered wheels. Lunokhod 1 was equipped

with a cone-shaped antenna, a highly directional helical antenna, four television cameras, and special extendable devices to impact the lunar soil for soil density and mechanical property tests. An X-ray spectrometer, an X-ray telescope, cosmic-ray detectors, and a laser device were also included. The vehicle was powered by a solar cell array mounted on the underside of the lid. Lunokhod 1 was intended to operate through three lunar days but actually operated for 11 lunar days, ceasing operations on October 4, 1971. Lunokhod had traveled more than 10 km, transmitting more than 20,000 television pictures and conducting more than 500 lunar soil tests.

Figure 2.28: One of the Lunar Surveyor Spacecraft.



Lunokhod 2

Lunokhod 2 was equipped with three TV cameras returning images to Earth, where a team of controllers sent driving commands to the rover in real time. There were 4 panoramic cameras mounted on the rover. Scientific instruments included a soil mechanics tester, solar X-ray experiment, an astrophotometer to measure visible and UV light levels, a magnetometer deployed in front of the rover on the end of a 2.5 m boom, a radiometer, a photodetector (Rubin-1) for laser detection experiments, and a French-supplied laser corner-reflector. The lander and rover together weighed 1814 kg.

Power was supplied by a solar panel on the inside of a round hinged lid that covered the

instrument bay, which charged the batteries when opened. A polonium–210 isotopic heat source was used to keep the rover warm during the lunar nights. The rover would run during the lunar day, stopping occasionally to recharge its batteries via the solar panels. At night the rover would hibernate until the next sunrise, heated by the radioactive source. Lunokhod 2 operated for about 4 months, covered 37 km of terrain including hilly upland areas and rilles, and sent back 86 panoramic images and over 80,000 TV pictures. Many mechanical tests of the surface, laser ranging measurements, and other experiments were completed during this time. On June 4 it was announced that the program was completed, leading to speculation that the vehicle probably failed in mid-May or could not be revived after the lunar night of May–June. A sudden failure was suggested by the fact that the Lunokhod was left in a position such that the laser retroreflector could be not used.

2.3.3 Mars

After an early attempt by the Soviet space agency to place a lander on Mars, NASA has launched five successful in situ Mars missions to date that have experienced thermal cycling environments with diurnal variations of -120°C to $+20^{\circ}\text{C}$, beginning with the two Viking landers that collected science data for several years in the 1970s. Landed Mars missions are summarized in Table 2.9.

Table 2.9: Survival times for past landed missions to Mars.

Mission	Agency	Launch date	Status	Surface time	Thermal control
Mars 3	Soviet SA	1971	20 seconds	N/A	Radiators
Viking 1	NASA	1975	79 months	Yes	RTG
Viking 2	NASA	1975	43 months	Yes	RTG
Mars Pathfinder Rover	NASA	1996	6 months	Yes	WEB, radiators
Mars Polar Lander	NASA	1999	Failed	Yes	Thermal enclosure
Mars Exploration Rover–A (Spirit)	NASA	2003	30 months (ongoing)	Yes	WEB, radiators
Mars Exploration Rover–B (Opportunity)	NASA	2003	30 months (ongoing)	Yes	WEB, radiators

Mars 3

The Soviet lander Mars 3, launched on May 28, 1971, was the first spacecraft to make a successful soft landing on Mars. It was powered by batteries charged by the orbiter prior to separation. Temperature control was maintained through thermal insulation and a system

of radiators. On December 2, 1971, Mars 3 impacted the surface, the four petal shaped covers opened and the capsule began transmitting to the Mars 3 orbiter 90 seconds after landing. After 20 seconds, transmission stopped for unknown reasons and no further signals were received at Earth from the surface.

It is not known whether the fault originated with the lander or the communications relay on the orbiter. A partial panoramic image returned showed no detail and a very low illumination of 50 lux. The cause of the failure may have been related to the extremely powerful dust storm taking place at the time, possibly inducing a coronal discharge that damaged the communications system. The dust storm would also explain the poor image lighting.

Viking

The Viking project consisted of launches of two separate spacecraft to Mars, Viking 1, launched on August 20, 1975, and Viking 2, launched on September 9, 1975. Each spacecraft consisted of an orbiter and a lander. Power was provided by two plutonium-238 radioisotope thermal generator (RTG) units affixed to opposite sides of the lander base and covered by wind screens. Each generator had a mass of 13.6 kg and provided 30 W continuous power at 4.4 volts. Four wet-cell sealed nickel-cadmium 8 Ah, 28 V rechargeable batteries were also onboard to handle peak power loads.

Viking 1

The Viking 1 lander touched down on July 20, 1976. Transmission of the first surface image began 25 seconds after landing. The seismometer failed to uncage, and a sampler arm locking pin was stuck and took 5 days to shake out. Otherwise, all experiments functioned nominally. It operated for 79 months until November 13, 1982, when a faulty command sent by ground control resulted in loss of contact.

Viking 2

The Viking 2 lander touched down on September 3, 1976. The cameras began taking images immediately after landing. The Viking 2 lander operated on the surface for 1281 Mars days, or 43 months, and was turned off on April 11, 1980, when its batteries failed.

Mars Pathfinder

Mars Pathfinder, the first NASA mission to Mars to use an airbag landing system, was conceived primarily as a technology flight experiment. It was launched on December 4, 1996 and landed on July 4, 1997. Over 2.5 m^2 of solar cells on the lander petals, in combination with rechargeable batteries, powered the lander. The Sojourner rover (Figure 2.29) was powered by 0.2 m^2 of solar cells, providing energy for several hours of operations per sol. Nonrechargeable lithium thionyl chloride (LiSOCl_2) D-cell batteries provided backup. All rover communications were done through the lander. Images were taken and experiments performed by the lander and rover until September 27, 1997, when communications were lost for unknown reasons.

Figure 2.29: The Sojourner rover from Mars Pathfinder.



Mars Polar Lander

The Mars Polar Lander employed the three-legged landing architecture used by Viking, but with solar array power. It was to touch down on the southern polar layered terrain near the edge of the carbon dioxide ice cap in Mars' late southern spring, with mission objectives of recording local meteorology, analyzing samples of the polar environment, and performing imaging and spectral analysis of the environment. Attached to the lander spacecraft were a pair of small probes, the Deep Space 2 Mars Microprobes, to be deployed to fall and penetrate beneath the surface when the spacecraft reached Mars.

The mission was launched on January 3, 1999, and reached Mars on December 3, 1999. Unfortunately, communication ceased for unknown reasons and it is not known if any of the final mission stages were successfully executed. The failure was not a consequence of environmental effects.

Because the Mars Polar Lander was intended to reach the polar region, with an estimated ambient temperature at landing of -72°C , the avionics were located inside a thermal enclosure that provided protection for the electronics and temperature control to keep them operating at temperatures of -15°C to $+10^{\circ}\text{C}$. The layout of the lander and the thermal enclosure are shown in Figure 2.30. The DS-2 probes were mounted in their own aeroshells on the side of the spacecraft, as shown in Figure 2.31.

The two probes each were contained in independent aeroshells with thermal protection.

Figure 2.30: Mars Polar Lander Flight System, showing lander thermal enclosure.

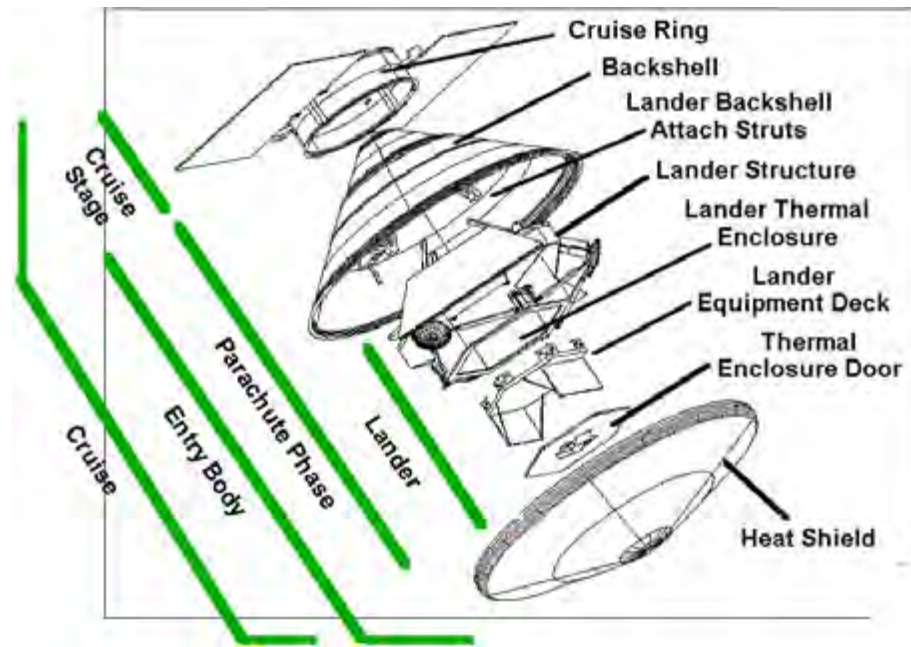
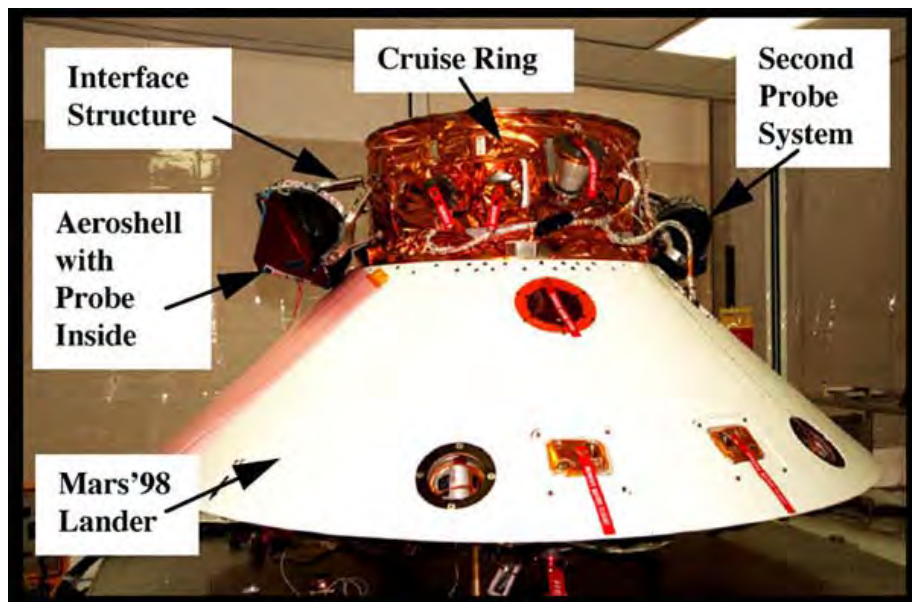
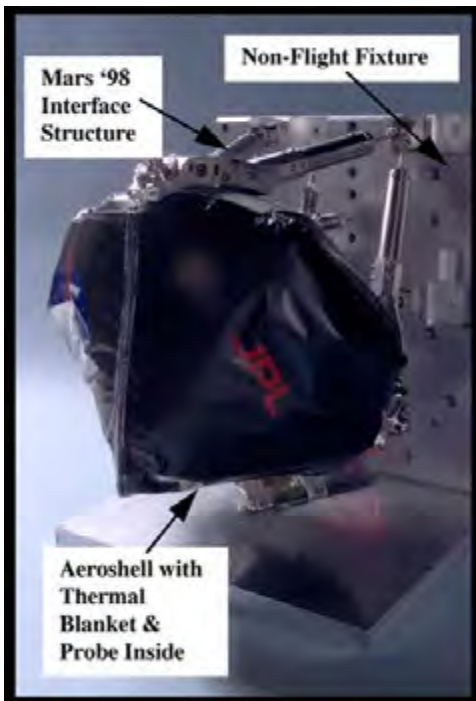


Figure 2.31: Mars Polar Lander spacecraft, with both DS-2 aeroshells mounted in place.



When the Mars Polar Lander spacecraft separated from its cruise ring, the Deep Space 2 interface structure was to initiate the aeroshell release sequence. Each aeroshell contained its own thermal blanket, as shown in Figure 2.32.

Figure 2.32: Deep Space 2 architecture with thermal protection and probe.

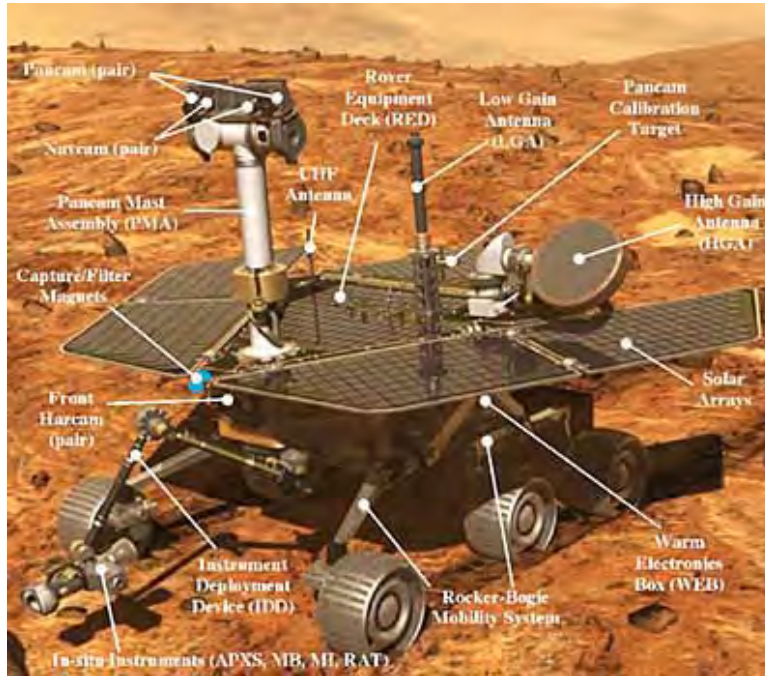


Mars Exploration Rovers

The Mars Exploration Rover mission (MER) comprised two identical landers, MER-A (known as “Spirit”), and MER-B (known as “Opportunity”). Spirit was launched on June 10, 2003, and landed on January 4, 2004, while Opportunity was launched on July 7, 2003, and landed on January 25, 2004. At the time of publication of this document, these two rovers were still operational.

In each rover, power is provided by the solar arrays, generating up to 140 W of power under full Sun conditions. The energy is stored in two rechargeable batteries. These more recent missions utilized a centralized system architecture to house all of the electronics and batteries in a thermally controlled (-40°C to $+40^{\circ}\text{C}$) warm electronics box (WEB), heated by a plutonium radioisotope heating unit and resistive heating units. Thermal control is achieved through the use of gold paint, aerogel insulation, heaters, thermostats, and radiators. The WEB’s placement in the rover is shown in Figure 2.33.

Figure 2.33: Location of the warm electronics box (WEB) in the Mars Exploration Rover.



This design connects the WEB electronics to the extremities of the system and ultimately results in an extremely complex wiring harness, consisting of tens of hundreds of total wire length. Integration is thus tedious, timely, and costly, particularly because any fault in the harness requires that the entire system be completely de-integrated for debugging. One photograph contained in Figure 2.34 shows the connections between the six controllers and the connections to the rover motors; these controllers are protected inside the WEB. The second photograph demonstrates the additional integration and test cabling from the WEB to the peripherals. This architecture is clearly limited physically and will not be feasible for more capable rover systems.

2.4 High Radiation

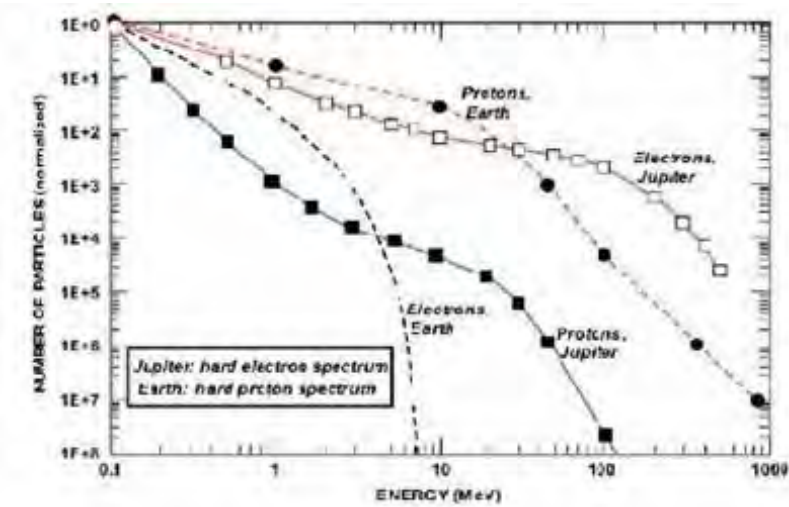
The environment surrounding Jupiter has an unusually strong magnetic field; in addition, it appears that this field has a strong quadrupole moment, giving it an unusual spatial shape. As a result of this field, particles ejected by the solar wind, such as electrons and protons, may be captured by this strong field and given additional energy. This phenomenon produces a strong radiation field around Jupiter. In addition to the energetic light particles, heavier ions have also been measured; it is possible that this flux is related to volcanic eruptions from Io.

Figure 2.34: Implementation of the MER warm electronics box (WEB).



Unlike Earth's Van Allen belts, comprising high-energy (up to 1 GeV) protons and lower energy (1–8 MeV) electrons, the radiation environment at Jupiter shows significant fluxes of much higher energy electrons (up to 500 MeV), and lower energy protons (up to 100 MeV). The spectra of electrons and protons are shown in Figure 2.35.

Figure 2.35: Radiation spectra at Earth and at Jupiter.



Early measurements were conducted by the Pioneer 10, 11, and Voyager spacecraft. These

spacecraft executed Jupiter flybys, collecting valuable but limited data on the temporal and spatial extent of the radiation. These data were integrated into the initial model used in developing Galileo, the spacecraft launched in 1989 to orbit Jupiter in 11 passes.

Subsequently, the Galileo data have been used to develop a new model with better spatial, temporal, and spectral fidelity. This new model, known as the Divine–Garrett radiation model, describes the environment more completely. The radiation environment at Jupiter is dominated by electrons ranging up to 500 MeV in energy, with some proton flux up to approximately 20 MeV, as well. Earth’s Van Allen belts, in contrast, are dominated by protons of only 100 MeV maximum energy, with electrons showing very little strength after 7 MeV. Because our general understanding of the impact of radiation on electronics is driven by experience near Earth, we have not yet developed the capability to fully understand the implications of the radiation and subsequently protect against such high fluxes and high energies of incident electrons.

2.4.1 Galileo

The Galileo spacecraft was launched in 1989 and injected into the orbit around Jupiter in December, 1995. The spacecraft was designed for a prime mission of 11 orbits extending over two years but survived far beyond its designed lifetime, completing 34 orbits. When the onboard propellant was nearly depleted and remote control would no longer be possible, mission engineers directed the spacecraft to impact with Jupiter. On September 21, 2003, the Galileo spacecraft entered the Jovian atmosphere, where it ultimately disintegrated.

Because Galileo did not carry a dosimeter, doses at various points in time could only be estimated. Furthermore, while Galileo was not intended to operate as a laboratory, testing its own tolerance to radiation, several science detectors provided information regarding ambient radiation levels for off-line correlation studies of detector responses. The following detectors collected radiation data:

- Energetic Particle Detector (EPD): detected electrons from 15 keV to 11 MeV, and protons and ions from 20 keV to 55 MeV
- Heavy Ion Counter: detected ions from 6 to 200 MeV/nucleon
- Star Scanner: Photomultiplier tube was calibrated with EPD to measure the flux of electrons with energies exceeding 1.5 MeV

Shielding Architecture

Most of the spacecraft was designed to a radiation design margin (RDM) of 2 for both electrons and protons. Electronics were generally placed within an equivalent shielding of at least 2.2 g/cm^2 (approximately 300 mils of aluminum). In addition, spot shielding was

used to protect particularly valuable subsystems, such as tantalum boxes for instrument sensors and tungsten cylinders surrounding photomultiplier tubes. Two instruments utilizing this shielding were the Solid-State Imaging (SSI) system and the Extreme Ultraviolet Spectrometer (EUVS). Schematics of these two instruments are shown in Figures 2.36 and 2.37.

Figure 2.36: Schematic of the Solid-State Imaging system on Galileo, including tantalum radiation shielding.

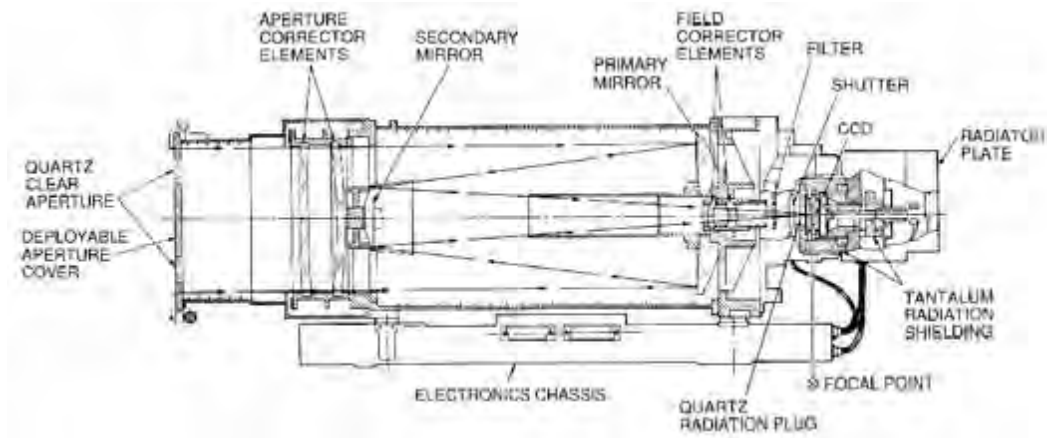
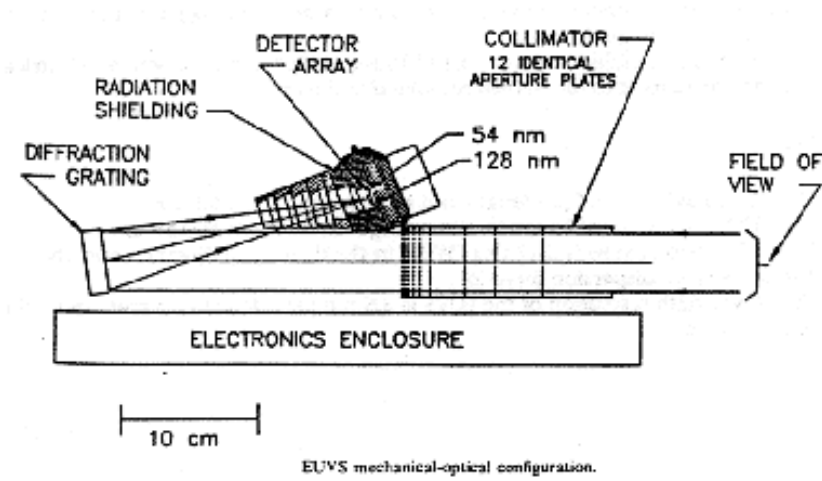


Figure 2.37: Schematic of the Extreme Ultraviolet Spectrometer on Galileo, including radiation shielding.



Observed Failure Modes

According to the Divine–Garrett model, the total ionizing dose (TID) behind the 300 mils aluminum shield was expected to reach 150 krad(Si)² at the end of the prime mission. In December 1997, Galileo began extended mission operations and by the end of the mission, the estimated TID reached 600 krad(Si) behind 300 mils of aluminum.

This extended exposure led to a number of failures in the subsystems and instruments on the Galileo spacecraft. These failure modes are detailed below. Table 2.10 lists the failure modes in the communications system and Table 2.11 identifies failures in the Attitude Control System.

Table 2.10: Radiation-induced failure modes in the avionics and communications systems on the Galileo orbiter.

Element	Failure	Cause	Consequence	Recovery
Tape recorder	Recorder will not play data back	Radiation damage to GaAs LED located in the drive electronics of the tape recorder's motor encoder wheel	Loss of science data	“Annealing” of radiation-induced defects in LEDs by passing the current. Recorder could operate for up to an hour at a time after recovery.
Ultra-stable oscillator	Frequency change during passing through radiation belt	Changes in properties of dielectric capacitor induced by electron flux	DSN failure to find the downlink, loss of science data	Galileo project learned to predict the expected frequency jump
S-band antenna	S-band phase dispersion, phase error	Electron radiation	Lost telemetry	De-weight or remove telemetry data when noise observed
Voltage controlled oscillator	Frequency jumps	Amplifier failure	Loss of downlink data	Passing electrical current through device to neutralize ions

²A krad(Si) is a unit of energy absorbed by silicon from radiation. It is equivalent to 0.01 J/kg

Table 2.11: Radiation-induced failure modes in elements of the Attitude Control System on the Galileo orbiter.

Element	Failure	Cause	Consequence	Recovery
Spin detector	Increase in noise level in detector electronics	Specific failed parts not known	Is only needed with single-star detection mode	Spacecraft used other source of spin data
Spin-Bearing Assembly	Spurious signals generated in a pair of sliprings throughout the mission	Radiation induced electromagnetic pulse-charge built-up in insulators	Power on reset condition leading to safing — total loss of science in 16, 18, 27, and 33rd orbit	Flight control re-programmed software to bypass safing routine if a bus reset indication was seen
Star Scanner	False star identification in E12 due to radiation noise in photomultiplier tube	Radiation noise	Rapid correction of platform pointing, science loss	During primary mission: use of gyroscope; after gyroscope failure: rely on single-star mode
Gyroscope	Defective outputs beginning in 9th orbit	Leaking p-n junction in DG-181 solid-state switch	Spacecraft in an unknown attitude, loss of science	Turning off gyro electronics throughout periapsis pass (radiation annealing with no bias)

Returned science was also compromised by failures in various instruments. Table 2.12 lists the failure modes for imaging instruments, while Table 2.13 lists failure modes for particle and magnetic flux instruments.

An additional major malfunction, unrelated to radiation, occurred when Galileo's high-gain antenna failed to fully deploy after the spacecraft's first flyby of Earth. Despite attempts to generate thermal cycling in the antenna motors by turning them on and off over 13,000 times, the antenna failed to open. The low-gain antenna was used to transmit the data to Earth for the duration of the mission. In order to increase the data throughput, advanced data compression techniques were implemented and the sensitivity of receivers in the Deep Space Network was upgraded. Although the mission was successful, the associated reduction in available bandwidth significantly limited the amount of returned data, particularly

Table 2.12: Radiation-induced failure modes in imaging instruments on the Galileo orbiter.

Failure mode	Cause	Consequence	Recovery
Near infrared spectrometer			
Started reporting noisy data at the Callisto orbit	Designed to take less than 10krad (Si) during primary mission (was protected in 3 mm tantalum enclosure)	Some science data loss	None
Memory resets in 100 krad Si gate CMOS RAM	Radiation related but not well understood	Some science data loss	None
Solid state imager			
White images	Failed dual FET due to lack of proper grounding. Only 30 mil shield	Many tens of images lost	Power cycling
Summation mode failure-started at C22	Radiation at periapsis	Scrambled images	New algorithm required to de-scramble images
Noise in CCDs	Hot pixels due to neutrons from RTGs and RHUs	Increased down-link time due to difficulties in compressing noisy images	None
Photopolarimeter			
The lithium tantalate pyroelectric detector records increased noise; spikes near Jupiter periapsis	No detailed analysis	Some science data loss	None
Ultraviolet spectrometer			
Total failure in grating encoder after C22; problems started at C19	Either GaAs IR LED or section of Si solar cell used as receiver failed due to radiation	The only instrument totally lost to Galileo	None

Table 2.13: Radiation-induced failure modes in particle, dust, and magnetic field detectors on the Galileo orbiter.

Failure mode	Cause	Consequence	Recovery
Energetic particle detector			
Microprocessor lockup six times (E12, E16, C22, I25, E26, C30)	Not clear—could be SEU or ESD related	Loss of data	New strategy to automatically power cycle and reload instrument
Sensitivity loss	TID (total ionizing dose)	Some science loss	Point detector away from calibration source while not taking data
Loss of Jb detector (one of two detectors measuring delta-E)	Build up of the dead layer on detector due to radiation	Ion energy loss data unobtainable	Project used predicted star intensity to eliminate false data
Dust detector			
Subsystem experienced increased noise during the first orbit and increased towards periapsis	Suspected electron radiation	Some science data loss	None
Magnetometer			
Processor lock-up	Memory chip radiation problem	Loss of data	Power cycles followed by memory reloads

by reducing the number of returned images.

Lessons Learned.

The experience with Galileo provided a great deal of insight on the details of the radiation environment around Jupiter, as well as on mitigation strategies. Some of the key insights are the following:

- The Galileo spacecraft suffered through a range of system failures traced to radiation.

- Several of these failures could have been mission-terminating, but spacecraft architecture and software allowed for in-flight reconfiguration.
- Because Galileo did not carry a dosimeter, the total dose could only be modeled or/and estimated.
- Mission architects benefited from the elliptical orbits of Galileo because they had several months to identify and address each failure before each periapsis.
- Evidence of electrostatic charging was seen twice, with both failures due to spacecraft design deficiency.
- Both temporary and permanent degradation of instrument SNRs (signal-to-noise ratios) due to particle flux was observed. While data quality was sometimes degraded, no instrument was rendered unusable by noise.
- The spacecraft design was robust against single-event upsets (SEUs).
- The “Chicken Mode” scheme — where components stay behind the shield most of the time — provide extra shielding for sensitive components or detectors, effectively minimizing radiation degradation in some instances.
- A unique spike in radiation flux occurred during the C22 periapsis, causing many problems. Data suggest that this occurred when the spacecraft and Io were at the same longitude and that it might have been related to volcanic activity on Io. Therefore, monitoring Io activity from a ground- or space-based infrared observatory may allow radiation “weather prediction” to help with future operation at Jupiter or Europa; for instance, critical electronics or detectors could be turned off prior to a rise in radiation levels.

3 Mission Impact of Extreme Environment Technologies

In order to prioritize the technology investment areas, it is necessary to understand NASA planning activities and the mission concepts currently under consideration. This chapter describes the mission planning process, then focuses on the missions called for in the roadmaps in the Science Mission Directorate.

3.1 NASA planning activities

The Solar System Exploration Decadal Survey by the National Research Council (NRC) of the National Academies summarized the current state-of-knowledge of the Universe and identified key science goals, objectives and priorities for future explorations. It also identified the understanding of our Solar System's formation as one of the highest priority science objectives.

In response to the NRC recommendations, Solar System Exploration (SSE) pathways were identified in the Vision for Space Exploration. The pathways included the Moon, Mars, the Solar System and beyond. To implement this plan, NASA's Advanced Planning and Integration Office (APIO) established two sets of teams in fiscal year FY05, with one focusing on strategic goals and the other, on capability goals. The teams addressed activities performed within the Science Mission Directorate (SMD) and Exploration Systems Mission Directorate (ESMD). These roadmap studies were completed by May 2005, with the conclusions for Solar System Exploration documented in the SRM-3 report.

Subsequently, NASA's Administrator initiated the Exploration Systems Architecture Study (ESAS) to further refine future plans related to ESMD. The SRM-3 document was updated and expanded in 2006, with a revised NASA Roadmap for SSE. Science advisory groups, such as the Outer Planets Advisory Group (OPAG), the Venus Exploration Assessment Group (VEXAG), and the Lunar Exploration Assessment Group (LEAG), provide further science input to NASA.

In support of the above activities, relevant missions were compiled into Design Reference Mission (DRM) sets. These in turn provide the current best estimates for missions and associated requirements under consideration for up to the next three decades. This chapter discusses a subset of the DRMs under NASA's Science Missions Directorate (SMD), with a special focus on Solar System Exploration. These missions are then grouped according to the extreme environments they would encounter, in order to discuss the associated enabling or enhancing technologies.

3.2 Overview of Science Missions Directorate Missions

SMD's primary objective is to implement a set of science-driven strategic and competitive missions. Planning for these missions takes place for many years and even decades in advance. Strategic missions are usually directed and larger in their scope, while smaller mis-

sions are competitive and selected through periodic Announcements of Opportunity (AO).

Technology planning for directed missions is reasonably well defined and the mission impacts are comparatively straightforward to discern; on the other hand, competitive missions are only planned a few opportunities ahead, translating sometimes to five years or less of planning. Missions under the small (Discovery and Mars Scout) and medium (New Frontiers) classes are also cost-capped, providing other limitations to technology development. Therefore, technology development plans for these smaller missions are harder to forecast.

SMD missions, both under the Mars Exploration Program (MEP) and Solar System Exploration (SSE) Program, can be significantly affected by exposure to extreme environments. In addition to these planning efforts, ESMD is developing plans for robotic and manned missions to the Moon and subsequently to Mars. While these ESMD plans are still in a formulation phase, it is expected that although they may also benefit from this technology development, these missions are out of the scope of this report.

3.2.1 Mars Exploration Program

The Mars Exploration Program is governed by four goals, established by the Mars Exploration Program Analysis Group (MEPAG). These goals are:

1. Determining if life ever arose or currently exists on Mars;
2. Understanding the process and history of climate on Mars;
3. Determining the evolution of the surface and interior of Mars; and
4. Preparing for human exploration.

It also addresses recommendations by the NRC, provided in the SSE Decadal Survey.

The first three goals are science driven, while the fourth is primarily technology focused. All of these may be translated into a number of robotic and human precursor missions, leading to a possible human landed mission by around 2035 (see Table 3.1). While the order of these missions could change from the current model, it is anticipated that similar mission types would be required to address the four MEPAG goals, programmatic and budgetary considerations. Therefore, this report briefly discusses potential next-decade Mars exploration missions and the associated options and technology implementation.

Current missions in flight or in advanced development phases include the Mars Reconnaissance Orbiter (MRO), the Phoenix lander and the Mars Science Laboratory (MSL) rover. The Mars Exploration Program is currently in a preplanning phase to define missions for the next decade beyond MSL (i.e., for the 2010 to 2020 timeframe). The final program is expected by the end of FY06, and would include a mixture of Large, Moderate, and Small missions, with cost caps shown in Table 3.2.

Table 3.1: Mars mission classes and estimated cost caps.

Mission class	Cost cap (\$M FY06)
Mars Scout	475
Moderate	750
Large	1,000
Large Flagship	Several 1,000

Table 3.2: Proposed Design Reference Mission set for Mars exploration.

Selected & Potential Mission Concepts	Mission Class	Earliest Launch
Mars Orbiters (MRO and MSO)	Moderate/Large	2005 & 2013
Mars Phoenix	Scout	2007
Mars Science Laboratory (MSL)	Large	2009
Scouts (small missions)	Scout	2011 & 2018
Mars Multi-Lander Network	Moderate/Large	2020
Mars Astrobiology Field Lab (AFL) rover Large	2016 or 2018	
Mars Sample Return (MSR)	Flagship	Third decade
MSR Mid-rover (MER / sub-MER class)	Scout to Large	2016 or 2018
Mars Deep Drill	Large	Third decade
Mars ISRU Testbed, Tech demo	Large	TBD
Mars Large human precursor & manned	Flagship	TBD

Possible next-decade missions could include a Scout mission in 2011 and a Mars Science Orbiter (MSO) in 2013; and some sort of rover mission in 2016–2018 (e.g., two mid-size Mars Exploration Rover (MER) class, or two MSL heritage rovers, or one Astrobiology Field Laboratory rover). The Mars Sample Return mission may be moved to 2024 and beyond, due to its high cost, estimated at ~\$5B and above. The program could potentially afford an additional moderate class mission during the 2010–2020 timeframe, namely either the Mars Multi-Lander Network mission or smaller MER class or sub-MER class Fetch rovers.

3.2.2 Exploration of the Solar System

For the present discussion, Solar System Exploration includes proposed Solar System missions, but not the exploration of the Sun or Earth. Missions are organized in classes with cost caps shown in Table 3.3.

Budgetary considerations limit the total cost for a given decade to approximately \$9B,

Table 3.3: Solar System Exploration mission classes and estimated cost caps.

Mission class	Cost cap (\$M FY06)
Discovery	425
New Frontiers	750
Small Flagship	1,500
Large Flagship	3,000

excluding some of the programmatic components, such as Research and Analysis (R&A), Education and Public Outreach (E/PO) and technology development.

Smaller New Frontiers and Discovery missions are not well defined, but funding is allocated to these programs in NASA’s budget. On the other hand, while Flagship class missions for the next three decades are relatively well defined, based on science goals identified by the NRC and the science community; Flagship class missions are not funded under the current budget.

After identifying these classes, mission concepts to a number of types of targets were organized into one of these three groups. Mission concepts to primitive bodies and the inner planets are summarized in Table 3.4, while Table 3.5 lists concepts to giant planets, and large moons.

This oversubscribed set helped guide SSE Roadmap teams in defining and ordering the missions for the next three decades. This summary is shown in Figure 3.1.

Among the Flagship class missions, the Europa Explorer (EE) mission is the leading candidate for the first Flagship class program, with an earliest launch date of 2015. Second decade missions would include the Titan Explorer and the extended Venus Mobile Explorer. For the third decade, the options could be influenced by the findings of the EE mission, leading to a potential selection between the Neptune/Triton Orbiter/Lander or a Europa Astrobiology Lander.

The initial New Frontiers class missions include the 2006 New Horizons Pluto–Kuiper Belt mission (launched in January 2006) and Juno (a Jupiter Polar Orbiter mission without probes), planned for a 2011 launch. Potential New Frontiers missions for the 2015 opportunity include: Comet Surface Sample Return, Lunar South Pole Aiken Basin Sample Return, Venus In Situ Explorer (short-lived), or Saturn Flyby with Shallow Probes (SFSP).

Figure 3.1: NASA's 2006 Solar System Exploration Roadmap.

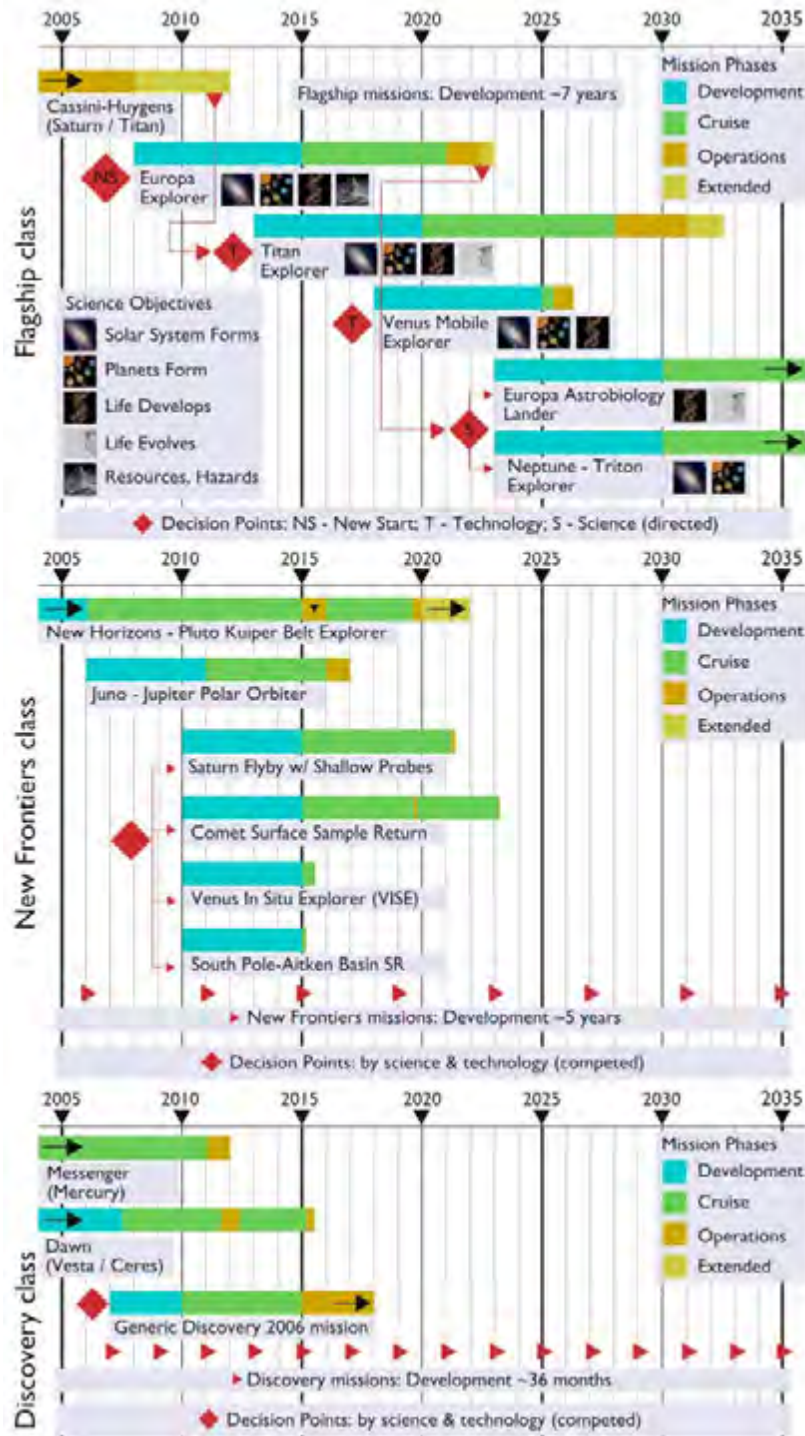


Table 3.4: SSE DRM set for ongoing and proposed missions to primitive bodies and inner planets (without the Moon).

Selected & Potential Mission Concepts	Mission Class	Earliest Launch
Primitive Bodies		
<i>Stardust</i>	<i>Discovery</i>	1999 (ended: 2006)
<i>Deep Impact</i>	<i>Discovery</i>	2005 (end: 2006)
<i>Dawn</i>	<i>Discovery</i>	2007 (end: 2016)
Comet Surface Sample Return	New Frontiers	2015 – TBD
Asteroid Rover Sample Return	New Frontiers	TBD
Trojan/Centaur Recon Flyby	New Frontiers	TBD
Inner Planets (without the Moon)		
<i>Messenger</i>	<i>Discovery</i>	2004 (end: 2012)
Venus In Situ Explorer (VISE) (short-lived)	New Frontiers	2015 – TBD
Geophysical Network – Venus	New Frontiers	TBD
Geophysical network – Mercury	New Frontiers	TBD
Venus Mobile Explorer	Flagship	2025
Venus Surface Sample Return	Flagship	TBD
Mercury Sample Return	Flagship	TBD

3.3 Mission Impact of Technology Development for EEs

The following section discusses the subset of the proposed SSE missions requiring technologies in extreme environments.

3.3.1 Mission Set

The DRM set for Solar System Exploration and Mars Exploration comprise an oversubscribed set of missions. Some of these missions target planetary destinations with harsh conditions and others will go to environments similar to those explored over the past 40 years. Specifically, Mars orbiter and planetary flyby missions would not require significant technology development because the the spacecraft environment is well understood and well controlled. Some of these missions with fewer technology investment needs include orbiter missions to Mars (e.g., MRO or smaller Scout missions) and to Neptune, flyby missions to Trojan/Centaur objects and to giant planets (e.g., Neptune, Uranus, and Saturn), and missions to the inner planets (e.g., Mercury Geophysical Network and Sample Return).

On the other hand, other missions would require significant technology development. Extreme environments discussed in this report include high or low temperatures, high pressures, and high-radiation environments. In general, high temperature and pressure are coupled and typical for Venus in situ and deep entry probe missions to giant planets, such as to Jupiter. High radiation and low temperature are also coupled for missions to the Jo-

Table 3.5: SSE DRM set for ongoing and proposed missions to giant planets and large moons.

Selected & Potential Mission Concepts	Mission Class	Earliest Launch
Giant Planets / Outer Planets		
<i>Galileo with probe</i>	Flagship	1989 (ended: 2003)
<i>Cassini-Huygens — Saturn Titan</i>	Flagship	1997 [†]
<i>New Horizons: Pluto-Kuiper Belt Explorer</i>	New Frontiers	2006
<i>Jupiter Polar Orbiter — Juno</i>	New Frontiers	2011
Jupiter Flyby with Deep Entry Probes	NF / Flagship	2020 [‡]
Neptune flyby	Flagship	TBD
Uranus flyby	Flagship	TBD
Neptune flyby with probes	Flagship	TBD
Uranus flyby with probes	Flagship	TBD
Saturn flyby with shallow probes	New Frontiers	2015
Neptune Triton Orbital Tour	Flagship	2030–2035
Neptune orbiter with probes	Flagship	2030–2035
Neptune orbiter / Triton Explorer	Flagship	2030–2035
Uranus Orbiter with probes	Flagship	TBD
Saturn Ring Observer	Flagship	TBD
Large Moons		
Io Observer	New Frontiers	TBD
Ganymede Observer	New Frontiers	TBD
Europa Explorer	Flagship	2015+
Europa Astrobiology Lander	Flagship	2035
Titan Explorer no Orbiter	Flagship	2020
Titan Explorer with Titan Orbiter	Flagship	2020

[†] End of mission scheduled for 2008, with a 6-year extension.

[‡] May vary as Juno science is returned.

vian system; relevant mission concepts are the Jupiter orbiter and Europa lander missions. Low-temperature missions are associated with surface missions to the Moon, Mars, Titan, Triton, and comets. Thermal cycling with fluctuations of 60–100°C would affect missions where the frequency of the diurnal cycle is relatively short, such as for Mars (similar cycle to Earth) and on the Moon, where the day length is 28 Earth days.

To analyze the technology needs, missions facing similar extreme environments were grouped together, with attention to the mission stage in which the extreme is faced. This analysis is shown in Table 3.6.

In order to understand the timeline of technology investment, mission concepts were then

Table 3.6: Extreme environments affecting planned missions.

Mission stage		Space	Entry		In situ					
Target	Proposed Mission Architecture	Radiation	Heat flux at atm. entry	Deceleration	High Pressure	Low temperatures	High temperatures	Thermal cycling	Chemical corrosion	Physical corrosion
High temperatures and high pressures										
Venus Surface	Air mobility, lander or rover		✓	✓	✓		✓		✓	✓
Saturn	Atmospheric entry probes		✓	✓			✓			
Jupiter	Atmospheric deep entry probes		✓	✓	✓		✓			
Low temperatures										
Lunar polar regions	Lander / rover					✓		✓		
Comet nucleus	Sample return		✓			✓				
Titan surface	Balloon, aerobot, lander / rover		✓	✓		✓				
Low temperatures and high radiation										
Europa orbit	Orbiter	✓				✓				
Europa surface	Orbiter w/ lander	✓				✓				
Thermal cycling										
Mars	Lander/rover					✓		✓		✓
Moon	Lander/river					✓		✓		✓
Mercury	Lander					✓		✓		

grouped by extreme environment, but sorted by launch date, rather than mission phase. This enabled the assessment team to develop an orderly plan for the investment. Technology readiness dates were also calculated, assuming a six-year lead time for Flagship missions and five years for New Frontiers. This analysis is shown in Table 3.7.

Table 3.7: Planned DRMs to extreme environments until 2035.

Mission	Class	Earliest Launch Date	Projected Technology Readiness Date
High Temperatures and Pressures			
Venus In Situ Exploration (VISE)	NF	2015	2010
Venus Mobile Explorer (VME)	Flagship	2025	2019
Saturn Flyby with Shallow Probes (SFSP)	NF	2015	2010
Jupiter Flyby with Deep Entry Probes (JDEP)	NF	2020	2010
Low Temperatures			
Lunar South Pole Aiken Basin Sample Return	NF	2015	2010
ESMD Lunar Surface Missions	TBD	2011+	2007
Comet Surface Sample Return (CSSR)	NF	2015	2010
Titan Explorer	Flagship	2020	2014
Low temperatures and high radiation			
Europa Explorer (EE)	Flagship	2015+	2010
Europa Astrobiology Lander (EAL)	Flagship	2030–TBD	2024

The next step was to create a set of tables describing the impact of specific technologies on specific missions. The tables use a graphical approach to illustrate the relative impact, with a code given by Table 3.8.

Technology investments may be reduced by limiting technology development to mitigate the environmental effects until traditional methods suffice. For example, radiation tolerance for a Europa mission could be either increased to about 5 Mrad at a significant cost, or to only 1 Mrad, to be supplemented by traditional shielding methods. Unfortunately, the additional shielding would require a sizable portion of the payload mass. This demonstrates the importance of understanding mission studies that trade the cost of technology development against the added mass and power costs resulting from an incomplete solution.

Table 3.8: Symbol codes for mission impact analysis.

Symbol	Level of Impact
○	Low
◐	Medium
●	High

3.3.2 High Temperature and High Pressure

High-temperature and high-pressure conditions are typical for Venus in situ missions and deep entry probe missions to the giant planets. Relevant issues related to these missions are discussed below.

Venus In Situ Exploration

The Design Reference Mission set includes four Venus in situ missions, namely the Venus In Situ Explorer with a short duration, the extended Venus Mobile Explorer, the Venus Surface Sample Return, and the Venus Geophysical Network missions.

Venus In Situ Explorer (VISE)

VISE is proposed as a New Frontiers class mission, and it would explore the composition and perform isotopic measurements of the surface and atmosphere of Venus. It would operate for several hours on the surface of Venus, acquiring and characterizing a core sample to study the mineralogy of the surface. Its earliest launch date would be 2015.

Venus Mobile Explorer (VME)

VME, shown in Figure 3.2, would be a Flagship mission that could launch as early as 2025. VME would explore and characterize the surface with a wheeled or an aerial vehicle and would acquire and characterize core samples. It would need to operate in the Venus surface environment for at least 90 Earth days. After passing through the sulfuric acid clouds, this mission is envisioned to perform survey imaging (in the case of an aerial vehicle) and acquire samples from about 10–20 cm depth and to perform science measurements in situ. An even greater interest to the scientific community is an extended (up to 90 days or longer) mission, allowing for significantly more extensive coverage of the surface and thus, more returned science.

Although the VSSR proposed mission may not require urgent technology development within the next ten years, due to its anticipated launch date, it is important to see the progression from short-lived to long-lived missions and on to sample return in order to understand the importance of various technologies, particularly that of high-temperature

Figure 3.2: Artist's concept for Venus Mobile Explorer.



sample acquisition. The Venus Geophysical Network (VGN) mission requires a subset of the technologies needed for VME.

Technology needs for in situ exploration at Venus

High-temperature sample acquisition is an enabling technology for all surface missions (except network missions), with requirements driven by the mission duration. On the other hand, high temperature electronics are only required for those surface missions designed to operate for days to months, when passive thermal protection technology is insufficient. The combination of passive and active cooling systems will need to strike a balance between required technology investment and the reduced costs of mass reduction.

Active cooling technology would be needed for extended missions calling for greater improvements in returned science. A corollary investment would result from the need for extended active cooling and power generation to have suitable power system, such as a Stirling Radioisotope Generator (SRG) with active cooling to the spacecraft. Certain mission functions will remain impractical for implementation at high temperatures and pressure; this group includes items such as most scientific sensors and microprocessors requiring active cooling.

A pressure vessel is required regardless of mission duration, and thus for all in situ missions. Advanced materials, such as honeycomb structures or composite materials could significantly reduce the weight of the pressure vessel. The mass savings could increase the

size and consequently the volume of the pressure vessel, potentially adding science instruments to the payload. An envisioned air mobility system for extended in situ investigations would use metallic bellows, requiring buoyancy control, corrosion resistance from the environment, and leak resistance and mitigation.

Venus missions do not require new entry probe thermal protection systems because the entry velocity is similar in magnitude to that of Mars, Titan, and Earth re-entry, although improvements in TPS could improve payload fraction.

These technology needs are summarized in Table 3.9.

Table 3.9: Impact of technology development on missions to Venus.

	Venus In Situ Explorer (VISE)	Venus Mobile Explorer (VME)	Venus Surface Sample Return (VSSR)
Earliest launch date	2015	2025	TBD
Temperature (°C)	460–480	460–480	460–480
Pressure (bar)	92	92	92
Architecture	Short-lived [†] surface	Extended [‡] surface	Sample return
Protection Systems			
Hypervelocity entry	<input type="radio"/> Medium	<input type="radio"/> Medium	<input type="radio"/> Medium
Hypervelocity impact protection	<input type="radio"/> Low	<input type="radio"/> Low	<input type="radio"/> Low
Pressure control	<input checked="" type="radio"/> High	<input checked="" type="radio"/> High	<input checked="" type="radio"/> High
Passive thermal control	<input checked="" type="radio"/> High	<input checked="" type="radio"/> High	<input checked="" type="radio"/> High
Active thermal control	<input type="radio"/> Low	<input checked="" type="radio"/> High	<input type="radio"/> Low
Component hardening			
High-temperature electronics	<input type="radio"/> Low	<input checked="" type="radio"/> High	<input type="radio"/> Low
High-temperature energy storage	<input type="radio"/> Low	<input checked="" type="radio"/> High	<input type="radio"/> Medium
Robotics			
High-temp. sample acquisition	<input checked="" type="radio"/> High	<input checked="" type="radio"/> High	<input checked="" type="radio"/> High
High-temperature aerial mobility	<input type="radio"/> Low	<input checked="" type="radio"/> High	<input checked="" type="radio"/> High

Note: For Venus surface missions, a detailed study quantified the mission impact in the following scheme: “Low” impact technologies produce a 2× increase in functionality; “Medium” impact implies a 5× increase; “High” impact technologies produce a greater than 5× increase in functionality; and “Very high” technologies are mission enabling.

[†] “Short-lived” for Venus implies durations of hours.

[‡] “Extended” for Venus implies durations of days or weeks.

Deep Probes to Giant Planets

The NRC recommended entry probe missions to the giant planets to provide in situ measurements, complementing and validating remote-sensing observations, such as the ones provided by the New Frontiers class Jupiter Polar Orbiter mission, Juno. The Galileo probe, the only probe mission to date into the atmosphere of a giant planet, entered Jupiter in 1995. Although extensive research and development work took place throughout NASA, much of this institutional knowledge has been lost.

In support of NASA's Solar System Exploration Roadmap for the next three decades, it was important to assess the current state-of-the-art on planetary probes and to identify steps needed to enable deep probe missions to Jupiter and potentially to other giant planets. Among the giant planets, Jupiter represents an extreme because it has the largest gravity well and highest radiation environment. Deep-entry probes to Jupiter also encounter extreme environments in the form of high temperatures ($>450^{\circ}\text{C}$) and high pressures (>100 bars), similar to those on the surface of Venus. Therefore, the present assessment discusses the feasibility of Jupiter Deep Entry Probes (JDEP) to or below a pressure elevation of 100 bars. The aeroshell design of these probes would likely be built from Galileo probe heritage.

Jupiter Flyby with Deep Entry Probes (JFDP)

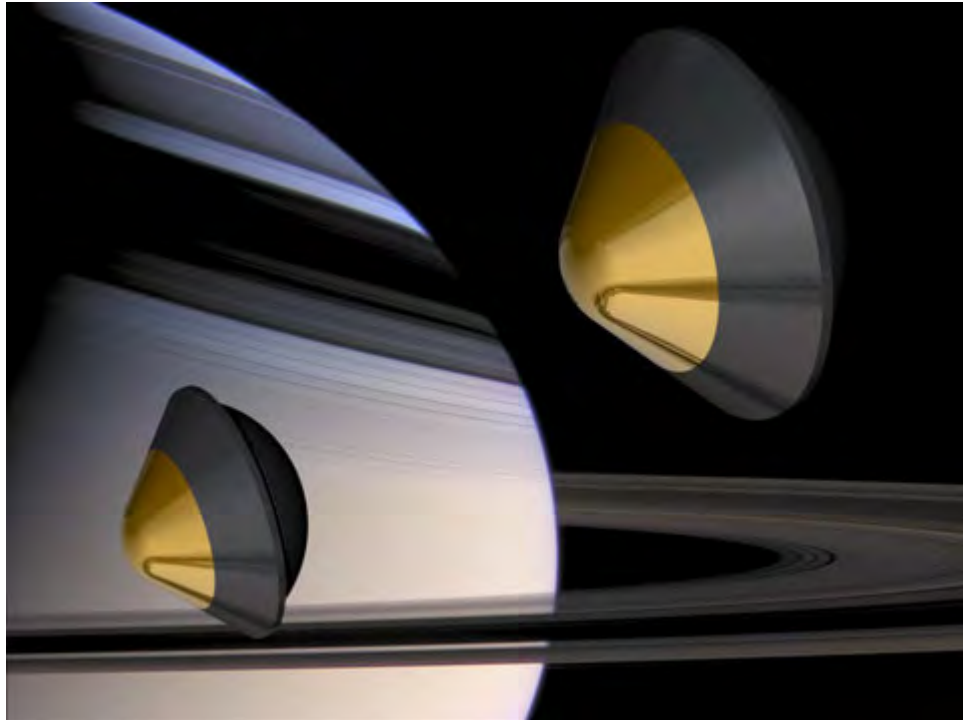
JFDP, a potentially solar- or RPS-powered New Frontiers class mission with a nominal launch date of 2020, would use a flyby architecture to release three probes into the atmosphere of Jupiter within 30° of the equator. These probes would reach a depth of 100 bars to measure atmospheric composition and other properties. Improvements to communication, pressure vessel, and thermal designs could greatly enhance penetration depth, compared to the Galileo probe's design. Therefore, deep entry probe pressure vessel designs would be similar to those for Venus in situ missions.

Saturn Flyby with Shallow Probes (SFSP)

SFSP, targeting a pressure depth of 10 bars, would likely use Galileo mission heritage (see Figure 3.3). In addition, water abundance to ~ 100 bars pressure depth would be measured using microwave radiometry (MWR), similar to the technique used on the proposed Juno mission. Measurement of the magnetic and gravity fields were also identified as science objectives, although this would require a polar trajectory for the carrier. On one hand, it would allow for the decoupling of the carrier from the probes, thus permitting the carrier to target any trajectory from approach, including a polar flyby or orbit. On the other hand, however, this option would result in a significantly longer flight time to Saturn, and would necessitate direct-to-Earth communication from the probes. DTE feasibility from Saturn has not yet been demonstrated, and even if it is possible, it would result in very restricted data rates, and would require new designs and qualifications for almost all elements of the telecom architecture. Typically, the communication window from the probes is limited to ~ 70 minutes. For a probe relay trajectory option the probes would communicate with the carrier, utilizing its co-rotation with the planet and good visibility to the probes. For a DTE trajectory option, the data link time would be limited by the probe's entry location

and the rotation of Saturn, which is $\sim 40^\circ$ in 70 minutes. This limited descent time and shallow pressure depth reach by the probes relax the requirements for improved technologies for passive thermal control and energy storage designs, as well as for parachute and balloon materials.

Figure 3.3: Artist's concept of Saturn Flyby with Shallow Probes.



Technology needs for in situ exploration at the Outer Planets

Deep probes will require innovative designs for sampling mechanisms because of ripple effects on structural and thermal designs. Short-lived probes would likely use primary batteries for energy storage. Advancements in specific energy for batteries could reduce battery size and volume, or the same volume and mass could provide higher power to instruments and to the communications system. Improved probe instruments could reduce payload mass and volume, as well as power requirements and associated heat generation. For a Jupiter probe mission, radiation tolerance requirements are not significant because of the limited exposure to the radiation environment.

TPS development may significantly impact probe missions to the giant planets. Estimated entry velocities on prograde orbits, utilizing the rotation of the planet, are listed in Table 3.10. Polar and retrograde orbits may require entry velocities that are 50% higher. Jupiter represents the extreme because its stagnation point heating was estimated at 30 kW/cm^2

for the Galileo probe. The TPS design requirements would be less stringent at Saturn. The entry velocities are tabulated in Table 3.10.

Table 3.10: Estimated entry velocity at the outer planets.

Velocity (km/s)	Jupiter	Saturn	Uranus	Neptune
Inertial	59.8	35.9	21.8	23.8
Prograde	47.3	26.0	19.2	21.2
Retrograde	72.4	45.8	24.4	26.5
Polar	62.9	38.7	22.2	24.2
Rotation	12.6	9.9	2.6	2.7

SFSP could use Galileo heritage to construct a vented design for the shallow probes to mitigate the extreme environment. Microwave radiometry on the flyby spacecraft or entry probes (released before atmospheric entry) could accompany these probes; however, the associated increased power and mass requirements would present further challenges to a solar-powered configuration. Like Jupiter deep probes, Saturn deep probes to 100 bars would necessitate pressure vessel and thermal designs, but with fewer constraints on the TPS and radiation protection. Furthermore, both JFDP and SFSP would benefit from systems providing protection from hypervelocity impacts, such as from micrometeoroids. Some well-known streams of cometary residue, such as the Leonids, may pose a threat to missions to the outer planets, although the exact threat depends on the detailed trajectory and length of cruise. Missions to Saturn, such as SFSP, experience additional challenges from crossings of Saturn's ring plane.

Table 3.11 shows the impact of technology development on the mission concepts. Entry probe missions to Neptune and Uranus would have similar considerations to the ones discussed above.

3.3.3 Low Temperatures

A number of targets would expose missions to extremely low temperatures, although each target has its own set of additional challenges. Mission concepts to each target are discussed in detail.

Lunar Surface Missions

Extreme environmental conditions on the Moon will likely shape and constrain lunar architectures in far-reaching ways. The lunar surface environment can be characterized by:

- *Lack of an atmosphere:* Vacuum

Table 3.11: Impact of technology development on probe missions to the outer planets.

	Jupiter Flyby with Deep Probes (JFDP)	Saturn Flyby with Shallow Probes (SFSP)
Earliest launch date	2020	2015
Temperature (°C)	~450	~70
Pressure (bar)	~100	~10
Architecture	Deep probes	Shallow probes
Protection Systems		
Hypervelocity entry	● High	● High
Hypervelocity impact protection	○ Medium	● High
Pressure control	● High	○ Low
Passive thermal control	● High	○ Medium
Active thermal control	○ Low	○ Low
Component hardening		
High-temperature electronics	● High	○ Low
High-temperature energy storage	○ Medium	○ Low
Robotics		
High-temperature sample acquisition	○ Medium	○ Low
Aerial mobility	○ Low	○ Low

- *Partial gravity:* 0.18 g
- *Radiation:* Galactic cosmic rays and solar particle events
- *Impacts:* Micrometeoroid
- *Thermal cycling:* Diurnal cycle is 28 Earth days long (14 days each of sunlight and night)
- *Physical corrosion:* Pervasive dust

Sortie missions that would amass man-made surface elements on the Moon could also pose potential environmental hazards. Consequently, the design and development of lunar technologies and habitats must respond effectively to these threats, potentially making lunar architectures complex and challenging.

Lunar architectures could target equatorial regions, polar craters, and permanently or near-permanently sunlit crater rims. Equatorial regions are characterized by the diurnal cycle resulting in extreme thermal cycling, where the surface temperature could rise above +100°C (212°F) at lunar “noons” and could sink below -155°C (-247°F) at night. Permanently

shadowed craters are targeted by robotic missions for potential in situ resource utilization (ISRU), under the assumption that these craters could hold a significant amount of easily accessible water ice, convertible into resources for future missions. Near-permanently illuminated crater rims, such as those of the polar Shackleton and Peary craters, could be chosen for their proximity to possible in situ resources at the bottom of the craters, combined with solar availability for human bases.

Comet Surface and Asteroid Sample Returns

The New Frontiers class Comet Surface Sample Return (CSSR) mission would obtain a 250–500 cc sample from the surface of a comet’s nucleus, assumed to be rich in organics. The targeted comet will be likely selected at several astronomical units (AU) from the Sun. It would present a dusty and cold environment, although radiation would not be an issue. Measurements conducted in situ would provide context for analysis of the returned sample prior to its return to Earth.

Titan Explorer

Following the success of the Huygens probe, Titan remains one of the highest priority science destinations. The SSE roadmap identified the in situ Titan Explorer (TE) as a potential second-decade flagship class mission. Possible architectures, considered in NASA’s Vision Missions studies and in focused RPS technology studies, include concepts both with and without an orbiter. Without an orbiter to relay data, the in situ vehicle (e.g., the hot air balloon) would be forced to communicate directly with Earth, requiring a directional antenna.

The Titan environment is unique because it contains methane and heavier hydrocarbons (tholins) in the form of aerosols and/or precipitation. The recent evidence from Huygens suggests a methane-soaked surface with clearly observable river channels and possible lakes, prompting the development of a mission to investigate the role of methane hydrology in sculpting these surface features. The Titan Explorer mission is envisioned to have either aerial or surface mobility to address these science goals. With a minimum lifetime of at least 90 days and possible duration of years, TE would acquire samples to characterize surface and subsurface materials, particularly with respect to prebiotic chemistry and extinct life.

Neptune Orbiter/Triton Lander Mission

Neptune’s moon Triton is one of the coldest surface environments in our Solar System, with a temperature of -235°C (or 38 K) due to its extreme distance from the Sun (30.06 AU). Two mission architectures under NASA’s Vision Missions studies included Neptune orbiters with probes, utilizing either the Prometheus architecture with nuclear electric propulsion or a high-thrust trajectory architecture with aerocapture. Both possibilities addressed potential exploration of Triton with or without a lander, with multiple lander concepts under consideration.

Technology Needs for Low Temperatures

Lunar missions

For permanent human bases, radiation shielding will likely introduce a significant technology challenge, although the impact on robotic science and human precursor missions is not expected to be significant. Sample return missions, such as the proposed Lunar South Pole Aitken Basin mission, would return approximately 2 kg of material from a region of permanent shade, where material from the Moon’s upper mantle is exposed on its surface. Sample return missions would be enhanced by the development of low temperature electronics and energy storage and would also require low temperature sample acquisition systems.

Radioisotope power system (RPS)-enabled lunar surface missions could utilize the excess heat from the power system, while solar-powered missions would need to provide resistance heating overnight powered by secondary batteries, and potentially augmented by radioisotope heater units. In general, lunar surface missions could be designed to mitigate the cold environment by effective insulation and active heating.

Therefore, the highest impact of the low-temperature environment is expected to be on the external components that need to be outside the warm electronics box (WEB), such as those of the actuators and motors on rovers, the instruments on the masts, and most importantly the sample acquisition mechanisms. As noted in Section 2, placement of electronic components outside the WEB can greatly simplify cabling.

Cometary missions

A cryogenic sample return mission would require keeping the sample temperature below -10°C , posing an additional challenge to the aeroshell/capsule as it must tolerate the high heat flux upon Earth re-entry. Two additional factors adding to mission complexity and cost are the low-temperature tolerant sampling mechanism and the mitigation of the impact of high-velocity particles from the comet during the initial approach.

Titan Explorer

Among the proposed Roadmap missions to low-temperature environments, the Titan Explorer is the one that would most benefit from advanced technologies (see Figure 3.4). Depending on the mission’s trajectory, cruise time, and location of crossing Saturn’s ring plane, the Titan Explorer may require protection from hypervelocity impacts of small particles.

For operations at Titan, the sample acquisition systems would require significant development, as well as the balloon materials for the air mobility system. However, all of the low-temperature technologies discussed in this report would be either strongly enhancing or enabling for the Titan Explorer, suggesting that the feasibility of such a mission depends strongly on the development of low-temperature technologies.

Figure 3.4: Artist's concept for Titan Explorer balloon.



Neptune Orbiter/Triton Lander

Lander architecture and design strongly influences the need to address the extreme environment. The cold ambient temperatures suggest that an internal power source, such as a radioisotope power system (RPS), would be required to power the lander, where the excess heat from the RPS could be directed to a lander's warm electronics box (WEB). However, elements external to the WEB and providing direct interface with the environment, such as a mast or a sample acquisition system, would need to tolerate the environment through a combination of low-temperature electronics and local component heating with resistance heaters, heatpipes or radioisotope heater units (RHUs).

The mission stage would dictate the extreme environment of concern. As studied, because of the long cruise duration there is a need for protection from hypervelocity impacts. Both the orbiter and the lander would have to be encapsulated in an aeroshell to enable aerocapture at Neptune. Temperature-control needs would vary with mission stage; during the cruise phase, the excess RPS-generated heat would be removed through active cooling and rejected to space. Later, through the aerocapture phase, a phase change material (PCM) could remove the heat from the RPS, keeping the electronics at a required temperature. Once on the surface of Triton, the lander must be capable of tolerating the extremely low temperature.

Summary

Technologies for missions impacted by low temperatures are detailed in the mission impact matrix shown in Table 3.12.

Table 3.12: Impact of technology development for missions to low-temperature environments.

	SPAB L/R	CSSR	TE		NO/TL
Earliest launch date	2015	2015	2020		2030
Temperature (°C)	-230	-270	-180		-235
Pressure (mbar)	~0	~0	1400		0.01
Architecture	Surface return	Surface	Lander	Aerial	Lander
Protection Systems					
Hypervelocity entry	N/A	N/A	N/A	N/A	N/A
Hypervelocity impact protection	○	●	●	●	●
Passive thermal control	●	●	●	●	○
Active thermal control	●	○	●	●	○
Component hardening					
Low-temperature electronics	●	○	●	●	●
Low-temperature energy storage	●	○	●	●	●
Robotics					
Low-temp. sample acquisition	●	●	●	●	●
Low-temperature aerial mobility	N/A	N/A	○	●	N/A

SPAB L/R — South Pole Aitken Basin Lander/Rover; CSSR — Comet Surface Sample Return;

TE — Titan Explorer; NO/TL — Neptune Orbiter / Triton Lander

● — High; ○ — Medium; ○ — Low

3.3.4 Low Temperatures and High Radiation

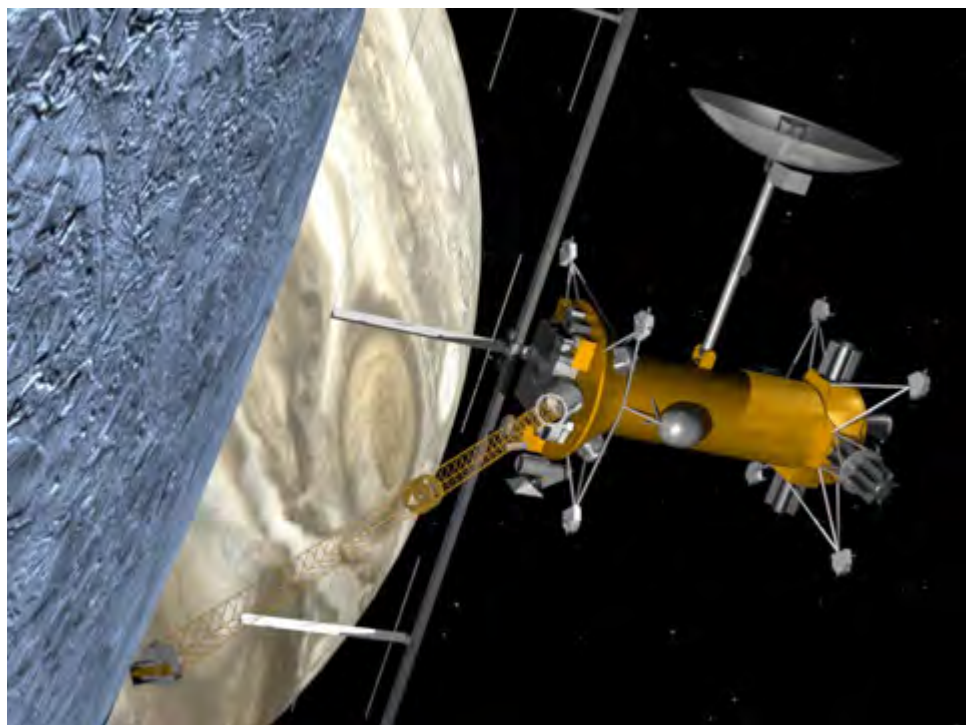
Missions to the Jovian system, especially potential landers, must address the simultaneous challenges of low temperatures and a high radiation environment. Missions considered in this section include a Europa Explorer mission with or without a small lander, a Europa Astrobiology Lander, an Io Observer (orbiter), a Ganymede Observer with or without a lander, and Juno (Jupiter Polar Orbiter), the second New Frontiers mission to be launched in 2011.

Europa Explorer and Europa Astrobiology Lander

The surface of Europa presents a fascinating target for life-detection missions because of

strong indications that a liquid water ocean may lie beneath the icy shell. However, missions to Europa would have to tolerate the intense Jovian radiation environment, dominated by electrons ranging up to 500 MeV in energy. Two Flagship class missions were defined in NASA's 2006 Solar System Exploration Roadmap: the Europa Explorer (EE) — see Figure 3.5 — that could launch after 2015, and the Europa Astrobiology Lander (EAL), proposed as a third-decade mission — see Figure 3.6. The proposed EE mission may include a small (340 to 375 kg) landed element, while the EAL would be a much more sophisticated lander with a powerful instrument payload. These two landers would have the mutual goals of characterizing the surface and subsurface ocean, and would further explore the surface composition and pre-biotic chemistry of Europa.

Figure 3.5: Artist's concept for Europa Explorer.



The effects of the potentially damaging radiation cannot be remedied simply with shielding because the secondary radiation (i.e., radiation caused by deceleration, or bremsstrahlung) may still potentially damage the electronics. In general, radiation-hard electronics are often augmented by incorporating shielding directly into a part's electronic package. In cases where certain radiation hard parts are not available (e.g., nonvolatile memory), a particular subsystem can be locally shielded, as has been considered in the past in mission studies for a Europa Orbiter.

Figure 3.6: Artist's concept for Europa Astrobiology Laboratory.



An issue unrelated to the radiation is the activity level of the surface of Europa, presenting the possibility of local contamination transport via the global ocean and associated planetary protection concerns. This poses problems for energy storage, since radioisotope power systems are perennial heat sources and potentially could, in a non-nominal landing or other mission operations, be introduced to close contact with water ice — potentially forming environments that could accommodate the growth of contaminant organisms.

Power system options for a lander would be defined by duration on the surface. A shorter 3–4 days' mission could use a primary battery, while a longer mission would likely use an RPS with a secondary battery. The impact of technology development on proposed Europa in situ missions is summarized in Table 3.13. The Jovian system, and in particular Europa, is considered to be one of the most challenging destinations for solar system exploration because of the high radiation environment and low temperature.

Io Observer and Ganymede Observer

Potential Io and Ganymede Observer missions would also encounter the Jovian radiation environment. However, at Ganymede the radiation environment would be significantly lower, due to the distance from Jupiter, while at Io it would be higher than at Europa. Since the total ionizing dose (TID) is a function of radiation intensity and exposure time, shielding requirements should be assessed in that context. For example, on a Ganymede Observer, with a similar operational lifetime to a Europa Explorer mission, the electronics would

Table 3.13: Impact of technology development for missions to Europa, a low-temperature, high-radiation environment.

	Europa Explorer (EE)	Europa Astrobiology Lander (EAL)
Earliest launch date	2015+	2023
Temperature (°C)	N/A	-160
Radiation levels (krad/day)	40	20 [†]
Architecture	Orbiter	Conventional lander
Protection Systems		
Hypervelocity entry	N/A	N/A
Hypervelocity impact protection	● Medium	● Medium
Thermal control	○ Low	○ Low
Radiation shielding	● High	● High
Component hardening		
Low-temp. / rad-hard electronics	● High	● High
Low-temperature energy storage	○ Low	● High
Robotics		
Low-temperature sample acquisition	○ Low	● High
Low-temperature aerial mobility	N/A	N/A

[†]Does not reflect shielding by Europa.

require less shielding and lower radiation tolerance. This would impact shielding mass allocation for the mission and the technology investment for radiation-tolerant components, thus potentially reducing mission complexity and cost. For an Io Observer, radiation exposure could be kept low by designing a highly elliptical orbit, where the spacecraft would spend a significant amount of time away from the highest radiation levels and would perform observations during repeated Io flybys.

Jupiter Polar Orbiter — Juno The second New Frontiers mission, Juno, is a Jupiter Polar Orbiter mission, designed with low-intensity low-temperature (LILT) solar panels. Although LILT promises higher conversion efficiency compared to triple junction solar panels, the lower solar flux at Jupiter would still result in a significant increase in surface area, impacting the mass of the power system. Juno’s polar orbit will minimize the interaction with Jupiter’s radiation belts. This approach, combined with a limited number of planned orbits, is expected to reduce the radiation shielding requirement on the spacecraft. Because the temperature environment for the orbiter is expected to be similar to that for other orbiter missions, most of the necessary technologies would not require significant development.

Lunar and Mars Missions

Radiation exposure on robotic lunar and Mars exploration missions is significantly lower than the Mrad range doses encountered at Europa, due to the relatively short mission durations, and to the lower radiation levels. However, since the radiation tolerance levels for electronics and humans are significantly different, manned missions should address the radiation environments for both galactic cosmic rays and solar particle events. The required shielding for human missions would significantly increase landed mass and consequently would add complexity and cost to the missions.

3.3.5 Thermal Cycling

Thermal cycling impacts in situ missions close to the Sun (e.g., out to Mars or 1.5 AU), and with a relatively short diurnal cycle. The many roadmap activities suggest that potential extraterrestrial targets facing this challenge include Mercury, Venus, the Moon, and Mars.

Because shorter diurnal cycles impact thermal cycling more significantly, lunar and Mars in situ missions are most affected. However, the impact of thermal cycling is also influenced by landing location. Due to the tilt of a planet's or moon's axis, polar landers at regions can experience season-long sunlit or dark periods, influencing the frequency of thermal cycling. A comparison of typical average lunar and Mars conditions are shown in Table 3.14.

Table 3.14: Diurnal cycles of targets experiencing thermal cycling.

Target	Diurnal cycle in Earth days or hours	Maximum Temperature (°C)	Minimum Temperature (°C)	Average Temperature (°C)
The Moon	28 days	+197	-233	+31
Mars	24.6 hours	+27	-143	-63

Lunar Missions

The effects discussed in the section on low temperatures are those of principal concern here. Generally, lunar surface missions could be designed with insulation and active heating systems to protect electronics from the cold environment. However, operational systems designed to tolerate a high number of cycles would have the strongest effect on these missions.

Mars Missions

Proposed and ongoing Mars in situ missions are shown in Table 3.2, including the Phoenix Mars Scout lander (in flight), the Mars Science Laboratory (MSL) rover (in development), and proposed and studied missions such as the Mars Multi-Lander Network, the Astrobi-

ology Field Laboratory (AFL) rover, the Mars Sample Return (MSR) mission, MER class mid-rovers, and the Mars Deep Drill, with these missions eventually leading to technology demonstration human precursor missions (e.g., an ISRU testbed) and then to large scale human precursor and manned missions.

Surface missions are affected by thermal cycling. Temperatures vary with the diurnal cycle, latitude, aerocentric longitude of the Sun (L_s), shadowing, and atmospheric effects. Temperature variations are characterized in Table 3.15, and the pressure is about 1% of that on Earth.

Table 3.15: Impact of technology development for missions to the thermal cycling environments of the Moon and Mars.

	Moon	Mars
Spacecraft configuration	Lander/rover	Lander/rover
Earliest launch date	2010	2009
Temperature (°C)	-155 to +100	-143 to +27
Pressure (bar)	~0	~6 mbar
Architecture	Extended [†] surface	Extended surface
Protection Systems		
Hypervelocity entry	N/A	N/A
Hypervelocity impact protection	<input type="radio"/> Low	<input type="radio"/> Low
Passive thermal control	<input checked="" type="radio"/> High	<input checked="" type="radio"/> High
Active thermal control	<input checked="" type="radio"/> High	<input type="radio"/> Medium
Component hardening		
Low temperature (with thermal cycle resistance)	<input checked="" type="radio"/> High	<input checked="" type="radio"/> High
Low-temperature energy storage	<input checked="" type="radio"/> High	<input type="radio"/> Medium
Robotics		
Low-temperature sample acquisition	<input checked="" type="radio"/> High	<input checked="" type="radio"/> High
Low-temperature aerial mobility	N/A	<input type="radio"/> Low

[†] Extended missions to the Moon and Mars refer to durations of months.

Therefore, the most significant impact of extreme environment effects on Mars missions is related to thermal cycling of various landed elements. Thermal cycling could lead to failure of solar panel soldering joints, or to the breakdown of other external connections. From a functional standpoint, electronics should be able to operate over the entire temperature range. In particular, the maximum temperature falls well within the operating range of conventional electronics. Although the minimum falls considerably below that for which conventional and even high-reliability electronics are designed or tested, it is well estab-

lished that electronic devices can operate in such low temperatures.

The reliability of the complete electronic system poses the greatest concern in light of the high number of daily temperature cycles experienced during the entire mission. Thermal cycling can be mitigated by keeping the component temperatures within a required range by a suitable insulation design combined with louvers, resistance heating, or by utilizing the excess heat of a radioisotope power source or radioisotope heater units.

Technology Needs for the Moon and Mars

In general, all missions are expected to benefit from component hardening, energy storage, and operational systems designed for low temperatures, but able to tolerate cycling between extremes. The needs are summarized in Table 3.15.

4 Emerging Capabilities in Technologies for EEs

4.1 Systems Architectures for Missions to Extreme Environments

The term “systems architecture” is used here to describe both the spacecraft (hardware) and mission design. In principle, architectures for extreme environments may be categorized in the following way:

- Isolation of sensitive materials from hazardous conditions;
- Development of sensitive materials tolerant to hazardous conditions; and
- Appropriate combinations of isolation and tolerance.

This systems approach combining the best of isolation techniques and new materials will be described more fully in Section 4.1.3.

4.1.1 Environmental Isolation

One possible solution for extreme environment mission architectures is to simply maintain all electronics and sensitive components in an environmentally controlled vessel. While this sounds feasible, the environmental protection is seldom complete nor does it come without cost. A good example of this is the bremstrahlung produced by radiation shielding. While radiation shielding may reduce the energy of the incident particles, the conversion into secondary electrons or photons may still produce additional damage to the electronics. A second example is the active refrigeration needed for thermal isolation in hot environments. Such systems will require additional mass and power resources to maintain a heat sink.

As a result, environmental isolation architectures typically require added resources and may not provide ideal solutions for all missions to extreme environments.

4.1.2 Environmental Tolerance

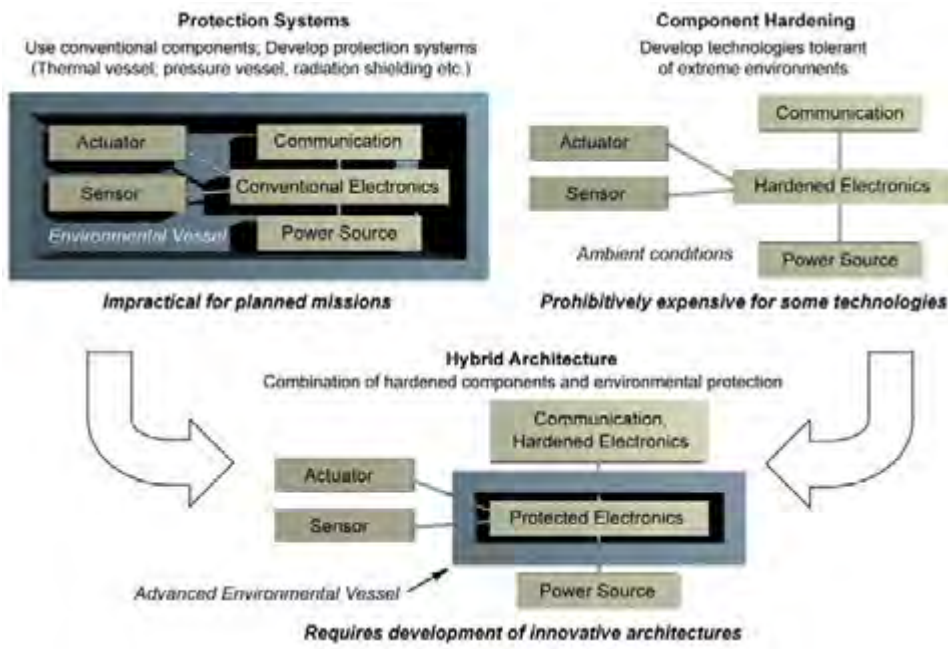
An alternative approach is to develop hardware components that can reliably operate and survive in extreme environmental conditions, thus eliminating the need for environmental control. While this approach is ideal on a purely technological level, some of the key technologies would require a large investment to achieve the desired performance (e.g., an avionics systems capable of operating at $\sim 500^{\circ}\text{C}$). Other technologies have fundamental limitations precluding them from functioning in some environments, such as battery technology, which becomes severely kinetically limited at temperatures lower than -100°C .

Therefore, environmentally tolerant technologies may pose elegant solutions to some technology challenges, but technology development may not be able to answer problems posed by fundamental physical limitations or impractical investment strategies.

4.1.3 Hybrid Systems

In a hybrid architecture, some environmental-sensitive components are maintained inside a protective enclosure, while other more tolerant components remain outside. This approach requires simpler and lighter environmental controls, enabling more functionality with less cabling. In addition, this approach is also cost-effective if technologies are selected for systems engineering capabilities, as well as for tolerance. The integration of isolation and tolerance to form a hybrid system is illustrated in Figure 4.1.

Figure 4.1: Hybrid systems architectures for extreme environments.



Such architectures are already maturing. For example, the Mars Science Laboratory (MSL) project has taken initial steps in hybrid architectures by co-locating each motor's controllers with the motor and actuator at the vehicle's extremities. The rover will use brushless motor-based actuators rather than the brush-contact motors used by the Mars Exploration Rovers (MER), thus requiring fewer control cables. These controllers operate in the Mars environment and are able to withstand hundreds of thermal cycles without deterioration in performance. By connecting them to the motors via redundant serial data and power buses, a simple and reliable bus loop can replace the older system of connecting hundreds of discrete wires to tens of motors with their drive electronics in the WEB.

For Venus landers, a hybrid architecture shows promise. Subsystems such as avionics, telecommunications, advanced instruments, and low-temperature energy storage will likely

require thermal/pressure control zones. On the other hand, with technology investment, subsystems such as in situ sensors, drilling, sample acquisition mechanisms, high-temperature energy storage, and limited electronics may be capable of tolerating full exposure to the extreme environment.

4.2 Protection Systems

In general, protection systems refer to those systems providing isolation from the extreme environment. Protection from hypervelocity entry is required for the high peak or total heat fluxes experienced during atmospheric entry. Hypervelocity particles can impact spacecraft throughout the cruise phase, with risks that are potentially increased during transit through particle-rich environments. Protection from high pressures and temperatures are integrated in architectures for landers on Venus. Specific technologies follow.

4.2.1 Hypervelocity Entry

The TPS protects or insulates a body from the severe heating encountered during hypersonic flight through a planetary atmosphere. Since TPS is a single point-of-failure subsystem, it is critical and its performance needs to be validated through ground test and analysis.

Two classes of TPS exist:

- Reusable TPS
- Ablative TPS

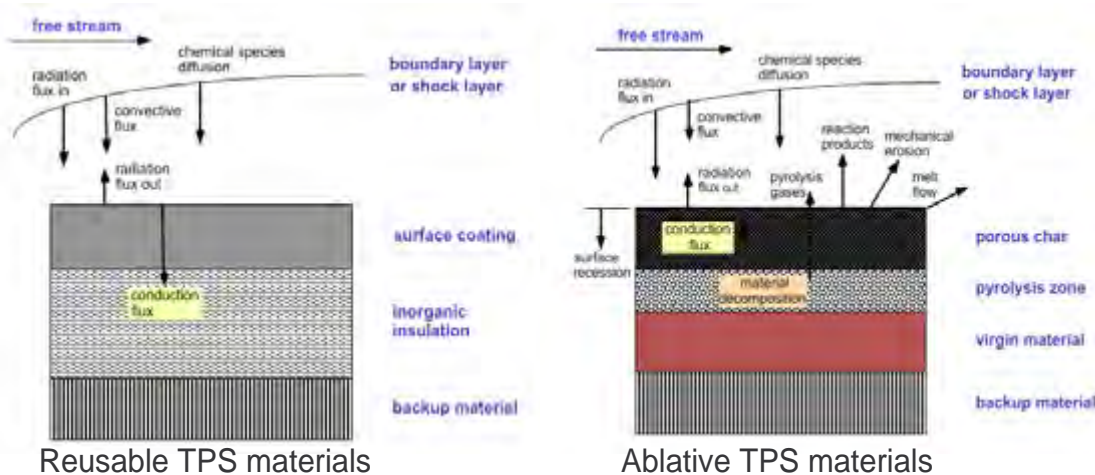
In reusable TPS systems, exposure to the entry environment produces no changes in the system's mass or other properties. Typically, reusable TPS applications are limited to relatively mild entry environments. A portion of the heat that is deposited onto the TPS system from the shocked gas is radiated away while the remainder is conducted into TPS material. Thus, the surface coating that is often used in these systems must have high emissivity to maximize the radiated energy flux, and low surface catalycity to minimize convective heating by suppressing recombination of dissociated boundary layer species at the heated surface. The primary insulation, usually made of inorganic materials, should also possess low thermal conductivity to minimize the material required to insulate the primary structure (known as the backup material).

Ablative TPS materials, in contrast, accommodate high heating rates and heat loads through phase change and mass loss. These materials represent the classical approach to TPS, used for over 40 years in a broad range of applications, including in all NASA planetary entry probes to date. TPS materials are typically reinforced composites; as binders, they use organic resins that are pyrolyzed upon heating. This process produces gases (mostly hydrocarbons) that percolate toward the heated surface, absorbing some energy in the form of heat. The pyrolysis gases are then injected into the boundary layer, altering it and reducing

convective heating in the process. These gases also react chemically with the boundary layer gases, affecting the net heat to the surface. Energy deposition to the material is usually high enough that breakdown of the material bonds occurs and the material recedes. The net energy deposited to the surface is affected by the reaction kinetics, as the reaction may be endothermic (vaporization, sublimation) or exothermic (oxidation). Resin pyrolysis also produces a carbonaceous residue, termed “char,” on the reinforcement.

Ultimately, ablative TPS materials dissipate energy through many more mechanisms than those available to reusable TPS materials as illustrated in Figure 4.2.

Figure 4.2: Energy dissipation mechanisms in reusable and ablative TPS materials.



Aerothermodynamic and material response modeling tools provide critical information regarding several parameters, including:

- Time-resolved profiles of instantaneous heat flux,
- Heat load,
- Material temperature profiles (including bond line temperature),
- Surface pressure, and
- Surface recession, as appropriate.

Because the material properties of TPS systems are best determined empirically, different types of transducers embedded inside or along the surface of the material provide data to both scientific and engineering models. While surface pressures in varying atmospheric conditions may be fairly accurately predicted, the aerothermal heating is not as well determined, as the TPS energy dissipation process makes the analysis of the local heating

environment more complex. These models are most useful when coupled to other onboard instrumentation data, such as acceleration or velocity, to refine atmospheric models.

Potential Benefits to Missions

Mars

The NASA landed missions to date (Viking, Pathfinder, and Mars Exploration Rover) all employed a blunt, 70° half-cone angle aeroshell and the same forebody TPS material, Lockheed–Martin’s SLA–561.

Aerocapture at Mars is of interest because the low density of the Martian atmosphere and estimated aerothermal environment suggest that existing materials, including some newer low-density materials, are adequate for direct entry or aerocapture. On the other hand, a Mars Sample Return (MSR) mission would pose new challenges because direct entry from Mars into the Earth’s atmosphere would be at velocities of 12–14 km/s. Because the Planetary Protection requirements would be very stringent, a highly reliable TPS would be necessary. However, the only current heritage material, carbon phenolic, would not provide the optimum mass fraction, and other flight-qualified carbon fabrics may not be available.

Venus

Future landed missions could, in principle, use the same forebody TPS as Pioneer Venus if the same aeroshell shape is used. However, the heritage material employed for Pioneer Venus may no longer be available since it used a carbon cloth derived from a specific rayon fabric produced in the 1970s. Currently, new carbon phenolic composites using carbon cloth derived from alternate rayon fabrics or other precursors are under evaluation. Characterization and qualification of such composites is straightforward but will require time and resources.

To place an orbiter around Venus, NASA is evaluating the use of aerocapture, a process that would generate lower peak heat fluxes but significantly larger total heat loads. Fully dense carbon phenolic would probably not be appropriate because the large heat load would impose a significant TPS mass penalty. Therefore, a mid-density TPS with better insulation properties would probably be more suitable. Alternatively, a multilayer system employing a robust ablator backed by a high-temperature, low-density insulator would be attractive for a Venus aerocapture mission.

During the period when the Pioneer Venus probes were designed, the Giant Planet Facility did not exist. Testing TPS materials for a Venus entry mission was a challenge then and remains so today because no existing arc jet facilities operate on CO₂. Existing arc jet facilities do simulate the peak heating rates and pressures, albeit in air and on small samples. Radiative heating rates can be simulated with existing high-energy laser facilities, although the radiative spectrum would not be representative. Fortunately, high-density carbonaceous materials are surface absorbers over a broad range of wavelengths, making

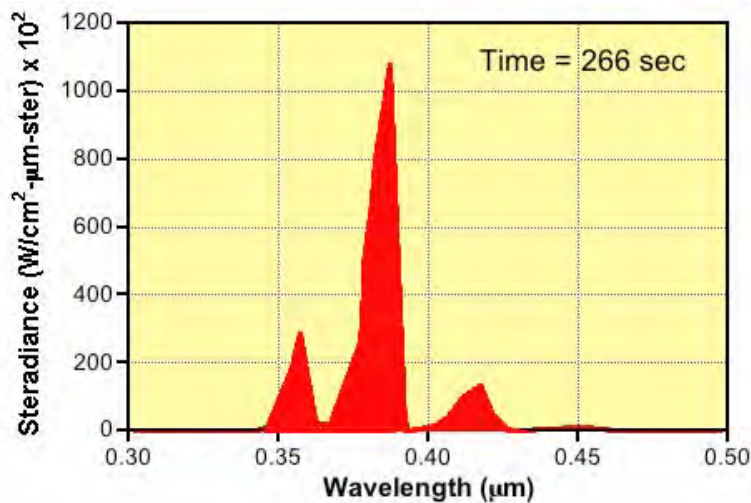
the simulated spectrum less critical. High-density carbonaceous TPS materials are reasonably well understood, and analytical scaling of their performance in air to the Venus atmosphere is straightforward.

Titan

In 2002, a NASA systems analysis team composed of technical experts from several NASA centers led a study to develop a conceptual design for an aerocapture mission at Titan. The team concluded that aerocapture was possible at Titan with a blunt 70° (half angle) rigid aeroshell entering the Titan atmosphere at an inertial entry velocity of 6.5 km/s. TPS sizing analyses were conducted for a broad range of candidate TPS materials and, as expected, low-density materials are the most attractive from a TPS mass standpoint.

However, there is significant uncertainty associated with the interaction of low-density TPS materials with UV radiation (i.e., the potential for in-depth absorption). Aerothermal analyses demonstrated that the cyano radical, CN, contributes to the large radiative heating rates, approximately twice those of convective heating and contained within the narrow UV band from 3500 to 4200 Å, as shown in the spectrum of Figure 4.3.

Figure 4.3: Spectral distribution of CN radiation on Titan.



This ultraviolet radiation raised a concern as a result of tests conducted 20 years ago, where materials were exposed to high-energy continuous wave (CW) and repetitively pulsed (RP) lasers at wavelengths ranging from visible ($0.53\mu\text{m}$) to infrared ($10.6\mu\text{m}$). Although specifics varied with the material and the incident heat flux, the data suggested that the performance of ablative materials degraded at the shorter wavelengths. Further studies demonstrated that the materials did not become semi-transparent at the shorter wavelengths, but rather

the absorption length increased with decreasing wavelength. The potential for in-depth radiant absorption is of concern since it could lead to char spallation that would significantly degrade material performance. The materials tested during these studies spanned the range from low-density organic resin composites to fully dense carbon–carbon composites, but none of the materials currently under consideration as candidates for Titan aerocapture was included in these studies.

Unfortunately, little is known about the specific performance of the AQ60 material used on the Cassini–Huygens probe. Apparently, design tests used an IR source but not UV sources.

Jupiter

Jupiter represents the most severe entry environment for probes due to the highest gravity well in the Solar System after the Sun, combined with the predominantly hydrogen atmosphere. Entry heat flux is contributed to both convective and radiative heating, which can reach over 30 kW/cm^2 . Fully dense carbon phenolic, used on the Galileo probe, is the only TPS material that could tolerate this heat flux. However, the Galileo recession data suggest that for a similar Jovian equatorial entry probe, the TPS mass fraction would probably exceed the 50% used on Galileo. Probes at higher latitudes, such as those envisioned in the Jupiter Flyby with Deep Probes, would require even higher mass fractions because the heating increases with the cube of entry velocity, and at higher latitudes the probe would benefit less from Jupiter’s rotation, thus would have higher entry velocities ($\sim 55 \text{ km/sec}$ at 30° latitude, compared to $\sim 47.3 \text{ km/sec}$ at the equator). As a result, the increased heating rates would cause char spallation to dominate the ablation process. Estimates suggest that the TPS mass fraction for such a mission using carbon phenolic would exceed 70%, leaving little mass for science payload. Retrograde probe entry results in velocities and entry heating that are beyond current TPS tolerance capabilities (see Table 3.10).

Neptune

Significant interest exists for both direct entry probes and aerocapture at Neptune.

Direct Entry Probes: Mission studies have determined that entry velocities at Neptune lie in the range of 28–32 km/s. Predicted stagnation point heating rates are very high, i.e., higher than Venus entry but lower than Jupiter entry (see Table 3.10). While fully dense carbon phenolic would be the primary forebody TPS candidate, the heritage carbon phenolic used in Pioneer Venus and Galileo may no longer be available.

Similar composites are under development, but need to be characterized and qualified. As for Jupiter, improvements in physics-based models are needed, specifically in the areas of radiative heating, turbulent convective heating, and the coupling of the shocked gas (which could be substantially ionized) with the recent materials in the presence of ablation products. Improvements in these models can reduce uncertainty and TPS mass fraction significantly as well as the high costs associated with the frequent operations of high-power arc jet facilities. As with Jupiter entry, limitations in existing ground test facilities present

significant challenges to validating any of these models. Thus, a qualification plan that carefully combines rigorous modeling with testing in existing facilities, or limited testing in future large-scale facilities, may be the best way to reduce both the risk and cost associated with TPS materials qualification for these missions. NASA is already considering qualification by analyses and test in other areas such as electric propulsion, where long-duration life tests are costly and in some cases impossible due to mission launch constraints.

Aerocapture: In 2003, a NASA systems analysis team conducted a detailed conceptual design study of a Neptune aerocapture mission and described an environment requiring a suite of solutions. The team demonstrated the requirement for an aeroshell shape providing a higher lift-to-drag (L/D) ratio than that of a blunt aeroshell. Aero thermal studies for an entry velocity of 29 km/s demonstrated that very high convective and radiative heating rates of 10–15 kW/cm² would be experienced in the stagnation region. Furthermore, the long flight time through the atmosphere would lead to enormous stagnation region heat loads of 1000–1500 kJ/cm². While the high heat fluxes suggest that only fully dense carbonaceous materials are viable candidates, the large heat loads dictate thicknesses that may exceed reasonable limits for uniformity. In areas away from the stagnation region, heat fluxes decrease and heat loads, although proportionately lower, are still very large.

State-of-the-Art

TPS Materials

Early NASA missions, including Gemini, Apollo, and Viking, employed new ablative TPS materials tailored for each specific entry environment. However, after Viking, NASA-sponsored ablative TPS development essentially ceased as the research focus shifted to reusable TPS in support of the Space Shuttle. For this reason, the Pioneer Venus and Galileo missions employed fully dense carbon phenolic developed by the United States Air Force for ballistic missile applications. Over the past 30 years, NASA adopted an approach to use historically flight-qualified materials exclusively, with the unintended consequence that the ablative TPS community in the United States has slowly disappeared. The Stardust and Genesis missions represented rare exceptions in developing new TPS materials, because those missions could not be accomplished with existing, flight-proven TPS materials.

Heritage materials are summarized in Table 4.1 and discussed in more detail in Table 4.2.

Over 40 years, NASA entry probes have employed relatively few ablative TPS materials, as shown in Figure 4.4.

Figure 4.5 shows the peak heat flux, associated stagnation pressure, and TPS mass fraction. NASA entry probes have successfully survived entry environments ranging from the very mild entry at Mars for Viking (25 W/cm² and 0.05 atm) to the extreme environment experienced at Jupiter by Galileo (30,000 W/cm² and 7 atm).

Table 4.1: TPS materials with flight heritage or under development.

TPS	Flight heritage or TRL level	Heat flux (W/cm ²)	Pressure (atm)
PICA	Stardust	>1000	<1
ACC	Genesis	<2000	>1
AQ60	Huygens	~250	<1
SLA 561 V	Mars	~300	<1
SLA 561 S	Mars	<20	<1
SIRCA	Mars	~150	>1
Carbon–Phenolic CMCP & TWCP	Venus, Jupiter	~100,000	≥1
Mid–Density Carbon–Phenolic including ARA PhenCarb Family	TRL 4–5	800 – 10000	>1
SRAM Family	TRL 5–6	~300	~1
Multi–Layer Systems (Carbon/Silica)	TRL 4–6	TBD	TBD
AVCOAT	Apollo/Earth Entry	~1000	~1

Table 4.2: TPS materials used on past and planned Mars and sample return missions.

Material	Mission	Heat flux (W/cm ²)	D _{aeroshell} (m)	Mission status
SLA 561 V	Mars Pathfinder	106	2.65	Completed
SLA 561 V	Mars Polar Lander / DS-2	100	2.4	Failed
SLA 561 V	Mars Exploration Rover	44	2.65	Completed
SLA 561 V	Mars Phoenix	65	2.65	Implementation
SLA 561 V	Mars Science Laboratory	155	4.6	Implementation
PICA	Stardust	1,200	0.83	Completed
ACC	Genesis	700	1.51	Completed

Mass fraction does not correlate well with peak heat flux and/or pressure, depending instead on the total integrated heat load, as shown in Figure 4.6. TPS material selection requires an assessment of the entry environment and a trade between ablation and insulation performance, thus requiring an analysis of the optimal performance characteristics. This optimization process can lead to lower mass fractions, such as the 13% for Pioneer Venus. The mission requirements to tolerate high heat fluxes, high pressures, and a relatively modest total heat load led to the selection of carbon phenolic, a relatively poor

Figure 4.4: Chronology of ablative TPS for NASA entry missions.

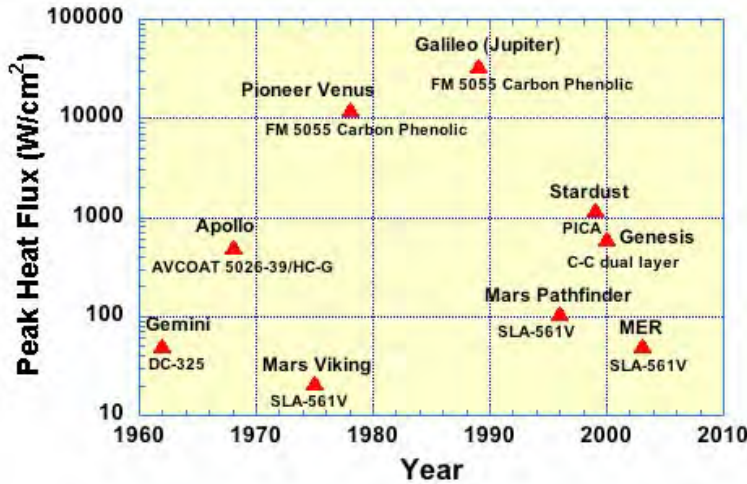
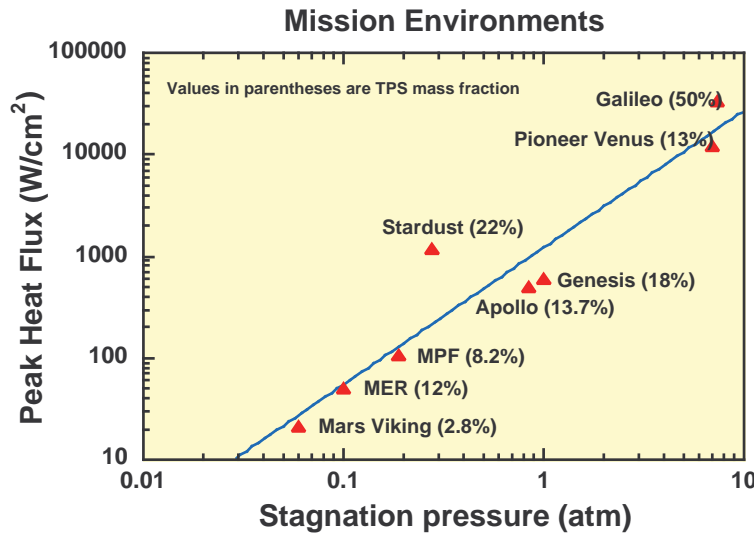


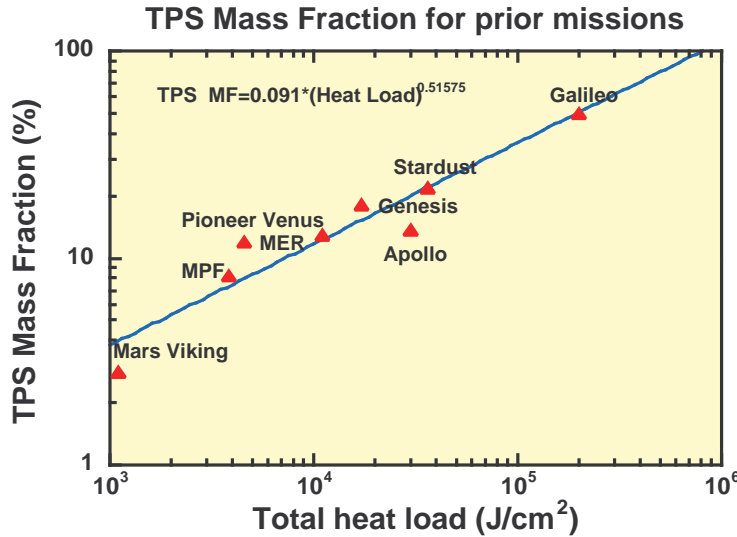
Figure 4.5: Mission environments for ablative TPS applications.



insulator but an excellent ablator.

For a given entry environment, materials selection requires a balance between ablative and insulation efficiency. Because both material strength and thermal conductivity increase with density, ablative TPS materials are often categorized by density, i.e., low density, mid density, and high density. Figure 4.7 illustrates material selection for a number of missions

Figure 4.6: Ablative TPS mass fraction for prior missions.



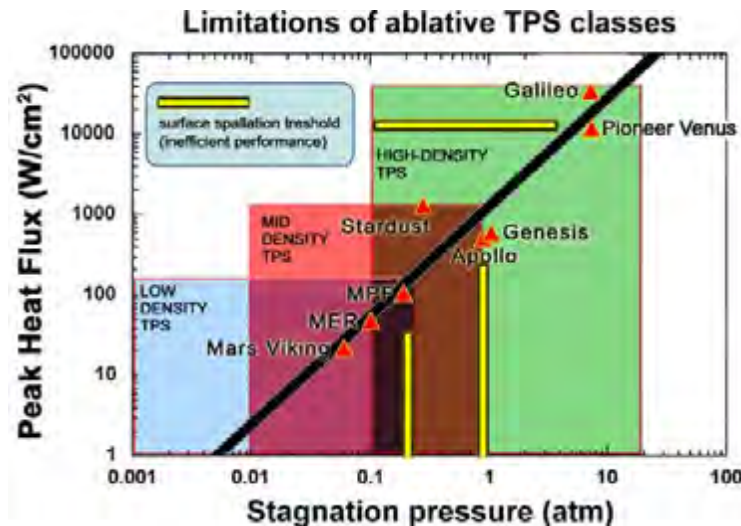
and shows that with increasing density, the threshold for char spallation moves to higher pressures and heat fluxes. A material used outside of its optimal zone leads to inefficient performance, resulting in a mass fraction less than optimal. Furthermore, providing minimal loss of thermal energy, char spallation consumes mass periodically in a way that is hard to model, making it highly undesirable.

Pressure Sensors

Many types of transducers exist to measure pressure. In the most common diaphragm transducer, two measurement and reference regions are separated by a diaphragm. The reference side is kept at a constant pressure of vacuum, one atmosphere, or another reference pressure. A pressure differential causes diaphragm displacement, converted to an electronic signal by measuring the change in resistance, capacitance, or inductance. Systems at TRL 9 have stainless steel or Inconel diaphragms. Although metal diaphragms are not suited for high-temperature applications because of plastic deformation and creeping, other materials may be more suitable. A ceramic diaphragm transducer is available for the automotive industry with integrated electronics on the same ceramic substrate. Micromachined silicon diaphragms with silicon-on-insulator (SOI) electronics transducers are available for high-temperature use. This is attractive for spacecraft applications because micromachining enables miniaturization of both the diaphragm and the surrounding unit. In addition, a smaller diaphragm gives an increased frequency response.

Electrochemical partial pressure sensors are either potentiometric, with an output varying exponentially with partial pressure, and amperometric, with an output linear in the partial

Figure 4.7: Limitations of ablative TPS classes.



pressure. The former sensor has a stronger variation with temperature than the latter. Electrochemical sensors are more tolerant at high temperatures and may be used to investigate catalycity. For instance, a zirconia-based oxygen partial pressure sensor operates only at temperatures exceeding 450°C, with a ceramic-based construction surviving temperatures of 1000°C. Unfortunately, thermal control presents a challenge as does power consumption.

Heat Flux Sensors

Heat flux is estimated by inputting measured temperatures into an appropriate heat transfer model. Direct measurements of incident heat flux require flux sensors to be mounted on the surface; otherwise, the TPS thermal properties must be well known to deduce the surface heat flux, although the accuracy diminishes with depth. Off-the-shelf heat flux sensors are typically fashioned from materials that function only in temperature ranges near room temperature. At high temperatures, reradiation of heat plays an important role in determining incident flux. For these applications, flux sensors with ceramic substrates and temperature sensors using precious metals have been fabricated for laboratory use.

Temperature Sensors

Measured temperature depth profiles allow TPS performance evaluation. Widely used thermocouples require no excitation power to operate, but they provide small output signals. While a thermocouple measures the small region defined by the junction, a resistance temperature detector (RTD) measures the line or area averaged temperature. This device requiring voltage or current excitation for operation, but provides high output and high accuracy.

Recession Sensors

Ablation processes alter the shape of the heat shield, changing both the mass and the lift-to-drag ratio. Ablation measurements provide additional information on TPS performance; however, this process is difficult to measure directly because the typical ablating surface temperature is 3000 K.

For the Galileo mission, the Analog Resistance Ablation Detector (ARAD) successfully recorded ablation even after encountering initial engineering challenges. However, the ARAD is not a true ablation detector because it follows the char layer instead of the ablating surface. The ARAD utilized a Kapton insulator because it becomes a conductor when it gets charred at approximately 700°C. Currently, several conceptual designs exist for non-Kapton-based isothermal devices with higher isotherms than Kapton.

Physics-Based Models

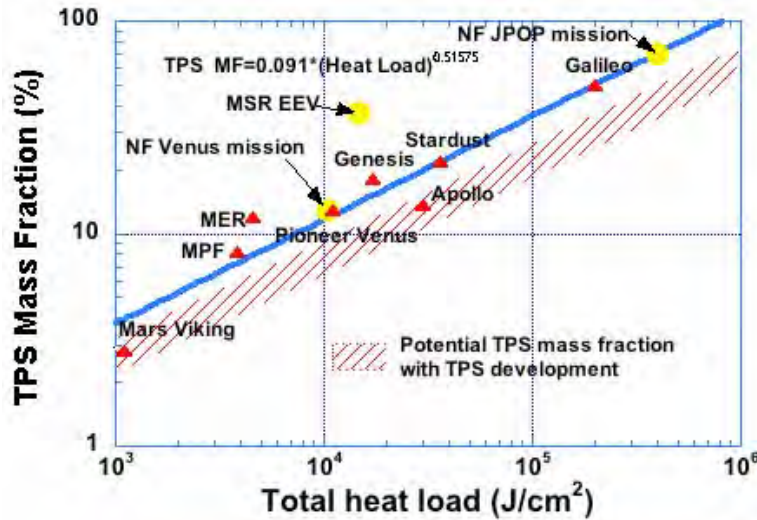
The flight data from the ten Galileo probe ARAD sensors showed that the predictions made by early models [MS82] overestimated the stagnation region recession (by about 30%) and substantially underestimated the frustum region. Great advancements have been made in the area of modeling high-speed flows over ablating bodies since that early (1982) work. For example, a Japanese study in 2005 showed that if injection-induced turbulence is included in the Galileo flow field simulation the final recession profile of the flight data at the frustum region can be closely reproduced; however, the stagnation region recession result from this study continued to overestimate the measurement. In earlier (2001) work performed in the U.S., the significance of the strong solid-fluid coupling on the predictions of the heat flux and recession shape was appreciated, and the effort led to the development of TITAN, a computer model for predicting charring material ablation and shape change of TPS materials. TITAN was developed in recognition of the need for advanced multidimensional modeling capability for the temperature response of the solid, which existing one-dimensional codes could not fulfill. TITAN was also “loosely-coupled” with a Navier-Stokes solver (called GIANTS) and benchmarked against typical arcjet models to demonstrate the fully-coupled, multidimensional solid-fluid modeling capability. Although the benchmarking problems were associated with heat fluxes much lower ($<0.8 \text{ kW/cm}^2$) than the Galileo probe entry values ($>30 \text{ kW/cm}^2$), the results demonstrated that accurate predictions of the ablator recession can not be achieved without using a fully-coupled solid-fluid multidimensional model.

Technology Development Needs

TPS Materials

Thermal Protection Systems can be mission enabling, at times significantly impacting the launch mass (with factors of 30–100) or science and instrumentation payload (1:1 trade with TPS). Figure 4.8 presents TPS mass fraction estimates for selected future mission concepts currently in the planning stages.

Figure 4.8: Ablative TPS mass fraction for past and selected future missions.



The crosshatched region of Figure 4.8 represents an estimate of the 20–50% potential savings in TPS mass fraction achievable with investment in TPS technology development. For Jupiter Polar Orbiter with Probes (JPOP), TPS mass fractions are estimated at 70%, while for Mars Sample Return (MSR), they are estimated at 37%. TPS technology development includes ground test facilities and improvements in models to predict the heating environment, as well as in TPS materials.

The general requirements are:

- Faster entry speeds (shorter trip times) lead to higher heat fluxes, demanding more efficient TPS.
- Aerocapture missions and in situ exploration via probes and landers must tolerate higher heat loads, requiring higher TPS mass fractions or more efficient TPS solutions.
- Sample return missions facing Earth re-entry requirements require robust and very efficient TPS, to reduce system mass and to assume containment of the sample where biological materials are concerned.

Pressure Sensors

Room-temperature pressure transducers at TRL 9 are commercially available. Both diaphragm and electrochemical pressure transducers are commercially available for use in limited temperature ranges.

Heat Flux Sensors

No high-temperature heat flux sensor is available commercially. A heat flux sensor in calorimeter mode can be fabricated in a few weeks. Emissivity analysis requires work on the timescale of months to years.

Temperature Sensors

Thermocouples with different sheath designs are commercially available, although applications to extreme environment require evaluation. An RTD good to 600°C is commercially available, and an RTD with a limit of 900°C can be fabricated with an estimated accuracy of 2°C in a few weeks. Insulation techniques need investigation.

Recession Sensors

No commercial product is currently available. ARADs or similar derivatives can be fabricated in a few months, although comprehensive studies are needed to give higher accuracy and reliability. Other recession designs are at the concept stage.

Physics-Based Models

Although the environment around bodies under benign entry conditions is well understood, the more extreme environments, such as those associated with Jupiter Deep Probes and Neptune-Triton Explorer missions, is not, as demonstrated by the Galileo TPS recession data. High-fidelity, multidimensional models that can resolve the physics of the shocked gas (which may be substantially ionized and turbulent), and can account for the radiation-rich hydrodynamic environment around highly-hypersonic planetary entry probes are needed. These models should take into consideration the strong coupling that exists between the fluid and the solid, which is very complex. Therefore, such model development must be part of a rigorous program with strong emphasis on validation.

4.2.2 Hypervelocity Impact Protection

Hypervelocity impacts from meteoroids during cometary flybys and passages through planetary rings or from space debris near Earth pose a potentially serious threat to spacecraft. Possible implications could include surface damage, unexpected changes in orientation, penetration of fuel tanks, damage to circuits.

Analysis of this risk requires description of the incident particles' mass and velocity distributions, as well as the shielding architecture. If this analysis is not conducted during the early phases of spacecraft design, it can provide severe constraints later and may impose a significant mass penalty for extra shielding.

NASA risk analyses show hypervelocity impacts to be one of the greatest threats to the survivability of the Space Shuttle³. Unfortunately, an expert committee commissioned by the

³Hypervelocity impact poses a greater risk than foam release at launch velocities.

NASA Engineering Safety Committee concluded that the Bumper II code, the primary tool for evaluating hypervelocity impact risk to the Space Station and Space Shuttle, is limited in applicability due to current uncertainties in hypervelocity particle environments, impact damage estimation equations, and impact-induced failure modes. The same problems exist for interplanetary and lunar missions, but the problems are arguably worse due to increased uncertainties in the environment definitions and the known decreased applicability of the vast majority of available impact test data to these environments. These uncertainties grow in severity with increased duration, particularly because current risk estimates for interplanetary missions are only valid to approximately one order of magnitude.

Potential Benefits to Missions

Accurate environmental and impact models could help reducing the risk of loss or damage associated with hypervelocity impacts. Furthermore, when used in conjunction with appropriate ground test capabilities simulating *in situ* conditions such as velocity, particle shape, and density, these models would permit potentially significant savings in mass, mission complexity, and performance.

State-of-the-Art

Modeling Particle Environments

Particle impacts, regardless of their mass and velocity, can be devastating for sensitive spacecraft components and should be assessed carefully. Impacts can range from low velocities (~ 1 m/s) with the mass of a bullet (~ 5 grams) to ~ 500 km/s at the 4 solar radii perihelion of a proposed “Solar Probe” mission. The latter could result in an impact energy over 60,000 J/mg. Therefore, it is very important to consider both the mass and the velocity of a particle population.

Particle distributions currently analyzed are shown below in Table 4.3. Masses range from micrograms up to several grams.

Table 4.3: Particle environments and associated representative velocities of hypervelocity impacts.

Environment	Velocities (km/s)
Earth's space debris	10
Interplanetary space	10–70
Planetary dust rings	5
Cometary debris clouds	70
Near-Sun dust cloud	500

While models (listed in the References) have improved, there is not an actual Solar Envi-

ronment Model for debris. Furthermore, these models are limited in their data sources to primarily 1 AU and masses below 1 mg. There are several national and international efforts underway to improve this situation, but progress is slow, and a resolution is not likely for several more years.

The Earth Space Debris environment definition is mainly the responsibility of the NASA Johnson Spaceflight Center. The debris environment is not currently well modeled above 2,000 km. It is a very dynamic environment as new launches are taking place globally and occasionally explosions in the existing debris take place, such as from booster stages.

Models of cometary dust environments and planetary ring environments are still in their initial stages, with unique models describing each body. In the short term, Cassini is rapidly improving the understanding of Saturn's rings, but those of Jupiter are still under study, as are those of Neptune and Uranus. Models of comets have similarly met with limited success, though preliminary studies suggest that comets present unique characteristics in their jets and surface structure.

Modeling hypervelocity impacts

The effects of hypervelocity impacts are typically simulated phenomenologically from data or from physical models. Empirical models are typically limited to particle sizes and velocities that are easily simulated in the laboratory; this translates to large particle simulations of 1 g and 7 km/s, or 1 g particles traveling at 1–70 km/s⁴. Resulting damage to hardware or shields varies with many different physical parameters; for the incident particle, these parameters include particle velocity, impact angle, mass, and density, and for the target, the thickness, strength, density, and physical separation with a shield are relevant.

Each shielding or hardware configuration requires a unique failure prediction equation, determined empirically or from sophisticated hydrodynamic impact computer codes (e.g., CTH, PICES). Typically, hypervelocity impact tests are used to populate a database to calibrate a computer model, then used to extrapolate to other particle masses, velocities, or variations in the shielding parameters. Unfortunately, even under the most ideal modeling and testing conditions, many uncertainties remain, making shielding design and evaluation difficult at best. Indeed, the need for a set of well-validated codes is one of the major problem areas for hypervelocity impact analysis.

The historical focus on “penetration” does not address the fact that impacting meteoroids often pass through multiple elements before hitting the critical component, producing an evolving debris cloud as each component is perforated. In this case, the debris cloud’s behavior often determines the damage in the ultimate critical component, rather than the “penetration” into a single element. Debris cloud behavior is much more complex than penetration into a single plate or semi-infinite surface. Penetration damage to critical

⁴Goller and Grun [1989] presented results of 40 km/s velocities for 1.13×10^{-16} g.

components may not lead to perforation, but may still cause component failure, especially lightweight, filament-wrapped pressure vessels.

Hypervelocity Testing

Appropriate testing facilities able to deliver solid masses to the target and accurately simulating impact conditions currently do not exist. Hypervelocity impact tests must replicate the composition, size, and shape of the impacting particle, its velocity vector, the shielding configuration, and the target configuration⁵. Of these, the particle's mass and velocity are typically the most difficult to simultaneously simulate. Currently, although a few hypervelocity impact facilities are capable of accelerating test masses representative of the environment up to 18 km/s, the great majority of impact testing lies in the range of 3–7 km/s. This latter range is unfortunately below the 10 km/s (space debris) to 30 km/s (meteoroids) representative of the actual space environment.

New facilities use laser or shaped charge accelerators, where a particle or flyer plate is accelerated by a high-energy, short-duration laser pulse or by a shaped explosive charge. Higher velocities can be achieved by electrostatic techniques, but facilities of this type are no longer operational nor relevant because the simulated velocities describe particle masses from ng to μg , a range typically not considered a threat to spacecraft. Although the newer techniques are somewhat more expensive and difficult to use, the gas gun's limit of velocities below 7 km/sec falls below the velocities of interest.

Hypervelocity impact damage is stochastic, with no two impacts producing identical damage even if produced by identical projectiles and velocities on the same targets. This makes statistical analysis rise in importance, suggesting that per-test costs must be minimized.

Shielding Technologies

Hypervelocity particle impact shielding technology has been typically based on military vehicles, protecting for masses from grams to kilograms, but with velocities far below 1 km/s. Although this lies well outside the range appropriate to spacecraft, the basic shielding paradigms still apply. Furthermore, much of the recent technology development has supported the Space Station and Space Shuttle, minimizing risks from higher particle masses with shields much too heavy for NASA's typically mass-constrained unmanned spacecraft, requiring significant extrapolation for robotic vehicles and ultimately suggesting impractical, massive shield designs.

Shielding for single surfaces is based primarily on mass per unit area, so that higher masses absorb greater amounts of impact energy. Recently, advanced materials like Kevlar and Nomex have proven very useful in reducing shielding mass, as have foam techniques developed for spacecraft. Multiple surface shields, such as a Whipple shield or more complex designs, work by providing a thin sacrificial shield or shields serve to break up the impacting

⁵Relevant configurations might differentiate between a pressurized vessel or an operating electronic circuit.

particle. The resulting debris cloud with smaller particles or gases then releases its energy over a larger area, thereby reducing the local effects⁶.

Given enough information, shielding can be tailored to specific configurations and environments. Often, designers conservatively assume that only a shield provides protection, not the supporting hardware. This assumption adds mass to the design, saving time because it is then not necessary to determine the impact response of the underlying hardware. Furthermore, critical hardware performance following shield failure has historically not been included in testing programs. Commonly used hardware requiring further study include honeycomb panels, pressurized tanks, multilayer insulation, power and signal cables, and carbon composites.

One new technology is the foam core shield (FCS), developed recently with the goal of improving on the performance of Multilayer Insulation (MLI).

Systems Engineering

Systems concerns for shielding architectures include prioritizing different system elements. An example is the shielding analysis of the Space Station, shown in Figure 4.9. Modules are ranked in importance by the population inside; i.e., crewed sections are ranked higher than empty modules. Different modules may thus require different strategies. This systems engineering process has not been formalized.

The NASA Bumper II code structure may be useful for this activity, but it has not been optimized for the environments relevant to unmanned exploration.

Technology Development Needs

Modeling Particle Environments

Protection against meteoroids requires data and models at distances other than 1 AU. Debris fields for altitudes exceeding 2000 km are needed.

Modeling Hypervelocity Impacts

Standardized, validated empirical cratering and penetration models for impact velocities of 5–40 km/s are needed, as are validated codes capable of modeling complex shielding geometries.

Hypervelocity Testing

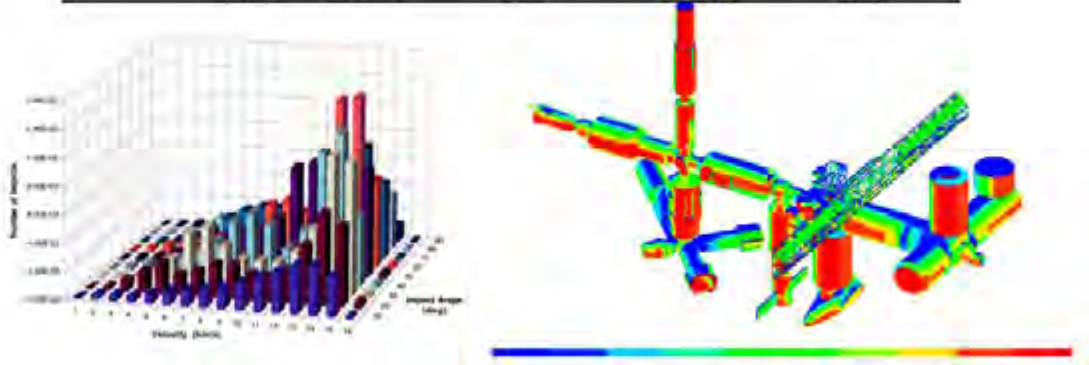
Rapid and cost-effective techniques are needed for impacting particles of 1 mg mass and 40 km/s velocity. Standardized test protocols are needed to evaluate new shielding configurations.

⁶This technique works optimally over a narrow range of masses and velocities and can, under some conditions, actually worsen the impact effects.

Figure 4.9: Impact shielding analysis for the Space Station.
Failure probabilities for each module are shown. (Based on the NASA Bumper II code; courtesy M. Matney and J.C. Liou, NASA JSC.)

Computation of Penetrating Flux and PNP (SHIELD) Graphical Interpretation of Results (EXCEL & I-DEAS)

Space Station Orbital Debris Threat Assessment				
Station Region	Impact Risk From 1mm Ø Debris		Debris Penetration Risk	
	Probability No Impact	Odds of Impact	Probability No Penetration	Odds of Penetration
FGB	0.995338	1/214	0.995541	1/224
Service Module	0.999335	1/1505	0.999796	1/4912
Node 2	0.990465	1/105	0.999998	1/625000
Hab Module	0.965074	1/29	0.998923	1/928
Lab Module	0.965522	1/69	0.999022	1/1023
CRV	0.997443	1/391	0.999839	1/6223
TOTALS	0.934622	1/15	0.993132	1/146



Shielding Technologies

Shielding materials of lower mass are needed for impacting particles of 1 mg mass and 40 km/s velocity.

Systems Engineering

A standardized methodology to evaluate shielding architectures for efficiency and reliability is needed.

4.2.3 Radiation Shielding

Radiation shielding provides protection from particles trapped in planetary magnetic fields, and emitted from the Sun. It may also be used to shield spacecraft subsystems from gamma/neutron radiation from onboard nuclear sources. These particles pose a serious hazard for electronic devices, electromechanical devices, thermal control materials, optical coatings, and dielectric materials used in a spacecraft.

The traditional method of protection against radiation has been the application of shielding mass in concert with radiation-hardened components to achieve the required end-of-mission performance. The next generation of space missions is expected to have increased mission duration and scientific observation time in regions of high radiation, such as the trapped particles at Jupiter or Saturn or the solar energetic particles at Mercury or Venus. Therefore, radiation shielding will be increasingly used to protect radiation-sensitive electronic devices, materials, and coatings.

The effective use of shielding mass depends on the mission's average radiation environment, the environment local to a sensitive device or material of interest, and the radiation tolerance of that element. Some mitigation measures may include added shielding mass, rearranged component placement to provide more protection, or even device or material substitution. Protection for electronic devices, dielectric materials, and electromechanical devices may be both expensive and design constraining. Unfortunately, the process of modeling the global and local radiation environments and validating mitigation measures has proven to be uncertain to date, requiring large design margins.

Potential Benefits to Missions

The potential benefits to missions are a reduction in required shielding mass to protect the spacecraft electronics and dielectric materials, as well as an increased spacecraft lifetime in severe radiation environments. Improvements are needed in modeling the charged particles trapped in planetary magnetic fields or in solar energetic particle (SEP) events, as well as in attenuation effects of shielding materials and geometries. Such analysis would allow more reliable estimates of the mission radiation environments, leading to reduced shielding masses and better assessments of science instrument performance over the mission's life. Model validation of shielding attenuation through ground testing would improve shielding design.

State-of-the-Art

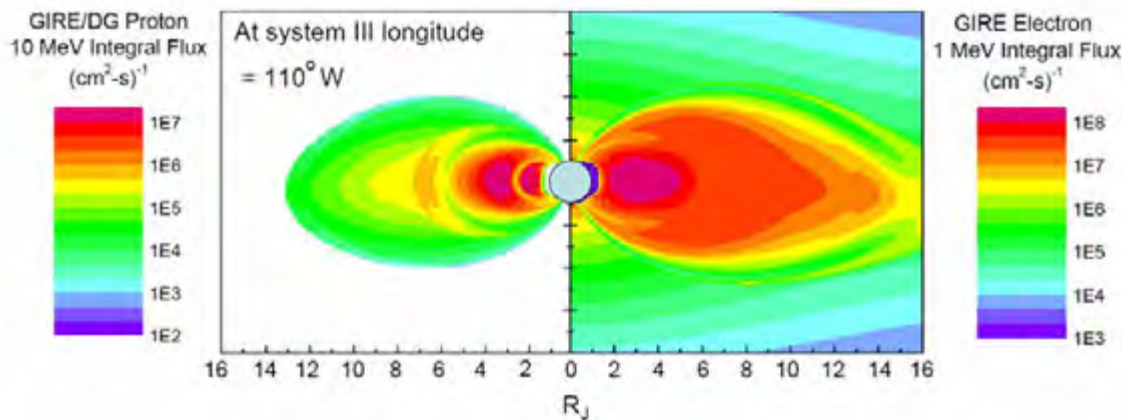
Models at the Outer Planets

Work on models of the energetic particle environment at Jupiter began in 1970s and was based originally on data from the Pioneer 10 and 11 spacecraft returned from flybys of Jupiter in 1973 and 1974, respectively. The models were then refined with data returned by Voyagers 1 and 2, both of which flew by Jupiter in 1979. For electrons and protons, this work led to the Divine model, the standard Jovian radiation belt model for the last three decades. However, this model is limited because the Pioneer and Voyager data only provided quick snapshots of the Jovian magnetosphere, thus covering only a limited temporal and spatial range.

On the other hand, the Galileo spacecraft orbited Jupiter between 1995 and 2003, executing 34 orbits and completing the mission through Jupiter entry on the 35th orbit. The

extensive scientific data returned from Galileo has improved the understanding of the Jovian radiation environment; specifically, the data from the Galileo spacecraft's Energetic Particle Detector (EPD) has been used to refine and update the Divine electron model. Galileo provided a manyfold increase in spatial and temporal coverage over the previously existing data set. The equatorial electron model developed from the Galileo EPD data was combined with the Divine model's pitch angle information to generate a complete Jovian trapped radiation model, the Galileo Interim Radiation Electron (GIRE) model that provides updated electron radiation environment estimates for radii in the range $8 \leq L_J \leq 16$. The GIRE model still uses the Divine analysis for proton fluxes at all spatial ranges, and for electron environment fluxes outside a proscribed range. These models are still being updated by additional data recorded on Galileo science instruments. Figure 4.10 illustrates the trapped particle distribution at Jupiter obtained with the Divine and GIRE models.

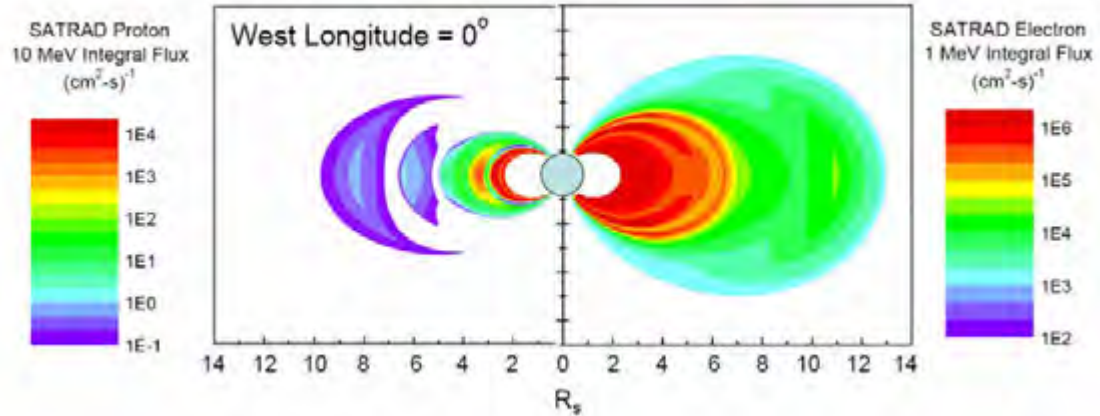
Figure 4.10: Proton and electron distributions at Jupiter.



The radiation belts at Saturn have not received as much attention as those at Jupiter because they are not nearly as intense; the famous particle rings tend to deplete the belts near the expected peak. As a result, a systematic development of engineering models for Saturn's radiation environment has not taken place, except for the model of Divine. That study used the published data from several charged-particle experiments aboard the Pioneer 11, Voyager 1, and Voyager 2 spacecraft during their flybys of Saturn to generate numerical models for the electron and proton radiation belts between 2.3 and 13 Saturn radii.

Recently, a computer model (SatRad) of Saturnian radiation belts based on the Divine numerical model has been developed. It is expected that this model will be updated with data returned by Cassini, currently orbiting Saturn. Figure 4.11 shows the trapped particle distribution obtained using the SatRad model.

Figure 4.11: Proton and electron distributions at Saturn.



The magnetically trapped charged particle populations at Uranus and Neptune were sporadically mapped by instruments onboard the Voyager 2 spacecraft. Models of the particle populations similar to those developed for Jupiter and Saturn can be developed with the Voyager data.

Modeling at the Inner Planets

The radiation environment at Mercury and Venus depends strongly on the solar energetic particle (SEP) flux. The radial variations of fluxes and fluences of ions have been approximated by a R^{-3} dependence and a R^{-2} form, respectively, based on a model where high-energy particles were produced in gradual events, accelerated by the flares, then scattered and propagated within the corona to large distances from the flare site. The accelerated particles then leave the corona over a broad range of angles from the flare site and propagate in the interplanetary medium.

However, this model has been largely replaced by one in which coronal mass ejections (CMEs) play an important role in producing energetic particles. CMEs occur in association with flares, but they are not believed to be causally related. Instead, flares and CMEs are two forms of energy released into the solar atmosphere. High-velocity CMEs travel through the interplanetary medium at supersonic speeds and cause shocks to form in the solar wind. Particles accelerated at these shocks form SEP events by leaking from the acceleration region and propagating in the interplanetary medium. The particles' path generally follows the field lines connecting to the CME shock area as it travels through space, rather than the field lines connecting to the flare site. As they propagate, the particles diffuse along and across the field lines, and are trapped in the vicinity of the shock area for some time

prior to escape.

When the CME shock passes over the spacecraft, it will enter a region of enhanced fluxes. As particle acceleration continues behind the shock, it forms the largest and most dangerous fluxes. Historically, events have been categorized as flare-accelerated impulsive events or shock-accelerated gradual events, each with its own radial dependence. However, this categorization may not be appropriate because some events may have particles, accelerated by both flares and shocks, with different radial variations for each component. This is complicated further by the fact that flare-associated events are only observable for flare sites that are well-connected via magnetic field lines to the observation point and can be distinguished. In addition, other structures associated with CMEs, such as high-energy particles trapped in closed magnetic configurations, have recently been suggested as SEP sources.

Several groups are developing theoretical models with different approximations and assumptions. The fluxes and fluences depend on the shape and velocity of the CME, which is affected by its interaction with the ambient solar wind as it propagates through space. The interaction of the accelerated particles with the solar wind magnetic fields and waves also affect fluxes and fluences. Research has shown that the radial dependencies vary strongly with energy and that the simple approximations used in older models do not sufficiently describe the data.

SEP fluences often show enormous longitudinal variance, as well. Major proton events are produced by a series of CMEs from a single activity center as the solar rotation carries it across the face of the Sun. When a CME propagates outward, it is probed by the magnetic field lines back to Earth as well as by the direction; this may manifest itself as a probe moving from the shock's flank to its nose or vice versa. Since the shock strength differs at the nose versus the flank, both the temporal profile and energy spectrum of energetic protons reaching 1 AU and beyond vary with the solar longitude. This is seen in measured proton fluences; those proton energies, $E > 10$ MeV, are associated with CMEs near the central meridian, but the largest fluences, $E > 100$ MeV, are from CMEs on the receding limb, magnetically connected to the observation platform. The magnitude of the longitudinal variation has not yet been well constrained; this represents another needed modeling and analysis effort.

Modeling Spacecraft Shielding

A spacecraft and its components must be designed to tolerate all the anticipated radiation environments it is expected to encounter. The use of additional shielding mass is undesirable due to the considerable mass penalty. Materials commonly used in spacecraft shielding, listed in Table 4.4, are often used in multilayer systems comprising combinations of materials to minimize the shielding mass. Multilayer structures are optimized through modeling the incident particle distribution and energy spectrum. A standardized shielding design protocol would accelerate the design of optimized systems with minimized mass penalties.

Table 4.4: Radiation-shielding materials and atomic weights.

Material	Atomic number Z (amu)
Aluminum	13
Copper	29
Tantalum	73
Tungsten	74

The spacecraft’s structure provides the bulk of material shielding the sensitive electronic devices and materials from the radiation source. Radiation transport codes use the external charged-particle population, neutron, or gamma-ray source as inputs and transport those particles through a spacecraft model describing structural elements, fuel tanks, the electronic chassis, circuit cards, and other elements. The outputs of the radiation codes are the attenuated spectra at the location of interest. The spacecraft model must accurately preserve geometry, material thickness, and material composition. This model is typically constructed manually, a process that may be extremely labor intensive, depending on the required fidelity. This practice has inspired the development of computer-assisted drawing (CAD) conversion routines, a process requiring continued attention to reduce labor costs and minimize mass penalties.

Ground Tests of Shielding Materials

The charged-particle shielding effectiveness of materials in the energy regime of interest to spacecraft designers, 0.01 to 100 MeV, has been estimated primarily with Monte Carlo radiation transport codes, such as ITS3, MCNPX, NOVICE, and GEANT4. Peer reviews for the Prometheus Project noted the absence of associated ground test measurements. This is problematic because the models’ adequacy of the radiation transport codes and the derived designs cannot be accurately assessed, ideally for multilayered shielding in simple geometries at varying energies for different particle. A ground test program using electron and proton beam testing would address these issues; the Prometheus Project identified suitable electron beam facilities at Renssalaer Polytechnic Institute and the Massachusetts Institute of Technology that would be appropriate.

Validation of Radiation Transport Codes

Due to limited computational power, early radiation transport codes used ray-tracing to convert all materials in the spacecraft mass model to an equivalent thickness of aluminum⁷ with a dose-depth database to determine energy deposition at specified locations. This quick analysis produced conservative results and lost spectral information in the process.

⁷Equivalent thickness calculations convert all other materials to aluminum by scaling the density appropriately.

Monte Carlo radiation transport codes use actual geometry and material effects to calculate local radiation environments.

Monte Carlo radiation transport codes can be divided into two types: forward and adjoint codes. Forward codes, such as MCNPX and GEANT4, transport particles from the source region to the point of interest and effectively compute local environments in complex geometries with directional radiation sources, such as monoenergetic beams. However, they do not efficiently analyze large geometries with small targets in an isotropic poly-energetic particle environment because the radiation transport model discards a large fraction of source particles. Adjoint Monte Carlo codes transport the particles from detector to source, thus minimizing losses of relevant source particles and making these codes desirable for space radiation modeling. The major charged-particle adjoint transport code available to the U.S. spacecraft industry is the NOVICE code, the standard for at least a decade and in development for 20+ years. Unfortunately, the NOVICE code must now be considered a sunset technology, due to the likely retirement of the code author in the next decade.

The Sandia National Laboratory has recently announced the development of ITS5, a new adjoint Monte Carlo charged-particle radiation transport code. This code requires review to determine its compatibility with existing codes and its readiness as a potential successor to the NOVICE code. Historically, code validation has been done by comparison to other codes, primarily MCNPX or GEANT4. The Prometheus Project peer review also noted that experimental validation is desirable to address potential deficiencies that may surface during use for space environment radiation transport. New irradiation data generated during ground tests could be used for code validation through modeling at the test facility and a thorough peer-reviewed comparison of results.

Technology Development Needs

Models at the Outer Planets

Galileo data must be integrated into models at Jupiter and Cassini data are required for models at Saturn. Preliminary models are needed for charged particles at Uranus and Neptune.

Modeling at the Inner Planets

Charged-particle models are needed for Mercury and Venus.

Modeling Spacecraft Shielding

Multilayer shielding design guidelines should be standardized. The CAD interface to the NOVICE code should be evaluated and continued. Spacecraft geometry models should be refined further to accelerate modeling capabilities and minimize mass penalties.

Ground Tests of Shielding Materials

Various materials should be evaluated as shielding materials for high-energy electrons and

protons.

Validation of Radiation Transport Codes

The upcoming sunset of the NOVICE code should be addressed by evaluating the ITS5 code or other charged-particle adjoint Monte Carlo radiation transport code. New codes must be evaluated and compared to the existing codes MCNPX, NOVICE, and GEANT 4. Ground test data should be incorporated into forward and adjoint codes.

The Europa Explorer pre-project at JPL has recently initiated a reassessment of environments, shielding and radiation codes. The results are expected to be available in late 2007.

4.2.4 Pressure and Thermal Control Technologies

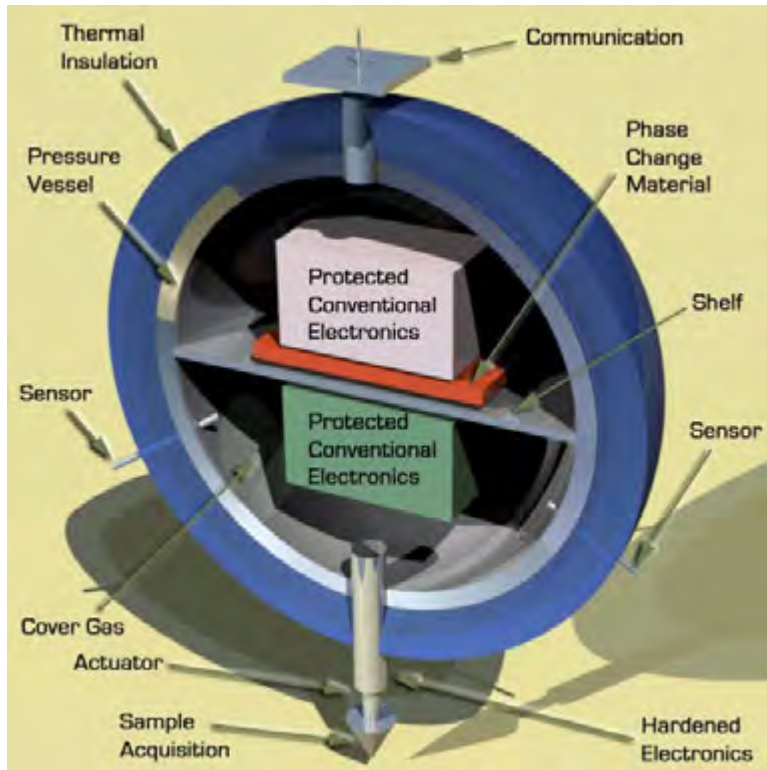
Spacecraft electronic systems will require varying degrees of thermal protection from the Venus thermal and pressure environment. Development of high-temperature electronics will allow many components to operate at either Venus ambient temperatures of 460°C or at some other intermediate elevated temperature, such as 200–300°C. Systems operating in these temperature regimes can simplify the spacecraft thermal control system and potentially reduce the overall system mass. However, it is likely that some electronic components will not be able to survive in environments of high temperatures and pressures. Specific science instruments, for example, may fall into this category since these are typically one-of-a-kind components and requiring them to operate at high temperatures may be impractical. Thermal systems for these kinds of electronic devices can use several techniques to keep them operational for the duration of the mission. Figure 4.12 shows a general schematic describing an application of a hybrid architecture to a pressure and thermal vessel.

Thermal control methods rely on isolation from external heat sources, removal of self-generated heat by local thermal energy storage, or active cooling. Isolation and thermal storage work well for short durations, but long-term service will require active cooling techniques. Development of thermal systems and pressure vessels will require additional developments in power systems and electronic components to become viable systems suitable for operating under extreme environment conditions.

Potential Benefits to Missions

Several mission scenarios exist for exploring Venus and the outer gas giant planets. Mission configurations for Venus typically include balloon platforms, atmospheric probes, landers, rovers, or seismic probes, among others, with lifetimes varying from hours to months for different architectures. For the gas giants, the mission architectures usually are either atmospheric probes or balloon platforms. The breadth of possible mission architectures dictates that technology developments in thermal systems and in pressure vessels will be multi-faceted. For this reason, this report summarizes a variety of thermal control systems that may enable several different mission architectures. While giving an indication of some of the

Figure 4.12: Schematic of a hybrid architecture for a pressure and thermal control vessel for Venus landers.



leading candidate thermal technologies, it is by no means an exhaustive study of the subject.

Future missions to the Venus surface or deep within the Jupiter atmosphere will require capabilities far exceeding those of Pioneer Venus or the Galileo Probe. Extending mission lifetime beyond one or two hours will call for much lighter pressure vessels and thermal control systems that can keep all components operational significantly. The mass saved in the pressure vessel could be reallocated to the thermal control system or in additional science instrumentation. Furthermore, successful mission architectures will need to permit communication back to Earth for more than just a couple of hours.

State-of-the-Art

Pressure Vessels

Most pressure vessels consist of a monolithic metal shell such as steel, titanium, or aluminum. Steel and aluminum do not have the specific strength of titanium and therefore are not competitive alternatives for a Venus probe. Carbon fiber reinforced composite over-

wrapped pressure vessels for space applications are well developed and offer significant mass reductions, compared to metallic shells. However, composite vessels are unable to survive the extreme temperatures encountered in the Venus environment because of the intolerance of the matrix resins used in fabrication.

Previous missions to the Venus surface by the Soviets and the U.S. used titanium to construct the pressure vessel. Because the pressure vessel represents the single largest mass in a Venus surface spacecraft, any pressure vessel mass reduction will have significant benefits, particularly in designing for tolerance of the 200–400 G deceleration loads experienced during atmospheric entry.

Thermal Control Systems

Thermal control systems have made several significant developments since the last missions to Venus. The Soviet Venera Landers used a rigid porous, silicon-based material for insulation on the exterior of the pressure vessel, as well as lithium nitrate trihydrate, with a heat of fusion of 106 Wh/kg (295 kJ/kg), as a phase change material (PCM) for thermal energy storage. The modules probably had an aluminum casing with aluminum fins for increasing heat transfer into the PCM. Even today, most PCM modules used on spacecraft utilize a paraffin PCM, with a heat of fusion of 82 Wh/kg (230 kJ/kg). Since the mass of paraffin in a PCM module is roughly half the total module mass, the effective energy absorption at the melting point is approximately 41 Wh/kg (115 kJ/kg).

Lithium nitrate offers significant advantages over paraffin or water as a PCM material. Since it has a specific gravity of 1.5, it has twice the density of most paraffins and a 50% improvement over water. Thus, the lithium nitrate PCM mass fraction is 65% of the total module mass and the effective energy absorption at the melting point is 70 Wh/kg (195 kJ/kg). Furthermore, the specific heat of lithium nitrate is higher than typical paraffins, granting even greater thermal storage capacity over a wide temperature range.

The Pioneer Venus mission used 41 layers of MLI to insulate the interior of the pressure vessel and protect the internal electronics from the Venus environment. The large probe was filled with xenon gas and the small probes were filled with nitrogen, both at about 100 kPa. The gas fill served to eliminate the possibility of corona discharge of interior electronic equipment, should the vessels leak in the Venus atmosphere. Although MLI is most effective in hard vacuum environments, the large number of layers used on Pioneer Venus enabled the blanket to work effectively at reducing convection from the hot pressure vessel wall. The use of beryllium for equipment shelves took advantage of the high specific heat to provide thermal storage.

Few significant advances in PCM module technology, other than the use of carbon foams as filler materials, have taken place. This application provides increased thermal conductivity into the PCM over aluminum fins and reduces mass.

Aerogel represents a significant advance in insulation technology because it has extremely low density and conductivity and it is effective over a wide range of temperatures. Other insulation advances include metal foams and ceramic foams suitable for high-temperature, high-heat flux applications.

Long-term missions on Venus will require a form of active refrigeration to keep sensitive electronics operating for periods longer than a day. Active refrigeration technology has been focused on cryocooler development and has become a mature technology. However, none of this “high heat lift” capability has been directed toward systems that could operate in a Venus environment. Typical cryocooler technology provides less than 5 W of cooling at low temperatures, while consuming on the order of 100 W of power. Most temperature lift magnitudes are on the order of 250°C.

Technology Development Needs

A 90 cm O.D. Venus lander pressure vessel absorbs an average of 1,700 W during the 1 hour descent, then an average of 1,500 W for the first 10 hours on the surface⁸. Because the bulk of energy is absorbed by the shell itself as its temperature increases, novel shell architectures and material integration may extend mission duration. Novel architectures include innovative materials used in pressure vessel construction, and the integration of specific materials for added thermal control. Finally, lander design may also include active cooling or refrigeration systems.

Pressure Vessels

The extremely high deceleration loads experienced by spacecraft entering the atmosphere of Venus or Jupiter amplify the benefits of reducing the mass of the pressure vessel. Significant opportunities for improvement in this area exist because the mass of a titanium pressure vessel can be reduced by approximately 50 to 65% using new materials and manufacturing methods.

At 500°C, the shell must have a compressive yield strength, compressive modulus, and creep strain rate such that it satisfies the following criteria:

- No buckling at the ultimate load of 150 atm pressure using the standard NASA knock-down factor of 0.14 for pressure vessels. Knockdown factors account for imperfections in the material and the manufacturing process leading to deviations from the ideal case; the common industry standard knockdown factor is 0.30. The elastic modulus

⁸These are based on a thermal model, developed at JPL, that accounts for a descent profile of ambient temperature, pressure, and velocity to compute an average convection coefficient. In general the descent heat absorption roughly corresponds to a velocity of 15 m/s and a convection coefficient of 130 W/m²K. The vessel has interior and exterior insulation. The average temperature difference between the exterior shell and the ambient environment is about 5°C. For the landed case, the average convection coefficient is 28 W/m²K. Although the convection coefficient is ~1/5 as large in the landed case the overall heat flow is dominated by the insulation resistance so the variation in external convection is damped. The average temperature difference between the exterior shell and the ambient environment is about 21°C when landed.

determines the buckling limit.

- No yielding at the proof load of 125 atm pressure. The yield strength determines the yield limit.
- The total allowable creep in 10 hours under 100 atm external load must be less than 0.5%.

Further relevant mechanical properties include fracture toughness, heat capacity, and thermal expansion coefficient. In addition, the shell must be impermeable to gases and compatible with the chemical environment. While low conductivity would also benefit thermal properties, better insulation can mitigate the risks of using conductive materials.

An extensive study by JPL revealed the advantages and limitations of several materials:

- Inconel 718 showed the best performance in both creep and tensile property comparisons and is the best metallic candidate for a pressure shell using a honeycomb sandwich construction.
- Ti-6Al-4V was the second-best performer in the creep and tensile comparisons at temperature. This is the traditional Venus lander spacecraft pressure vessel material and is fabricated in a monolithic shell.
- Beryllium is lightweight and has high elastic modulus, high thermal conductivity, and high specific heat, but low creep resistance in tension at temperature. Toxicity issues raise concerns regarding fabrication; however, established vendors exist to fabricate beryllium products.
- Of composite materials, a SiC/Ti matrix composite has superior strength/density performance compared to other materials and is creep resistant at 500°C; it is suitable for fabricating a monolithic shell configuration.

In all the metal candidates, buckling was the limiting criteria except for beryllium because of its high elastic modulus. A comparison of elastic modulus as a function of material density at room temperature is shown in Figure 4.13 for the metallic candidates. At 500°C, the magnesium and aluminum alloys drop out of consideration. Beryllium clearly has the highest modulus per unit mass of all candidates even at 500°C, but it is limited by yield and creep.

These materials are characterized in Table 4.5. However, these parameters do not capture the significant challenges to manufacturing methods presented by these technologies.

Three different pressure vessel configurations have been identified for these materials. The traditional manufacturing process for spacecraft landing on Venus's surface is to fabricate monolithic shells from titanium or beryllium. Composite wrapped shells are commonly seen in pressure cylinders and the technology is well developed. This manufacturing technique

Figure 4.13: Modulus comparisons of various metals at room temperature.

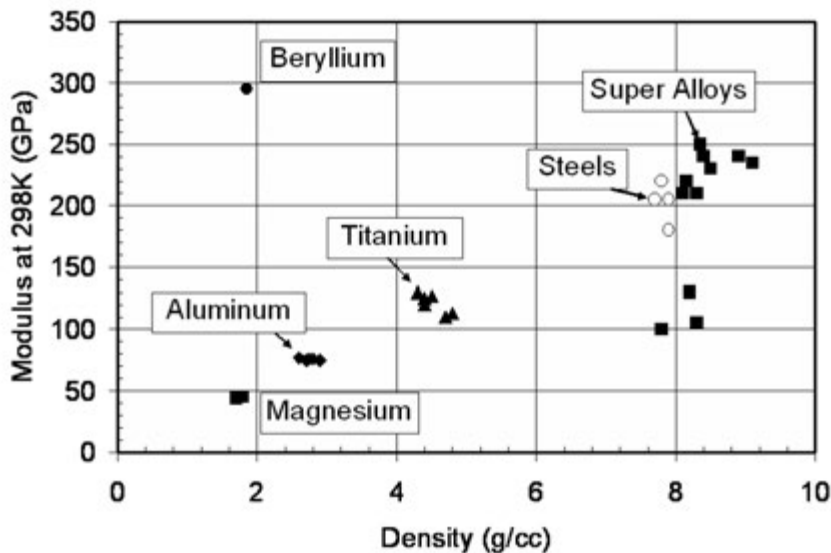


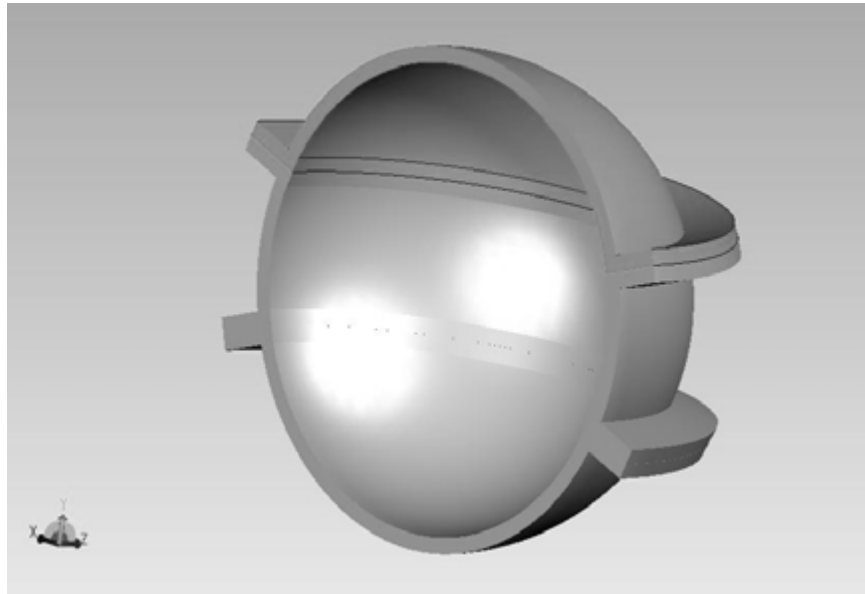
Table 4.5: Candidate materials for pressure vessel shell structure.

Material	Elastic modulus (MPa)	Yield strength (MPa)	Poisson's ratio	Density (kg/m ³)
Ti-6-4	79,293	448	0.31	4,429
Inconel 718	176,512	931	0.29	8,221
Ti matrix	213,745	1,696	0.28	3,332
Beryllium	227,535	171	0.10	1,855

would be used for aluminum/sapphire or aluminum/silicon carbide or Polymer Matrix Composite materials. An appropriate fabrication technique for Inconel 718 would be to form honeycomb sandwich shells into curved geometries, as is commonly done for aircraft engine cowlings.

Fabricating a monolithic shell for a pressure vessel uses fairly common manufacturing processes. A titanium hemisphere can be shaped using spin forming. Features such as flanges, windows, feedthroughs, and brackets may be welded onto the shell to create the spacecraft pressure vessel. A three-piece sphere allows two equipment shelves to be mounted to a central ring, while the forward and aft sections of the sphere serve as caps mounted to the center section. An example of a three-piece sphere is shown in Figure 4.14.

Figure 4.14: Cut-away sectional view of a three-piece monolithic shell.



Because beryllium is brittle and cannot be shaped by spin forming, fabricating a monolithic shell can be more difficult than it would be for titanium. The spherical sections would have to be machined from solid billets; features, such as flanges and windows, could not be welded to a beryllium shell and would therefore have to be machined as part of the shell from the parent billet material. A three-piece spherical shell is preferred for beryllium because the billets for each section would be smaller than if the shell were made into hemispheres. This process is also more forgiving of rework processes because only 1/3 of the sphere, rather than half, would be at risk at one time. Unfortunately, the number of vendors qualified to work with beryllium is limited.

Composite-wrapped tanks are now commonplace and the latest innovations involve linerless tanks. The impermeable aluminum liner has been replaced by using resins that form a gas-tight barrier that resists microcracking as the pressure cylinder is repeatedly loaded and unloaded. The manufacturing process consists of passing the wrapping fibers through a wet adhesive, such as molten aluminum or epoxy. The wetted matrix is then wrapped around a mandrel to form the tank shape. The composite-wound tank is then cured at an elevated temperature to set the tank.

A picture of composite-wound linerless tanks is shown in Figure 4.15. While this process is suitable for fabricating pressure cylinders or composite tubes, it has not been used to fabricate hemispherical sections. Thus, the manufacturing process for creating a structural

shell for a spacecraft with flanges, windows, feedthroughs, etc. still requires development.

Figure 4.15: Linerless composite tanks.

Developed by Composite Technology Development Inc. The wrapped tank may be used as the pressure vessel if it can be made with flanges and feedthroughs. It will also have to be insulated to keep it from coming apart at high temperatures. This is being developed between JPL and Ceramic Composites Inc.



While most honeycomb structures are flat panels, honeycomb sandwich construction produces strong lightweight panels for many applications, particularly for curved components. Manufacturing a spherical segment in this fashion requires forming the inner and outer facesheets into the desired shape using a bulge-form technique. A picture of a bulge forming tool is shown in Figure 4.16.

The honeycomb core is made by diffusion bonding thin corrugated sheet (ribbon) sliced to the desired web thickness. The core is then bulge-formed to match the inner and outer facesheets and assembled to the facesheets in a special toolset; a braze alloy is added to bond the facesheets to the core. For a titanium structure, TiCuNi braze alloy would be used, while for Inconel, the braze alloy would be BNi-8. Several methods for completing the brazing process exist, but typically the assembly would be placed in a vacuum braze furnace, as shown in Figure 4.17. When the brazing process is complete, the tool set is removed and the part is ready for attaching features, such as windows, flanges, and brackets, by cutting the shell for openings and brazing the features in place.

Figure 4.16: A typical bulge forming tool for fabricating honeycomb facesheets.



Thermal Control Systems

Thermal control systems can be categorized as passive or active technologies. Passive techniques are suitable for short-duration missions, typically less than 24 hours, while active systems manage heat flows for systems operating for longer durations. Both would take advantage of phase change materials (PCM), solids with high heats (enthalpies) of fusion. Like most materials, the temperature of a PCM in its solid phase rises as it absorbs heat. At the melting point, PCMs can absorb significant amounts of heat without a temperature increase, making them valuable for missions to extremely high temperatures.

Passive cooling: Significant breakthroughs in the mature areas of thermal energy storage or insulation technology are unlikely. However, innovative designs using known materials may significantly extend the surface lifetime in the Venus environment. Water and lithium are two simple materials that can be used in lander designs.

Water alone may be used effectively because by transitioning from a frozen state at -20°C to a vapor state at 315°C and 92 bars, water can absorb about 900 Wh/kg. With a mass fraction of approximately 40%, the effective energy storage capacity would be around 360 Wh/kg (1,000 kJ/kg). Thus, the heat storage capacity of the pressure vessel could be significantly increased if it incorporated several kilograms of water within its structure. The water vapor (at 315°C and 92 bars) would then have to be vented to the atmosphere to drive the vaporization process to completion. A sketch of such a system is shown below in Figure 4.18.

Figure 4.17: A vacuum braze furnace for bonding honeycomb structures.



The heat storage capacity of the pressure shell may also be increased by including a layer of lithium. Lithium, with the highest specific heat of any solid (nearly twice that of beryllium), melts at 180°C and has a heat of fusion (429 kJ/kg) exceeding that of water at (333 kJ/kg). While its low density (530 kg/m³) causes volume concerns, lithium does not require a high-pressure containment system nor a vent to the atmosphere, compensating for a storage capacity (500 Wh/kg) that is only half that of water. Furthermore, it can continue absorbing heat until the shell reaches the Venus ambient temperature, whereas when all the water is vented, the shell would increase in temperature more rapidly. The estimated mass fraction of lithium in the thermal energy storage system is about 40%, providing an effective thermal energy absorption of around 251 Wh/kg (700 kJ/kg). A model is shown in Figure 4.19.

An alternative concept, based on water evaporation and lithium–water chemistry, allows the electronics and shell parasitic loads to generate heat that vaporizes water, taking advantage of the high heat of water vaporization, 667 Wh/kg (2,400 kJ/kg). This vapor is then absorbed by lithium metal, acting as a water–getter; as the vapor exits the electronics, it may absorb additional parasitic heat from a radiation shield inside the shell, then piped to an exterior vessel containing a lithium metal matrix. A highly exothermic reaction takes place, forming liquid LiOH, a low–density LiH powder, and Li₂O powder. This system can potentially remove 3 to 4 times more energy per unit mass than the best PCM technology,

Figure 4.18: Schematic of a Venus lander pressure vessel with a water PCM shell liner.

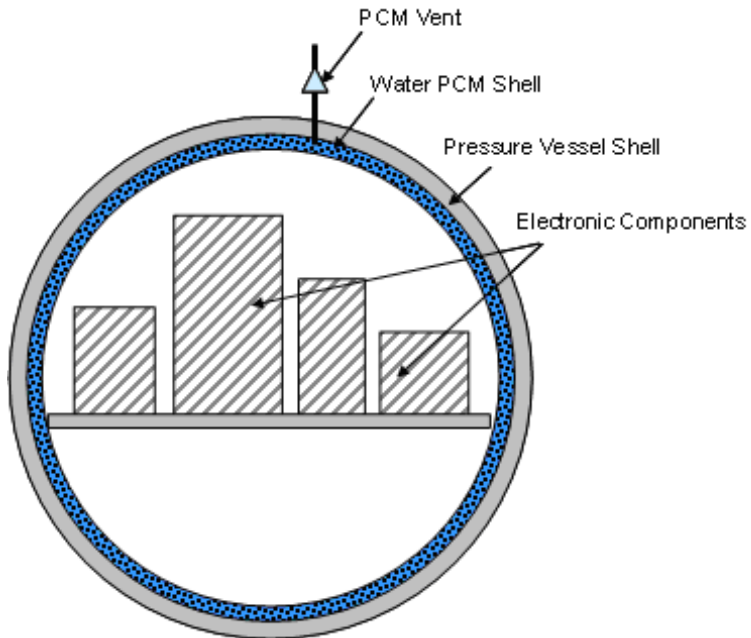
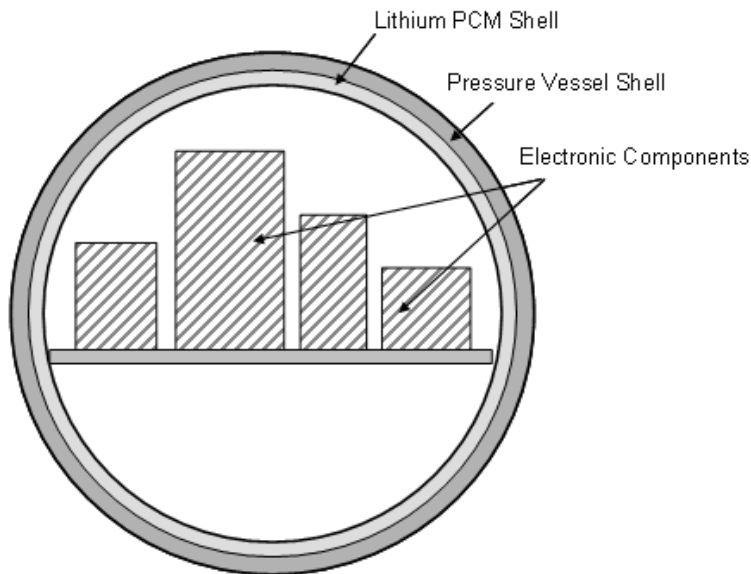


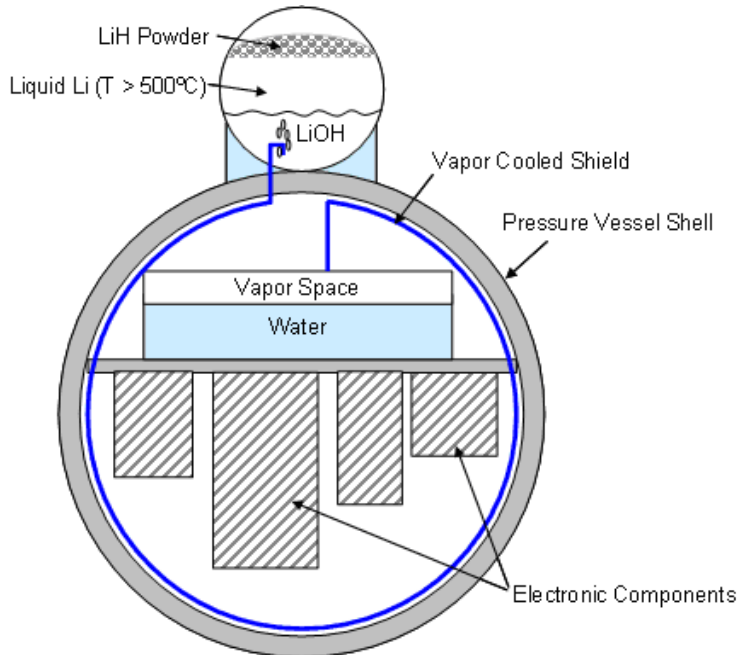
Figure 4.19: Schematic of a Venus lander pressure vessel with a solid–liquid lithium PCM shell liner thermal energy storage system.



including the mass of the lithium and the water. This technique has not yet been experimentally demonstrated.

In another version, the high-temperature lithium/water reaction could generate electric power. Like the first system, the water starts at a frozen state, absorbing 900 Whr/kg of water mass. This system would be combined with lithium, reducing the storage capacity to 500 Whr/kg for the combined lithium–water mass (see Table 4.6). It is estimated that the mass of water and lithium would be about 30% of the total thermal energy storage system mass, providing an effective energy storage capacity of 180 Wh/kg (500 kJ/kg). A schematic of this water–lithium system [Jon93] is shown in Figure 4.20.

Figure 4.20: Schematic of a Venus lander pressure vessel with a water–lithium thermal energy storage system.



A number of other materials have been considered for similar concepts. These materials are characterized below in Table 4.7.

Active cooling: Active cooling or refrigeration is required to sustain an extended mission (in excess of a few days) on the surface of Venus. Certain vital components of exploration vehicles, such as microprocessors and imaging sensors, cannot be hardened to operate at the temperature of the Venus surface with their desired functionality intact. The Venus surface refrigeration system would be designed to remove heat leaking in from the environment, as

Table 4.6: Thermal storage of water– and lithium–based passive cooling.

Architecture	Storage capacity (Wh/kg)	Comments
Water	360	Improved mass fraction (higher density)
Lithium	251	Does not require venting
Water–lithium	180	Not experimentally demonstrated

Table 4.7: Estimated material thermal properties at 92 bars in order of increasing melting temperature.

Material	Formula	Melting temperature (°C)	Density of solid (kg/m ³)	Density of liquid (kg/m ³)	Heat of fusion or vaporization [†] (kJ/kg)	Storage capacity (Wh/kg)
Water (melt)	H ₂ O	0	897	1,000	333	119
Gallium	Ga	30	5,900	-	80.3	29
Sodium hydrogen phosphate	Na ₂ HPO ₄ :12H ₂ O	36	1,520	1,450	280	100
Sodium hydroxide monohydrate	NaOH:H ₂ O	64	1,720	-	272	98
Cerrobend	Alloy	70	9,400	9,200	33	12
Water (vapor)	H ₂ O	100	-	-	2260	812
Lithium [‡] (solid)	Li	180	530	-	260	94
Methyl fumarate	(CHCO ₂ CH ₃) ₂	102	1,045	-	242	87
O–mannitol	C ₆ H ₁₄ O ₆	166	1,489	-	294	106
Aluminum chloride	AlCl ₃	192	2,440	-	272	98

[†] The energy storage associated with solid–liquid transformations is the heat of fusion, while that associated with liquid–gas transitions is the heat of vaporization.

[‡] Lithium is highly reactive and therefore is not expected to absorb heat in its liquid state prior to undergoing a reaction with radicals in the environment.

well as heat dissipated by electronic components, such as microprocessors and image sensors, in the cooled volume. This section reviews the fundamental limits on the performance of such a refrigerator for the Venus environment, summarizes some of the past work on practical refrigeration solutions, and discusses some of the more promising technologies for future application.

High–temperature mitigation is typically referred to as active cooling or refrigeration. The term “refrigeration” is rooted in the act of bringing the temperature below the freezing point; in space applications, it is generally used for cryocoolers, which are heat pumps operating in cryogenic environments. Temperature mitigation in the extremely high tem-

peratures of Venus will also require heat pumps on long-lived missions. Therefore, the terms “active cooling” and “refrigeration” will be used interchangeably throughout this discussion.

Principles of Refrigeration Applied to Venus

The efficiency of a power-generating or refrigeration cycle can be expressed as:

$$\begin{aligned}\text{Efficiency} &= (\text{Work Performed})/(\text{Total Energy}) \\ &= (Q_h - Q_c)/Q_h \\ &= 1 - Q_c/Q_h\end{aligned}$$

where Q_c and Q_h represent the heat flow at the cold and hot ends, respectively. The ideal or “Carnot” efficiency has been shown to be $(1 - T_c/T_h)$.

For practical refrigeration cycles on Venus,

$T_h = 500^\circ\text{C}$ (773 K), for heat rejection to the Venus ambient at 460°C (733 K).
 $T_c = 50^\circ\text{C}$ (423 K), for typical electrical component operation.

Thus, the maximum refrigeration efficiency is $1 - 423/773 = 0.453$.

For practical power generation on Venus,

$T_h = 1000^\circ\text{C}$ (1273 K), due to material considerations.
 $T_c = 500^\circ\text{C}$ (773 K), for heat rejection to the Venus ambient at 460°C (733 K).

Thus, the maximum power generation efficiency is $1 - 773/1273 = 0.393$.

The major associated challenges of this Venus surface mission are to develop a system capable of efficiencies approaching the Carnot limit of efficiency and to furnish the power required to drive the refrigeration system. Six refrigeration system concepts are discussed below:

1. *Thermoacoustic Refrigeration*: As part of an assessment of active cooling of electronics in high-temperature well holes, a team at the Los Alamos National Laboratory considered various options for a high-efficiency refrigerator. This study team recognized that while the common vapor compression (Rankine cycle) refrigerator had very high efficiency, it was only practical for modest temperature differences. Extending this concept to a multistage refrigerator based on the Rankine cycle would require a complex system using many different fluids.

On the other hand, the study team determined that a thermoacoustic refrigerator with a purely gaseous working fluid could achieve reasonably high efficiencies; consequently, they built and tested a prototype for cooling components to 150°C in a

300°C environment. In this study, electric power could be furnished through a power cable from a generator at the wellhead, leaving the problem of generating power in a high-temperature environment unaddressed.

2. *Multistage Rankine/Brayton:* A multistage reverse Rankine and reverse Brayton cycle refrigeration cycle was designed by Allied-Signal AiResearch for a Discovery Workshop Mission Proposal for a Venus surface mission (<http://www.msss.com/venus/vgnp/vgnp.txt.html>). The system was designed to provide 14.5 W of cooling at 93°C with a R-11 reverse Rankine cycle, which was staged to a AlBr₃ reverse Rankine cycle at 149°C, which was then staged to an argon reverse Brayton cycle at 400°C. The total input power was 230 W, yielding an efficiency of 0.063. A sketch of the refrigeration system is shown in Figure 4.21.
3. *Coupling Refrigeration with Power Generation:* In a NASA study conducted at Glenn Research Center under the Revolutionary Aerospace Systems Concepts (RASC) program, it was recognized that for Venus surface operations, the approach to power generation and refrigeration needs to be coupled. The power source for an active cooling system on the surface of Venus is assumed to be based on radioisotope heat generation. Because approaches based on solar photovoltaic energy, wind energy, and the energy in the atmospheric temperature gradient appear to be less practical, they were not explicitly evaluated in this study.

NASA has been involved in the development of a power generator designed to operate over a temperature range similar to that of the proposed refrigerator (50–500°C). The Stirling Radioisotope Generator (SRG), currently under development at Glenn Research Center, is a free-piston machine operating on a Stirling thermodynamic cycle. The heat input to the converter results in a temperature at the hot end of 650°C, while heat is rejected from the cold end at 80°C. Approximately 250 W of input heat is converted with a linear alternator into reciprocating motion, resulting in an electrical power output of 62 W. The resulting electrical efficiency is almost 25%, compared with the theoretical value of 62% for an ideal (Carnot) generator operating over the same temperature range. On Venus, the SRG would need to reject heat at a temperature of approximately 500°C; the temperature of the generator's hot side would likely be limited by material properties of both the General Purpose Heat Source (GPHS) bricks and generator components to approximately 1000°C, further limiting the efficiency.

The Glenn team studied a “free-piston” Stirling-cycle refrigerator using a helium working fluid, with a compression ratio of about a factor of 10. Like the Los Alamos thermoacoustic refrigerator, this free-piston refrigerator used an inert gas working fluid to exploit the Stirling thermodynamic cycle. Stirling Radioisotope Generators (SRG) operating on the same thermodynamic cycle as the refrigerator and using a plutonium-238 heat source for energy provided power to the refrigerator. The

plutonium–238 is encapsulated in GPHS modules, with each module containing approximately 600 g of plutonium dioxide and producing about 250 W of thermal power at the beginning of life (BOL). In the Stirling Radioisotope Generator, this thermal power is converted first to mechanical power and then to electrical power. It is more efficient to drive the Venus refrigerator directly with the mechanical energy, although electrical power would still need to be generated to operate sensors, computers and communications systems.

Accordingly, the refrigerator was based on a “kinematic” design with a large stroke crankshaft, driven by the generator using a chain and sprocket approach. The efficiency for the Stirling–cycle refrigerator was projected to be 0.376 to provide a compartment cooled to 200°C in a 500°C environment. A block diagram of the cooler is shown in Figure 4.22.

4. *Thermoacoustic Stirling Heat Engine:* In a more recent study of operating vehicles at the surface of Venus, a JPL team developed a concept for powering a Venus rover and refrigerating electronics and sensors using the Thermoacoustic Stirling Heat Engine (TASHE), developed by a team at Los Alamos National Laboratory and Northrop Grumman Space Technology (NGST). The system converts high-temperature heat into acoustic power that provides both electric power and cooling for the rover. The TASHE system provides thermal control through a pulse tube cooler that keeps the rover’s electronics at temperatures below 50°C. With a total cooling load of 414 W and 3,000 W input power, the efficiency was determined to be approximately 0.14.

The energy budget for the TASHE system is shown in Figure 4.23. Figure 4.24 shows a prototype, and Figure 4.25 illustrates a concept for a rover on Venus using TASHE to provide power and cooling.

While the TASHE concept has been demonstrated as both a cryocooler and a heat engine, no components have been built to operate at the high temperatures needed for power generation. For many missions exploiting the technologies discussed elsewhere in this report, it should prove possible to reduce thermal parasitics and generation in the cooled volume to well below the 414 W indicated; a system with just a few kW of heat input may prove to be quite feasible.

5. *Thermoelectric Power Generation:* Thermoelectric technology that converts radioisotope heat directly into electricity represents the only conversion technology flown in space to date. For the Venus application, the low conversion efficiency relative to the Stirling cycle is a shortcoming; however, novel thermoelectric materials can operate at the high temperatures of the Venus environment. The simplicity of thermoelectric conversion, requiring neither moving parts nor control electronics, may make it attractive for a range of missions. Malin Space Science Systems has suggested that a thermoelectric conversion efficiency for a Venus surface RTG would be about 0.04.

6. *Lithium Refrigeration with Power Generation:* An alternative one-month surface cooling system has been proposed by Jack A. Jones [Jon93] in which liquid water would be stored in a cooling cavity of a Venus surface vessel; the water would be evaporated and reacted with a lithium water getter. All the products of reaction are significantly below 0.01 bar atmospheric pressure at temperatures well above the Venus surface temperature of 460°C, thus providing cooling at or below about 0°C. For a well-insulated vessel, a one-month mission would remove 50 W total (10 W electrical, plus 40 W parasitic heat) and would require about 44 kg of lithium and 57 kg of water (Figure 4.20). The total reactant mass is thus about 101 kg. Assuming the use of battery power, no vibration takes place. The battery mass would be about 18 kg for a 30-day mission, assuming a primary battery energy density of 400 Wh/kg.

Alternatively, the system's waste heat of reaction of 600 W could potentially be used to power a Stirling cycle refrigerator without the need for an RPS. However, the refrigeration system assumes very low radiation emissivities of $\varepsilon = 0.010$ and $\varepsilon = 0.005$, thus essentially eliminating the possibility of axle protrusions through the vacuum vessel. For higher ε values of 0.06 and 0.03, allowing for axle protrusion, the system would produce a total heat load of 250 W (10 W electrical plus 240 W parasitic heat), and the system lifetime would be reduced to about 6 days.

Figure 4.21: Three-stage diagram of Rankine/Rankine/Brayton mechanical cooling system.

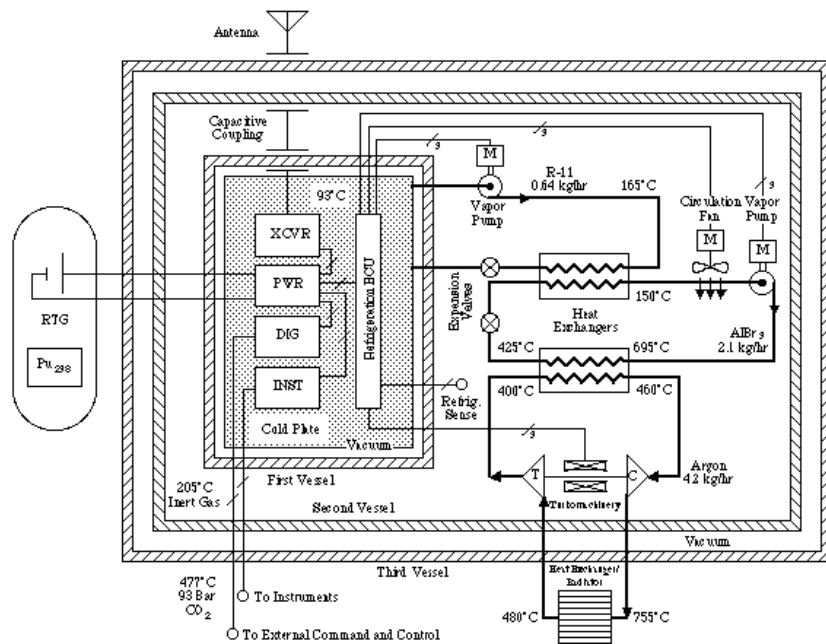


Figure 4.22: Block diagram of a Stirling mechanical cooler.

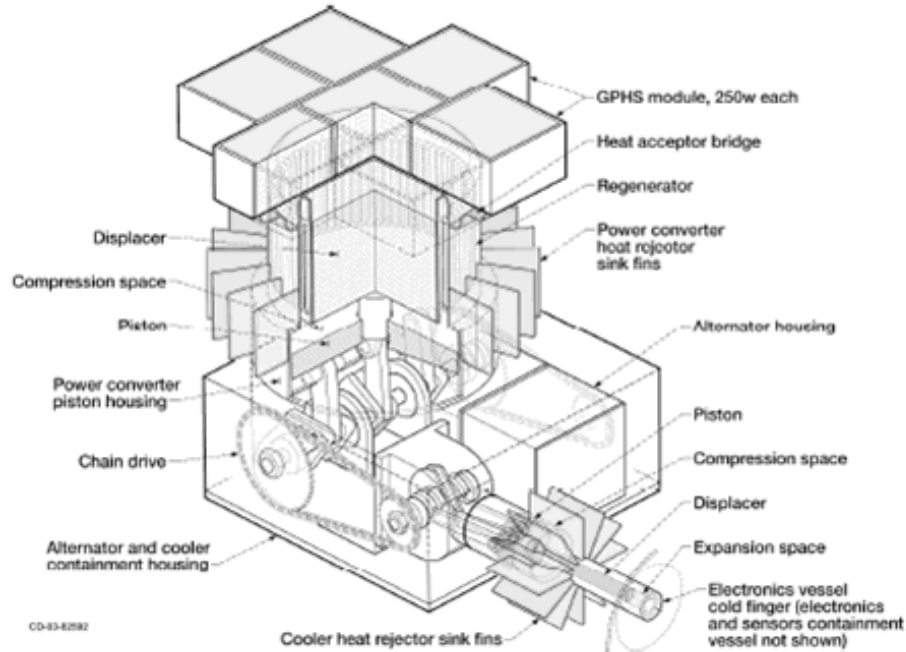


Figure 4.23: Energy budget for a Venus cooling system based on the Thermoacoustic Stirling Heat Engine (TASHE) technology.

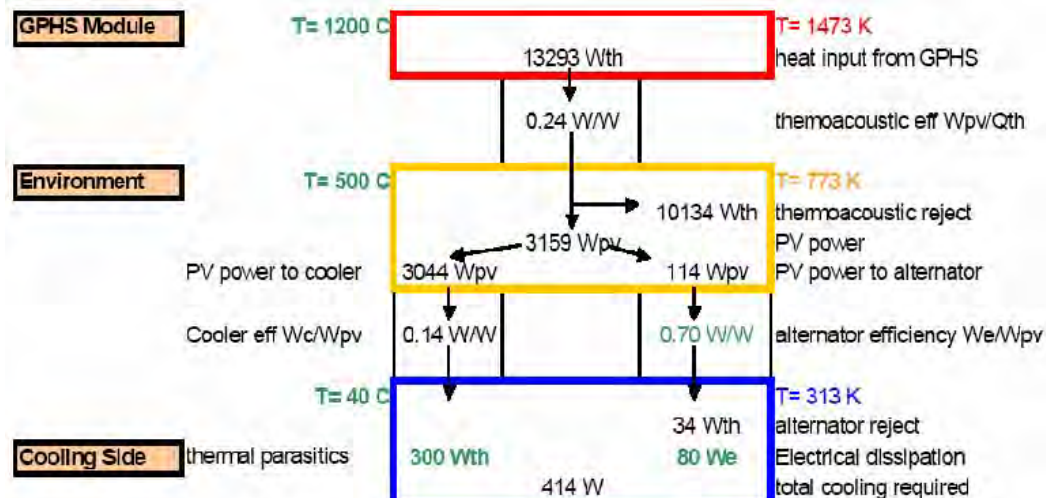


Figure 4.24: Prototype for the Thermoacoustic Stirling Heat Engine (TASHE).

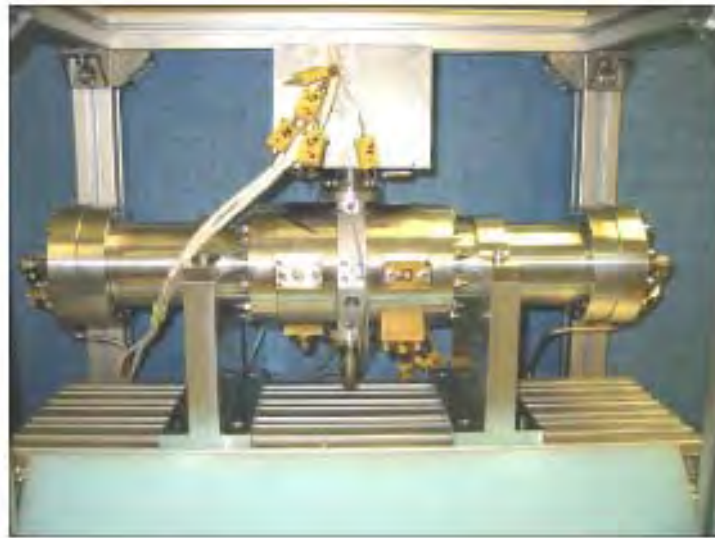
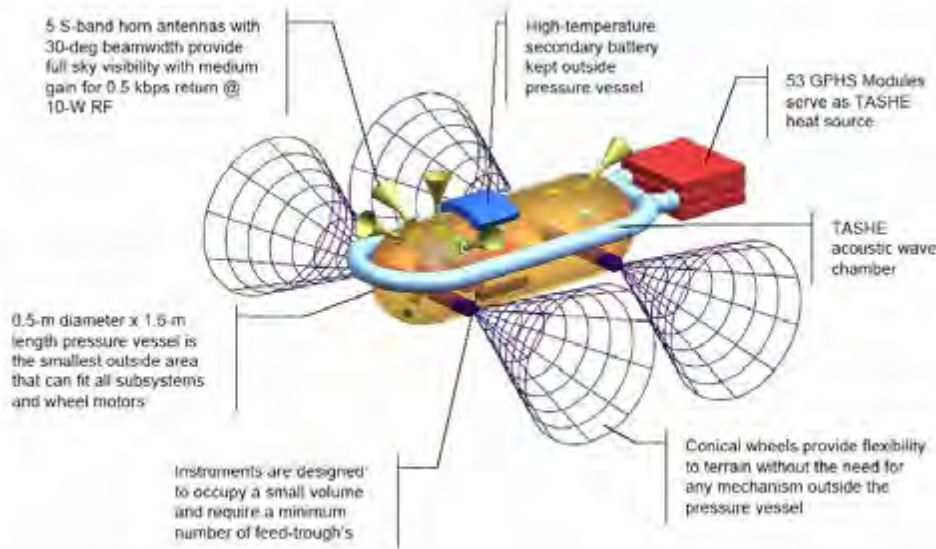


Figure 4.25: Concept for a Venus rover using a Thermoacoustic Stirling Heat Engine (TASHE) to provide power and cooling.



Technology Development Needs

Pressure Vessels and Passive Thermal Control

Development of improved materials and manufacturing methods for fabricating space-qualified pressure vessels or structural shells is far from complete. Some of the remaining technology development tasks to improve the current state-of-the-art include:

- Develop more detailed manufacturing engineering plans for the leading candidate materials. Many issues arise in fabricating a simple hemispherical shape sealed with a mating part. Adding features, such as optical windows, electrical feedthroughs, flanges, and brackets, makes manufacturing a spacecraft shell even more challenging.
- Estimate comparative fabrication costs for the different manufacturing technologies to guide selection of cost-effective technologies.
- Obtain samples or prototypes of shells from leading candidate materials to demonstrate that the technology is practical.
- Perform testing on subscale prototypes under Venus-like environmental conditions for temperature and pressure survivability.

Active Cooling

Preliminary assessments indicate that several feasible approaches exist for providing both power to, and cooling of, electronics on the surface of Venus for long-lived in situ missions. Radioisotope-based power-generation methods, in conjunction with active cooling, appear to be quite promising. These RPSs would be based on the Stirling power conversion technology in either the free-piston or thermoacoustic implementations. However, little has been done to address the materials problems of operating these devices at temperatures of 1000°C or higher; this capability would be needed to provide satisfactory generation efficiencies, given the high rejection temperatures imposed by the Venus environment.

RPSs currently under development are not suitable to operate in the Venus environment, even with customization or modifications. Thus, a long-lived Venus in situ mission using this approach would require a dedicated RPS with active cooling, beginning with an analysis focused on operations on Venus.

Alternatively, a 6-day Venus rover mission or a 30-day Venus seismometer mission could potentially be powered by batteries and cooled with a lithium/water reaction, thus eliminating the use of an RPS and resulting in no vibration for seismometer measurements.

Unfortunately, studies to date on this subject have been limited in scope, making it difficult to choose an appropriate power system for the proposed Venus Mobile Explorer mission with sufficient data. In order to refine the understanding of the power system options for VME, it is recommended to carry out dedicated studies related to potential VME mission

architectures, integrated with analysis at the system and component levels.

4.3 Component Hardening

“Component hardening” refers to technologies expected to be exposed to the ambient environment. The general categories include electronics, electromechanical systems, and energy storage.

4.3.1 High-Temperature Electronics

Most commercially available electronic devices have rated operating temperature limits of 125°C, far below the requirement for the Venus environment (480°C). Conventional silicon (Si) devices cannot be used at temperatures exceeding 200°C, due to increased leakage current and latch-up at reverse bias junctions. For functionality to 300°C, these problems may be managed by the use of silicon-on-insulator (SOI) technology, where the integrated circuits are dielectrically isolated from the base substrate.

Because SOI becomes unusable due to leakage beyond 300°C, alternatives like wide bandgap semiconductors are needed. The most highly developed of these are silicon carbide (SiC) and gallium nitride (GaN). Another alternative set of non-solid-state devices capable of operating at 500°C are thermionic vacuum devices.

In addition to these active devices, passive components have been studied, with mixed success. Currently, thick film ruthenium oxide resistors are capable of operating for long periods at 500°C. However, general-purpose ceramic capacitors, the best candidate technology for high-temperature operation, often exhibit wide variations in capacitance with increased temperature, particularly with an increased dielectric constant.

Finally, the packaging of high-temperature devices requires the careful selection and evaluation of substrate, die attach, and interconnect materials capable of withstanding high temperatures without decomposing, forming excessive brittle intermetallics, Kirkendall voiding, or cracking due to mismatched coefficients of thermal expansion. Development of new packaging materials and processes will be required.

Potential Benefits to Missions

Missions to Venus represent the strongest challenges to operation in a high-temperature and high-pressure environment. Maintenance of all the electronics in thermally insulated, near-Earth temperatures requires significant energy, and under some circumstances limits the mission’s science return. Certain subsystems for Venus surface missions, such as sensor and actuator systems, will be required for operation in the ambient surface environment (480°C) to obtain the desired sample extraction and measurement. Placing high-temperature electronics in the immediate vicinity of these sensors will enable signal conditioning and amplification and will also increase the sensor signal-to-noise ratio. In

addition, sample acquisition systems, such as drills, will require high-temperature position sensors and drive electronics.

For Venus surface missions and Jupiter deep probes, thermally controlled pressure vessels would be used to protect much of the remaining electronics and instruments from the high temperatures and pressures of the external environment. Since thermal control is mainly achieved through insulation (Venus In Situ Explorer or Jupiter Probes) or a combination of insulation and active cooling (Venus Mobile Explorer), subsystems generating significant heat within the vessel are counterproductive and greatly increase the required power to maintain the desired internal environment. Therefore, development of 500°C electronics will eliminate high heat-dissipating subsystems, such as signal transmitters for telecommunications, power converters, and actuator drive electronics, from the pressure vessel. Such technologies would greatly improve the efficiency of the cooling system and increase the overall lifetime, reliability, and science capability of the mission.

Over the shorter term, the small integration scale of 500°C electronics will limit their use to the applications identified above. However, other critical spacecraft functions, such as a solid-state data recorder, digitizer, and avionic computer, will require technologies capable of large-scale integration. With sufficient technology investment and development over the longer term (more than a decade), large-scale integration of wide bandgap 500°C electronics to carry out these functions will eventually become possible, which would in turn facilitate complete elimination of semiconductor electronics cooling to perhaps enable greatly prolonged Venus surface mission. Nevertheless, in the shorter term, increasing the operating temperature of the electronics within the vessel will improve the component lifetime and the efficiency of the cooling system. Increasing the operating temperature of the electronics within the pressure vessel impacts the system in two ways:

- *Active cooling systems:* Increasing the operating temperature of the electronics from 125°C to 300°C reduces the differential temperature between the external environment and that maintained by the cooling system, resulting in increased system efficiency and reducing the required power.
- *Passive cooling systems:* Increasing the operating temperature of the electronics improves survival time because a longer time will be necessary for the system to reach a state exceeding the electronics' operating temperature.

In addition, electronics capable of operating at 300°C could be used without additional cooling for Venus balloons at altitudes of 25 km or higher. Fortunately, at intermediate high temperatures of 300°C, it becomes feasible to exploit the use of very large scale integrated (VLSI) electronics based on Silicon-on-Insulator (SOI) technology.

State-of-the-Art

The theoretical temperature limits of various solid-state semiconductors are usually determined by bandgap calculations, intrinsic carrier concentrations, and carrier mobility. These

estimates often exceed experimentally determined limits, as shown in Table 4.8. These measured limits are determined by the metallurgical contacts of the devices, electromigration and reaction of the interconnects, time-dependent breakdown of gate dielectrics, and defects within the semiconductors. An overview of high-temperature semiconductor technology applications, capabilities, and development challenges is given in [NOC02].

Table 4.8: Theoretical and empirical limits for high-temperature materials.

Materials	Theoretical temperature limit (°C)	Experimental temperature limit (°C)
Bulk Si	400	225
SOI	400	300
SiC	900	600
GaN	900	600
Vacuum devices	1000	600

The operating characteristics of a number of materials are shown in Table 4.9 and will be discussed further below.

Table 4.9: Characteristics of high-temperature materials.

Materials	Transistor normal state	Operating voltage (V)	Demonstrated temperature (°C)	Power consumption	Commercial integration scale [†]
SOI	Off	3–5	300	Low	MSI
SiC	On	>200	500	High	SSI
GaN	On	>15	300	Medium	SSI
Vacuum devices	On	>200	500	High	Discrete

[†] SSI denotes small-state integration; MSI denotes medium-state integration; discrete elements are not yet integrated.

SiC technologies

Currently, discrete SiC diodes and metal semiconductor field effect transistors (MESFET) are available commercially, and junction field effect transistors (JFET), bipolar junction transistors (BJT), and metal oxide semiconductor field effect transistors (MOSFET) are currently being developed, although even gate turn-off thyristors (GTO) have now been demonstrated. Almost none of these commercial or developing SiC devices are targeted for ambient application temperatures above 300°C where electronics functionality could no longer be provided by SOI technology.

The inherent properties of SiC limit the commercial applications to high-power circuits, such as the discrete high-voltage SiC transistors currently available⁹. Current estimates suggest that they can survive 500°C operation for at least tens of hours, a limit determined by the degree of electromigration within the metal traces and oxidation of the ohmic contacts, as they were not designed for use at 500°C.

Normally-on JFETs are the most widely available for high-temperature applications, but development of normally-off JFETs and BJTs is ongoing. While the SiC MOSFET would be the most desirable transistor to support large-scale integrated circuits, the development of a gate dielectric for such a transistor to operate reliably above 300°C (temperature limit of SOI) is a problematic challenge that remains to be overcome.

GaN Technologies

Commercial GaN devices have been developed for high-speed and microwave applications. They are currently available at small-scale integrated levels for military and defense applications; however, their operation at 500°C has not yet been demonstrated, even at the discrete transistor level.

SOI CMOS

SOI CMOS devices suffer from high leakage currents, and therefore from high power requirements at elevated temperatures.

Vacuum Technologies

An alternative approach to solid-state devices is the use of thermionic vacuum transistors, well-suited for extreme temperatures because they require high internal temperatures in order to operate. Thermionic vacuum devices are capable of long-term operation at 500°C, with negligible degradation. They are low-noise, linear devices, with electrical performance parameters that are virtually independent of temperature. Hence, high-temperature circuits made with vacuum transistors do not need elaborate circuitry to compensate for variation of transistor performance with temperature, presenting a significant advantage compared to semiconductors. The low-noise, temperature-insensitive properties of the vacuum tube transistors make them ideally suited for telecommunications applications. However, careful design and improvement of the device packaging (vacuum enclosure) and materials are required to enable operation at 500°C. Furthermore, these vacuum devices are inherently unlikely to achieve the high levels of integration and functionality possible with semiconductor transistors.

⁹It should be emphasized that this statement relates to **commercial** SiC transistors not designed for high-temperature operation. When a SiC transistor is designed and packaged for high temperatures, over 1000 hours of 500°C packaged SiC transistor and amplifier circuit operation has been demonstrated by NASA GRC. NASA GRC is targeting to further develop and demonstrate 10,000 hours of 500°C SiC device and circuit operation.

Passive Devices

Passive elements for high-temperature applications depend not only on the survivability of resistive elements, dielectrics, or magnetic core materials, but also on the component packaging and interconnection technology. This is the most common source of failure for devices not designed for high-temperature operation. Specific failure modes exist for various passive elements.

Thin film and thick film resistors deposited on ceramic substrates provide the best performance and miniaturization of currently available resistor technologies. Potential problems include oxidation of thin film resistive elements after extended exposure to high temperatures and resistance value drift in thick film resistors. Degradation of potential candidate resistors must be characterized in detail to use them in 500°C circuits.

Capacitors present particular challenges to high-temperature operation since capacitance varies with increased temperature, particularly as the dielectric constant and dielectric dissipation are increased. At elevated temperatures, the capacitors' leakage currents increase significantly, making it difficult for the capacitor to hold a charge. The most promising candidates for high-temperature (500°C) capacitors are NP0 ceramic capacitors and piezoelectric-based capacitors. NP0 capacitors have minimal variation in capacitance with temperature, but unfortunately they exhibit a significant increase in dissipation above 300°C. Piezoelectric capacitors are designed for operation at a specific temperature, where they exhibit optimum properties. Unfortunately, the temperature window for this peak performance is very narrow, and these capacitors change significantly with increasing temperature. Various capacitor technologies, such as diamond capacitors and other alternative dielectric materials with high bandgaps, are currently under development and may eventually offer superior properties throughout the entire 23–500°C range.

High-Temperature Packaging

Electronic packaging for high temperatures presents many challenges compared to conventional packaging, including the following:

- Decomposition (including oxidation) or melting of materials,
- Mismatch of the coefficient of thermal expansion (CTE),
- Intermetallic diffusion at the contacts/interconnects,
- Electromigration in conductors, and
- Diffusion and degassing in encapsulate materials.

For example, the maximum use temperature for most polymers is less than 300°C. Therefore, above 300°C, no polymers exist for circuit boards, underfills, encapsulants, cable/wire insulation, die attach or a variety of other applications used in conventional electronic packaging. Regarding melting, various solders and die attach materials used at lower temperatures are not applicable at higher temperatures. To further complicate matters, solders

are usually selected to have reflow temperatures at least 50°C higher than their use temperature. Increasing the processing temperatures of solid-state electronics to 550°C from 500°C could significantly reduce the survivability of the active circuitry, particularly for an extended reflow process. Table 4.10 summarizes the current state of high-temperature die attach materials.

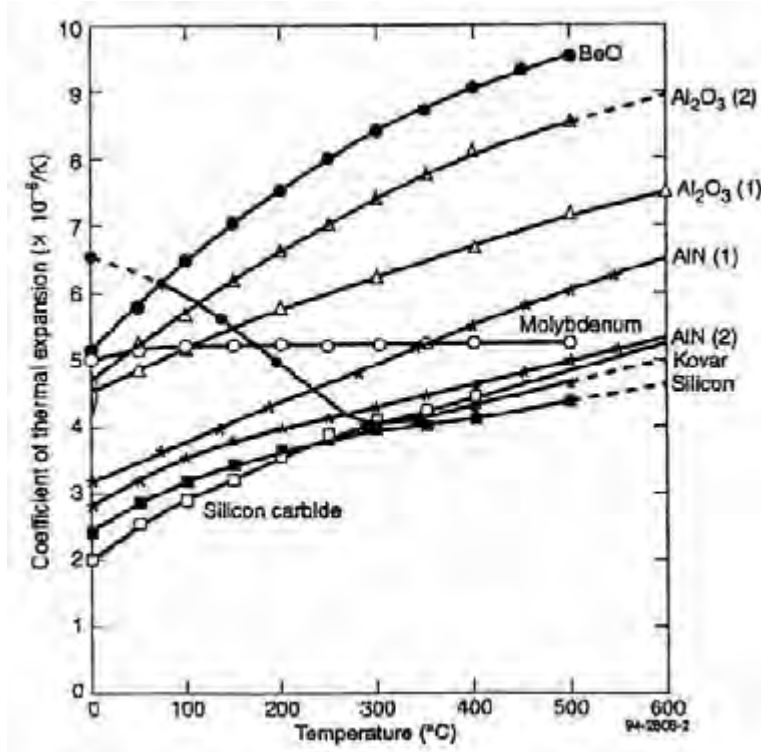
Table 4.10: High-temperature behavior of die attach materials.

Material	Maximum Temperature (°C)	Comments
Solders		
Au80Sn20	280	Eutectic
Au88Ge12	356	Eutectic
Au97Si3	363	Eutectic
Sn5Pb95	308	Solidus
Pb92In5Ag3	300	Solidus
Brazes		
82Au/18In	451	Solidus
45Ag/38Au/17Ge	525	Eutectic
72Ag/28Cu	780	Eutectic
82Au/18Ni	950	Eutectic
Other		
Au thick film paste	>600	High firing temperature
Au thermo-compression bonding	>800	Assumes Au to Au interface

Even if all the materials of the packaged assembly survive exposure at the required temperatures, careful materials selection to minimize mismatch in coefficients of thermal expansion (CTE) is critical due to the significant operating temperature range and the stiffness of die attach materials capable of withstanding high temperatures. Differences in CTE between the substrate and the die could lead to fatigue and eventual die fracture after experiencing thermal cycling; in particular, stresses at the die edge can cause horizontal crack propagation and die lifting. The temperature variations of the CTEs for a number of materials are shown in Figure 4.26.

Finally, diffusion, oxidation, and electromigration are all significantly affected by increased temperatures. Interdiffusion of different metals at the die bondpad can result in failure of the electrical interconnect. A commonly cited example is the Au-Al system, in which the diffusion of Au into Al leads to the formation of intermetallics in the Al side and voiding in the Au side of the interface. A summary of the maximum service temperatures and limiting properties for a selection of die bondpad wirebond combinations is provided in Table 4.11.

Figure 4.26: Coefficients of thermal expansion for various materials in the 0–600°C range.



Prototype ceramic substrates based packaging systems composed of chip-level packages and printed circuit boards (PCBs) for small scale low power high temperature devices have been preliminarily demonstrated. The packaging system facilitated the test of a SiC MESFET in a 500°C oxidizing environment for over 560 hrs at NASA GRC. These packaging systems need further development and long-term reliability evaluation to meet future space applications. Some of these packaging technologies may also apply to 300°C SOI circuits.

Medium Temperature Electronics

At 300°C, it becomes feasible to exploit traditional Si-based electronics for large scale integrated (LSI) electronic functions. Past investments by the Department of Energy, the oil industry, and the automotive industry have produced small- and medium-scale integrated (SSI and MSI) Si-based electronic circuits operational at 250–300°C. These circuits are fabricated with SOI technology to reduce their leakage current at higher temperatures. Currently available SOI circuits qualified for 225°C operation¹⁰ include gate arrays (40K gates, 20 MHz), a 83C51 microcontroller (20 MHz), a 256K SRAM, and operational amplifiers.

¹⁰Operations have been demonstrated at 300°C.

Table 4.11: Maximum temperatures and limiting properties for select bondpad–wire metallurgical combinations.

Metals: Pad–Wire	Maximum Temperature (°C)	Limiting Properties / Comments
Al–Au	175	Forms brittle intermetallic phases that reduce bond strength and conductivity.
Ni–Al	300	Interdiffusion creates excessive voids that decrease bond area and strength.
Al–Al	660	Melting temperature of Al.
Au–Au	1064	Melting temperature of Au.

fiers.

Passive components for 300°C would use similar resistors to those used at 500°C. Capacitors pose significantly fewer problems at this temperature, and the currently available NP0 should function well for low-value capacitor needs. Electronic packaging for 300°C would be similar to that developed for use at 500°C, where it exists.

Technology Development Needs

Although brief operation of various devices has been proven at the desired elevated temperatures, a number of the technological improvements are necessary to develop systems with extended capabilities. The most critical and difficult technological challenge for 300–500°C electronics is sufficiently prolonged, stable, and reliable electrical operation at these high temperatures. Current commercial SiC devices are available as discrete, normally-on, high-voltage devices targeted for application temperatures below 200°C. In order to use SiC for 500°C instrument amplifiers and other small signal circuits, transistors capable of working at low voltages is critical. Ten years ago, NASA GRC demonstrated low-voltage SiC device and logic gate operation for brief (1 h) time periods at 600°C. Since then, NASA GRC has greatly prolonged the operational life of its SiC transistors to over 1000 hours at 500°C. Using these advances, NASA GRC is presently attempting to realize SiC integrated circuits that will operate at 500°C for many thousands of hours.

In addition, complementary devices (normally on and normally off), as well as the resulting integrated circuits, are available and allow device matching and the capability to tailor device properties to the application. For power circuits, normally-off devices would allow power switches to default to the off position in the case of failure. For logic circuits, complementary devices reduce required power. Low-voltage, small-scale integrated circuits are already available in GaN but the capability to survive at high temperatures has not been established and may require modification of metal layers.

Similar to the development required for SiC devices, thermionic vacuum devices are available as discrete, normally-on, high-voltage devices, and their use in small signal circuits would greatly benefit from the availability of low-voltage, complementary devices and small-scale integrated circuits. With this technology, a 500°C S-band telecom system, actuator drivers, sensor amplifiers, and power converters become feasible.

As with any modern electronics design process, extreme environment circuit and system design requires accurate models of the semiconductor devices and passive elements that are valid over the anticipated operating conditions. These models are used to repeatedly analyze the system during design and if they are unavailable, the designer is merely guessing about the performance at extreme temperatures. To predict circuit reliability, both custom-designed components and commercial-off-the-shelf (COTS) components must include lifetime assessment effects in their models. Models, modeling methodologies to include end-of-life predictability, and modeling tools to expedite this process are requirements for rapid development of extreme environment electronic design in NASA applications.

SiC Technologies

Needs include 500°C normally-off transistors that can operate at low voltages, stable long-term 500°C device operation, and reliable 500°C SSI integration. Such capability can initially be developed and realized using SiC JFET or BJT devices and suitable high-temperature on-chip interconnect. Over the longer term, a complementary CMOS-like insulated gate transistor technology in SiC is desirable because it would more easily enable higher levels of integration with less power consumption — provided that reliable 500°C SiC transistor gate insulator could be developed.

GaN Technologies

Like SiC technologies, this area requires development of 500°C normally-off transistors that can operate at low voltages, stable long-term 500°C device operation, and reliable 500°C SSI integration.

Vacuum Technologies

Like SiC technologies, this area requires development of 500°C normally-off low voltage transistors, reliable 500°C SSI integration, and reliable vacuum packaging at 500°C with thermal cycling.

SOI CMOS

These technologies require ultra-low power (0.2 W/gate/MHz) 300°C LSI technology development with a minimum operating frequency of 40 MHz.

Passive Devices

Capacitors with a low-temperature coefficient of capacitance and low dissipation factor over the entire temperature range are greatly needed for a full range of capacitance values.

High Temperature Packaging

Potential solutions to several of the current challenges with high-temperature packaging exist. Ceramic substrates with high-temperature metallizations and relatively close CTE matching with SiC or GaN active elements are available, as well as potential high-temperature die attach solutions. In addition, the use of Au wirebonds with Au bondpads on active circuitry will reduce the formation of intermetallics at the interface. Options may exist for coating of finished assemblies with ceramics. Unfortunately, little work has been done to clearly determine whether these solutions will meet NASA's needs for high-temperature electronic systems, since these needs far exceed those of current commercial terrestrial applications. Finally, high-temperature electronic packaging for target applications, such as high-frequency packaging for Venus telecom, must be developed and evaluated in detail.

Medium-Temperature Electronics

As discussed previously, currently available SOI circuits that have been demonstrated to work at 300°C include gate arrays (40K gates, 20 MHz), 83C51 microcontroller (20 MHz), 256K SRAM and operational amplifiers. While these circuits can be used to build the essential systems of a spacecraft, their overall power consumption and performance fails to provide the optimal benefits for the Venus missions. Low-power, medium-temperature Si-based electronics can be developed through additional optimization of film thicknesses and scaling of the transistor geometries. Low-power, LSI-scale medium-temperature Si-based electronics, once developed, can be used to integrate most essential functions in Venus In Situ Explorer (VISE) or atmospheric probes.

4.3.2 Low-Temperature Electronics

Most commercially and military available electronic circuits (COTS) are rated to operate between -55°C to $+125^{\circ}\text{C}$. This temperature range is far narrower than those needed for a number of NASA targets:

- The Moon (-230°C in the permanently shadowed regions and -180°C to 110°C cycles),
- Mars (-120°C to 20°C cycles),
- Titan (-145°C), and
- Comets (-180°C).

However, Si and SiGe transistors are known to function down to -269°C , suggesting that it should be possible to build electronics that function at the low temperatures of NASA's anticipated targets. Lack of commercial demand, design methodology, and accurate device simulation models has prevented the development of cold-temperature integrated circuits.

The development of cold-temperature and wide-swing, low-temperature tolerant Si-based circuits calls for understanding of the following phenomena:

- At temperatures below -150°C , Si-based bipolar transistors suffer from carrier freeze-out.
- Hot carrier injection accelerates the aging of MOSFETS as a function of reducing temperature.

However, SiGe-based heterojunction bipolar transistors (HBT) do not suffer from this carrier freeze-out problem. A further complication is that the combined effects of radiation and colder temperatures (such as the surface environment of Europa) on Si-based devices are not well understood.

Finally, packaging of devices for the temperature range of NASA's missions requires the careful selection and evaluation of substrate, die attach, and passivation materials capable of operating at low temperatures without transitioning to a glass phase, forming excessive or brittle intermetallics, or breaking due to mismatched thermal expansion coefficients.

Potential Benefits to Missions

The lowest temperature seen in NASA targets in the 2006 SSE Roadmap is that of the South Pole – Aitken Basin in the permanently shadowed regions of the Moon. Rovers and hoppers that begin at nonshadowed regions and move into those regions of permanent shadow will experience the widest temperature swings. Missions to Mars pose a different challenge in the form of the largest number of temperature cycles. Titan missions also present low temperatures of -180°C (90K).

In the absence of electronics capable of operating across the full temperature ranges of these environments, robotic systems on the surface of the Moon, Mars, Europa or other deep space destinations will require thermal control systems such as a centralized warm electronics box (WEB) to protect their electronic subsystems from the temperature extremes. Unfortunately, the WEB approach uses power relatively inefficiently. It also severely complicates the design because it requires a large wire harness to connect the protected electronics to the various unshielded loads at the extremities of the robotic system; for Mars Exploration Rover (MER), this required about 1,800 individual wires. This approach is clearly not robust, modular, or scalable to significantly more complex robotic exploration systems.

Electronics that operate in low temperature ranges can eliminate the need and expense for sustaining local artificial, Earth-like environments to protect sensitive electronic parts. The resulting integrated system is simpler and easier to maintain, and the approach opens the design space for integrated, modular subsystems located at the point of use and loosely coupled in distributed networks. Each node of the collaborating robotic system can be constructed without elaborate thermal control, saving both power and mass, and avoiding the complex, heavy, and difficult-to-integrate “point-to-point” wiring harnesses of present-day

designs. In their place, multiple redundant serial, data, and power buses can be used to significantly simplify interconnects and cabling, and wireless communications links can be implemented for mobile units.

State-of-the-Art

Transistors

Silicon-based transistors have been demonstrated to operate down to -269°C . Commercial manufacturers of electronic circuits support various state-of-the-art technologies including complementary-symmetry¹¹/metal-oxide semiconductor (CMOS), SOI CMOS, BiCMOS, and SiGe BiCMOS¹² with devices capable of operating down to -230°C .

In many cases, the operating speed, noise margins and gain-bandwidth of semiconductor devices improve with cooling due to increased carrier mobility, saturation velocities, and interconnect conductivity. On the other hand, low temperatures also may lead to severe device reliability and performance problems. With the current aggressive size reduction of devices in the deep submicron regime, hot-carrier-degradation (HCD) becomes a critical reliability issue at low temperatures. HCD leads to severe performance degradation and eventual failure, significantly limiting device reliability and lifetime. Temperatures approaching -230°C overlap with the carrier freeze-out temperature region of commonly used Si devices, often rendering them inoperable. Low-temperature exposure also aggravates the deleterious effects of radiation in many devices. Table 4.12 summarizes the issues associated with low-temperature electronics.

Table 4.12: Theoretical and empirical limits for low temperature electronics.

Technologies	Theoretical Temperature Limit ($^{\circ}\text{C}$)	Empirical Temperature Limit ($^{\circ}\text{C}$)	Concerns for Operation at -230°C
Si Bipolar	-269	-150	Carrier freeze-out
CMOS	-269	-180	HCD for short-channel MOSFETS [†]
SOI	-269	-230	HCD for short-channel MOSFETS
SiGe BiCMOS	-269	-269	HCD for short-channel MOSFETS

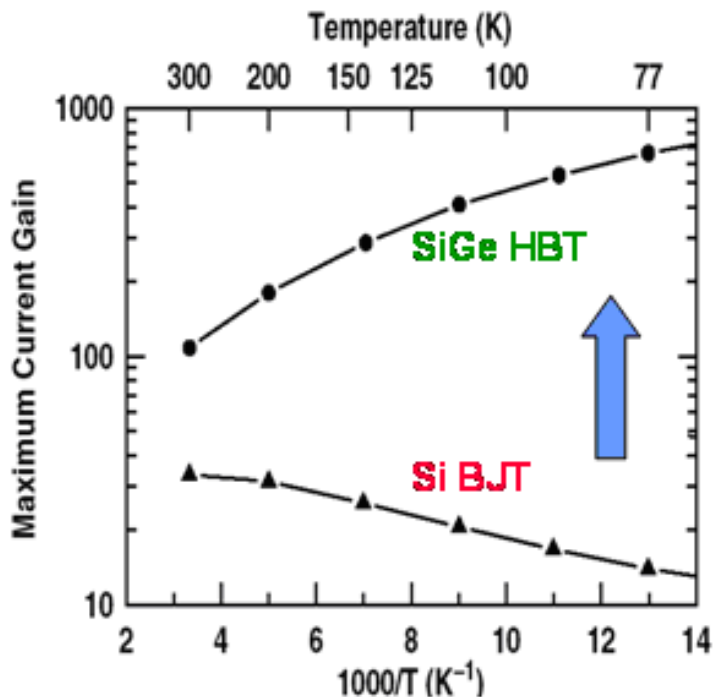
[†] MOSFETs are metal-oxide-semiconductor field-effect transistors, the most common field-effect transistors in digital and analog circuits.

¹¹The words “complementary-symmetry” refer to designs using symmetrical pairs of p-type and n-type MOSFET transistors for logic functions, only one of which is switched on at any time.

¹²BiCMOS devices integrate bipolar junction transistors with CMOS devices, a relatively recent technology advance in integrated circuit design currently used in small- to medium-scale integration.

Commercially available electronic circuits capable of working at -230°C do not currently exist. Si-based bipolar transistors experience degraded performance due to carrier freeze-out at temperatures as low as -130°C . However, SiGe-based bipolar transistors do not suffer from carrier freeze-out and are capable of operating to -269°C , or 4 K, as shown in Figure 4.27. Although Si-based MOSFETs apparently show improved performance at lower temperatures and have been demonstrated to operate down to -269°C , the operating life of short-channel MOSFETs is severely degraded due to injection of hot carriers at low temperatures.

Figure 4.27: Low-temperature operations of SiGe HBT and Si BJT. The arrow indicates the increasing performance gain from SiGe HBT with decreasing temperatures. Heterojunction bipolar transistors (HBT) and bipolar junction transistors (BJT) differ because HBTs use different semiconductor materials for the emitter and base regions, creating a heterojunction. This improvement on the BJT allows for significant doping, providing electron mobility and thus, improved efficiency.



Because silicon-based transistors evidently function at temperatures below -55°C , it is only natural to assume that commercially available electronics COTS may also operate down to a lower temperature range. Under the Mars Focused Technology program, NASA has demonstrated operation at temperatures as low as -155°C for a number of COTS, including digital IC's, memory circuits, analog IC's, mixed-signal IC's, and radio frequency IC's.

However, the wide temperature range impacts circuits and components in a number of ways.

Digital Integrated Circuits

State-of-the-art field programmable gate arrays (FPGA¹³), digital application-specific integrated circuits (ASICs), microcontrollers, and digital signal processing (DSP) circuits are fabricated using deep submicron CMOS transistors. Leakage current in such circuits doubles for every 10-degree rise in temperature; for example, during the “programming” mode at temperatures below -40°C , certain reconfigurable FPGAs draw excessively large currents (one to two orders of magnitude higher than currents required for reprogramming at room temperature), impacting both their reliability and lifetime. At the other extreme, many FPGAs also exhibit a large static leakage above $+80^{\circ}\text{C}$ that translates to an excessive supply current (on the order of several amperes), leading to rapid performance degradation.

Memory Circuits

State-of-the-art memory circuits using dynamic random access memory (DRAM) or static random access memory (SRAM) are fabricated using CMOS-based high-density building blocks that may not function at extremes in temperature. At low temperatures, the rise in threshold of the CMOS transistors in DRAMs can compromise the refreshing operation, while at high temperatures ($+120^{\circ}\text{C}$), the increased leakage current of CMOS transistors reduces the amount of time a bit can be dynamically stored in a DRAM cell. On the other hand, static memory devices (high-density SRAMs) generally perform very well at low temperatures (-180°C) but can consume a large amount of power due to increased leakage currents at the high end of the range ($+120^{\circ}\text{C}$). Nonvolatile ferroelectric RAM (FRAM) fails to operate below -100°C , and little is known about the electrical performance of other types of radiation-hard, nonvolatile memories (chalcogenide, magnetoresistive, etc.) at extremes in temperature.

Analog Components

Discrete power transistors, amplifiers, precision voltage and current sources, multipliers, phase-lock-loops and other analog circuits have very precise operating performance requirements (gain, noise, frequency, etc.) that vary strongly with temperature. Existing components can only operate at peak performance in a very narrow temperature range. Also, Si bipolar transistors frequently used in high-performance analog designs suffer from rapid decline in gain with cooling, and are practically unusable below -150°C . At the high end of the temperature range, transistor leakage current (in both bipolar and CMOS) can severely degrade the performance of the analog circuits.

Mixed-Signal Integrated Circuits

Integrated circuits often contain analog to digital (A/D) converters, digital to analog (D/A) converters, and analog multiplexing circuits as core elements, and employ a digital core (microcontroller or DSP) for signal processing. Wide-temperature-range, radiation-tolerant,

¹³FPGAs are semiconductor devices with programmable logic components and interconnects.

high-performance A/D or D/A converters are currently not readily available.

RF Electronics

Typical RF electronics used for space telecommunication are rated operational in the range between -55°C and $+125^{\circ}\text{C}$, precluding their use through lunar nights without proper thermal management. In addition, the transmit amplifiers for most of these systems have relatively low efficiencies that strongly depend on power and frequency of operation, and are therefore marginal for operation during the lunar day because the temperature of the output stage will likely rise above the ambient temperature of $+120^{\circ}\text{C}$.

To avoid bulky heatsinks or active thermal management, RF devices and circuitry capable of tolerating these extreme temperatures are clearly needed. This is especially important for UHF systems envisioned as components of small fixed or mobile units in distributed surface networks.

Silicon-based components show significant variation with temperature because of the performance of the Si transistor, described below in Table 4.13. Specifically, the compromised performance impacts the performance of traditionally designed analog circuits over this temperature range. However, it may be possible to design appropriate Si-based custom ASICs, an attractive option that minimizes NASA investment requirements because a mature commercial manufacturing infrastructure for Si-based electronics already exists.

Table 4.13: Temperature variations of silicon device parameters.

Device	V_{th} (mV/ $^{\circ}\text{C}$)	Mobility (cm 2 /Vs/ $^{\circ}\text{C}$)	V_{be} (mV/ $^{\circ}\text{C}$)	Beta (/ $^{\circ}\text{C}$)	Drain breakdown (mV/ $^{\circ}\text{C}$)	BV_{CEO} (/ $^{\circ}\text{C}$)
nMOS	0.5	4	N/A	N/A	125	N/A
pMOS	0.5	4	N/A	N/A	125	N/A
Si PNP BJT	N/A	N/A	2.2	2	N/A	0.01
Si NPN NPN	N/A	N/A	2.2	2	N/A	0.01

Device physics at low temperatures differs from that applicable to military applications, necessitating new models appropriate to the transition from traditional charge-control physics cryogenic operation. Furthermore, significant changes in device parameters require the development of new, wide-temperature-swing design methodologies that consistently produce reliable, high-performance Si circuits.

Radiation-Hardened Low-Temperature Electronics

The effects of combined radiation and cold temperatures are not well understood or mod-

eled. Many of the self-annealing mechanisms that help repair radiation damage in Si-based circuits slow down or stop at cold temperatures. Wide-bandgap devices, such as SiGe-based transistors, apparently show significantly better resistance to damage caused by radiation at room temperature.

Passive Elements

At low temperatures, applications using passive elements suffer from performance variation with temperature. In particular, electrolytic capacitors will not function at cold temperatures, and the other types of capacitors experience changing capacitance values under temperature variation.

CAD Design Tools

Current device models used in standard IC design tools are only suitable for commercial, or at best, military temperature ranges. As a result, circuit simulation for wide-temperature-range mixed-signal ICs is severely handicapped due to a lack of accurate models and because current designs are optimized with empirical data at lower temperatures. While many COTS components may be capable of operating outside the environmental range specified in the catalog, the lack of models predicting their behavior outside this range excludes them from consideration for low-cost extreme-environment electronic systems.

Increased use of distributed architectures require modeling tools that enable the simulation of multidisciplinary systems, in addition to the electronics. The simulators and modeling languages exist, but the tools to create the models do not.

High-Density Packaging

Currently, there is a lack of basic material data and performance data on combinations of packaging materials appropriate to low temperatures or thermal cycling. Existing performance data typically fall within the commercial temperature range, or less often in military specification range, and may not have been collected with a suitable breadth of materials combinations (e.g., characterization of a die attachment material with multiple substrates). Material combinations subjected to wider temperature ranges may undergo phase changes that compromise performance, or they may experience new failure mechanisms not encountered under less severe conditions. Testing over this wider range is critical to establish the temperature limits of the materials, to characterize thermally induced stresses and fatigue due to thermal cycling, and to identify any new failure modes.

The most critical issue facing electronics operating under thermal cycling is the capability of the electronics packaging to survive the repeated passes to low temperatures. An advanced chip-on-board packaging technology is currently being developed in the Mars Focused Technology Program with the goal of being able to survive 1500 cycles between -120°C to $+80^{\circ}\text{C}$.

Technology Development Needs

To support NASA's missions to extreme cold environments, the development of long-life, radiation-tolerant, low- and, ultra-low power integrated electronics and electronic packaging technology capable of operating at temperatures as low as -230°C is needed.

The two major groups of technologies, CMOS and SiGe, are compared in Table 4.14. The principal difference is that SiGe technologies can improve short-range communications capabilities, while CMOS would not. However, both classes of devices would benefit data acquisition, power management and distribution (PMAD), motor drives, and actuator systems.

Table 4.14: System impact of CMOS and SiGe technologies.

Subsystem	CMOS	SiGe
Short-range communications	No	Yes
Data acquisition	Yes	Yes
Power management and distribution (PMAD)	Yes	Yes
Motor drives	Yes	Yes
Actuators	Yes	Yes

Transistors

While Si transistors operate across this wide temperature range, significant circuit design challenges remain to be addressed for circuits operating reliably over such a broad temperature range.

Digital Integrated Circuits

Cold-temperature VLSI class ASICs can be fabricated with several technologies such as CMOS, SOI CMOS, and SiGe BiCMOS; however, radiation considerations narrow the technology choices to SiGe BiCMOS and SOI CMOS. Unfortunately, because commercial technologies are only modeled to -55°C , the lack of proper performance models at very cold temperatures severely handicaps the development of mixed-signal ASICs in all of these technologies. In addition, scaling of CMOS technologies aggravates the degradation of the CMOS transistors due to hot carrier injection.

Memory Circuits

Low-temperature memory circuits are needed, particularly with radiation-hardened properties.

Analog Components

High-gain transistors with minimal leakage currents at -150°C are needed.

Mixed-Signal Integrated Circuits

Rovers and hoppers to permanently shadowed regions of the Moon may have to start their missions from the nonshadowed regions. Consequently, they may experience temperature changes between -230°C and 110°C . Coping with this wide temperature range, especially for the mixed-signal circuits, will demand the development of new design methodologies that include the temperature-dependent effects in transistor performance, such as the performance variations of mixed-signal circuits that can be corrected using companion digital circuits and look-up tables.

Alternatively, an aggregate set of analog circuits with optimized performance for specific narrow temperatures can be multiplexed in different temperatures to produce a wide-temperature, mixed-signal circuit.

RF Electronics

Designing Si-based custom ASICs minimizes NASA investment requirements because a mature commercial manufacturing infrastructure for Si-based electronics already exists. Furthermore, accurate models to simulate low-temperature performance are needed because the underlying physics changes from that applicable to military applications. In addition, new, wide-temperature-swing design methodologies are needed to consistently produce reliable, high-performance Si circuits.

Radiation-Hardened Low-Temperature Electronics

Electronics in the Europa Lander package will experience the combination of radiation and low temperatures. Devices developed for operation at low temperatures will require further testing and design for use in environments with risks of radiation damage.

Passive Elements

Low-temperature capacitors require development.

CAD Design Tools

Development of accurate models and optimal design rules are needed.

High-Density Packaging

The requirements for the rapid change of temperature in some of the missions also demand the development of new material combinations for system-level packaging of the cold-temperature IC's. These new combinations should eliminate the reliability concerns that arise from mechanical stress and fatigue of the IC package.

4.3.3 Radiation Tolerant Electronics

At present, the space industry relies on three distinct sources for radiation-tolerant electronics:

1. Commercial components that are determined to be — perhaps serendipitously — radiation tolerant.
2. Electronics built at manufacturing lines with radiation hardened materials processes. These are known as radiation hard by process (RHBP).
3. Components built on commercial lines with commercial materials but designed to tolerate higher radiation levels. These are known as radiation hard by design (RHBD).

Each of these approaches may play an important role in furnishing technologies for future missions. For total ionizing dose (TID), the biggest driver for technology development will be missions to the Jupiter system and specifically for exploration of Jupiter's moon Europa, where the radiation dose rate is approximately 750 krad per month. Radiation-tolerant parts are defined as parts capable of meeting specification after exposure to 100 krad (Si), whereas radiation-hard parts are defined as parts capable of meeting specifications after exposure to 300 krad (Si).

At present, the space industry relies on commercial or government dedicated manufacturing lines to produce radiation-tolerant/hard components. Electronics built at manufacturing lines with radiation-hardened materials processes have the most flight heritage and tend to provide the best radiation hardness. However, these special processes require dedicated manufacturing facilities; currently operational commercial rad-hard manufacturing lines are owned by Atmel, BAE Systems, and Honeywell SSC. In addition, government-owned manufacturing lines for radiation-hard electronics are located at Sandia National Laboratory (SNL) and Defense Micro-Electronics Activity (DMEA). These latter two facilities are prohibited from competing with commercial industry and are considered foundries of last resort. Parts manufactured in these government-owned installations are restricted to product segments not offered by private industry or address obsolescence problems and cater primarily to the military market. The parts are typically latchup immune, impervious to single-event upset (SEU), prompt dose hardened, and total dose hardened well beyond 1 Mrad(Si)¹⁴.

Generally, the time and cost associated with qualifying and maintaining dedicated rad-hard facilities dictates a much slower upgrade cycle; consequently, a technology lag of 3 to 4 generations exists behind the state-of-the-art consumer electronics market. Part families available in RHBP versions tend to be less capable than their commercial equivalents and are restricted, for example, to low density (<4 Mb) static random access memories (SRAMs), low-density (~4 Mb) nonvolatile (NV) memories, medium-performance, medium-power dissipation microprocessors (~200 MIPS), selected analog-to-digital converters (ADCs), field programmable gate arrays (FPGAs) and structured application-specific integrated circuits (ASICs).

¹⁴A rad(Si) is a unit of radiation energy absorbed by silicon, equivalent to 0.01 J/kg. Therefore, 1 Mrad(Si) is equal to 10 J/kg.

Some candidate radiation-tolerant components may be electronics manufactured for purely commercial purposes that happen to have special design features or materials that are serendipitously radiation tolerant. The space industry resorts to purchasing entire manufacturing lots from various vendors and screens parts for their suitability. Digital VLSI parts with a reasonable upset immunity and a TID tolerance of up to 100 krad(Si) (in rare cases) are well suited for near-Earth or low radiation environments when used in conjunction with error correction and detection (ECAD), redundancy, and/or shielding. Searching for serendipitously rad-tolerant parts provides access to a much broader spectrum of digital parts with lower cost and comparatively high performance. There are usually significant additional costs associated with the testing and screening of these types of parts. Generally, suitable analog or mixed-signal devices are much more difficult to find, although more are becoming available every day.

Radiation hardened electronics by design (RHBD) has opened a third avenue for manufacturing and acquiring radiation tolerant/hard electronics. In conjunction with on-chip circuit redundancy implemented at commercial foundries, changes in the transistor shape, placement, on-chip temporal, and functional voting have resulted in chips/designs with a total dose hardness of more than 5 Mrad(Si), latchup immunity, and SEU immunity. The space community benefits from direct access to higher performance manufacturing technology, relatively low cost, and a performance boost of 1–2 generations over the RHBP electronics. The RHBD approach is relatively new to the space sector. Qualification procedures are still being developed to address how designs that use multiple die/parts/components to achieve radiation tolerance can be qualified for flight. Traditional qualification methods evaluate each part's ability to meet its specification after exposure to radiation. This new RHBD approach cannot be qualified in the same manner. Performance for commercial, RHBP, and RHBD digital applications are shown below in Figure 4.28.

Companies currently offering RHBD parts include Aeroflex, ATK Mission Research, BAE Systems, Boeing, and Peregrine. In contrast to the dedicated hardened process foundries, RHBD requires trades between integration density, power dissipation, and performance. Table 4.15 compares a single logic block made with a commercial design, a RHBD process, and with a technology typical for dedicated rad-hard foundries (RHBP). As indicated, expected benefits of RHBD approach result from increased integration density, improved power efficiency and higher clock speeds compared to dedicated foundries.

State-of-the-Art

Nonvolatile Memories

Nonvolatile memories with high density, low operating power, high write/read speed, high endurance, and high radiation tolerance will be important to any deep space mission. The radiation-tolerant memories available currently or in near-term advanced development are listed in Table 4.16. Performance data for memories still under development are estimated based on preliminary test results.

Figure 4.28: Performance of radiation-hardened electronics for military space applications (RHBP), commercial markets, and RHBD.

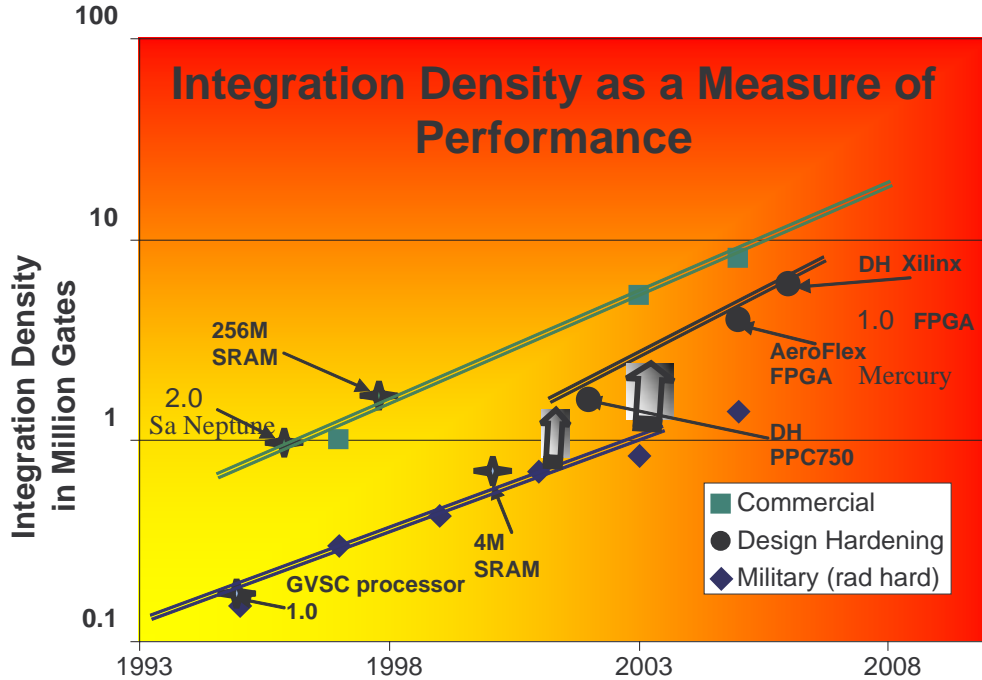


Table 4.15: Measured parameters for a single NAND logic gate manufactured with commercial, RHBD, and rad-hard processes (adapted from R. Lacoé, the Aerospace Corporation).

	HP 0.35 μm Commercial	HP 0.35 μm RHBD	HP 0.5 μm Rad Hard
Lambda (μm)	0.20	0.20	0.30
Cell area (μm²)	51.00	88.44	114.75
W/L (n)	5.00	12.00	5.00
W/L (p)	9.00	20.00	9.00
Supply voltage (V)	3.30	3.30	5.00
Propagation delay (ns) (FO=2)	0.10	0.09	0.14
Power dissipation (μW/MHz)	0.29	0.64	1.10
Power delay product (aJ/MHz)	38	80	168
Gate density (Mgates/cm ²)	1.96	1.13	0.87
Maximum operating frequency (MHz)	376	402	328
Thru-put/Watt (Mgates-Mhz/cm ² /μW)	6.82	1.75	0.79

Table 4.16: Memory characteristics of nonvolatile memory available currently or in the near future.

Type	Vendor [†]	Density (Mb)	Write speed (ns)	Read speed (ns)	Endurance (cycles)	Status
EE PROM	NG	0.256	10000	250	10^6	Available
PROM (read only)	Aeroflex	0.256	N/A	40	N/A	Available
Flash	Commercial	1000	10000	10000	10^5	Available
CRAM	BAE	4	500	70	10^8	Available
FeRAM	Celis/TI	0.008	45	20	10^{13}	Prototype
MRAM	HW	1	100	60	10^{15}	Available
MRAM	HW	4	~100	~60	10^{15}	Prototype

[†] Vendors are identified as follows: NG = Northrop–Grumman; BAE = British Aerospace; TI = Texas Instruments; HW = Honeywell.

Radiation tolerance for these chips is summarized below in Table 4.17.

Table 4.17: Radiation tolerance characteristics of radiation-tolerant, nonvolatile memory available currently or in the near future.

Type	Vendor [†]	TID krad(Si)	SEU (MeV/mg/cm ³)	SEL (MeV/mg/cm ³)
EE PROM	NG	300	>35	Immune
PROM (read only)	Aeroflex	1000	>70	>110
Flash	Commercial	~30	2	~10
CRAM	BAE	1000	>60	>100
FeRAM	Celis/TI	1000	TBD	>75
MRAM	HW	300	>75	Immune
MRAM	HW	1000	>75	Immune

[†] Vendors are identified as follows: NG = Northrop–Grumman; BAE = British Aerospace; TI = Texas Instruments; HW = Honeywell.

The highest density memory (1000 Mb) currently available is flash memory, but it is only tolerant of a TID of 30 krad. Prototype devices of 4 Mb projected to handle a TID of 1 Mrad are under development.

At this time, the single chip 1 Mbit, 300 krad, MRAM from Honeywell is the only commercially available nonvolatile, rad-hard memory. Additionally, the MRAM and CRAM are expected to be offered in 5 \times stacked die modules that will increase the highest available memory to 16 Mb or 64 Mb. Currently, Celis/TI is planning to develop 64 Mbit chips, but with an availability date that is yet undetermined. Packaging of individual die may also allow for increased chip/package densities in the future.

In addition, the Japanese Aerospace Exploration Agency (JAXA) is investing in the development of the fully depleted SOI (FDSOI) based FeRAM memory. These parts are expected to operate at 1 GHz, be latchup and SEU immune, and have a density of up to 16 Mb, but it is still difficult at this time to determine the schedule and readiness for this technology.

Other emerging memory technologies are too early in their development to be considered viable for any missions expected in the next decade. However, they may offer viable options for future missions to Europa, such as Europa Astrobiology Lander. These novel memory technologies include the carbon nanotube (CNT), nanoparticles, holographic memories, and ionic metal-based memories.

High Speed, Volatile Memory

A host of command and data handling (C&DH) subsystems require various startup, cache, and main computer memories. The most commonly used solutions are based on SRAM and DRAM architectures. The poor radiation performance of synchronous dynamic random-access memory (SDRAM) and dynamic random-access memory (DRAM) lead to much more difficult design solutions for a high radiation environment; therefore, SRAM memories often make more practical design solutions.

The highest single chip density available at present is 4 Mb SRAM. Chips with higher density are based on multichip modules (MCM), stacked die (3D-Plus), or multidie flat packs. Single-chip densities of 16 Mb are expected to be available from Honeywell and BAE Systems in 2007 and 2009, respectively. Both vendors are planning on developing 4 \times or 5 \times stacked die modules that will increase the highest available memory options to 64 Mb. Although it is likely that other vendors will release higher-density SRAM options, this review did not have access to definitive roadmaps with assured funding sources. Of particular interest to C&DH is a high-speed L2 cache for the commonly used 167 MHz version of the IBM RAD750, and the upcoming 200 MHz enhanced radiation-hardened version (discussed further in the section on microprocessors). Currently, a 4 Mb, 5 ns access speed SRAM is nearing completion at BAE Systems. This part, manufactured on the new BAE Systems 0.15 μ m radiation hard foundry line, has a total dose hardness greater than 1 Mrad.

Unlike nonvolatile memories, the SRAM-based memory requires stand-by power for the memory to store the data. The required stand-by power is specific to the particular SRAM architecture and manufacturing process and is usually related to the memory cell leakage current. If SRAM is used for the spacecraft mass memory, the required power can be significant. Fortunately, the increased demand for lighter portable electronic applications with extended battery life has fueled the development of technologies that provide low stand-by power. These technologies, although developed for commercial markets, can be applied in the future to space-rated SRAM memory systems. SRAM memory options are summarized in Table 4.18.

Table 4.18: Radiation-tolerant SRAM memory available currently or in the near future.

Type	Vendor [†]	TID krad(Si)	SEU (MeV/mg/cm ³)	SEL (MeV/mg/cm ³)	Stand-by power (mW)	Status
HW	4	1000	40	Immune	14	Available
HW	16	1000	40	Immune	~20	2007
BAE	4	200	~70	Immune	25	Available
BAE	4	1000	~70	Immune	15	2007
BAE	16	1000	~70	Immune	10	2008
Aeroflex	16	300	53	100	20	Available
Maxwell	16	100	20	68	10	Available
Atmel	4	300	TBD	80	1	Available
Atmel	16	200	TBD	80	1	Available

[†] Vendors are identified as follows: HW = Honeywell; BAE = British Aerospace

Microprocessors

It is imperative for rad-tolerant processors within the C&DH system to be latchup immune and have a high SEU threshold for a reliable performance, while maintaining a high data throughput. Table 4.19 provides an overview of many of the processors suitable for a prolonged deep space mission. The Rad750 manufactured by BAE Systems and Honeywell's PPC603e are the most advanced processors specifically designed for low power and high reliability. The "enhanced" version to BAE Systems RAD750 is currently manufactured at the new BAE Systems 0.15 μm radiation-hard foundry line. This part is concurrently developed with an 4 Mb SRAM L2 cache (see above) to provide an overall radiation-hard board-level solution, with a performance boost of about 2 \times over the existing RAD750.

This review does not include the LEON processor developed by the European Space Agency because the specific performance characteristics have not yet been published. The Japanese Aerospace Exploration Agency (JAXA) is developing a MIPS64 processor that passed initial production; however, radiation performance tests are not expected to be completed until

Table 4.19: Radiation-tolerant commercial and radiation-hardened space processors available currently or in the near future.

Processor	Vendor	Clock [MHz]	DMIPS [†]	TID [krad(Si)]	SEU	Latchup	Availability
RAD750	BAE Sys	132	242	300	5×10^{-5} / device	immune	available
RAD750 enhanced	BAE Sys	200	400	1000	TBD	immune	4Q 2006
PPC 750FX	Motorola	1000	1500	>100	2×10^{-9} cm ² /bit	immune	available
PPC 603	HW	100	167	1000	5×10^{-5} /day	immune	available
Rad 6000	HW	25	25	1000	5×10^{-5} /day	immune	available
Mongoose V	HW/Synova	12	20	300		>80	available
MIPS64 5kf	JAXA	200	320	tests in progress			1Q 2007
SCS750A [‡]	Maxwell	800	1800	>100	5×10^{-5} /day	immune	available

[†] DMIPS refers to Dhrystone MIPS, a score used to represent benchmarks more meaningfully than MIPS (million instructions per second) because MIPS is not used across different instruction sets (i.e., RISC vs. CISC) for the same computation requirement from users. The main score is therefore Dhrystones (number of interactions of the main code loop) per second; the DMIPS is the Dhrystone score divided by 1,757.

[‡] Board solution

2007.

Maxwell's SCS750A is a single board computer solution using commercially available PPC 750FX chips. With chip-level triple modular redundancy (TMR) and EDAC (error detection and correction), it achieves an upset rate of 10^{-5} errors/device/day in a galactic cosmic ray (GCR) environment. This approach is useful because it yields a very high-throughput of 1800 Dhrystone MIPS at less than 25 W, while maintaining at the board level a relatively low SEU rate. Qualification methods for this board still require investigation.

The BAE's system RAD 750 processor was used in Deep Impact, XSS-11, and MRO, and the enhanced version is being baselined for the MSL mission, currently in implementation phase.

Analog-to-Digital Converters

The analog-to-digital converter (ADC) is a critical component for the design of electronic hardware for flight projects. Key performance requirements and drivers include: bit res-

olution, driven by sensor applications; power, driven by general applications; and speed, required predominantly by communication applications. Each mission may have tens of ADCs distributed throughout the electronics. Each ADC may have differing performance specifications based on its specific application. With the number of suppliers of flight-worthy components dwindling, it is now necessary to evaluate COTS products for mission suitability.

In general, several latchup immune solutions exist for 8-bit and 14-bit ADCs covering a broad spectrum of sample rate, low power dissipation, and good conversion efficiencies for most applications. Similarly, numerous vendors offer latchup-immune and reasonably TID-hardened 12-bit, 14-bit, and 16-bit ADCs. Although the sample rate for the 12-bit ADC is lower than desirable, it may be the only option because no suitable radiation hard solutions currently exist for 10-bit and 24-bit ADCs. Tables 4.20 and 4.21 summarize the currently available ADCs.

Table 4.20: ADCs available currently or in the near future.

Resl (bit)	Vendor	Part Number	Process
8	FSC/SPT	SPT7725	Bipolar
8	Analog Dev.	7684RP	CMOS
8	National	ADC1175	CMOS
8	Atmel	TS8388B	Bipolar
12	Analog Dev.	AD9871XE	CMOS
12	Analog Dev.	AD6640	Bipolar/SOI
12	Analog Dev.	AD1672	CMOS
12	Honeywell	RH9225	CMOS/SOI
14	Raytheon	AL2	CMOS
14	ADI/Maxw	7871RP	CMOS
14	ADI	AD6644	Bipolar/SOI
14	Linear Tech.	LTC1417	CMOS
16	TI/Maxw	7809LPTRP	CMOS
16	Linear Tech	LTC1604	CMOS

Field Programmable Gate Arrays

For deep space missions, NASA has a long tradition of using highly reliable, and preferably radiation-tolerant, electronics. COTS parts are used on many missions to augment the limited selection of military-grade parts and/or to reduce costs. Driven by the need to further reduce part cost and increase spacecraft performance, NASA has gradually shifted the part pedigree away from the customary path of choosing military-grade parts electronics to the path of choosing COTS parts. One key example of NASA's new strategy is the increasingly

Table 4.21: Specifications for ADCs available currently or in the near future.

Resl (bit)	Vendor	Part Number	Power Dissipation (W)	Analog Input Voltage (V)	Conversion rate/time (Msps)	TID (krad)	SEL (MeV–cm ² /mg)
8	FSC/SPT	SPT7725	2.2	0 to –2	300	100	>100
8	Analog Dev.	7684RP	0.45	0 to 5	15	100	Immune
8	National	ADC1175	0.06	0 to 4	20	100	No data
8	Atmel	TS8388B	3.4	±1	1000	150	No data
12	Analog Dev.	AD9871XE	1	±1	5	200	Immune
12	Analog Dev.	AD6640	0.7	2	65	100	Immune
12	Analog Dev.	AD1672	0.24	5, 2.5, –2.5	65	100	Immune
12	Honeywell	RH9225	0.24	4	20	300	Immune
14	Raytheon	AL2	0.325		10	300	Immune
14	ADI/Maxw	7871RP	0.05	±3V	1	100	Immune
14	ADI	AD6644	1.3	±2	65	100	Immune
14	Linear Tech.	LTC1417	0.15	±2.5	0.8	20	>67
16	TI/Maxw	7809LPTRP	0.15	±5, ±10	0.1	10	20
16	Linear Tech	LTC1604	0.22	±2.5	0.33	100	55

common use of Field Programmable Gate Arrays (FPGAs).

Generically, FPGAs fall into two categories: 1) Antifuse-based, one-time programmable devices; and 2) reprogrammable FPGAs, based on SRAMs or nonvolatile memories. The state-of-the-art FPGAs (Table 4.22) available to space and military users are limited to latchup hardened SRAM-based (Xilinx) and antifuse-based (Actel) FPGA parts, with total dose capabilities at or below 300 krad and system gates totaling of 6 M or less. Currently, multiple efforts are focused on assessing the overall radiation performance of FPGAs. This part has one or two processor cores embedded in the FPGA fabric, blurring the line between FPGAs and processors.

The state-of-the-art FPGA market is largely limited to radiation-tolerant parts, some of which have significant SEU tolerance issues. Only one new radiation-hard FPGA is under development at BAE Systems for space use. The part is based on the Actel RHAX 250 series, with a design shrink to the BAE Systems 0.15 micron rad-hard line. The total dose performance of >1 Mrad(Si) is only a projection of the radiation performance based on test structures.

Improvements in embedded processors and other items, such as nonvolatile memory, high-speed SRAM, microcontroller functions, and bridge chip functions, would benefit the space community through the improvements in mass, volume, and performance. However, these improvements bring added complexity, making radiation assessments much more difficult.

Table 4.22: Radiation-tolerant and radiation-hardened FPGAs available currently or in the near future.

Vendor	Device #	Core (V)	I/O supply (V)	System gates (000's)	Avail.	TID (krad(Si))	SEL (MeV–cm ² /mg)	SEU (MeV–cm ² /mg)
Actel	RTSX72SU5	2.5	3.3/5	108	Yes	100	>100	
Actel	RTAX1000SU	1.5	3.3	1000	Yes	200	>100	>50
Actel	RTAX2000SU	1.5	3.3	2000	Yes	200	>100	>50
Aeroflex	Eclipse UT6325	2.5	2.5/3.0	320	Yes	300		
Atmel	AT40KEL040	3.3	3.3	50	Yes	200		
BAE Sys	RH AX 250	2.5	3.3	250	1Q2009	>1000		
Xilinx	XQR2V1000	1.5	1.8–3.3	1000	Yes	200	>125	1
Xilinx	XQR2V3000	1.5	1.8–3.3	3000	Yes	200	>125	1
Xilinx	XQR2V6000	1.5	1.8–3.3	6000	Yes	200	>125	1
Xilinx	XQR2VP40	1.5	1.8–3.3	4000	Yes	200	>100	1
Xilinx	XQR2VP70	1.5	1.8–3.3	7000	Yes	250	>100	1

Commercially, integrated circuits today are increasingly produced as ASICs, circuits designed for a specific use. Because contemporary ASIC devices have such high capabilities, gate arrays today are evolving into “structured ASICs”; these consist of a processor core, a digital signal processing unit (DSP), peripherals, interfaces, SRAM, and extra logic gates. Unfortunately, despite a growing presence of structured ASICs in consumer electronics, radiation-hardened structured ASICs do not currently exist for the space market.

Custom rad-hard ASICs are currently available from Honeywell that are qualified for both digital and mixed-signal uses and are highly reliable. This type of ASIC requires long development times and is not reprogrammable. Also, the costs associated with these types of ASICs can be substantial. This approach has been successfully used on previous mission such as Cassini, NPOESS, and many military missions.

User-Programmable Gate Arrays

NASA’s assessment of future availability of military-grade, radiation-hardened ASICs sees this industry under continued strain, particularly since the military may not sponsor further development of ASICs. The relatively small radiation-hard electronics market requires that hardware and technology development costs be amortized over small part counts. This, in turn, yields a purchase price approximately 100 times higher than those of their commercial counterparts, making radiation-hardened parts less attractive to suppliers to the commercial aerospace market and accelerating the market’s decline. This self-perpetuating cycle reduces the hardware upgrade rate of radiation-hard foundries and continues to widen the performance gap of commercial parts.

To replace high-cost components fabricated in dedicated foundries, technology development should focus instead on customer-configurable, radiation-tolerant technologies configurable by the end user in the lab (i.e., reprogrammable and one-time programmable FPGAs) or the manufacturing floor (i.e., Structured ASICs or S-ASIC — see Table 4.23). Although FPGAs have a lower unit cost and are therefore preferable for applications requiring short development time the cost of additional screening and qualification for flight may be prohibitively high for many missions.

Table 4.23: A model radiation hard PPC750 implementation using customizable gate arrays or standard ASICs.

	Full custom ASIC (180 nm)	Structured ASIC (180 nm)	FPGA (130 nm)
Design NRE [†] costs (\$M)	5–15	0.5–2	0.5–1
Chip cost (\$)	1,000 [‡]	1,000	5–15,000
NRE schedule (months)	12–18	2–10	1–6
Fabrication schedule	3 months	2 weeks	1 day
Density (M Gates)	2	2	0.3
Speed (MHz)	250	200	75
Typical uses	Microprocessor, CPU	General logic, including processors	General logic, reconfigurable logic
Performance level	High	Medium	Lower

[†] Nonrecurring engineering activities are known as NRE.

[‡] Excludes intellectual property licensing costs

NASA and the aerospace industry have extensive experience with one-time programmable and reprogrammable FPGAs. Structured ASICs, on the other hand, are relatively new in the commercial arena and are not used in any fashion in the space industry. All of the various flavors of commercially available structured ASICs are prefabricated gate arrays, without the final 1 to 3 metal layers. The end customer can specify a final personalization of the die as designed with a vendor-specific design tool.

Technology and Advanced Development Needs

Two primary directions of development have been identified to meet the needs of those solar system exploration missions identified in the 2006 Strategic Roadmap that would be exposed to the most severe radiation environments. This assessment includes the advanced development needs for missions that would fly within the next decade and second on the needs and opportunities for missions in the subsequent decade.

Jupiter Radiation Environments

The most severe radiation environments in the solar system are encountered in the Jovian radiation belts. The most intense radiation is found in a torus-shaped zone that includes the orbits of Io and Europa. The New Frontiers Juno mission, currently in Phase B, has a highly inclined and eccentric orbit with a perijove very close to Jupiter itself and initially close to the Jupiter equator, which significantly mitigates the dose rate received. The Europa Explorer mission, which is currently in pre-Phase A, is exposed to much higher dose rates. The accumulated dose for two years in Jupiter orbit followed by a 90-day nominal mission in Europa orbit is about 3.5 Mrad. The Europa Astrobiology Lander could take place at least a decade later, and would experience a lower dose because of shielding by Europa.

Near Term Advanced Development Needs

At present, the basic technology exists for implementing a Europa Explorer mission that would enable the spacecraft to achieve its design life in the extreme radiation environments of the Jupiter system. However, significant advanced development and engineering challenges remain that must be addressed by the Europa Explorer pre-project. Here we review the radiation design approach for the Europa Explorer and what would be required during the implementation of this mission to assure success.

The Europa Explorer mission concept of 2006 [Cla07] has been designed to accommodate the state-of-practice in rad-hard electronics described above. It takes advantage of rad-hard components that have become available over the last five years. It also makes use of the generous mass margins that are enabled by an indirect trajectory to Jupiter, which allow more radiation shielding to be used than in earlier mass-constrained mission concepts. Another feature of the Europa Explorer mission concept is the use of a radiation-hard, volatile memory for the mass memory. Since the mission has been designed to minimize mass memory needs, a memory based on currently available 4 Mbit devices is feasible and the spacecraft has sufficient power to accommodate standby power needs.

While the basic technology is there to make the mission possible, the development of parts for spacecraft systems and instruments would require significant investment and would require early investments during the formulation phase and will extend the development phase of the mission. Areas where particular attention will be needed are as follows:

Next Decadal Developments

In planning technology investments, which will have impacts beyond the first decade, two important factors will enter in. First, new technologies will appear and the rad-hard technologies we have today will become obsolete. Second, future missions will demand improved capabilities in terms of signal processing, driving the need for DSPs, custom data handling (pushing the development of FPGAs) and precision measurement (driving the need for 24 bit A/D converters). Most of these technologies are not currently available even for use in moderately severe environments. Finally, for the second generation of exploration, in situ

exploration with an Europa Astrobiology Laboratory is recommended, which means that mass margins will be constrained and limit shielding.

The commercial introduction of Field Programmable Gate Arrays with embedded processors is one pathway to an onboard computational capability with more computational power per watt. A radiation-hard version of these components may offer solutions for future Europa missions. The embedded intellectual property, including processor modules, bridge chip functions, memory elements, and bus controller, could permit future missions to drastically reduce the discrete part count and integrate a large number of components into a single chip. In addition to its mass, schedule, cost, and power savings, the FPGA is well-suited to augment the central C&DH computer with substantial additional processing. Furthermore, the development of a mixed-signal Structured ASIC is advisable, as it could permit the user to build application-specific designs into the radiation-hard gate array fabric with minimal design or manufacturing cost. This development is expected to achieve performance numbers only 25% lower than pure ASICs. The understanding of technology needs external to NASA may permit subsequent collaborations responsible for developing parts even without NASA's participation; this process can be conducted by reviewing the plans of the Department of Defense's Radiation Hardened Oversight Council (RHOC) and continued active participation in their further evolution. In general, the RHOC has been focused on the needed digital components for the DoD; however, space exploration requires development of radiation-tolerant analog electronics.

Summary

NASA's solar system exploration program calls for electronics capable of implementing missions that would travel deep into Jupiter's radiation belts. For a Europa Explorer mission, if implemented during the present decade, NASA would be able to leverage past and current NASA and DoD investment in rad-hard electronics technology to meet missions needs. However, a significant amount of advanced development work would be needed during the mission development phase, particularly for avionics and scientific instruments. For missions with ample power and limited data storage needs, volatile memories could provide an adequate solution. Advances in nonvolatile memory would improve performance and would be enabling for future landed missions.

For missions in the subsequent decade, advances in electronics technology will create new opportunities and new challenges. Next-generation missions will demand more computing power, and more precise measurements, and will have less mass for shielding. This is best met by closing the current wide gap between the capabilities of state-of-the-art commercial electronics and currently available space-qualified processors. For low-power applications, exploiting the recent development in FPGA with embedded processors is one promising pathway to accomplishing this.

4.3.4 High-Temperature Energy Storage

Background

NASA is currently planning robotic missions for the exploration of the inner planets. Venus exploration missions pose significant challenges for energy storage systems. These missions require energy storage systems that have the capability to operate at high temperature and high pressure. The Venus temperatures ranges from 460°C at the surface to 0°C at an altitude of 55 km. The pressure ranges from 90 bars at the surface to 1 bar at an altitude of 55 km.

The types of missions that are being examined include: orbiters, atmospheric probes, short- and medium-duration landers, short- and medium-duration aerial platforms, surface sample return, and long-duration exploration systems. Venus Orbiters require energy storage systems with large cycle life capability and operational temperature capability in the range of 0–30°C similar to Mars and Earth orbiters. Venus surface missions (probes, landers, and rovers) require mass- and volume-efficient energy storage systems that can operate at temperatures as high as 480°C. Venus atmospheric exploration missions (aerial platforms, atmospheric probes) require energy storage systems that can operate at 50–480°C depending on the altitudes.

A detailed description of Venus exploration missions under consideration and projected launch dates is given in Section 3.3.2 of this report. The Venus Design Reference Mission set includes four Venus in situ missions, namely the short-duration on the surface Venus In Situ Explorer (VISE), the extended stay on the surface Venus Mobile Explorer (VME), the Venus Surface Sample Return (VSSR), and the Venus Geophysical Network missions. VISE is proposed as a New Frontiers class mission, and it would explore the composition and perform isotopic measurements of the surface and atmosphere of Venus. VISE would operate for several hours on the surface of Venus, acquiring and characterizing a core sample to study the mineralogy of the surface. The earliest launch date for VISE would be 2015. VME would be a Flagship mission that could launch as early as 2025. VME would explore and characterize the surface with a wheeled or an aerial vehicle and would acquire and characterize core samples. VME would need to operate in the Venus surface environment for at least 90 Earth days. The Venus Sample Return, proposed for the third decade, is a very difficult mission that would follow a successful Mars Sample Return and an effective Venus Mobile Explorer mission.

Energy Storage Systems

The energy storage systems that are under development can be classified into:

- a) primary batteries,
- b) rechargeable/secondary batteries,
- c) fuel cells,

- d) capacitors, and
- e) fly wheels.

Among these energy storage systems, primary batteries, rechargeable batteries, fuel cells and capacitors have been used widely in various space missions. Primary batteries ($\text{Zn}-\text{AgO}$, $\text{Li}-\text{SO}_2$, $\text{Li}-\text{SOCl}_2$, and $\text{Li}-\text{CF}_x$) are used in missions that require one-time use of electrical power for a few minutes to several hours. Primary batteries cannot be recharged. Rechargeable batteries, also referred to as secondary batteries ($\text{Ag}-\text{Zn}$, $\text{Ni}-\text{Cd}$, $\text{Ni}-\text{H}_2$, $\text{Li}-\text{Ion}$), can be recharged several hundred or thousands of times with an external source of electrical power. They are used mainly for load leveling in nuclear-powered missions and for providing electrical power for survival during eclipse periods in solar-powered missions. Fuel cells (alkaline and polymer electrolyte membrane) are used in missions that require large amounts of electrical power (several kilowatts) for periods of up to 10 days, such as human space missions (Gemini, Apollo, and Shuttle), but they have not been used on space science missions. Capacitors (double layer and electrolytic) are used for applications that require repeated high-power, short-duration pulses (seconds). Flywheels are still under development and have not been used so far in any space mission.

Some of the important characteristics of state-of-the-art, high-temperature batteries are shown in Table 4.24. These space-qualified batteries are designed to operate at -20°C to 40°C and are therefore not suitable for missions that encounter extreme environments such as high temperatures. The state-of-practice fuel cells are also not suitable for operation at high temperatures.

In the past (1960s and 1980s), the Soviet Union and the U.S. conducted a number of Venus exploration missions using state-of-practice batteries. The Soviets carried out more than 10 such missions for the exploration of Venus, including orbiters, probes, balloons, and landers. The U.S. launched four probes (Pioneer) for the exploration of Venus during the 1970s. The batteries for these missions were housed (along with the electronics and other scientific instruments) in a container that was thermally controlled by passive cooling along with insulation materials. This approach has resulted in significant mass and volume penalties at the container level. Further, the duration of these missions was limited to a few hours. The ideal solution is to employ energy storage systems that can operate outside the chamber at 460°C . Use of such high-temperature energy storage systems would result in significant mass and volume savings, as they do not need to be housed in the thermal container.

Operation of the batteries and fuel cells at high temperatures presents a number of technical challenges, including:

- Stability of electrode materials at elevated temperatures;
- Electrolyte stability and undesirable side reactions such as electrolyte oxidation at the cathode and reduction at the anode;

- Corrosion of the current collectors and the seals;
- Increased electrolyte vapor pressure;
- Stability and compatibility of the separator materials at elevated temperatures;
- Safety issues due to high reactivity of the electrode materials with electrolyte, separator; and
- Hardware issues arising from CTE mismatch.

In spite of these challenges, some high-temperature batteries ($\text{Li}-\text{FeS}_2$, $\text{Na}-\text{S}$ and $\text{Na}-\text{NiCl}_2$) have been developed for some defense and commercial applications. The battery systems were shown to have a capability to operate at temperatures from 225–450°C. These batteries are referred to as high-temperature batteries in this report and appear to offer the possibility of meeting the high-temperature operational requirements of the Venus exploration missions. However, further development of these batteries is required to make them space qualified.

In addition, there are a number of existing terrestrial batteries that have the potential to operate at temperatures up to about 250°C after some modifications/advancements. This type of batteries is referred to as Intermediate Temperature Batteries in this report. These batteries could be used for atmospheric missions (probes aerial platforms) that require operation up to 250°C. They could also be considered for surface exploration missions by keeping them in a thermally controlled chamber consisting of insulation and active cooling (with less mass and volume penalties than the state-of-practice ambient temperature batteries).

Finally, there has been a considerable amount of research on the development of advanced electrode materials and electrolytes required for the development of advanced batteries that can operate over a wide range of temperatures (including the High-Temperature Batteries) and deliver substantial energy densities. These are referred to as Advanced High-Temperature Batteries in this report. These are based on solid-state electrolytes as well as molten salt electrolytes. Some of these are projected to operate over a wide range of environmental temperatures, including the very high temperature range. Batteries employing these materials offer several potential advantages over existing high and intermediate temperature types. Developmental status of these Advanced High Temperature Batteries lags behind those of existing of High-Temperature Batteries and no hardware versions have yet been made. Nevertheless, these are considered promising candidates for future missions with environments that range from the intermediate through the high temperature ranges (250°C through 500°C).

Fuel cells also have the capability to operate at high temperatures. Some of the high-temperature fuel cells under development for terrestrial applications include: molten carbonate fuel cells and solid oxide fuel cells. The operating temperature of the molten carbonate fuel cells is about 600°C and the solid oxide fuel cells operate at temperatures higher

than 800°C. These fuel cell systems are suitable for long-duration missions. However, there are several system issues (including fuel and oxidant handling) that need to be resolved before considering them for future Venus missions.

The prospective energy storage systems for future planetary exploration missions in high-temperature environments can be classified into three types:

- i) High-Temperature Batteries;
- ii) Intermediate-Temperature Batteries;
- iii) Advanced High-Temperature Batteries; and
- iv) High-Temperature Fuel Cells.

A brief discussion of the status of the development of these batteries and fuel cells, as well as the technical issues that need to be still resolved before they can be considered for future space missions, are presented below.

High-Temperature Batteries (>450°C)

High temperature batteries that are under development can be classified into two groups:

- a) Thermal Batteries; and
- b) High-Temperature Rechargeable Batteries.

Thermal batteries were developed primarily for use in weapons and missiles by DOD and DOE. These are primary batteries and are activated thermally before use. The impetus for the development of high-temperature rechargeable batteries came primarily from the electric vehicles and load leveling applications. These batteries appear to offer promise for meeting high-temperature operational requirements of the future Venus exploration missions (surface as well as atmospheric). However, further development of these batteries is required to make them space qualified.

Thermal Batteries

Thermal batteries were developed by DOD and DOE for use in weapons and missiles. These are primary batteries and are activated thermally before use. A signal from an external source initiates the ignition of pyrotechnic materials (heat pellets) within the battery. This ignition in turn results in melting the electrolyte and the battery produces electrical power for a short period of time (from a few seconds to an hour). The exact lifespan of individual thermal batteries depends on both design and application.

Thermal batteries contain an alkali or alkaline earth metal anode, a molten salt electrolyte, a transitional metal salt cathode, and a heat source (usually positioned between the cells). Lithium alloys are the most commonly used anode materials in the thermal batteries, though magnesium metal and calcium are also used. Transition metal sulfides (FeS_2 , CoS_2) are

presently used as the cathode materials in the present-day versions of the thermal batteries, although calcium chromate, potassium dichromate, potassium chromate, lead chromate, and metal oxides have also been used. A eutectic mixture of lithium chloride and potassium chloride is often used as the molten salt electrolyte in these batteries. In addition, thermal insulation is positioned around and at both ends of the cell stack to reduce heat loss rates and thereby maintain operable internal temperatures for longer periods, and the battery is designed to remain hermetically sealed throughout its service life. Thermal batteries have specific energy of about 45 Wh/kg and can function in a thermal environment that ranges from 7°C to 74°C (45°F to 165°F).

These batteries are not suitable as such for use in future Venus exploration missions. Major modifications in design and chemistry of the thermal batteries are needed before they can be considered for future space missions. The modifications required include:

- a) removal of the heat pellets;
- b) removal of the activation squib;
- c) thermal design changes (removal of the insulation materials);
- d) use of advanced molten salt electrolytes to achieve operation in the desired temperature range;
- e) cell hardware and seal designs; and
- f) increase of electrode thickness.

The modified design can be somewhat simpler and provide improved performance. These modified thermal batteries are projected to have specific energy of about 200 Wh/kg and could operate at temperatures up to 500°C.

High-Temperature Rechargeable Batteries

Significant work was carried out in the 1970s and 1980s on the development of high-temperature (300°C to 600°C) rechargeable batteries. DOE and several contractors examined high-temperature rechargeable batteries for over 30 years for electric vehicle and load leveling applications. These systems include: a) LiAl-FeS₂, b) Na-S, and c) Na-metal chloride. Several functional and full-scale electric vehicle (EV) demonstration units were developed and tested. Although these batteries were designed as rechargeable versions, they can function in the primary battery mode as well. Some of the important characteristics of the three high-temperature rechargeable batteries are given in the Table 4.24.

The major issues that need to be addressed before these batteries could be considered for space applications include:

- a) adapting cell and battery designs for space applications;
- b) insuring the stability of seals and terminals;

Table 4.24: State-of-the-art high-temperature secondary batteries.

Characteristic	LiAl–FeS ₂	Na–NiCl ₂	Na–S
Operating temperatures (°C)	400–475	220–500	290–450
Open circuit voltage (V)	1.73	2.58	2.08
Discharge voltage range (V)	1.2–1.8	2.1–2.5	1.7–2.0
Theoretical specific energy (Wh/kg)	490	800	755
Specific energy for batteries (Wh/kg)	Near 100	90–130	80–120
Energy density for batteries (Wh/l)	Near 150	70–130	90–150
Cycle life (cycles)	>1000	>1000	2000
Energy efficiency (%)	80	80	80

- c) minimize the corrosion of current collectors at high temperatures;
- d) determine the effects of zero gravity upon performance;
- e) improving the safety; and
- f) optimizing the electrolyte composition to improve conductivity and reliability.

Development status of these three high-temperature rechargeable batteries is given below.

Lithium–Metal Sulfide (LiAl–FeS₂) Batteries: This is a molten salt rechargeable battery and was developed primarily at Argonne National Laboratory in the early 1970s for vehicular propulsion. These batteries use a lithium alloy anode such as Li–Al, an FeS₂ cathode, and a molten salt electrolyte, LiCl+KCl. Other metal sulfides, such as nickel and cobalt, may offer higher performance for some niche applications. The cell reaction is given by $2LiAl + FeS_2 \leftrightarrow Li_2FeS_2 + 2Al$. Electrolyte refinement and the development of stable chalcogenide ceramic sealants has led to the development of sealed electrolyte-starved bipolar LiAl/FeS and LiAl/FeS₂ cells and batteries. The most advanced version of these employs a cylindrical, bipolar configuration with disc-shaped elements. A unit cell is comprised of discs of anode and cathode, separator, electrolyte, and intercell connectors. The anode is made from pressed powders of the alloy plus some electrolyte. The operating temperature range of this battery system is about 375°C to 475°C, and the realized specific energy at the battery level is about 100 Wh/kg.

Several improvements are needed before this battery system could be considered for use in future space missions. These include: optimization of the operating temperature, safety improvements, cell hardware modifications, and use of improved cathodes such as CoS₂. The operating temperature range of the LiAl–FeS₂ system could further be optimized by replacing the binary (LiCl and LiBr) electrolyte melt with a ternary system, i.e., a mixture of LiCl, LiBr, and KBr. The effects of self-heating on these batteries in a high-temperature

ambient have not yet been determined and need to be examined experimentally. These effects are expected to depend on discharge rate, cell geometry, and thermal engineering.

Sodium–Sulfur (Na–S) Batteries: This system was the first high-temperature battery that was widely studied and well developed. Development was initiated in the beginning by the observation that sodium beta alumina ceramic permits rapid mobility of sodium ions. The Na–S battery is a solid electrolyte type that employs a molten sodium anode, a solid beta alumina electrolyte/separator, and a molten sulfur cathode. Beta alumina has a high sodium ion conductivity of 1–10 S/cm at operating temperatures and a low electronic conductivity. The operating temperature range of the battery is 290°C to 450°C, and the cell reaction is: $2Na + xS \leftrightarrow Na_2S_x$ ($x = 2.7$ to 5). The cell has a cylindrical configuration with an outer metal case and an inner thin cylinder of the solid beta alumina electrolyte. The sodium anode is located inside the electrolyte cylinder and partially contained within yet another thin safety can. A metal rod inside the inner can and in contact with molten sodium serves as an anode current collector. The sulfur is contained in the annular space between the electrolyte and the outer can. A graphite–felt material serves as the cathode current collector.

These batteries have a specific energy of about 80–120 Wh/kg at the battery level. This system has good cycle life but is plagued by the fragile nature of the ceramic separator and safety issues upon separator failure. The high vapor pressure of the sulfur precludes the use of Na–S systems for temperatures exceeding 450°C. However, a mixed sulfur–selenium cathode has been proposed to mitigate this effect.

Sodium–Metal Chloride (Na–MCl₂, M=Ni, Fe) Batteries: This battery, pioneered in the 1980s by the Beta R&D Company and known as the “ZEBRA” (Zero Emission Battery Research Activities) battery, is an offshoot of sodium–sulfur, with the sulfur cathode replaced with nickel or iron chlorides in contact with tetrachloroaluminate melt for improved safety. The battery is a solid electrolyte type that uses a molten sodium anode and a solid beta alumina electrolyte/separator to provide a full cell reaction of $2Na + MCl_2 \leftrightarrow M + 2NaCl$. The operating temperature is 250°C to 500°C.

A composite cathode is used in these batteries, where solid NiCl₂ is in contact with molten NaAlCl₄ to allow for rapid Na diffusion during operation. The cell has a cylindrical configuration with an outer metal case and an inner thin walled cylinder of solid sodium beta alumina electrolyte. The sodium anode is located in the annular space between the ceramic electrolyte and the metal case, while the MCl₂ cathode is located inside the electrolyte tube. Nickel chloride is now primarily used because of its high specific energy compared to iron chloride, though iron chloride is still used as a cathode dopant to prevent morphological changes in NiCl₂ upon cycling and to increase the specific energy by 40% to 130 Wh/kg. The metal case serves as the anode current collector and the metallic nickel inside the cathode material serves as the positive current collector. The development of a fluted or cruciform-shaped beta alumina electrolyte element providing an enhanced reaction area

represents an important advance in this technology. This system has good cycle life but is plagued by the fragile nature of the ceramic separator and safety issues upon separator failure.

Intermediate Temperature Batteries (50–250°C)

In this report, the batteries that can operate safely at temperatures 50–250°C are referred as Intermediate Temperature Batteries. There are no primary and rechargeable batteries (that are currently in use) that could operate in this intermediate temperature range. Some of the lithium primary batteries with liquid cathodes can function up to 150°C. Some primary and rechargeable lithium battery systems with solid cathodes could be modified/improved to operate up to 250°C.

Lithium Primary Batteries

There is no primary battery system currently in existence that could operate in this intermediate temperature range. The operation of the batteries with aqueous electrolytes ($Zn\text{--MnO}_2$, $Ag\text{--Zn}$) is limited to 60°C. The existing Li primary systems can only work up to 70°C, except for Lithium thionyl chloride ($Li\text{--SOCl}_2$) and lithium–sulfuryl chloride ($Li\text{--SO}_2Cl_2$) systems (Table 4.25). These two types of batteries have been demonstrated to operate up to 150°C. Some of the current Li primary battery systems with solid cathodes ($Li\text{--CF}_x$) could be modified to operate up to 250°C.

Table 4.25: State-of-the-art intermediate-temperature (50–250 °C) batteries.

	$Li\text{--SO}_2$	$Li\text{--SOCl}_2$	$Li\text{--MnO}_2$	$Li\text{--CF}_x$	$Li\text{--SO}_2Cl_2$
Operating range (°C)	To 70	To 150	150	To 70	To 150
Open circuit voltage (V)	3.0	3.6	3.0	3.2	4.0
Specific energy for batteries (Wh/kg)	240	390	~140	500	?
Energy density for cells (Wh/l)	375	880	~200	900	?

$Li\text{--SOCl}_2$ Primary Batteries: In these batteries, lithium functions as anode material, and the cathode active material is liquid thionyl chloride ($SOCl_2$). The electrolyte consists of tetrachloroaluminate ($LiAlCl_4$) dissolved in $SOCl_2$. $Li\text{--SOCl}_2$ cells are available in a cylindrical configuration. Each cell is composed of a spirally wrapped Li anode, carbon cathode current collector, and organic separator. The overall reaction is $4Li + 2SOCl_2 \rightarrow 4LiCl + SO_2 + S$.

The cell exhibits a high open-circuit voltage of 3.6 V, with a high specific energy near 390 Wh/kg and energy density near 880 Wh/l. This chemistry has a heritage with the Mars

Pathfinder and Deep Impact missions. This battery can operate at temperatures up to 150°C and was successfully used for through-hole drilling applications.

Li–SO₂Cl₂ Primary Batteries: These batteries are similar to Li–SOCl₂ batteries except that the active cathode materials are the sulfuryl chloride instead of thionyl chloride. Lithium functions as anode material in these batteries, and the cathode active material is liquid sulfuryl chloride (SO₂Cl₂). The electrolyte consists of tetrachloroaluminate (LiAlCl₄) dissolved in SO₂Cl₂. Li–SO₂Cl₂ cells are available in a cylindrical configuration. Each cell is composed of a spirally wrapped Li anode, carbon cathode current collector, and organic separator. The overall reaction is $4Li + 2SO_2Cl_2 \rightarrow 4LiCl + 2SO_2$.

The cell exhibits a high open-circuit voltage of 4.0 V, a high specific energy near 390 Wh/kg, and energy density near 880 Wh/l. This battery system can also operate up to 150°C and was considered for several weapons applications.

Lithium Primary Batteries with Solid Cathodes: The state-of-the-art Li primary batteries with solid cathodes are not operational beyond 70°C. However, some of them could be modified to operate up to 250°C. These modifications include: 1) the use of lithium alloys instead of lithium metal; 2) use of high-energy solid cathodes such as transition metal oxides and fluorides, e.g., CF_x and MnO₂; 3) use of high boiling point nonaqueous organic electrolytes (sulfolane or PC based); 4) use of ionic liquid-based electrolytes; and 5) thermally-resistant cell hardware.

Modified Rechargeable Lithium-Ion Batteries

There is no existing rechargeable battery system that could operate in this medium temperature range. The operation of state-of-the-art batteries with aqueous electrolytes (Ni–Cd, Ni–H₂, Ag–Zn) is limited to 60°C. State-of-the-art lithium-ion batteries that employ liquid organic electrolytes also operate only up to 70°C. However, the Li-ion systems could be modified to operate up to 250°C. These modifications include: 1) the use of lithium alloys instead of carbon anodes; 2) use of stable high-energy solid cathodes such as transition metal oxides; 3) use of high boiling point nonaqueous organic electrolytes (sulfolane or PC based); 4) use of ionic liquid-based electrolytes; and 5) thermally-resistant cell hardware.

Next Generation / Advanced High-Temperature Batteries

A great deal of research is being carried out on new battery systems that can operate at elevated temperatures. The work has included assessment of alternate anode and cathode materials as well as new electrolytes based on solid as well as molten salt electrolytes.

Based on one or more of these advanced anode and cathode materials and a solid-state or molten salt electrolyte, it is possible to develop high-temperature primary and rechargeable

batteries with an energy density far exceeding the LiAl/FeS₂ system. Laboratory versions of some cells employing these electrolytes have been shown to operate over a range of temperatures from the medium to high levels referred to above. Although actual battery hardware has not yet been developed with most of these advanced materials, the laboratory results to date have been quite promising. These batteries are expected to offer significant advantages over existing elevated temperature batteries in terms of simpler design and operation as well as increased energy density.

Sandia National Laboratories has developed a high temperature primary battery that can operate at temperatures up to 250°C. Also, JPL recently reported a primary battery that could operate up to 450°C. These two battery systems are based on fluoride ion-based, solid-state electrolytes. The major limitation of these batteries is that they can only operate at very low discharge rates. Further development work on these systems is expected to make them attractive for future Venus surface missions.

The research work that was reported on the development of advanced anodes, cathodes, electrolytes, and the batteries is given below.

Anodes: A number of anode systems, including Li-Al alloys, Li-Si alloys, Li-Mg alloys, molten Na, and carbon intercalation materials have been investigated. Many of these systems are well understood and studied. The lithium alloy-based anode systems are possibly appealing for intermediate temperature, such as 150–250°C. Table 4.26 lists some candidate anode materials.

Table 4.26: Anode candidates for solid electrolyte batteries.

Anode	Maximum temperature (°C)
Li-Al alloy	>500
Li-Si alloy	>500
Li-Mg alloy	>500
Carbon	>500
Molten Na	Unknown

Cathodes: Many cathode materials have high theoretical specific energy values and melting temperatures that exceed the targeted high-temperature environment. Table 4.27 lists a number of candidate materials for cathodes, their theoretical capacity or specific energy, the current TRL level, and the melting temperature.

Electrolytes: Several new solid-state and molten salt electrolytes are being developed for use in high-temperature batteries. Table 4.28 lists a number of electrolytes and suggested

Table 4.27: Cathode candidates for solid electrolyte batteries.

Cathode	Theoretical capacity (Wh/kg)	Melting temperature (°C)
MnO ₂	1005	535
CuCl ₂	1125	620
V ₂ O ₅	490	690
MoO ₃	525	795
Bi ₂ O ₃	640	817
CuO	1280	1326
(CF) _x	2180	Unknown
Bi ₂ Pb ₂ O ₅	544	Unknown
Ag ₂ CrO ₄	515	Unknown

operating temperatures.

Table 4.28: Electrolyte candidates for high-temperature batteries.

Electrolyte	Conductivity at 450°C (S/cm)	Maximum temperature (°C)
LiI based (Al ₂ O ₃)	0.1	270–450
LiBr based (Al ₂ O ₃)	0.1	270–550
LiCl/KCl (salt)	0.1	>500
Beta Al ₂ O ₃	0.1	>500
80(Li ₂ S)/20(P ₂ S ₅) (molten salt)	0.1	>500
LiSO ₄ /LiPO ₄	0.1	>500
LiSiO ₄	0.1	>500
Li ₅ MO ₄ (M= Al, Ga, Fe)	0.1	>500
LiMCl ₄	0.1	>500
LiSiCON	0.1	To 800
NaSiCON	0.1	Unknown
Li ₃ N	0.1	Unknown
MgO	0.1	Unknown

The solid electrolytes under development include:

- a) lithium ion conducting electrolytes;

- b) sodium ion conductive electrolytes;
- c) fluoride ion conducting electrolytes; and
- d) nitrate ion conducting electrolytes.

Lithium solid electrolytes of interest include LiSiO_4 and related phases, Li_5MO_4 ($\text{M}=\text{Al}$, Ga , Fe), LiSiCONs , Li–rare earth titanate perovskites, Li_2SO_4 , Li_3N , LiMCl_4 ($\text{M}=\text{Mg}$, Mn , Ti , Cd , Cr Co , Fe , Zn). The lithium solid electrolytes are suitable for use with lithium alloy anodes and metal oxide cathodes. The sodium ion conducting electrolytes (NaSiCONs) are attractive for use in advanced sodium–S/Se batteries or sodium–metal chloride batteries. The fluoride ion solid-state electrolytes (alkali and alkaline earth metal fluorides) are suitable for use with batteries employing metal fluoride-based cathodes. Nitrate ion conducting solid electrolytes are being considered for batteries employing metal chloride cathodes (CuCl_2). Figure 4.29 shows the variation of conductivity with temperature for several materials. In the temperature range of interest for this study, all of the materials show conductivities exceeding 0.1 S/cm.

The types of molten salt electrolytes under development include:

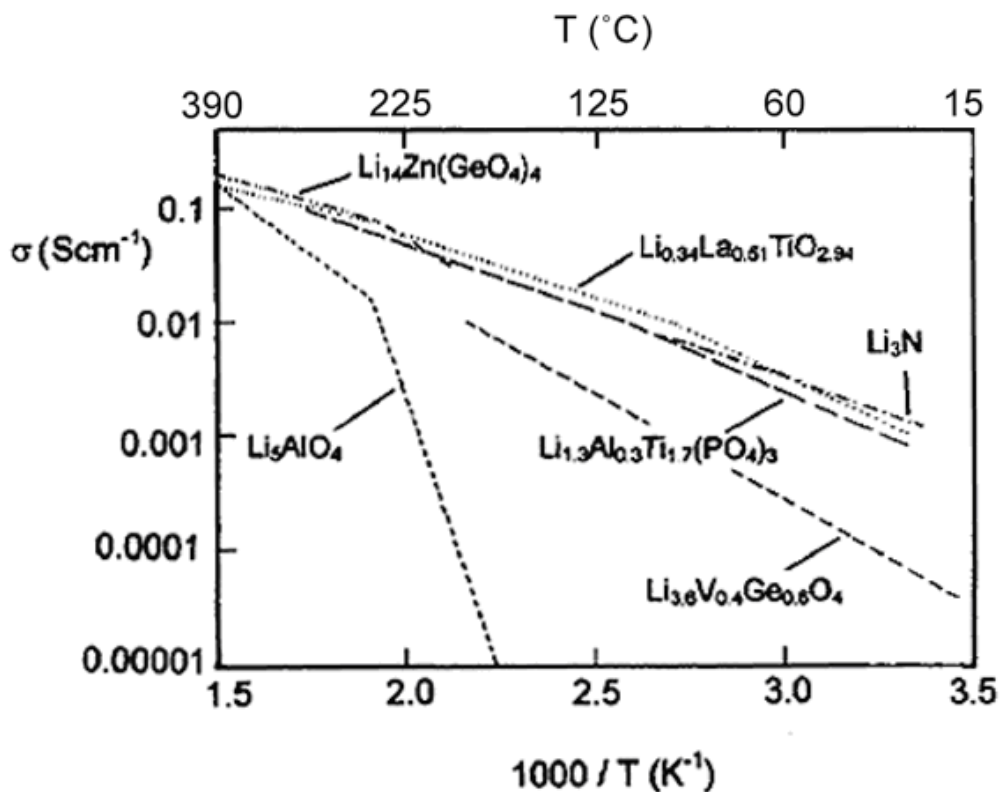
- a) eutectic mixtures of alkali or alkaline earth metal halides (300–500°C),
- b) molten nitrate salts (150–300°C), and
- c) imidazolium compounds such as 3–ethyl–1–methylimidazolium tetrafluoroborate (50–450°C).

The promising eutectic mixtures of alkali or alkaline earth metal halides molten electrolytes include $\text{LiCl}-\text{KCl}$, $\text{LiCl}-\text{LiBr}-\text{KBr}$, $\text{LiBr}-\text{KBr}-\text{LiF}$ (melts at 324.5°C) $\text{LiI}-\text{LiBr}-\text{LiCl}-\text{LiF}$, (melt between 325.4°C and 326.1°C), and 80(Li_2S)20(P_2S_5). These advanced eutectic mixtures of alkali or alkaline earth metal halides molten electrolytes are attractive for use with $\text{Li}-\text{FeS}_2$ and $\text{Li}-\text{CuS}_2$ type high temperature batteries. The current density that can be sustained is critically dependent on the temperature and electrolyte composition. The molten salt nitrate electrolytes were examined for the $\text{Li}(\text{Al})/\text{Ag}_2\text{CrO}_4$ battery system. The state-of-the-art imidazolium compounds such as 3–ethyl–1–methylimidazolium tetrafluoroborate (50–450°C) were found to be reactive with $\text{Li}-\text{Al}$ anodes at high temperatures and advanced imidazolium compounds are under development.

Sandia High-Temperature Primary Battery

Recently DOE Sandia National Laboratory has reported the development of an all solid-state battery for gas/oil drilling applications. This battery is reported to have the capability to operate from ambient temperature to 500°C. This battery system appears to be attractive for future Venus surface exploration missions.

Figure 4.29: Temperature variation of conductivity (Arrhenius plots) for selected crystalline Li-ion conductors.



The chemistry of the battery is not yet reported and the published information indicates that it employs solid-state fluoride ion electrolytes. It is reported that all the battery components (anode, cathode, and the electrolyte) are in the solid-state form.

These batteries are presently being produced in Russia under a joint program with Sandia and General Atomics Corporation. The major limitation of this battery is that it can operate only at very low rates. Use of advanced electrolytes may improve the rate capability of this type of battery system.

JPL High-Temperature Primary Battery

Recently JPL identified a battery system that is capable of operating up to 450°C. This battery system employs Ca metal as the anode, NiF_2 as the cathode, and fluoride ion based solid-state electrolyte. This battery uses a solid-state design and can operate for long periods of time at Venus surface temperatures without any requisite cooling. The solid electrolyte and electrodes provide for greatly enhanced safety and robustness, and mitigate

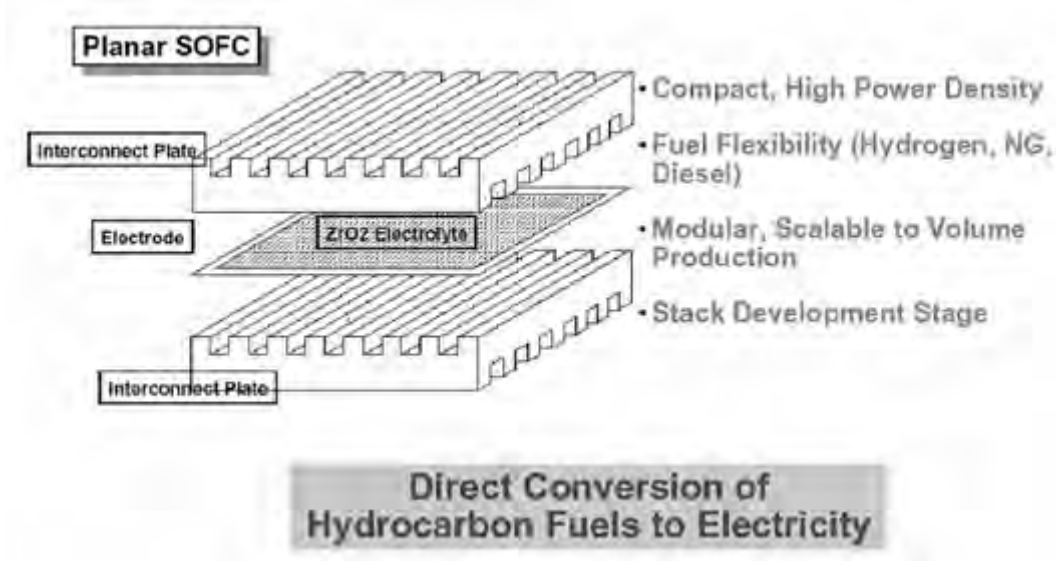
problems associated with electrode dissolution in molten electrolytes. These features result in a smaller, simpler, less expensive, and more flexible system compared to those design solutions that incorporate thermal management approaches or conventional thermal battery chemistries.

The cell has an open circuit voltage of about 2.93 V and projected specific energy of about 300–400 Wh/kg. The cell was shown to operate successfully at about 450°C. Further development of the system to improve its rate capability is in progress.

Solid Oxide Fuel Cells

Another possible high-temperature energy source is the solid oxide fuel cell (SOFC) that operates at temperatures exceeding 800°C. Though these systems now rely on a cooler ambient to enhance heat rejection, it is possible that a SOFC operating at 1000°C could function in a 460°C ambient. These fuel cells need to be heated to an operating temperature before they are able to produce full power. A SOFC started at 450°C would produce very limited power levels until its reaction layers become sufficiently hot to deliver the increased outputs. The operating life of the SOFC has been shown to be quite good. Single cell lifetimes of 34,000 hours were demonstrated at a constant output of 120 mA/cm² at 0.7 V DC. A schematic of this cell is shown in Figure 4.30.

Figure 4.30: Schematic of a solid oxide fuel cell.



The solid oxide fuel cell is typically fueled by a direct feed of pressurized natural gas. Internal reforming of the natural gas produces hydrogen and carbon monoxide that are oxidized in the fuel cell to produce electricity. Because of the ability to oxidize carbon monoxide,

various hydrocarbons can be pre-reformed and introduced into the cell without the need for carbon monoxide cleaning as required in other terrestrial fuel cells (thus simplifying the system considerably and adding fuel flexibility).

A SOFC yields high efficiency and could serve as a long-lived power source, assuming development of suitable materials and systems for fuel storage and cell operation at elevated temperatures. This presents a substantial challenge because at 460°C, the pressure in a fuel storage cylinder increases nearly threefold compared to room temperature. This review did not find evidence of a SOFC qualified in ambient temperatures exceeding 200°C. Also, there is some concern that the efficiency of the solid oxide system may be reduced somewhat with operation at the higher ambient temperatures; and this needs to be examined experimentally.

4.3.5 Low-Temperature Energy Storage Devices

Background

NASA is studying a number of robotic surface missions for the exploration of the outer planets and their moons. Some of the destinations under consideration include the Moon, Mars, Europa, Enceladus, Titan, and Triton. These missions require energy storage systems that have the capability to operate at very low temperatures. Mars surface missions require energy storage systems capable of operating at temperatures ranging from 20°C to as low as -140°C depending on the location. Europa surface exploration missions require energy storage systems that can operate at temperatures as low as -180°C. Enceladus surface temperatures are about -193°C at the equator. Titan surface exploration missions require energy storage systems that are capable of functioning at temperatures as low as -178°C. Lunar surface temperatures in the permanently shadowed regions can be as low as -230°C depending on the location. Neptune's moon Triton is possibly the coldest planetary environment in our Solar System, with a temperature of -235°C (or 38 K) due to its extreme distance from the Sun (30.06 AU). The potential missions that require low-temperature energy storage devices include: Mars landers and rovers, lunar outposts / habitat rovers, Europa lander/probes, Titan Explorer, and Triton Lander. In addition to low-temperature performance, these missions would also require energy storage systems with high mass and volume efficiency, as well as long life capability. A detailed description of these missions and projected launch dates is discussed in Section 3 of this report.

Energy Storage Systems

The energy storage systems that are under development can be classified into:

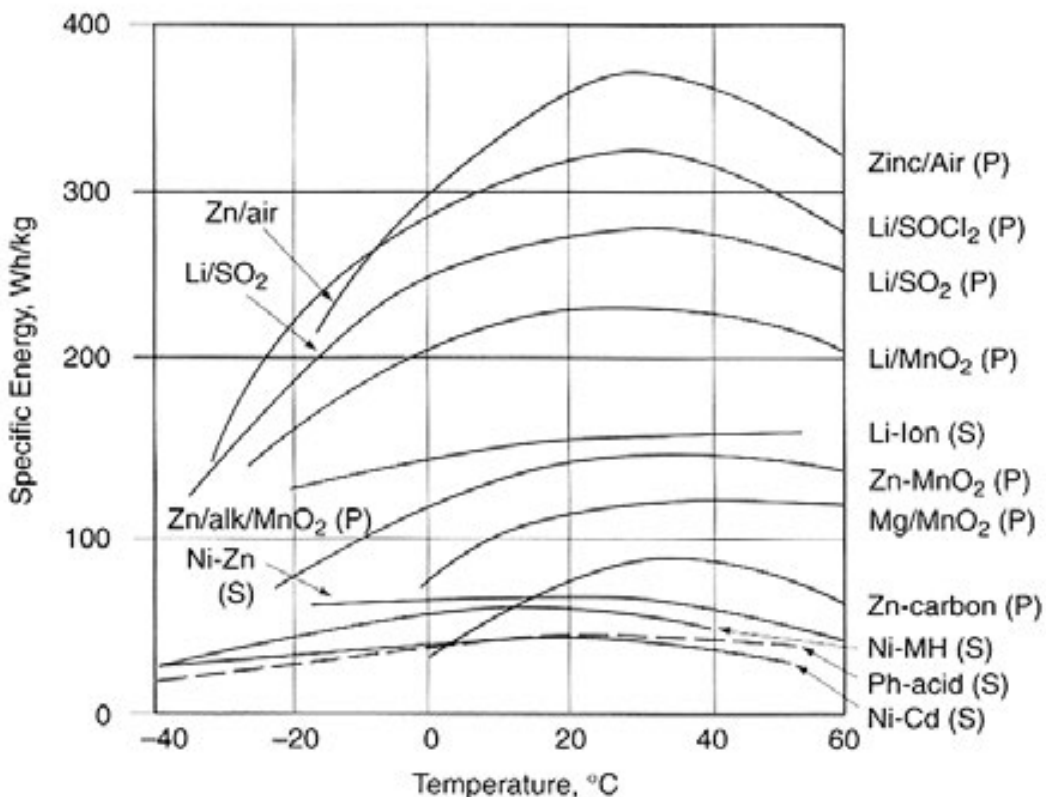
- a) primary batteries;
- b) rechargeable/secondary batteries;
- c) fuel cells;

- d) capacitors; and
- e) flywheels.

Among these energy storage systems, primary batteries, rechargeable batteries, fuel cells, and capacitors have been used widely in various space missions. A detailed description of state-of-practice space-qualified primary and rechargeable batteries and their performance capabilities is given in the High-Temperature Energy Storage Systems section of this report. These state-of-practice space-qualified batteries are designed to operate at -20°C to 40°C and they are not suitable for missions that encounter extreme environments such as low temperatures. The effects of temperature on the performance of various primary and rechargeable commercial batteries is given in Figure 4.31. The aqueous primary and secondary battery systems (Ni–Cd, Pb–Acid, Ni–MH, and Zn Carbon, Mg–MnO₂, and Zn–MnO₂) have low specific energy compared to the lithium primary and rechargeable/secondary batteries and their specific energy decreases rapidly as temperatures decline to -20°C . Even though the Zn–Air aqueous primary battery has the highest specific energy, it is not suitable for use in space missions. The specific energy of even the Li primary and rechargeable/secondary batteries declines at lower temperatures but remains above that of the aqueous batteries at -40°C . Though some of these batteries retain a significant fraction of their room temperature capacity at colder temperatures, virtually all of them cease to function at temperatures below -50°C . Also, state-of-practice fuel cells are not suitable for operation at low temperatures.

In the past, the Soviet Union and United States conducted a number of lunar and Mars surface exploration missions (landers and rovers). Most of these missions employed state-of-the-art primary and rechargeable batteries that can operate between -20°C and 40°C . The batteries were maintained at these temperatures by the use of a thermal management system that employs solar-powered electrical heaters or radioisotope heaters. During the period 1966–1968, NASA carried out several robotic missions (Surveyor missions) for lunar surface exploration and also to gather information for the subsequent lunar lander. Most of these missions were carried out near the equator where the temperatures are quite moderate. These Surveyor missions employed silver zinc-batteries for energy storage. Thermal control of these spacecraft was achieved through electrical heaters and effective insulation. Although the Surveyor 2 and 4 missions failed, the remaining five spacecraft landed successfully and transmitted images from onboard television cameras. In general, Surveyor craft survived 1–4 lunar days. Surveyor 1's mission was terminated after the first lunar night due to a dramatic drop in battery voltage. The Lunokhod 1 and 2 rovers launched by the Soviets used a hybrid power system (consisting of solar panels and batteries) that was thermally managed using polonium-210 radioisotope heat sources. The United States has conducted five Mars surface missions since the 1970s. These include two Viking landers, one Mars Pathfinder (that included a lander and a rover), and two Mars Exploration Rovers. The Viking landers were powered by two plutonium-238 radioisotope thermoelectric generators (RTG). Four flooded, sealed nickel–cadmium 8 Ah, 28 V rechargeable batteries were also onboard to handle peak power loads. The heat from the RTGs was used

Figure 4.31: The effects of temperature on the performance of various primary and rechargeable commercial batteries.



to keep the batteries and other parts of the payload warm. Mars Pathfinder was powered by solar panels and a silver zinc battery. Electrical heaters were used to keep the batteries warm. Sojourner rover on the Mars Pathfinder mission was powered by solar panels with load leveling power coming from the Li-SOCl₂ batteries. Radioisotope heaters were used to keep the Li-SOCl₂ batteries warm. The Mars Exploration Rovers are powered by solar panels and Li-Ion batteries capable of operating as low as -20°C. Radioisotope heaters were used to keep the Li-Ion batteries at temperatures higher than -20°C. In summary, energy storage requirements of the past surface exploration missions were met using the existing primary and rechargeable batteries in conjunction with good thermal management techniques (employing electrical/radioisotope heaters). This approach provided functionality but at the expense of large thermal system mass and volume and complexity as well as limited exploration sites. The ideal solution is to employ energy storage systems that can operate at low temperatures. Use of such low-temperature energy storage systems would result in significant mass and volume savings (as they need not be housed in the thermal container) and extend mission duration.

There are a number of existing terrestrial primary and rechargeable batteries that have the potential to operate up to about -100°C after some modifications/advancements. They can also be considered for other missions that require operation -100°C or below with minimal thermal management requirements. This type of battery is referred as Low Temperature Battery in this report.

There has been limited work on the development of batteries that able to function at very low temperatures (down to -200°C). This type of battery is referred in this report as Advanced Low Temperature Battery. Developmental status of these Advanced Low-Temperature Batteries lags behind those of Low-Temperature Batteries, considered above, and no hardware versions have yet been made. Nevertheless, these are considered promising candidates for future missions with environments that have temperature ranges from -100°C to -200°C .

In addition to batteries, there are alternative energy storage devices that have the potential to operate at ultra-low (below -180°C) temperatures. These devices consist of Flywheels, Superconducting Magnetic Energy Storage, Combustion-Driven Turbine Systems, and Hybrid Systems using thermal batteries.

The prospective low-temperature energy storage systems for future inner planetary exploration missions can be classified into three types:

- i) Primary Low-Temperature Batteries;
- ii) Secondary Low-Temperature Batteries; and
- iii) Alternative Low-Temperature Energy Storage Systems.

Status of the development of prospective energy storage systems and the technical issues that need to be still resolved before they can be considered for future space missions are presented below.

Low-Temperature Batteries

State-of-practice primary and rechargeable batteries can only operate effectively over a temperature range of -40°C to $+40^{\circ}\text{C}$. The factors that are responsible for the poor performance of the batteries at low temperature are:

- Poor electrolyte conductivity;
- Poor ionic transport kinetics in the electrode materials (i.e., bulk);
- Slow diffusion and charge transfer at the electrolyte/electrode interphase;
- Poor electrolyte wetting and/or transport across the separator material; and

- Seal integrity/brittleness and cell hardware CET mismatch.

In the past 10 years, JPL, U.S. Army laboratories DOE laboratories, and private industry (Lithion, SAFT etc;) have made significant progress in improving the low-temperature performance of the state-of-art primary and rechargeable lithium batteries. This work has resulted in the development of primary Li-SOCl₂ and Li-CuCl₂ batteries that can function at temperatures as low as -80°C. The major limitation of these batteries is that they can only function at very low discharge rates. Rechargeable Li-Ion batteries that can function at -40°C have been developed and performance capabilities were demonstrated in small capacity cells. Work is in progress to extend the performance of these batteries down to -100°C. Summary of the progress made to date on the development of primary and rechargeable lithium batteries is given below.

Low-Temperature Primary Li Batteries

The primary battery systems that have potential for improved low-temperature performance (down to -100°C) include Li-SOCl₂ and Li-CF_x. The rationale for this projection is that these systems have a wide temperature range of operation (generally operational to >100°C) and they have not been optimized for extremely low temperatures.

Primary Li-SOCl₂ Batteries: Among the various primary batteries, this system possesses the highest potential for improved performance at low temperatures (perhaps as low as -100°C). Further, these batteries have moderate to high specific energy and energy density, coupled with demonstrated long life capability.

JPL developed a special version of the Li-SOCl₂ primary cell (under the New Millennium DS-2 program in the late 1990s,) that functioned at temperatures as low as -60°C for a Mars microprobe mission. JPL (in collaboration with Yardney) modified the Li-SOCl₂ chemistry by using an alternate electrolyte salt (LiGaCl₄) and optimizing the salt concentration. The resultant cells showed improved power and energy density at -60°C compared to SOP Li-SOCl₂ cells. However, the performance of these cells declined significantly below -60°C and displayed a severe voltage delay at low temperatures. At these temperatures, the specific energy of this battery was between 35–45 Wh/kg.

This unique Li-SOCl₂ battery exhibited a severe delay at these low temperatures and became inoperable due to formation of an interfacial film between the anode and the electrolyte. Testing showed that this delay could be mitigated by application of a de-passivation step (high current pulse) at a much higher temperature. It was found that this de-passivation step must be done shortly before cooling and should be carried out at temperatures greater than -30°C. Completion of the step eliminated the delay and enabled the battery to be functional at -80°C.

The limited power and energy performance of these batteries at temperatures lower than -60°C is generally due to three factors:

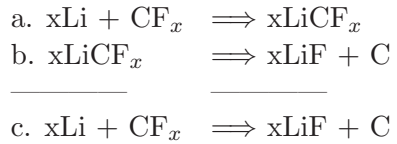
- a) low electrolyte conductivity;
- b) poor lithium–ion conduction across the lithium chloride film; and
- c) poor reduction kinetics of SOCl_2 .

The low–temperature performance of these batteries can likely be improved with the use of alternative electrolytes and improved cell designs. Addition of suitable solvent additives, investigation of alternate electrolyte salts, and controlling the purity of the electrolyte are anticipated to minimize voltage delay and improve low–temperature performance. Prospective candidate co–solvent additives include: thionyl fluoride, thionyl chloride fluoride, sulfonyl fluoride, sulfonyl chloride fluoride, and sulfonyl bromide fluoride.

Primary Li– CF_x Batteries: Li– CF_x cells have the highest specific energy at room temperature relative to the other primary lithium batteries. The major drawbacks of this system are poor performance capability at low temperatures and high discharge rates. However, this system can be modified or further developed to function effectively at temperatures as low as -80°C .

Li– CF_x cells employ Li as the anode material, solid CF_x as the cathode material together with conducting carbon powders, and a liquid organic electrolyte. These electrolytes employed solvents such as dimethylsulfite (DMSI), dimethoxy ethane (DME), propylene carbonate (PC), and electrolyte salts such as lithium hexafluoroarsenate (LiASF_6).

The chemistry of the Li– CF_x cell is described by the following reactions:



The cells are made in a cylindrical configuration. Li– CF_x cells and batteries are available from Eagle Picher Industries. This cell exhibits an operating voltage of 2.5–2.7 V and has the highest specific energy (400–600 Wh/kg) and energy density (up to 1000 Wh/l) of the lithium systems. The major limitations of this battery system are its extremely low power capability (~ 15 W/kg) and limited performance at low temperatures.

The poor performance of Li– CF_x cells is due to:

- a) low conductivity of the cathode material, CF_x , (this is the dominant limitation);
- b) low conductivity of the solvent–electrolyte at the very low temperatures; and
- c) low surface area of existing cells with thick electrodes.

The modifications required to realize significant improvements in low-temperature performance include use of thin electrodes, and advanced electrolytes.

Low-Temperature Rechargeable Li Batteries: The best existing secondary batteries for low temperatures use are: lithium-ion, Li-S, Li-CuO, and Li-CuCl₂. All of these have demonstrated good performance to temperatures of at least -40°C and they have the potential to operate at -100°C after some modifications/advancements.

Rechargeable Li-Ion Batteries: Among the rechargeable lithium batteries, lithium-ion batteries are especially attractive due to their high specific energy (~150 Wh/kg), good reversibility (>1,500 cycles), and superior safety properties. For these reasons, lithium-ion rechargeable batteries have been developed for various aerospace applications under a NASA-DoD Interagency Program. In addition to displaying high specific energy and long cycle life, the batteries can operate over a wide temperature range of -30°C to +40°C. One of the drawbacks of this system is poor performance capability at low temperatures. However, this system can be modified or further developed to function effectively at low temperatures as low as -80°C.

In the Li-Ion cells, carbon is used as the anode material, lithium cobalt oxide as the cathode material, and the electrolyte is an organic liquid solvent (propylene carbonate diethyl carbonate etc) containing 1.0M LiPF6.

The state-of-the-art commercial cells can only operate up to 0°C. In 1998, JPL had developed a Li-Ion cell that can function at -20°C, and this technology was transferred to Yardney and SAFT for manufacturing. These batteries are presently in use on the MER rovers (Spirit and Opportunity) and they have the best low-temperature performance of any commercial rechargeable Li-Ion battery. Under a DoD sponsored program, JPL identified a new electrolyte that permits the operation of Li-Ion cells effectively at temperatures as low as -40°C. Experimental cells fabricated by Lithion and SAFT using this electrolyte showed more than 20-30% higher capacity at -40°C compared to SOP Li-Ion cells. Recent advances in electrolyte compositions at JPL have led to demonstrations of good performance of lithium-ion cells at temperatures as low as -60°C at low rates (e.g., ~70% of the room temperature capacity, corresponding to 77 Wh/kg using a C/150 rate). These batteries can further be improved to operate effectively up to temperature as low as -100°C.

The poor performance of Li-Ion batteries at temperatures below -60°C is primarily due to the poor electrolyte conductivity (<10⁻⁵ to 10⁻⁶) and/or freezing at these temperatures. Another factor that influences the low temperature is that the electrode surface films (especially at the anode), produced when in contact with organic electrolytes, become highly resistive and rate determining. The third factor limiting performance is poor lithium diffusivity within the bulk of the electrode material.

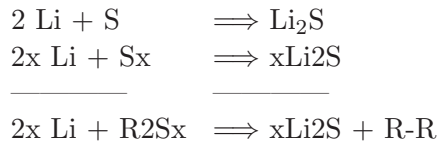
Viable technical approaches to improve the low-temperature performance of these systems

include:

- a) develop electrolytes that have sufficient conductivity at temperatures as low as -100°C ($\sim 10^{-4}$ S/cm);
- b) develop novel electrolyte additives that result in the formation of electrode passivation layers with improved ionic conductivity enabling facile kinetics at low temperature;
- c) develop high capacity cathode materials with high ionic diffusivity;
- d) develop high capacity carbon anode materials with high bulk diffusivity and/or lithium alloy anode electrodes with stable interfacial characteristics (e.g., no lithium dendritic growth and/or excessive reduction of electrolyte components); and
- e) develop improved cell designs.

Rechargeable Li–S Batteries: Li–S batteries are projected to provide very high specific energy (>400 Wh/kg) and energy density (>500 Wh/l) compared to other advanced rechargeable battery systems. Although projected to exceed the other advanced systems, this technology is presently at an early stage of development (TRL 1). Small–capacity cells (2 Ah) have been made and tested. Research of these batteries is carried out primarily by universities and start–up companies, such as Moltech, Polyplus, SION Power, and Tadiran, who are involved in developing this battery system.

Li–S batteries are based on the lithium metal anodes and sulfur or polysulfide cathodes. The following cell reactions are relevant.



Experimental cells with a specific energy of 400 Wh/kg have been developed and are under evaluation. The cells have limited cycle life (only 200 cycles to-date) and low rate capability. Good low–temperature performance has also been displayed by Li–S rechargeable batteries (e.g., SION Power Corp.), with reasonable performance at -60°C . At -50°C , approximately 50 Wh/kg is delivered at a high C/3 discharge rate. Although displaying impressive specific energy over a wide temperature range, Li–S technology is not as mature as Li–ion and generally has more safety issues associated with its implementation (i.e., use of lithium metal, formation of dendrites, etc.).

Rechargeable Li–Copper Chloride Batteries: Lithium Energy Associates is presently developing this battery system under an Air Force sponsored program. This system was shown to operate at temperatures as low as -80°C .

In these batteries, lithium metal is the anode, copper chloride is the cathode, and lithium tetrachloroaluminate/sulfur dioxide is the electrolyte.

The cells are made in a cylindrical configuration. The D size cells have a specific energy of about 175 Wh/kg at room temperature and energy density is about 300 Wh/l. The specific energy of the system however, decreases with temperature and the cell exhibits about 40 Wh/kg at -60°C . The unresolved issues of this battery are safety and poor rate capability at low temperatures.

Alternative Low Temperature Energy Storage and Conversion

No energy storage systems currently exist for operation at temperatures lower than -100°C . However, three technologies could, in theory, operate in these ambient conditions. These are:

- Flywheels;
- Superconducting magnetic energy storage; and
- Combustion–driven turbine systems.

Flywheels

Flywheels store kinetic energy from the rotation of high-speed rotors. They have the potential advantage over batteries in that they can supply energy to high depths of discharge (DOD), but they currently yield a much lower energy density. To act as a viable energy storage medium, flywheels need to operate at such high rotational frequencies that the main challenge becomes maintaining rotor structural integrity.

Flywheels show no taper charge and fewer thermal constraints than batteries. The kinetic energy or state of charge of the flywheel system is always well determined if the speed is known, unlike electrochemical systems where the state of charge depends on factors such as the system voltage or pressure, rate at which current is withdrawn, battery age, temperature, and charge/discharge history.

Flywheels have the potential for long cycle life at $>75\%$ DOD, with high discharge rates that are attractive for pulse power applications. Magnetic bearings and rotors have been demonstrated with operations up to 60,000 RPM, and accelerated life testing may be considered credible. Large flywheels are under development for various terrestrial applications; however, although they may be operable over fairly wide temperature ranges, these devices may be competitive with batteries at the ultra-low temperatures of space science applications.

The predicted performance of future flywheels depends upon assumptions for the specific energy. Because a specific energy of 25–30 Wh/kg has already been achieved with a rather crude rotor, flywheel technologists have projected mid-term achievable specific energies of

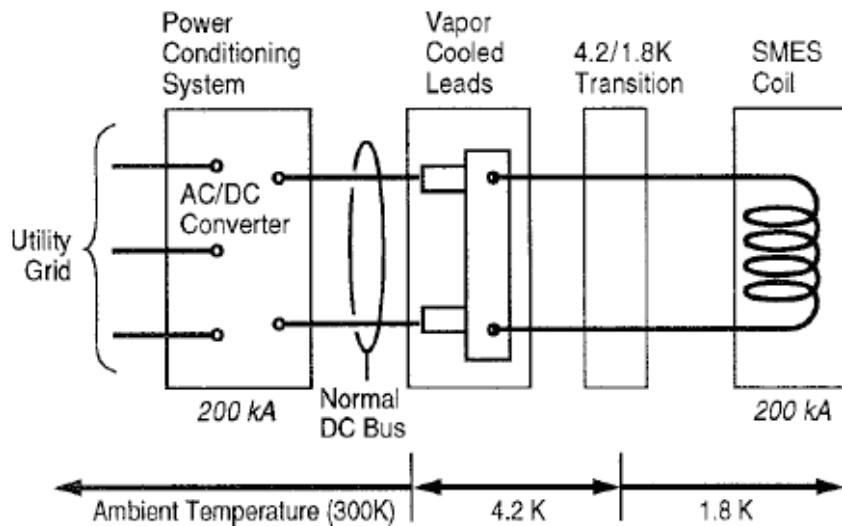
44–70 Wh/kg, using composite rotors and other mass-saving innovations.

Superconducting Magnetic Energy Storage (SMES)

The recent discovery of high-temperature superconducting materials with transition temperatures as high as 110 K (-163°C) makes SMES a possible energy storage solution. In their initial conception, SMES systems were envisioned as large-scale (megawatt-level) load leveling for large power-generation plants. There is no reason that this technology would not work on a much smaller scale, though the overall specific capacity and energy density might be lower than expected. Figure 4.32 shows a schematic diagram of a SMES system where the superconducting material has a wound wire form factor and is thought to be superconducting at 1.8 K. Some newer materials, such as $(\text{Bi},\text{Pb})_2\text{Sr}_2\text{Ca}_2\text{Cu}_3\text{O}_{10}$ (“BSCCO-2223”), have a transition temperature of 110K and could be used in a SMES system. Unfortunately, a SMES approach requires that the coils are maintained at cold temperatures at all times to prevent charge loss from electrical resistance.

Figure 4.32: Schematic of a typical SMES system.

In the case suggested for this study, high T_c superconducting materials would be used and would be fully functional at -180°C .



Though feasible, this approach would yield a power supply with a relatively short lifetime that would have to be “charged” after insertion into the cold environment. Because of this, and the low specific energy associated with flywheels, this approach is not recommended for further development as a low-temperature power source. Further challenges include development of low-temperature electronics and materials, with closely matched CTEs that would not separate upon thermal cycling.

Combustion-Based Turbine Systems

With proper fuel selection, a novel design combustion chamber combined with a traditional turbine system could supply energy efficiently. In this case, a thermal battery would be used to start the system by heating the fuel lines and combustion chambers. Once the generator system is started, it would keep itself warm while driving the turbine. Though this sort of approach would not be considered for most missions due to its relatively low specific energy, the extra issues associated with ultra-low-temperature ambient environments could make such an arrangement much more attractive.

4.4 Robotics

Mission operations require a set of technologies that directly support data collection activities. Some of the required technologies support other spacecraft systems, such as energy storage, and are already discussed elsewhere. The principal disciplines required for operations fall in two categories: Electromechanical systems for sample acquisition and mobility systems provide flexibility in site selection. Each of these disciplines faces distinct challenges for high and low temperatures and is thus discussed independently.

4.4.1 High-Temperature Mechanisms

Operating motors and actuators at 480°C on the surface of Venus presents an extreme challenge. Thermal cooling can ameliorate the problem for drive electronics and batteries; however, the actuators, bearings, cabling/insulation, solders, and control sensors may have to be located external to any environmentally controlled zone to operate on the surface. In addition to high temperature and pressure, chemical corrosion can significantly limit the motors' and actuators' useful life and performance. Other considerations include material compatibility and efficacy, chemical reactions, alloying, annealing, and diffusion. In addition, thermal expansion mismatch can be catastrophic to a system requiring precision fits.

Potential Benefits to Missions

Venus In Situ Exploration (VISE) and Venus Mobile Explorer (VME) missions would call for sample acquisition of unweathered samples from 10–20 cm below the surface. In addition, actuators needed for robotic exploration include lander pedal motors, drive/steering motors, manipulator joint motors, latching and deployment motors, and robotic arm motors.

State-of-the-Art

Standard actuators based on ferromagnetic or ferroelectric materials face an intrinsic challenge as they reach the Curie temperature, where the material transitions from ferro- to paramagnetic and loses its actuation capability. Magnetic actuators such as brush, brushless, or stepper motors require magnetic materials; currently, commercial units operate at a maximum temperature of approximately 200°C. In these actuators, the primary fault mechanism is shorting in the winding insulation, rather than operation above or near the

Curie temperature.

Some motors designed for extraction of smoke and deadly toxic fumes during fire emergencies are available for use up to 500°C; however, these are usually large and have lifetimes of a couple of hours. No COTS or known prototype motors exist with the capability of operating under Venus surface conditions for any appreciable or reliable amount of time. Honeybee Robotics has developed and demonstrated a first-generation prototype of an extreme-temperature, high-pressure (90 bars) motor for possible future use on the surface of Venus. Under Phase I funding from the NASA Small Business Innovative Research (SBIR) program, a small switched-reluctance type motor, which operates without permanent magnets, was built and successfully tested at temperatures up to 460°C. The motor continued to function as it was brought to temperature several times over two hours, during which it was started and stopped repeatedly. An optimized version of this motor could be used to power drills, robotic arms, and other devices that may be landed on the surface of Venus. It is shown in Figure 4.33.

Technology Development Needs

Motor and actuator technologies capable of operating in the high-temperature (460°C) and high-pressure (90 bars) Venus surface environment are needed for systems driving sample acquisition and mobility functions. Technologies required include motors and gearboxes, position sensors, high-temperature electrical cabling, mechanical devices related to drilling, sample containment mechanisms, and the mechanical transfer devices to move the sample from the collection point to the scientific instruments inside the lander.

The current technology for high-reliability electromagnetic actuators consists of copper wires with polyimide insulation installed into slots in a magnetic silicon-steel. The steel core is composed of individual laminations bonded together with a dielectric adhesive to electrically isolate each lamination from the others and prevent eddy currents along the length of the core that would reduce the motor's efficiency. The wires are then impregnated with an adhesive to lock them in place to protect the wires from vibration damage and improve the thermal conductivity of the motor stator. Since the aerospace industry has been building high-reliability electromagnetic actuators for over 40 years, various design rules have been developed through testing and failures. These rules limit the smallest allowable wire in a stator, the minimum bend radius of the wire, the minimum radius on the steel core to prevent cutting through the wire insulation, and the size of the end turns of the windings to allow for differences in thermal expansion of the steel and the copper.

A high-temperature actuator will not be able to use most of these standard materials and processes. As a result, the confidence that currently exists for electromagnetic actuators cannot be transferred directly to a high-temperature actuator. Consistent designs of flight actuators require studies of detailed properties of magnetic and insulating materials.

Figure 4.33: High-temperature (550°C) switched-reluctance type motor developed by Honeybee Robotics.



Electromagnetic Actuators

The winding methods currently used for high-reliability actuators would not be adequate, as a 460°C environment negatively affects winding insulation material and bearing life. High-temperature synthetic lubricants or a variation of the low-temperature lubrication method will be needed. Though some currently available permanent-magnet materials can function at high temperatures, these materials currently do not possess enough functional margin for a flight application. The rotor position sensors in cyclical actuators are typically electronic in nature and are therefore prone to failure at high temperatures. Use of actuators without rotor sensors is one possible solution, unless a suitably robust sensor can be identified.

Spring-Based Actuators

Variations of the elastic properties with temperature will result in changing operational margins. The friction/interfacial properties at temperature are important to understand the operational margins and reliability of the actuator. Many spring actuators are operated

without dampers, and all of the energy put into the moving components must be absorbed at the final position of the system. This requirement can lead to higher mass systems with shock loading mechanical coupling to the spacecraft.

Damping Mechanisms

If used to reduce overall system mass, damping systems will likely be electromagnetic in nature; the common fluid-based systems, including bearing lubrication, have many issues at high temperatures. One technology, the eddy current damper, creates a retarding force for the spring actuator with eddy currents generated by a conductor moving through a magnetic field. The conductor's resistance drops with decreasing temperature, improving the eddy current function. These devices need high-ratio gearboxes for adequate damping within a reasonable mass; this gearing poses the principal challenge for the actuator. Furthermore, the gearing has bearings and gear interfaces to keep lubricated, in addition to the bearings of the actuator, presenting additional challenges.

Thermal Actuators

Paraffin (and other low-temperature) actuators require thermal input to function. Because typical operating temperatures are significantly lower than those of the high-temperature environments, these actuators are not useful except for release at arrival; however, a high-temperature phase change material that melts at 500°C may be actuated with minimal heating above the 460°C ambient. Maintaining internal pressure and sealing the chamber are critical to prevent damage to the spacecraft and perhaps the environment.

Piezoelectric Materials

Since piezoelectric materials do not need windings, can be fixed to a structure, and do not require electrical or mechanical commutation. They are also candidates for high-temperature actuators.

4.4.2 Low-Temperature Mechanisms

Motors and actuators are needed to reliably operate in the -230°C to -193°C temperature range for extended periods of time, without or with very limited thermal control.

Potential Benefits to Missions

Low-temperature motors and actuators would be needed to operate Titan Aerobots, Lunar Aitken Basin explorers with rovers, and a lander on Europa. The motors would be needed for sample acquisition systems, mobility systems, robotic arms, and other applications.

State-of-the-Art

Current surface exploration hardware has demonstrated the capability to operate on Mars in ranges of -115°C to 0°C. Significant challenges remain in developing and demonstrating hardware to operate at 100°C colder than current capabilities, such as materials, bearings,

lubricants, sensors, actuators, motors, and thermal control. Additional concerns exist for control electronics and cabling.

The Mars Exploration Rovers and Mars Pathfinder represent the state-of-the-art in low-temperature robotic systems, with additional heritage from the Apollo rovers. Current operation of gears, bearings, and lubricants at -130°C is limited to 1,000,000 revolutions, and drives and mechanism position sensors are also limited to operating at -130°C . Harmonic gears are limited to operation at -80°C .

Technology Development Needs

Mission requirements, such as sampling location, operating temperature, and duration of exposure, drive electromechanical needs. These requirements dictate the required mechanism specifications for parameters including torque, viscosity, and load actuation distance. Anticipated technology development will lead to improvements in operating temperature ranges, extended life, and additional challenges imposed by operation in vacuum.

Goals include extending the operating temperature to -223°C and providing the capability for 50,000,000 revolutions for gears, bearings, and lubricants. These mechanisms should also be able to operate in vacuum. Furthermore, drives and mechanism position sensors should be able to operate at -230°C . Additional concerns exist in the development of low-backlash gear trains and manipulators.

4.4.3 High-Temperature Aerial Mobility

While an extended Venus program was carried out by the Soviets, basic limitations make it necessary to invest in technology development. The Soviet Vega balloons were fabricated from a material with high areal density limiting the payload mass fraction. Also, the material was not only highly permeable, but possessed optical properties that make it more susceptible to damage on the day side of the planet.

Potential Benefits to Missions

High-temperature balloon technology can enable aerial mobility missions near the Venus surface. Any concept for surface sample return will require a high-temperature balloon to lift the sample to a feasible launch altitude above the bulk of the Venus atmosphere. A long-duration Venus aerial explorer would need to be fabricated from a balloon material compatible with the ambient high temperatures.

Mission concepts generally focus on buoyant (balloon or aerobot) missions because of the lack of solar power below the clouds of Venus, and the desire to minimize or eliminate the consumption of onboard electrical power in the production of lift. The two balloon mission concepts of interest are the following:

- *Venus Surface Sample Return (VSSR)*: A short-duration, single ascent from the sur-

face to high altitude. This is required for any kind of surface sample return mission that must be brought out of the Venus atmosphere to avoid atmospheric drag losses to the rocket that would bring the sample back to Earth.

- *Venus Mobile Explorer (VME)*: A long-duration Venus aerial explorer. This vehicle would fly at an altitude ranging from 0 to 5 km for months over a range of interest (possibly global), providing aerial images of the surface, sampling the atmosphere, and descending and sampling the surface.

The atmospheric temperature near the surface at Venus is approximately 460°C, a value that falls to 380°C at an altitude of 10 km. Balloon material must have the capability to tolerate these high temperatures at low altitudes.

State-of-the-Art

Balloon Materials

Although extensive research has been conducted in the last decade to test various potential balloon materials up to 460°C, no polymer material has been found to be completely suitable. Polybenzoxazole (PBO) film has the temperature-tolerance capability, but no high-temperature adhesive exists to join PBO gores together and make enclosed balloon shapes. Polyimide films (e.g., Kapton) become brittle in the range of 400°C to 425°C. In addition to these problems, both PBO and polyimide films would require Teflon coatings to survive the corrosive sulfur-based gases at Venus. Teflon-coated glass fabrics have adequate temperature tolerance and corrosion resistance, but the glass fibers tend to break when the balloon is folded for transport in an uninflated condition.

Metal bellows balloons are the leading technical solution at the present time. Small-scale bellows constructed from stainless steel have been successfully tested up to 460°C. Effective balloons can be designed with areal densities of approximately 1 kg/m², densities attainable with existing fabrication technology.

Metal balloons are restricted to low volumetric expansion ratios (3:1) because this high areal density quickly leads to an unacceptable balloon weight in large-volume balloons; for a balloon starting at the surface, this limits the maximum altitude to approximately 20 km, which is quite adequate for VME because the peak of Maxwell Montes, the highest mountain on Venus, lies at 11 km altitude.

For operation at high altitudes in the region of Venus clouds, temperatures are much lower but the sulfuric acid environment still precludes conventional terrestrial balloons. A prototype of the next generation superpressure balloon has been designed, built, and tested successfully at JPL. Such balloons may be capable for long-duration global flight and able to tolerate the sulfuric acid of the Venus clouds by being coated with a fluoropolymer external layer. A photograph from recent development is shown below in Figure 4.34.

Figure 4.34: Venus superpressure balloon prototype, designed for Venus atmosphere.



A two-balloon system is required for the sample return mission concept because the sample must be lifted to an altitude exceeding 60 km. The second, large-volume balloon could be made from Kapton material and kept thermally protected until the moment of deployment. Development is needed for a system facilitating the transfer of buoyancy gas from the metal to the Kapton balloon during vehicle ascent.

Aerial deployment and inflation

The second key subsystem for Venus balloons is a deployment and inflation system that stores the balloon in a small volume for transit to Venus, releasing the balloon upon arrival and filling it with helium or hydrogen for buoyancy. In general, this technology is mature, given the Soviet Vega balloons that flew at high altitudes over Venus in 1985. It seems likely that the metal balloon would be inflated upon descent from the upper atmosphere, thereby relaxing the thermal protection requirements on the high-pressure storage tanks.

Other concepts with simpler storage requirements use low-molecular-weight liquids, such as water and ammonia, that can be readily stored as liquids on Earth and in space, but are transformed to gases at the temperatures of the Venus atmosphere.

No high-temperature deployment and inflation systems have ever been built and tested, but existing design concepts use only COTS structural, thermal, and high-pressure plumbing components. However, subsystem tests have been conducted recently. A photograph is shown below in Figure 4.35.

Figure 4.35: Aerial deployment and inflation tests for a Venus balloon prototype.



Technology Development Needs

Balloon Materials

Development of metal bellows balloon technology requires scaling up the bellows size from the 30–40 cm diameter sizes already tested in proof of concept experiments to the larger

sizes (1–3 m diameter) needed to float significant payloads (10–500 kg). This requires advances in manufacturing technology for new bellows sizes.

Research is also needed to evaluate the long-duration leak performance of the metal bellows balloon for the Venus Mobile Explorer mission concept. If the leak rate is found to be unacceptably high, a mitigation plan will need to be devised and pursued. Because the surface sample return mission is a short-duration one (hours), it has minimal leak rate constraints.

Aerial Deployment and Inflation

Research is necessary to verify deployment and inflation designs with full-scale prototype testing at temperature. Although this problem is generally viewed as an engineering challenge rather than a technology development issue, experimental data are required to verify reliable operation. Use of liquids, such as water or ammonia, will require heat exchangers that operate during descent to inflate the balloon.

4.4.4 Low-Temperature Aerial Mobility

The capability for aerial mobility at low temperatures would significantly benefit survey operations and in situ exploration of Titan, searching for prebiotic and biotic activity in the atmosphere, in volcanic regions, and in the surface water–ice.

The environment of Titan is very well suited to aerial mobility despite the very cold temperature and is characterized in Table 4.29 below. The thick atmosphere, low gravity, and gentle winds provide an excellent environment for balloon architectures, and the large scale–height makes atmospheric entry particularly low–risk.

Table 4.29: Characterization of the atmospheres of Earth and Titan.

	Earth	Titan
Atmospheric pressure at surface (bars)	1	1.6
Force of gravity (g)	1	0.14
Surface winds (m/s)	$\gg 1$	<1
Scale height (km)	6	20

Potential Benefits to Missions

Mission concepts generally focus on buoyant missions because of the lack of solar illumination at Titan, making solar–powered devices ineffective. Therefore, it would be desirable to minimize the consumption of onboard electrical power in the production of lift. The two architectures of interest are:

- A self-propelled aerobot (blimp) using electric motor-driven propellers to fly to specific targets of interest. Such a vehicle would use thrust vectoring and internal balloonets to enable altitude changes over a range of 0 to 8 km. Improved autonomous capabilities would enable ground approach and surface sampling maneuvers.
- A wind-blown drifting balloon with altitude control capabilities. The most likely candidate for this kind of balloon would be an RTG-Montgolfière, in which RTG waste heat is used to provide buoyancy by heating up ambient atmosphere gas in the balloon. Buoyancy modulation is achieved with variable gas venting through a valve at the apex of the balloon. Although less capable than the self-propelled aerobot option, this kind of altitude-controlled drifting balloon may still be capable of ground approach and surface sampling maneuvers.

Both types of aerobots would be designed for multi-month mission durations at a minimum. Given the use of RTG electrical power, the primary mission limiting factors would be gas leakage from the balloon or serious structural damage suffered in a ground collision.

New technologies are needed to develop compact, self-propelled balloon vehicles with “go-to” targeting capability that survey large regions of the planet while carrying substantial payloads for extended periods.

State-of-the-Art

Cryogenic Balloon Materials

The atmospheric temperature near the surface of Titan is approximately 90 K (-183°C), making cryogenic balloon material a key enabling technology for all Titan aerobot concepts. Materials have been developed for both the aerobot and balloon concepts. These materials are polyester film with fabric laminates, yielding areal densities around 100 g/m^2 and tensile strengths of $10,000\text{--}16,000 \text{ N/m}$, at cryogenic temperature. In addition, adhesives have been developed and successfully tested at this temperature, enabling the use of taped seams for gore-to-gore construction of balloons.

A 4.6 m long prototype blimp (see Figure 4.36) has been successfully constructed and tested at 93 K using new materials and adhesives. Continued research is focused on developing second-generation materials with Spectra, Technora, or Vectran fabrics, instead of polyester, to improve strength and low-temperature flexibility for the laminate material.

An alternative concept is a RPS-heated, double-walled Montgolfière. It would be expected to have a long life (88 year half-life power source), would be forgiving to numerous small leaks, and may likely attain global coverage by flying with the various winds at different altitudes. A diagram is shown in Figure 4.37.

Aerial Deployment and Inflation

It is anticipated that a Titan aerobot will be aerially deployed and inflated in a similar

Figure 4.36: Prototype for Titan aerobot.



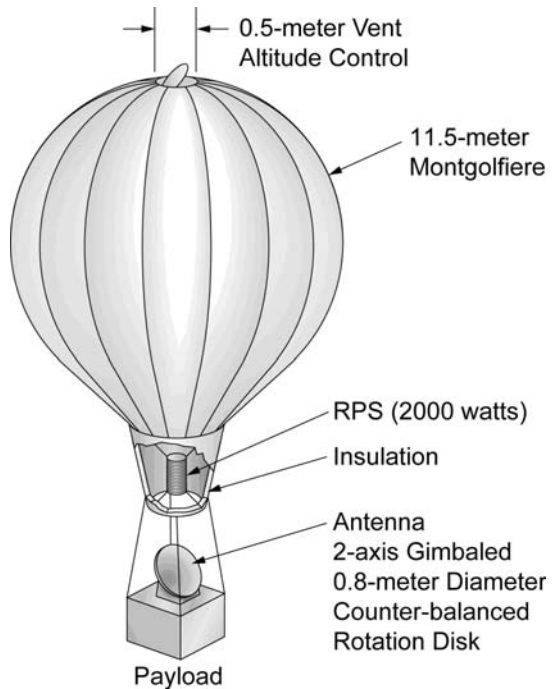
fashion to that of the Soviet Vega balloons in 1985. The thick, dense atmosphere allows for slow descent speeds under a parachute (hence, low aerodynamic forces on the system), providing many minutes to execute the deployment and inflation process. Some limited proof-of-concept deployment and inflation experiments have been conducted to date on Titan aerobot systems, and the results have confirmed the viability of the architecture and the strength and mechanical robustness of these fabric-reinforced balloon structures. Continued research is underway to conduct full-scale experiments in Earth’s atmosphere, with large-scale cryogenic testing anticipated in the more distant future. Figure 4.38 shows the sequence of an aerial deployment test for a Titan aerobot.

Preliminary concepts have been described for the deployment and inflation process for a Montgolfière balloon. The architecture is shown in Figure 4.39.

Aerobot Autonomy

The two-hour-plus round-trip light time between Titan and Earth precludes any kind of real-time control of the aerobot by terrestrial pilots. Therefore, any aerobot beyond a simple drifting balloon will require some level of onboard autonomy in the form of operating software and associated sensors and actuators for guidance, navigation, and control. Highly

Figure 4.37: Design concept of a Montgolfière balloon for use at Titan.



capable self-propelled aerobots with surface sampling capability will require substantial autonomy in the form of robust flight control, hazard detection and avoidance, localization and motion estimation, ground approach, and surface sample acquisition.

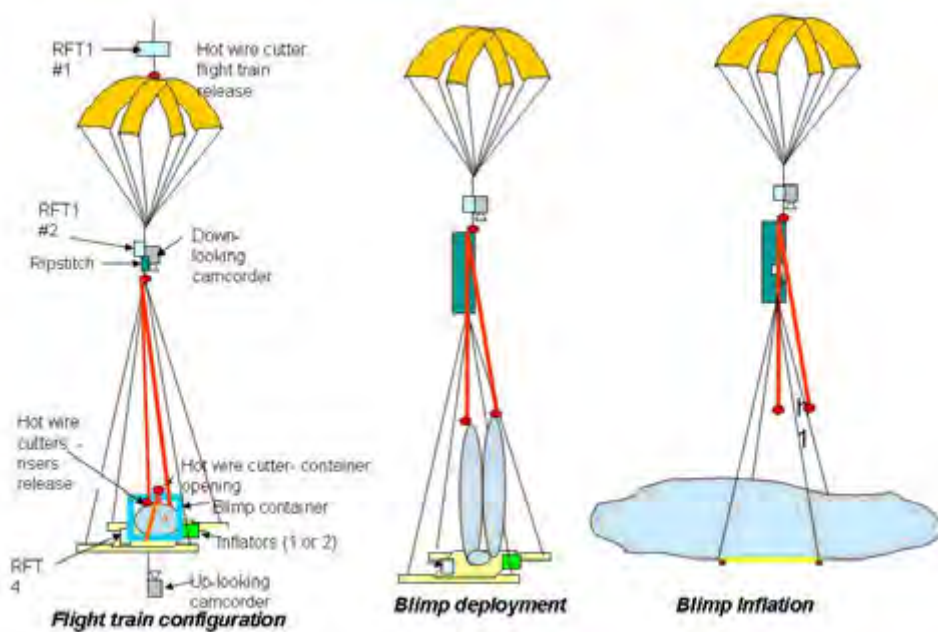
Preliminary Earth atmosphere test flights have been conducted in recent years, using self-propelled blimps to demonstrate low levels of autonomy. However, such efforts did not progress to the level required for robust, long-duration operations and therefore substantial further work is required. Furthermore, while additional tests have shown that direct-to-Earth telecommunications capability may be possible, it is anticipated that this will be used to retrieve science data and that onboard autonomy will still be necessary to retire risk.

Technology Development Needs

Cryogenic Balloon Materials

Fabrication of full-scale (10+ m size) balloons and blimps is needed to validate fabrication technology and provide prototypes for lab and field testing. One of the advantages of the Montgolfière concepts is that they do not suffer from leakage problems, like other pressurized aerobot concepts.

Figure 4.38: Deployment and inflation concept for a Titan aerobot.



These prototypes require long-duration cryogenic testing to quantify leak rates through pinholes and membrane diffusion. If the leak rates are found to be too high to support long-term missions, mitigation steps will be required, likely providing added gas or changing the balloon material and construction technique to reduce the leakage.

Although it will be difficult to simulate the environment appropriately, it is important to provide added tests because the low Titan gravity strongly affects free convection heat transfer rates. Cryogenic testing of RTG-heated Montgolfière balloon prototypes is needed to validate analytical models of heat transfer and buoyancy performance.

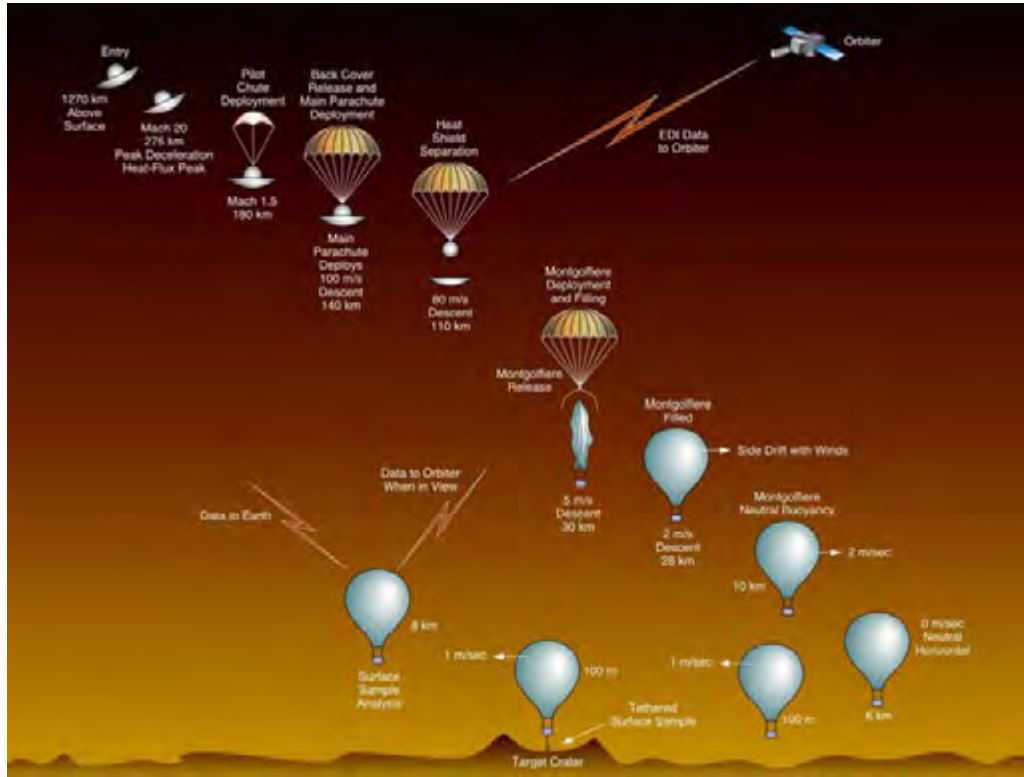
Aerial Deployment and Inflation

To validate at least one viable approach and confirm its predictive models, aerial deployment and inflation testing of full-scale Titan aerobot prototypes will be required. Furthermore, long-duration packaging and storage testing of folded prototype balloons will be key to assessing the impact of extended storage on membrane integrity and strength.

Aerobot Autonomy

Aerobot autonomy technology would consist of flight software integrated with sensor suites and actuator systems. This system requires further development and validation with flight

Figure 4.39: Block diagram of deployment concept of a Montgolfière balloon at Titan.



testing in the Earth's atmosphere. It is expected that the extensive autonomy development of the Mars Exploration Program will be leveraged here.

In addition, development is needed of a surface sample acquisition system and associated sample handling hardware suitable for use from aerobot platforms. Most current models are based on tethered devices that leave the aerobot tens of meters above the surface, minimizing the risks associated with autonomous landings on the Titan surface.

5 Roadmaps

The goal of the Solar System Exploration Division in sponsoring this study was to determine the gaps and to identify the most productive areas for technology investment. Developing a new technology and infusing it into space science missions is expensive. The technology must be integrated at a system level in order to be most effective. Accordingly, two factors must be considered when selecting the investment areas of highest priority and formulating the technology roadmaps:

- Impact of the potential technology advance on the portfolio of future space science missions; and
- Prospects for achieving the needed technological advance with acceptable risk and affordable investment.

The portfolio of future space science missions was derived from the Design Reference Missions used by the Solar System Exploration Directorate at JPL, in support of NASA HQ. These missions and associated launch dates are consistent with those used by NASA strategic planning groups and the Solar System Exploration Roadmap published in September, 2006.

The roadmaps assume the following development approach:

- Pursue parallel technology developments where alternative approaches exist and there is significant uncertainty as to which approach is most likely to succeed. Use readiness gates to monitor progress and down-select to the most promising technology for maturation of the technology at the earliest feasible time.
- Conduct a test and validation program to demonstrate the success of technologies. In this connection, it may be necessary to augment and modernize the existing infrastructure at various NASA centers as needed to support missions.
- Technology must reach Technology Readiness Level 6 approximately 4–5 years before the projected launch date in order to be infused into the mission.
- Metrics are expressed strictly for technical performance and do not implicitly include the impact on mission cost. Technology-specific down-select processes will include risk assessments and mission-specific cost assessments.

All listed mission milestones are projected technology readiness review deadlines and not launch dates, as those are most relevant to the mission-driven technology development program. These technology development roadmaps should be treated as a starting point, and later on should be updated based on detailed missions designs.

5.1 Roadmaps for Protection Systems

Protection systems describe those technologies that provide isolation from the surrounding environment. These are used in conjunction with hardened systems able to tolerate the environment and provide protection or shielding from the following challenges: hypervelocity entry, hypervelocity particle impact, radiation, and high temperatures and pressures.

5.1.1 Hypervelocity Entry

Objectives

The objectives for developing thermal protection systems for hypervelocity entry are to establish new materials and sensors for atmospheric entry at: 1) Earth, 2) Jupiter, and 3) Venus. The current state-of-the-art and suggested performance metrics for these capabilities are listed in Table 5.1.

Table 5.1: Performance metrics for hypervelocity entry protection.

For hypervelocity entry protection, the state-of-practice has regressed; while systems formerly existed capable of tolerating the heat fluxes stated in this table, they are no longer available.

Hypervelocity Entry	Metric	State-of-Practice	Goal (TRL 6)
Earth re-entry (sample return)	Peak heat flux kW/cm^2	1	1
	Mass fraction (%)	14	10
Venus entry	Peak heat flux kW/cm^2	10	10
	Mass fraction (%)	13	6
Jupiter entry	Peak heat flux kW/cm^2	30#	30
	Mass fraction (%)	50	40
# Galileo probe heritage – no longer available			

Benefits

Jupiter probes deployed to higher latitudes, such as those envisioned in some of the mission concepts (e.g., Jupiter Flyby with Deep Probes), would experience higher entry heating than the Galileo probe. Consequently, the TPS mass fraction is expected to increase from 50% to about 70%, if conventional fully dense carbon–phenolic systems are used. This would significantly reduce science payload mass fraction for a given entry mass. Advanced TPS materials could lead to a significant reduction of TPS mass fractions, thus enabling Jupiter probe missions to diverse latitudes. Venus missions, especially with direct entry would also benefit from this development. Furthermore, TPS materials developed for Stardust and Genesis could enable future Venus missions, with entry from orbit or using Venus aerocapture for orbit insertion. Missions to Titan would require low-density materials, tolerant to UV radiation.

Approach

Development would begin with multilayer materials applicable to many missions and architectures. Specific applications to each mission architecture would then be developed. Systems engineering to develop efficient architectures with optimized TPS payloads would require thorough assessments and implementation plans, in addition to simulation facilities. This development should leverage from NASA investments in crew exploration vehicle TPS (materials, facilities, models, expertise, etc.).

Technology Roadmap

The costs for each area of the hypervelocity entry task range as high as \$12M/year for the multiuse materials to approximately \$5 M/year for specific applications. The development plan is shown in Table 5.2.

Table 5.2: Development timeline for hypervelocity entry protection.

Hypervelocity Entry	08	09	10	11	12	13	14	15	16
Jupiter TPS					③	④	⑤	⑤	⑥
Systems analysis				No TRL level					
Missions: Dates for technology infusion									↓ JFDP

Technology Readiness Levels are shown from 1 to 6: ①; ②; ③; ④; ⑤; ⑥

5.1.2 Hypervelocity Particle Impacts

Objectives

The objectives for developing protective systems for hypervelocity particle impacts are to establish:

1. New environmental models for meteoroids (data and new models outside/inside 1 AU), cometary, planetary ring, and debris models above ~ 2000 km;
2. Standardized, validated empirical cratering and penetration models and validated hydrocodes capable of modeling complex shielding geometries for impacts of 5–40 km/s;
3. Techniques for rapidly and cheaply testing with new shielding configurations for masses up to 1 mg and for velocities up to 40 km/s;
4. Shielding technologies for light shielding designs for 1 mg particles at 5–40 km/s; and
5. Standardized methodology for evaluating the efficiency and reliability of complex shielding schemes.

The current state-of-the-art and suggested performance metrics for these capabilities are listed in Table 5.3.

Table 5.3: Performance metrics for hypervelocity particle impact protection.

Hypervelocity Particle Impact	Metric	State-of-Practice	Goal (TRL 6)
Environments	Mass/velocity inside 1 AU	Some data at 0.3 AU	0.1–1 AU
Meteoroids	Mass/velocity outside 1 AU	Some data at 0.3 Saturn	1–30 AU
Comets	Mass/velocity outside 1 AU	Some data at 0.3 Saturn	1–30 AU
Debris	Mass/velocity around Earth	Data below 2000 km	120 – 36,000 km
Impact modeling	Validated mass/velocity penetration	Some models	Validated codes
Hypervelocity testing	Mass (1 μg – 1g)	1–100 μg	1 g
	Velocity (km/s)	10	40
Shielding technologies	Areal density (g/cm^2)	3	$\ll 2$
System validation	Efficiency (reliability vs mass)	Space Station	General system

Benefits

The effects of hypervelocity particle impacts upon space systems can range from surface pitting and degradation to complete destruction of the spacecraft (e.g., damage to pressurized tanks or batteries). Aside from the obvious benefit of avoiding these problems, accurate environmental impact models, along with valid ground test capabilities, would permit potentially significant savings in mass, and mission complexity, and possible performance improvements. Improvements to models of the mass and velocity distribution of the meteoroid and debris environment would allow more reliable estimates of the threat environment and the likelihood of failure. Better models of the effects of hypervelocity impacts would permit better, more efficient shield designs. The utilization of better testing capabilities would greatly improve the ability to design shielding and maximize its effectiveness. Improved models and shielding techniques would enhance mission reliability and reduce the mass needed for shielding.

Approach

Hypervelocity particle impacts are a concern for virtually every NASA mission, particularly those in challenging environments such as a cometary coma. Technology development should leverage from and rely on historical approaches to the Space Station or the Deep Impact

and Stardust missions. Testing at velocity levels of 10 to 20 km/s should become more affordable in order to evaluate the designs for future missions like Comet Nucleus Sample Return.

The need for standardized shield models and test protocols will increase as hypervelocity impact mitigation becomes more important to ensure high reliability on upcoming missions. Complex future missions to come, including, for example, the Jupiter Flyby with Deep Probes and the Titan Explorer, will require extensive shielding designs. Even missions to Venus, like the Venus Mobile Explorer, will benefit from better shielding technology if they employ RTGs and fly by Earth, because of the unique nuclear safety issues driving mission design (e.g., Galileo and Cassini).

Technology Roadmap

The technology development plan is shown in Table 5.4, with milestones synchronized to most of the major SSE missions. The costs for each area of the hypervelocity task are on the order of at least 1-2 FTE per year for each area, plus the support required to develop at least one facility able to produce 40 km/s velocities for 1 mg masses. At least 3 flight experiments will be required to measure meteoroid environments (inside and outside 1 AU) and the debris environment above 2000 km. These experiments will likely cost on the order of \$2-3M each. Modeling and testing will likely cost approximately \$250K each year unless costs can be substantially reduced.

Table 5.4: Development timeline for hypervelocity particle impact protection.

Hypervelocity particle impact	08	09	10	11	12	13	14	15
Environments								
Debris		③	⑥					
Comets	②		④	⑥				
Meteoroids				③	④	⑤	⑥	
Impact modeling				③	④	⑤	⑥	
Hypervelocity testing								
<15 km/s	③	④	⑥					
<40 km/s					②	④	⑥	
System validation	②	③	④	⑤	⑥	⑦	⑧	
Shielding technologies	③	④	⑤	⑥	⑦	⑧	⑨	
Missions: Dates for technology infusion			↓ EE	↓ CSSR				↓ TE JFDP

TRLs are shown from 1 to 6: ①; ②; ③; ④; ⑤; ⑥

5.1.3 Radiation Shielding

Objectives

The objectives for developing radiation shielding are to:

1. Establish magnetically trapped charged particle population models, including completing a Jovian model with the remaining Galileo data, revising the Saturn model with Cassini data, developing models for Neptune and Uranus, and modeling the solar charged-particle environments near Venus and Mercury;
2. Develop shielding effectiveness and spacecraft modeling, including multilayer shielding design guidelines and CAD interface evaluation and development with NOVICE or ITS5;
3. Conduct ground testing of shielding materials, electron testing of single layer and multi-layer material shielding, and proton testing of single layer and multi-layer material shielding; and
4. Validate radiation transport codes and evaluate charged particle adjoint Monte Carlo codes, beginning with ITS5 by comparing outputs of other codes (NOVICE, MCNPX, GEANT4, and ITS5) with ground test results.

The state-of-practice of these models are listed in Table 5.5.

Table 5.5: Performance metrics for radiation shielding technologies.

Radiation Shielding	Metric	State-of-Practice	Goal (TRL 6)
Radiation environment models	Jupiter (with Galileo data)	Almost completed	Complete
	Saturn (with Cassini data)	Some data	Complete
	Neptune and Uranus model	Little data	Complete
Spacecraft shielding models	Multilayer design	Does not exist	Complete
	CAD interface	Prototypes	Complete
Ground testing of shielding materials	Electron shields	Little testing	Complete
	Proton shields	Little testing	Complete
Radiation transport code validation	ITS5 evaluation	Not evaluated	Complete
	NOVICE, MCNPX, GEANT4, ITS5 vs. Shielding Material Ground Tests	Not validated	Complete

Benefits

The benefits to missions are the reduction in shielding mass required to protect the space-

craft electronics and dielectric materials, as well as increased spacecraft lifetime in severe radiation environments. Improving charged particle environment models would allow more reliable estimates of the shielding mass required to protect the spacecraft and more accurate assessments of science instrument performance over mission life. Improvements in both modeling and ground testing shielding materials and geometry would allow optimization of the shielding design, thus reducing the shielding mass required on the spacecraft. Missions to the Jovian moons would particularly benefit from these technologies.

Approach

Improving radiation shielding requires better modeling of the environment at Jupiter, and Saturn, using the data returned from Voyager, Galileo, Cassini, and New Horizons. In parallel, spacecraft shielding models must be refined to account for the natural shielding properties of the spacecraft structure. Testing must be done in simulated environments to validate models. Radiation transport codes must also be validated to understand energy dissipation mechanisms in various shielding configurations.

Technology Roadmap and Resource Requirements

The plan to develop shielding technologies is shown in Table 5.6. The costs for the radiation shielding technology task are on the order of 1–2 FTE per year for each area, plus the costs associated with a test facility capable of studying electron and proton fluxes.

Table 5.6: Development timeline for radiation shielding technologies.

Radiation shielding	08	09	10	11	12	13	14	15
Radiation environment models								
<i>Jupiter</i>	④	●	⑥					
Spacecraft shielding models								
<i>Multi-layer design</i>	③	●	⑥					
<i>CAD interface</i>	④	●	⑥					
Ground testing of materials								
<i>Electron shields</i>	③	●	⑥					
<i>Proton shields</i>	③	●	⑥					
<i>Test facility</i>	③	●	⑥					
Radiation transport models								
<i>ITS5 evaluation</i>	③	●	⑥					
<i>Validate NOVICE</i>	③	●	⑥					
<i>Validate MCNPX</i>	③	●	⑥					
Missions: Dates for technology infusion				↓				
				EE				

TRLs are shown from 1 to 6: ①; ②; ③; ④; ⑤; ⑥

5.1.4 Pressure Vessel and Thermal Control Technologies

Objectives

The objectives are to develop:

1. A pressure vessel with a mass savings of 50-60% compared to a standard monolithic titanium shell;
2. A thermal energy storage system with twice the specific energy capacity of the current state-of-the-art;
3. A thermal energy storage system integrated with the pressure vessel with a tenfold improvement in storage capacity relative to the current PCM module technology; and
4. A scaleable and efficient powered refrigeration/cooling system, in order to maintain temperatures at operational levels for the payload and subsystems, for extended periods of time (e.g., for months).

The current state-of-the-art and approximate (order of magnitude) performance metrics for these technologies are shown below in Table 5.7.

Table 5.7: Performance metrics for pressure vessel and thermal control systems.

Pressure Vessel and Thermal Control	Metric	State-of-Practice	Goal (TRL 6)
Pressure Vessel (Materials)	Mass/Internal Volume at 500°C, 100 bar (kg/m ³)	~ 800	~ 300
Localized Thermal Energy Storage	Energy/unit mass (kJ/kg)	~ 100	~ 200
Integrated Thermal Energy Storage	Energy/unit mass (kJ/kg)	~ 100	~ 300
High Temperature Active Cooling	Energy/unit mass (kJ/kg)	None	~ 3

Benefits

Advanced passive thermal control and pressure vessels would be required for the short lived in situ Venus missions in order to extend the mission lifetime to more than two hours (i.e, Venera heritage). The Venus Mobile Explorer mission would require active thermal control for extended survival of days to months.

Approach

The technology development will focus on the VME mission. Although the VISE mission could also benefit from the proposed technology development, it should be noted that this

mission could be accomplished with existing capabilities. The timeline for the four technology development areas is shown in Table 5.8. The first two technical objectives, listed in Table 5.7, can reach TRL 6 within the next 5 years since the process for achieving these goals is well defined. These technologies could then be ready for infusion to the VISE mission. The last two technical areas will require significant program resources and will take up to 10 years to develop to TRL 6 because the associated development paths are still quite immature.

The pressure vessel material technology development program will focus on developing manufacturing engineering plans, followed by fabricating and testing doubly curved material samples from several candidates. The best material candidates will be selected to fabricate a subscale prototype pressure vessel to be tested in a Venus-like temperature and pressure environment.

Development of advanced phase change modules will focus on using high-density/high-capacity storage materials, such as lithium nitrate, with lightweight high-conductivity fillers, such as carbon foam or carbon fibers. These modules are suitable for locally storing waste heat generated by specific electronic devices. Sample modules will be fabricated and tested for thermal performance in the first year.

An integrated thermal energy storage system will be developed after the development of the lightweight pressure vessel is complete. The integrated thermal system increases the thermal energy storage capacity of the shell, which has the greatest storage capacity of any element on the spacecraft. Initially, a set of conceptual demonstrations will be designed, fabricated, and tested. This will be followed by a more extensive development of incorporating the system into the pressure vessel developed earlier. In the first five years, the integrated thermal energy storage development should be able to triple the energy storage capacity of existing localized systems using a liquid-to-vapor phase change. Further development of such systems should enable a tenfold increase over current technology in specific storage capacity within 10 years.

The active cooling systems will require making calls for technology development in this area to the engineering development community. A selection of the most promising technologies will be made based on detailed proposals for the design of cooling system architectures. Development of several competing architectures is desired because paper studies are insufficient to develop an optimized solution. Select prototype systems would then be developed and subjected to performance testing and life testing in a Venus environment to achieve TRL 4 within 5 years. A down-selection of the most promising technologies would then be made for further advancement to TRL 6 within 10 years.

Since these cooling systems require some usable source of energy, a program to develop radioactive power sources that can deliver thermal, mechanical, or electrical energy to the cooling system could be required as well.

Technology Roadmap

The development timeline is shown in Figure 5.8 and is synchronized to exploration initiatives on Venus.

Table 5.8: Development timeline for pressure vessel and thermal control technologies.

Pressure Vessel and Thermal Control	08	09	10	11	12	13	14	15	20
Pressure Vessel (Materials)	③	●	⑥						
Localized Thermal Energy Storage	③	●	⑥						
Integrated Thermal Energy Storage	③	●	●	⑥					
High Temperature Active Cooling	②	●	●	●	●	●	●	●	⑥
Missions: Dates for technology infusion				↓ VISE					↓ VME

TRLs are shown from 1 to 6: ①; ②; ③; ④; ⑤; ⑥

5.2 Roadmaps for Component Hardening

Component hardening is the process of developing technologies able to tolerate the external environment. This section describes the individual elements key to mission operation and survival.

5.2.1 High-Temperature Electronics

Objectives

The objectives for the high-temperature electronics are to develop:

1. High-temperature, long-life (500 hrs) SiC, GaN, and vacuum tube active components;
2. Small-scale, high-temperature (500°C) SiC, GaN, and microvacuum device-based integration technology;
3. High-temperature passive components and packaging technology;
4. Device characterization and modeling capability that results in the tools that enable extreme environment electronic design;
5. High-temperature integrated systems;
6. Medium-temperature (300°C) LSI-scale, ultra-low-power SOI CMOS;

7. Integrated medium temperature electronic systems, such as solid state recorder, flight microcomputer and actuator/sensor controller.

The current state-of-the-art and suggested performance metrics for these capabilities are shown in Table 5.9.

Table 5.9: Performance metrics for high temperature electronics technologies.

High T Electronics	Metric	State-of-Practice	Goal (TRL 6)
High T electronics	Lifetime at 500°C	1–100	2000
	Voltage (V)	60–200	5–12
	Transistor Type	Normally on	Normally off
Small-scale high T integration of SiC/GaN/vacuum devices	Integration level (transistor/chip)	5	100
High T packaging and passive components	Capacitor size (μF)	0.00001	10
	Lifetime at 500°C (hrs)	1–120	2000
Medium-temperature (300°C) SOI CMOS electronics	Performance (MHz)	20	40
	Power dissipation ($\mu\text{W/gate/MHz}$)	2.6 at 5 V	0.2 at 1.8 V

Benefits

High power electronic and telecommunications systems act as internal heat sources inside the thermally protected pressure vessel. Placing these systems outside the vessel may reduce internal heating and extend the life of the mission. Small scale integrated SiC, GaN high temperature technologies and heterogeneous high temperature packaging can support this need and produce components for power conversion, electronic drives for actuators, and sensor amplifiers.

For telecommunication systems, high temperature integrated vacuum electronics will provide a noise-performance advantage over SiC or GaN because high-temperature vacuum-based power amplifiers may operate directly in the Venus surface environment without any penalty in noise and linear performance. These technologies can also enable the development of light mass sample acquisition systems that could operate in the Venus surface environment without any thermal control.

In missions with active thermal control, medium-temperature large-scale integrated electronics can be used for fabricating all essential functions of the spacecraft. Electronics operating at medium temperatures can reduce the difference between the outside environment and inside the thermally protected system, significantly reducing the associated power requirements for cooling. As a result, this type of electronics can enable the aerial vehicles,

such as Venus Mobile Explorer, to operate for prolonged duration down to lower altitudes with 300°C temperatures.

Approach

The approach considers technology infusion dates for current NASA missions and assumes leveraging existing industrial infrastructures. Critical emphasis must be placed on prolonging reliable high-temperature electrical operation to time periods in excess of expected mission requirements. This plan emphasizes the optimization of existing wide-bandgap semiconductors (SiC, GaN) and vacuum transistor technology for high-temperature applications. In the high-temperature electronics, the plan will initially concentrate on the development and successively longer-term high-temperature demonstration of SiC, GaN and vacuum transistor components (currently at TRL 4) and their models. At this point, the wide-bandgap technologies with the best promise for meeting mission requirements will be selected and the program will rapidly transition to demonstration of TRL 5 small-scale integration technology for these components. In parallel with active component integration, this approach provides for the development of high-temperature heterogamous packaging technology with the necessary passive components at a TRL of 6. The technology demonstration for high-temperature electronics and/or high-temperature batteries should be considered on the VISE mission.

For medium-temperature electronics, we will look at 300°C ultra-low-power, SOI-based LSI technology. The key to this effort's success will be to leverage existing industrial infrastructure for fabrication of SOI CMOS technology and leveraging the DOE investment. As a result, process solutions that would reduce the leakage of the high-temperature SOI CMOS technology will be investigated and implemented. Next, the 300°C LSI electronic functions such as the solid-state recorder and the microcomputer needed for missions to Venus and Jupiter will be prototyped and demonstrated.

Technology Roadmap

Required development timeline is given below in Table 5.10 for the development of the SiC, GaN, and vacuum-tube-based SSI components for 500°C, ultra-low-power LSI-scale SOI CMOS for 300°C, and a corresponding HT packaging technology.

5.2.2 Low-Temperature Electronics

Objectives

The objectives for developing low-temperature electronics are to develop:

1. Design methodology for making reliable, ultra-low-power, wide-low-temperature and low-temperature VLSI class digital and mixed-signal ASICs;
2. Low-temperature and wide-low-temperature radiation-tolerant, VLSI class, ultra-

Table 5.10: Development timeline for high temperature electronics technologies.

High T Electronics	08	09	10	11	12	13	14	15	20
High Temp (500°C) Actives									
<i>SiC</i>	②	④							
<i>GaN</i>	①	④							
<i>Vacuum tubes</i>	②	④							
Small Scale Integration									
<i>SiC/GaN</i>		④	⑤						
<i>Micro Vacuum tubes</i>			④	⑤					
HT passives and packaging	②	③	④	⑤					
HT system integration									
<i>Telecom (PA)</i>							⑤	⑥	
<i>Actuator electr., sensors</i>							⑤	⑥	
<i>Power converters</i>					⑤	⑥	⑥	⑥	
300°C ULPE Si	②	③	④	⑤					
Integrated 300°C systems									
<i>Solid state recorder</i>					⑤	⑥	⑥	⑥	
<i>Microcontroller</i>					⑤	⑥	⑥	⑥	
<i>Sensor/actuator controller</i>					⑤	⑥	⑥	⑥	
Missions: Dates for technology infusion					↓ VISE JFDP				↓ VME

TRLs are shown from 1 to 6: ①; ②; ③; ④; ⑤; ⑥

low-power, long-life Si- and SiGe-based electronic components for sensor and avionics systems;

3. Wide-low-temperature passive components and high-density packaging technology;
4. Research and modeling tools that produce the models that enable low-temperature and wide-low-temperature rad-tolerant electronic design;
5. Low-temperature integrated systems, such as solid-state recorder, flight microcomputer, and actuator/sensor controller.

The current state-of-the-art and suggested performance metrics for these capabilities are shown below in Table 5.11.

Benefits

Avionics systems that can directly work at cold temperatures (down to -230°C) will enable the elimination of the warm electronics box and implementation of distributed architectures

Table 5.11: Performance metrics for low-temperature electronics technologies.

Low T Electronics	Metric	State-of-Practice	Goal (TRL 6)
SOI CMOS and SiGe electronic components	Lifetime of analog circuits at -230°C (hrs)	1–100	2000
	Power dissipation ($\mu\text{W/gate/MHz}$)	60–200	5–12
	Performance (MHz)	5	100
VLSI scale integration of SOI CMOS and SiGe	Integration at -230°C (transistors/chip)	N/A	1,000,000
Low T passives and packaging	Capacitor size (μF)	0.00001	10
	Lifetime at -230°C (hrs)	N/A	2000
	-230 to 120°C thermal cycling (number of cycles)	0	1000
Rad hard/low T electronics	Total dose (krad) at -160°C	N/A	1000

will enable the development of ultra-low-power, efficient, and reliable systems. Sensors, transmitters, and in situ systems using wheels, drills, and other actuators will require drive, control and interface electronics for greater system reliability, robustness, and versatility. At each target, specific benefits include:

- *Moon*: The ability to operate electronics through temperature extremes will effectively double the working time of lunar robotic systems by eliminating the necessity for hibernation during extremely cold nights. Modules and spares can also be sent ahead of the mission more easily since storage in a thermally controlled environment is not required.
- *Mars*: Wide-cold-temperature electronics capable of operating between -130°C and 20°C daily temperature cycles will enable the development of long-life, highly advanced, modular, highly reliable, efficient robotic and mobility systems.
- *Comets*: Cold-temperature electronics will enable the development of robotics for sample acquisition systems.
- *Titan*: Ultra-low-power cold temperature electronics will enable the development of lightweight, long-life, highly efficient mobile systems for sensing and sample acquisition.
- *Europa*: Low-power, radiation-hardened electronics will enable development of a lander package that can operate for longer periods of time and at lower power at the surface of Europa.

Approach

The two major technologies currently under development are complementary metal oxide semiconductors (CMOS) and SiGe semiconductors. These technologies already have wealthy libraries of scalable circuit blocks (soft IPs) and are producing, at high TRL levels, VLSI-scale electronics for operating temperatures between -55°C and 120°C . Both technologies have the potential to contribute to a number of critical systems, as shown in Table 5.12. Development of low-temperature electronic systems and subsystems using these technologies will require modeling and characterization of their performance down to -230°C , establishing design verification models and scalable CAD tools for this temperature range, and developing corresponding design libraries and the necessary verification methodology and reliability monitoring infrastructure. Once the necessary design infrastructure is established, almost all of the scalable circuit building blocks used for development of current VLSI circuits on these technologies can be used for building advanced VLSI subsystems reliable down to -230°C . Coupled into effective subsystems, CMOS and SiGe should be able to operate with a lifetime of months at temperatures as low as -230°C . Harvesting the potentials of these technologies for mixed-signal sensors and instruments will require the development of mixed-signal building blocks in both CMOS and SiGe building blocks independently. More importantly, these electronics need to be integrated into the appropriate subsystems.

As a whole, these subsystems must exhibit temperature, precision, and lifetime characteristics consistent with the mission requirements. This technology program impacts the Europa Astrobiology Lander, but not the Europa Explorer (EE) because the EE currently is envisioned to be an orbiter. However, if a battery powered landed package is included with the EE, these technologies would be necessary earlier. In addition, the low-temperature electronics will be needed at earlier TRL dates for use in integrated systems.

Technology Roadmap

Low-temperature Si CMOS and SiGe systems are primarily required for the Titan Explorer mission, requiring extensive milestones staggered in time, as shown in Table 5.12.

5.2.3 High-Temperature Energy Storage

Objectives:

The objectives for developing high-temperature energy storage are to:

1. Characterize the performance and stability of existing primary batteries at high temperatures (500°C) and if a promising candidate is found, select it for advanced development;
2. Develop an intermediate temperature secondary battery (250°C) based on current lithium ion technology; and

Table 5.12: Development timeline for low-temperature electronics technologies.

Low T Electronics	08	09	10	11	12	13	14	15	25
Si CMOS									
Tools, files and design	③	④	⑤	⑥					
SiGe									
Tools, files and design	③	④	⑤	⑥					
LT passives and packaging	③	④	⑤	⑥					
Integration into subsystems									
Data acquisition system					⑤	⑥			
Avionics					⑤	⑥			
Short range com					⑤	⑥			
PMAD					⑤	⑥			
Motor drive					⑤	⑥			
Rad hard/low T electronics				②	③	④	⑤	⑥	
Missions: Dates for technology infusion				↓ Moon				↓ TE	↓ EAL

TRLs are shown from 1 to 6: ①; ②; ③; ④; ⑤; ⑥

3. Select the most successful components and create a flight-qualifiable primary and secondary battery for the 250–500°C performance range.

The suggested performance metrics are listed in Table 5.13.

Table 5.13: Performance metrics for high-temperature energy storage.

High T Energy Storage	Metric	State-of-Practice	Goal (TRL 6)
Primary batteries	Specific energy at 500°C (Wh/kg)	200	300
Secondary batteries	Specific energy at 500°C (Wh/kg)	130	200
	Reversibility at 500°C (# of cycles)	2000	3000
Medium T Battery		190	300

Benefits:

These high-temperature batteries will enable and or enhance the Venus Design Reference Missions under study. The mission set under study includes four Venus in situ missions, namely the Venus In Situ Explorer (VISE) with a short duration, the extended Venus Mobile Explorer (VME), the Venus Surface Sample Return (VSSR), and the Venus Geophysical

Network missions. The VISE and VME missions are anticipated to operate on the order of hours and months, respectively, where at least part of the craft's subsystems are exposed to a high-temperature environment. The hybrid approach of creating two or three different environments within the pressure vessel may prove to be useful. It is possible that in addition to operation outside of the vessel (475°C), a battery will be used in more than one of these sub-environments within a vessel, creating a distributed, point-of-use power system. In this case, there will be a need for an energy source at temperatures ranging from 50°C to 475°C. Even though a primary battery system appears to be adequate for the VISE mission needs, rechargeable systems are also considered here, especially if they permit a wider or more extreme temperature. The rechargeable battery will be also needed for the VME mission, where long-term operation is targeted. Not having to cool the batteries will significantly lower the thermal load of the active cooling system.

Approach

The High Temp (HT) effort will initially consist of procurement of cells of the existing HT batteries and evaluation of their performance and stability at 500°C. If one or more of these is shown to be functional at this temperature, it will be selected for advanced development. The advanced development will consist of design, fabrication, and test of an aerospace version of the cell and then the battery.

The Intermediate Temp (IT) effort will initially be focused on screening the existing Li cells for capability to withstand elevated temperatures to 250°C. The work will consist of storage tests followed by discharge of groups of cells at increasing temperature increments from 50 to 250°C. The most promising will be selected for further development wherein attempts will be made to improve design for extended temperature capability. Finally, a Flight Type version of the modified cell will be designed, fabricated, and tested.

The Next Generation (IT-to-HT) effort will focus on selecting the most promising advanced cell components to enhance high temperature stability as well as performance. This work will initially consist of assembly and test of laboratory type cells based on the advanced components. Hardware versions of the most cells will then be fabricated, and tested. Finally, a Flight Type Cell and then battery will be designed, fabricated, and tested.

Technology Roadmap

The development timeline is synchronized to the VISE and VME missions to Venus and the JFDP mission to Venus.

The timeline is shown in Table 5.14.

5.2.4 Low-Temperature Energy Storage

Objectives

The overall objective of the program is to develop low-temperature (-100°C) primary and rechargeable batteries that are mass and volume efficient, required for the surface explo-

Table 5.14: Development timeline for high-temperature energy storage.

High T Energy Storage	11	12	13	14	15	16	17	18	19	20
High T Battery: Primary							4	6	6	
High T Battery: Secondary	2	3	3	4	4	6	6	6	6	
Medium T Battery	3	3	4	4	5	6				
Missions: Dates for technology infusion						↓ JFDP				↓ VME

TRLs are shown from 1 to 6: 1; 2; 3; 4; 5; 6

ration missions of outer planets and their moons.

The specific objectives of the program are:

- Develop low temperature (-80°C) primary battery for near-term missions;
- Develop low-temperature rechargeable battery (-60°C) for near-term missions;
- Develop improved low-temperature (-100°C) primary and secondary batteries (lower operating temperature capability and improved power and energy densities) for future missions.

The suggested performance metrics are listed in Table 5.15.

Table 5.15: Performance metrics for low-temperature energy storage.

Low T Energy Storage	Metric	State-of-Practice	Goal (TRL 6)
Primary batteries	Specific energy at -40°C (Wh/kg)	100	150
	Specific energy at -80°C (Wh/kg)	50	100
	Specific energy at -100°C (Wh/kg)	N/A	100
Secondary batteries	Specific energy at -40°C (Wh/kg)	150	200
	Specific energy at -100°C (Wh/kg)	N/A	50
	Reversibility at -40°C (# of cycles)	>2500	3000
	Reversibility at -100°C (# of cycles)	N/A	500
Low T/Rad hard energy storage	Radiation hardness at -160°C (Mrad)	N/A	1

Benefits

Low-temperature batteries could benefit future surface missions such as Mars landers and

rovers, lunar outposts/ habitat rovers, Europa lander/probes, Titan explorer, and Triton lander. The performance capabilities of several of these missions would be significantly enhanced with the use of low-temperature batteries. The mission impact/benefits of these technologies would be: a) Operation of the rovers/probes/landers in a cold environment; b) mass and volume savings associated with the heavy thermal system that is needed with SOP space batteries; and c) cost savings.

Unlike the missions in high-temperature environments, the extreme low-temperature missions can extend for longer than tens of hours or tens of days because reliability and life concerns are negligible at low temperatures. The batteries for such missions can therefore be sized such that the power densities are lower and the specific energies and energy densities are proportionately higher. Although many factors limit the performance of batteries at temperatures below -100°C , technology investment leading to improved performance would minimize constraints on thermal management designs and/or energy consumed by heating devices. The Titan Explorer, as well the Europa Astrobiology Lander, could benefit from all of these technologies.

Approach

Low-Temperature Primary Batteries: The approach to develop advanced low-temperature primary batteries will consist of an initial parallel development effort on the two most promising systems: Li-CF_x and Li-SOCl₂ (Li-interhalogens). The challenges in these systems are different. Li-CF_x already has high specific energy but only at exceedingly low rates, whereas Li-SOCl₂ requires an increase in specific energy. Both systems will benefit from new electrolytes that perform well at low temperatures. Subsequent efforts will require down-selection to the most promising technology for maturation to TRL 6.

The initial phase of the effort will focus on advancing both technologies to TRL 4, utilizing the following activities:

1. Identify electrolytes that have good lithium ion conductivity at these low temperatures;
2. Improve the Li electrode/electrolyte interfacial properties for enhanced charge transfer;
3. Improve the ionic and electronic conductivity of cathode material (CF_x); and
4. Demonstrate technology feasibility with experimental cells at appropriate rates of charge and discharge.

The second phase of the effort will focus on advancing the down-selected technology to TRL 6 and will consist of the following activities: a) cell design and fabrication; b) battery design and fabrication; c) electrical and life performance; and d) performance validation at the prototype cell and battery levels. The assessment team also recommends fostering

partnerships with various universities and industries for the initial phase of the development (TRL 2–4) and developing partnerships with the relevant industries for advancing the technology to TRL 6.

Low-Temperature Secondary Batteries: The approach to developing advanced low-temperature rechargeable batteries will consist of an initial parallel development effort on the two or three most promising systems, including Li-ion, Li-S, and other Li-metal based systems. The initial phase of the effort will focus on advancing this battery technology to TRL 4 and will consist of the following activities: a) the identification of electrolytes with improved lithium-ion conductivity at low temperatures; b) the development of improved electrode materials with enhanced kinetics for lithium intercalation and diffusion; and c) the demonstration of the technological feasibility with experimental cells. The second phase of the effort will focus on advancing the technology to TRL 6 and will consist of the following activities: a) cell design and fabrication; b) battery design and fabrication; and c) performance validation at the prototype cell and battery levels.

Technology Roadmap

It is anticipated that development will take place in parallel for most of the energy storage systems, with integration of radiation hardening to take place after the initial battery and flywheel development. The timeline is summarized in Table 5.16.

Table 5.16: Development timelines for low-temperature energy storage.

Low T Energy Storage	08	09	10	11	12	13	14	15	25
Primary Batteries				②	③	④	⑤	⑥	
Secondary Batteries				②	③	④	⑤	⑥	
LT/Rad Hard Energy Storage								③	⑥
Missions: Dates for technology infusion								↓ TE	↓ EAL

TRLs are shown from 1 to 6: ①; ②; ③; ④; ⑤; ⑥

5.3 Roadmaps for Robotics

Operation systems allow mission goals to be met and enable the collection of returned data. Technologies here include the mechanical systems required for in situ sample acquisition and analysis, as well as aerial mobility systems on Venus or Titan, where atmospheric conditions provide the opportunity for broad survey operations.

5.3.1 High-Temperature Mechanisms

Objectives

The objectives are to: 1) Develop a sample acquisition system operable at 500°C; 2) Develop mechanisms associated with aerial mobility; and 3) Provide for extended operations for tens of hours. The sample acquisition system would require a drill capable of collecting the sample from at least 20 cm below the surface in a short time (tens of seconds). The performance metrics are given in Table 5.17.

Table 5.17: Performance metrics for high-temperature mechanisms.

High T Mechanisms	Metric	State-of-Practice	Goal (TRL 6)
Sample acquisition system	Operation temperature (°C)	500 (USSR)	500
	Mass (kg)	23 (USSR)	5
	Drilling time (s)	230 (USSR)	100
Robotic arm and wheels	Operation temperature (°C)	N/A	500
	Lifetime (hrs)	N/A	tens

Benefits

High-temperature motors and actuators would be the key components of a sample acquisition and transfer system. The acquisition of unweathered samples from at least 20 cm below the surface layer of Venus would be desired for the VISE mission. In addition, motors and actuators are desired for a variety of functions, such as opening and closing valves, deploying landing gear, and operating robotic arms and antenna gimbals. For VME, mission motors and actuators may be crucial for mobility systems if a rover is selected as a mission baseline, requiring reliable operations for hundreds of hours.

Approach

Required technologies include motors and gearboxes, position sensors, high-temperature electrical cabling, mechanical devices related to drilling and containing a sample, and mechanical sample transfer devices. Magnetic materials with high Curie temperatures need to be identified and tested for the motor itself, while gearboxes and lubricants require suitable materials. High-temperature testing of the elements will precede motor assembly, integration, and environmental testing.

Technology Roadmap

Development of high-temperature mechanisms is synchronized primarily to in situ exploration for VISE and VME, posing longer lifetime requirements on all the systems. Table 5.18 shows the development timeline.

Table 5.18: Development timeline for high-temperature mechanisms.

High T Mechanisms	08	09	10	11	12	13	14	15	20
Sample acquisition	③	②	④	⑥					
Sample processing/handling	③	②	④	⑥					
Robotic arm	④			⑥					
Longer lifetime						④	⑤	⑥	
Missions: Dates for technology infusion				↓ VISE					↓ VME

TRLs are shown from 1 to 6: ①; ②; ③; ④; ⑤; ⑥

5.3.2 Low-Temperature Mechanisms

Objectives

The objectives for low-temperature mechanisms include development of: 1) An integrated wheel/ballute motor, with appropriate lubrication, capable of operation down to -180°C and 50,000 revolutions; 2) A low-temperature robotic arm for sample acquisition; and 3) Integration with technologies hardened to 1000 krad of radiation. The performance metrics are shown in Table 5.19.

Table 5.19: Performance metrics for low-temperature mechanisms.

Low T Mechanisms	Metric	State-of-Practice	Goal (TRL 6)
Integrated wheel/ balloon motor	Operating temperature ($^{\circ}\text{C}$)	-120	-180
	Number of revolutions	Limited	50,000
	Lowest operating lubricant T ($^{\circ}\text{C}$)	-120	-180
LT robotic arm	Actuation performance at -180°C	Varies	Insensitive
Rad hard/LT integration	Total dose (krad) at -160°C	N/A	500

Benefits

Low-temperature motors and actuators would be needed to operate the Titan Explorer, rovers associated with the Lunar Aitken Basin, and for the Europa Astrobiology Lander. The motors would be needed for sample acquisition systems, mobility systems, robotic arms, and other applications.

Approach

Advanced lubricants and/or lubrication delivery systems will be needed for long-lived mech-

anisms in an ultra-cold environment. Lubricant systems will be developed for highly loaded sliding and rolling mechanisms for lunar missions. Solid and novel liquid lubricants will be developed and deployed for mechanism contact zones throughout the system's projected lifetime.

Advanced drive components and systems will be needed to allow reliable and robust mechanical power transmission. New materials may be needed for gears, bearing, and harmonic drive components to survive for long-term survival at -233°C under high tensile and compressive loads. Alternate materials, such as titanium alloys, ceramics, and composites, will be investigated and fatigue tested at the component level under ambient and ultra-cold temperatures. Surface fatigue and bending fatigue will be used to screen candidate materials. New mechanical power transmission concepts with inherent design advantages for cold environments will also be investigated. Development will also take place for drive system design concepts compensating for large tolerance changes due to operation at a temperature significantly colder than that of assembly and delivery.

Technology Roadmap

The development of low-temperature mechanisms is linked to plans for Titan Explorer, with radiation hardness to be integrated later for the Europa Astrobiology Laboratory. Table 5.20 shows the development timeline.

Table 5.20: Development timeline for low-temperature mechanisms.

Low T Mechanisms	08	09	10	11	12	13	14	15	25
Integrated wheel/ballute motor					③	④	⑤	⑥	
LT sample acquisition system					③	④	⑤	⑥	
Rad hard/ LT integration				④	⑤	⑤	⑥	⑥	
Missions: Dates for technology infusion								↓ TE	↓ EAL

TRLs are shown from 1 to 6: ①; ②; ③; ④; ⑤; ⑥

5.3.3 High-Temperature Mobility

Objectives

The objective is to develop high-temperature balloon technology for use on the Venus Mobile Explorer. This technology would be required for a subsequent Venus Surface Sample Return mission, although this is outside of the planning horizon of the Roadmap. This consists of the balloon itself, plus the deployment and inflation system required to make the balloon operational upon arrival at Venus. The required performance metrics are summarized in Table 5.21.

Balloons for advanced missions have to be robust and capable for

- Heavy payloads: >40 kg
- Long duration: >6 days
- Global flights: multiple day/night cycles and circumnavigation at any latitude
- High payload mass fraction: >0.5
- Robust: safety factor (ratio of burst load to actual load) >2.5 in the most adverse combination
- Low gas permeability: metallized film
- Minimum day/night temperature variations: minimum optical absorptivity/infrared emissivity ratio (a/e)

This device requires ~1 degree pointing, comparable to the ~0.5 degree pointing needed at Titan.

Table 5.21: Performance metrics for high-temperature aerial mobility.

HT Aerial Mobility	Metric	State-of-Practice	Goal (TRL 6)
Venus Surface Sample Return	Areal density (g/m ²)	N/A	1000
	Altitude range (km)	N/A	0–15
	Operational flight time (days)	N/A	0.3
	Non-balloon floated mass (kg)	N/A	500
Venus Mobile Explorer	Areal density (g/m ²)	N/A	1000
	Altitude range (km)	N/A	0–4
	Operational flight time (days)	N/A	180
	Non-balloon floated mass (kg)	N/A	200

Benefits

High-temperature balloon technology would be enabling for aerial mobility missions near the Venus surface required for the Venus Mobile Explorer mission. Any kind of surface sample return mission would require a high-temperature balloon to lift the sample to a feasible launch altitude above the bulk of the Venus atmosphere.

Approach

The recommended approach is to focus on the metal bellows balloon concept and emphasize prototyping and high-temperature testing in the development program. The technological

needs can be addressed sequentially to a large extent: Fabricate large-size bellows, evaluate the long-term leakage performance, then validate deployment and inflation technology. One significant complication is the need for suitable high-temperature, high-pressure test facilities large enough for full-scale metal balloon prototypes.

Technology Roadmap

Because VME is the primary beneficiary of these systems, the milestones are synchronized to VME's launch, as shown in Table 5.22.

Table 5.22: Development timelines for high-temperature aerial mobility.

HT Aerial Mobility	08	09	10	11	12	13	14	15	25
Large-diameter bellows design, fabrication, and testing		③	●	●	●	●	●	●	⑤
Long-duration leakage tests				④	●	●	●	●	⑤
Deployment and inflation design, fabrication, and testing		③	●	●	●	●	●	●	⑤
System integration and testing								⑤	⑥
Missions: Dates for technology infusion									↓ VME

TRLs are shown from 1 to 6: ①; ②; ③; ④; ⑤; ⑥

5.3.4 Low-Temperature Aerial Mobility

Objectives

The objective is to develop low-temperature (cryogenic) aerobot (balloon) technology for use in the proposed Titan Explorer mission. This technology has several sub-components, including cryogenic balloon materials, balloon fabrication, aerial deployment and inflation, aerobot autonomy, and surface sample acquisition and handling. The required performance metrics are summarized in Table 5.23.

Benefits

The environment of Titan is well-suited to aerial mobility despite the cold temperature. The dense atmosphere (4.5 times that of Earth), low gravity (1/7 that of Earth), and low surface winds (<1 m/s) enable compact, self-propelled balloon vehicles with “go-to” targeting capability across the planet and the ability to carry substantial payloads for long periods of time. Several balloon component technologies would be enabling for these Titan missions, including cryogenic balloon materials, aerial deployment and inflation, and highly autonomous ground approach and surface sample acquisition.

Table 5.23: Performance metrics for low-temperature aerial mobility.

LT Aerial Mobility	Metric	State-of-Practice	Goal (TRL 6)
Aerobot: Self-propelled, surface-sampling	Operation time (days)	N/A	180
	Non balloon floated mass (kg)	N/A	200
	Altitude range (km)	N/A	0–8
	Balloon material areal density (g/m ²)	100	100
	Surface location targeting accuracy (m)	N/A	100
	No. of 100 g surface samples	N/A	20
Balloon: Altitude-controlled drifting (RTG– Montgolfière)	Operation time (months)	N/A	36
	Non balloon floated mass (kg)	N/A	100
	Altitude range (km)	N/A	0–8
	Balloon material areal density (g/m ²)	100	100

Approach

The recommended approach is to pursue development of both the two main aerobot concepts: self-propelled blimps and RTG Montgolfière balloons. Although both require basic feasibility and performance studies, substantial overlap between the two vehicles would mitigate the technology development costs. The areas of overlap include balloon materials, balloon fabrication techniques, aerobot navigation algorithms and sensors, and surface sample acquisition and handling systems. Note also that the science requirements of a future Titan mission may preclude the RTG Montgolfière approach if “go-to” targeting or highly precise surface sample acquisition capabilities are deemed necessary to achieve the scientific objectives.

Technology Roadmap

The technology development is summarized in Table 5.24 and proceeds along paths for the aerobot and balloon concepts separately.

Table 5.24: Development timelines for low-temperature aerial mobility.

LT Aerial Mobility	08	09	10	11	12	13	14	15
Self propelled aerobot	③	④	⑤	⑥	⑦	⑧	⑨	⑩
Montgolfière balloon	③	④	⑤	⑥	⑦	⑧	⑨	⑩
Missions: Dates for technology infusion								↓ TE

TRLs are shown from 1 to 6: ①; ②; ③; ④; ⑤; ⑥

6 Resources and Background Information

The Extreme Environment report provides an overview of technologies and related issues, and recommends a development plan for the addressed technologies. Additional information on these topics can be found in literature. Supporting background material for this report can be found in the references identified for the various sections.

State-of-Practice of Exploration of Extreme Environments

For further information on this topic, please consult the following references: [AAN⁺06], [AKG⁺05], [Bie04], [BWH⁺96], [BKM86], [CHV⁺02], [DG83], [FAF02], [Fie00], [GGS92], [GJR⁺03], [GH00], [Gri97], [HV78], [Zak07], [Mit07], [JPL07], [NAS07a], [KBC⁺99], [KH80], [Kra89], [Ksa83], [LWS⁺05], [LBCC05], [LM02], [Mar78], [MG98], [NH96], [PGB⁺02], [SLRJ03], [WMJW92], [ZLG⁺02].

Future Mission Concepts

For further information on this topic, please consult the following references: [AW05b], [ABGO06], [BAC⁺06], [ABC⁺04], [ABE⁺05], [Bal04], [BJ05], [Bal05], [Coh02], [HB06], [LEApr], [MEP07], [NAS07b], [NAS05], [NRC03], [OPA07], [NAS06], [VEX07], [The04], [Cla07].

Hypervelocity Entry

For further information on this topic, please consult the following references: [LV03], [Lau02], [MVT04], [VLW06].

Hypervelocity Impact Protection

For further information on this topic, please consult the following references: [NAS70a], [NAS70b], [Div93].

Radiation Shielding

For further information on this topic, please consult the following reference: [Fey88].

Pressure and Thermal Control Technologies

For further information on this topic, please consult the following references: [Ban01], [Gil02], [HV78], [Jon93], [Lan04], [LM04], [Mal], [Mee91], [Mel04a], [Mel04b], [DPK96], [Te73].

High-Temperature Electronics

For further information on this topic, please consult the following references: [AHRS04], [Ben99], [BW81], [CM02], [Coo03], [Fri95], [Har99], [McC97], [Jur99], [Kir00], [KHGS07], [MCM⁺], [NOC02], [Sad03], [SHC⁺04].

Low-Temperature Electronics

For further information on this topic, please consult the following references: [ABC⁺95],

[AS85], [Bri91], [CRD86], [Cre03], [Cre94], [DCF88], [EHG⁺02], [GPS96], [GDC01], [Len74], [PHD⁺02], [PHD⁺00], [Se93], [TYC85].

Radiation Tolerant Electronics

For further information on this topic, please consult the following references: [BDS03], [BMJ02], [CKRR96], [DJ84], [Dod96], [De04], [Ee01], [Fe97], [Fe01], [He01], [Ie02], [IF04], [JKS⁺94], [Joh96], [SR98], [Se01].

High-Temperature Energy Storage

For further information on this topic, please consult the following references: [SC68], [HKJ⁺98], [LR02], [KJHV96], [Coe96], [RWR97], [Cra03].

Low-Temperature Energy Storage

For further information on this topic, please consult the following references: [RCMR00] and [KBB⁺96].

High-Temperature Mechanisms

For further information on this topic, please consult the following references: [BCe01], [HAR⁺04], [LW05], [MV00], [Ree83].

Low-Temperature Mechanisms

For further information on this topic, please consult the following references: [Ae71], [JRH⁺04], [MSBE02], [Wig71].

High-Temperature Aerial Mobility

For further information on this topic, please consult the following references: [HFF⁺06], [KHYC05], [KHY01], [HMS⁺00], [LLC03].

Low-Temperature Aerial Mobility

For further information on this topic, please consult the following references: [HJK⁺06] and [HKY⁺06].

Acronyms and Abbreviations

A/D	analog to digital
ACC	advanced carbon carbon
ACP	Aerosol Collector and Pyrolyser
ADC	analog to digital converter
AFL	Astrobiology Field Laboratory
amu	atomic mass unit
AO	Announcement of Opportunity
APIO	Advanced Planning and Integration Office
ARAD	Analog Resistance Ablation Detector
ARC	Ames Research Center
ASIC	application-specific integrated circuit
atm	atmosphere
AU	astronomical unit
BAE	British Aerospace
BiCMOS	Bipolar CMOS
BJT	bipolar junction transistor
BOL	beginning of life
C&DH	command and data handling
CAD	computer-aided design / drawing
CCD	charge-coupled device
CDMU	Command and Data Management Unit
CET	Capacitance Equivalent Thickness
CMCP	chopped molded carbon phenolic
CME	coronal mass ejection
CMOS	complementary metal-oxide semiconductor
CNRS	Centre national de la recherche scientifique
CNT	carbon nanotube
CONTOUR	Comet Nucleus Tour
COTS	commercial off-the-shelf
CRAM	card random-access memory
CSR	Comet Surface Sample Return
CTE	coefficient of thermal expansion
CW	continuous wave
D/A	digital to analog
DCP	data and command processor
DISR	Descent Imager/Spectral Radiometer
DMEA	Defense Micro-Electronics Activity
DMIPS	Dhrystone million instructions per second
DRAM	dynamic random access memory
DRM	Design Reference Mission
DS-2	Deep Space 2
DSP	digital signal processing
DWE	Doppler Wind Experiment
E/PO	Education and Public Outreach
EAL	Europa Astrobiology Lander
ECAD	error correction and detection
ECT	Enabling Cross-cutting Technology
EE	Europa Explorer
EE	Extreme Environment

EEPROM	electronically erasable programmable read-only memory
ENSERG	École Nationale Supérieure d'Électronique et de Radio électricité de Grenoble
EPD	Energetic Particle Detector
ESA	European Space Agency
ESAS	Exploration Systems Architecture Study
ESD	electrostatic discharge
ESMD	Exploration Systems Mission Directorate
EUVS	Extreme Ultraviolet Spectrometer
EV	electric vehicle
FCS	foam core shield
FDSOI	fully depleted SOI
FET	field-effect transistor
FPGA	field-programmable gate array
FRAM	ferroelectric random access memory
FTE	full-time equivalent
g	gravity / gram
GaAs	gallium arsenide
GaN	gallium nitride
GCMS	Gas Chromatograph Mass Spectrometer
GCR	galactic cosmic ray
GIRE	Galileo Interim Radiation Electron (model)
GPF	Giant Planet Facility
GPHS	General Purpose Heat Source
GRC	Glenn Research Center
GTO	gate turn-off thyristor
HASI	Huygens Atmospheric Structure Instrument
HBT	heterojunction bipolar transistor
HCD	hot carrier degradation
HGA	high-gain antenna
HT	high temperature
HW	Honeywell
IC	integrated circuit
ICBM	Intercontinental Ballistic Missile
IR	infrared
ISRU	in situ resource utilization
IT	intermediate temperature
ITS3	radiation Monte Carlo code: Integrated Tiger Series, v.3
ITS5	radiation Monte Carlo code: Integrated Tiger Series, v.5
JAXA	Japanese Aerospace Exploration Agency
Jb	Galileo Energetic Particle Detector
JDEP	Jupiter Deep Entry Probes
JFDP	Jupiter Flyby with Deep Entry Probes
JFET	junction field effect transistor
JPL	Jet Propulsion Laboratory
JPOP	Jupiter Polar Orbiter with Probes
L/D	lift-to-drag ratio
LEAG	Lunar Exploration Assessment Group
LED	light-emitting diode
LILT	low-intensity, low-temperature
Ls	aerocentric longitude of the Sun
LSI	large-scale integrated
LT	low temperature
MCM	multichip modules

MCNPX	a general purpose Monte Carlo radiation transport code
MEA	main engine assembly
MEP	Mars Exploration Program
MEPAG	Mars Exploration Program Analysis Group
MER	Mars Exploration Rover
MESFET	metal semiconductor field-effect transistor
MLI	multilayer insulation
MOSFET	metal oxide semiconductor field-effect transistor
MRAM	magnetoresistive random-access memory
MRO	Mars Reconnaissance Orbiter
MSI	medium-state integration
MSL	Mars Science Laboratory
MSO	Mars Science Orbiter
MSR	Mars Sample Return
MTECH	MTECH Laboratories, LLC
NAND	not and
NASA	National Aeronautics and Space Administration
NF	New Frontiers
NG	Northrop–Grumman
NGST	Northrop Grumman Space Technology
NIST	National Institute of Standards and Technology
NO/TL	Neptune Orbiter/Triton Lander
NPOESS	National Polar-orbiting Operational Environmental Satellite System
NRC	National Research Council
NRE	nonrecurring engineering
OPAG	Outer Planets Advisory Group
ORNL	Oak Ridge National Laboratory
PBO	polybenzoxazole
PCB	printed circuit board
PCM	phase change material
PICA	phenolic impregnated carbon ablator
PMAD	power management and distribution
PROM	programmable read-only memory
PSA	Probe Support Avionics
PSE	probe support equipment
R&A	Research and Analysis
RAM	random-access memory
RASC	Revolutionary Aerospace Systems Concept
RDM	radiation design margin
RHBD	radiation hard by design
RHBP	radiation hard by process
RHOC	Radiation Hardened Oversight Council
RHU	radioisotope heater unit
RKA	Russian Aviation and Space Agency
RP	repetitively pulsed
RTD	resistance temperature detector
RTG	radioisotope thermoelectric generator
SBIR	Small Business Innovative Research
SDRAM	synchronous dynamic random-access memory
SEL	single-event latchup
SEP	solar energetic particle
SEU	single-event upset
SFSP	Saturn Flyby with Shallow Probes

Si	silicon
SiC	silicon carbide
SIRCA	silicon impregnated reusable ceramic ablator
SLA	superlightweight ablator
SMD	Science Mission Directorate
SMES	superconducting magnetic energy storage
SNL	Sandia National Laboratories
SNR	signal-to-noise ratio
SOFC	solid oxide fuel cell
SOI	silicon-on-insulator
SOP	state of practice
SPAB L/R	South Pole Aitken Basin Lander/Rover
SPIU	subsystem power interface unit
SRAM	silicone-reinforced ablative material
SRAM	static random access memory
SRG	Stirling Radioisotope Generator
SSE	Solar System Exploration
SSI	small-state integration
SSI	Solid-State Imaging
SSP	Surface-Science Package
TASHE	Thermoacoustic Stirling Heat Engine
TE	Titan Explorer
THSS	thermal subsystem
TI	Texas Instruments
TID	total ionizing dose
TMR	triple modular redundancy
TPS	thermal protection system
TRL	Technology Readiness Level
TV	television
TWCP	tape-wrapped carbon phenolic
UHF	ultra-high frequency
UV	ultraviolet
V	voltage
VEXAG	Venus Exploration Analysis Group
VISE	Venus In Situ Explorer
VLSI	very large scale integrated
VME	Venus Mobile Explorer
VSSR	Venus Surface Sample Return
WEB	warm electronics box
ZEBRA	Zero Emission Battery Research Activities

References

- [AAN⁺06] S.K. Atreya, E.Y. Adams, H.B. Niemann, J.E. Demick-Montelara, T.C. Owen, M. Fulchignoni, F. Ferri, and E.H. Wilson. Titan’s Methane Cycle. *Special Issue on the Outer Planets, Satellites, and Rings, Planetary and Space Science*, 54:1177–1187, 2006. [255](#)
- [ABC⁺95] A. Alessandrello, C. Brofferio, D.V. Camin, O. Cremonesi, A. Giuliani, A. Nucciotti, M. Pavan, G. Pessina, and E. Previtali. Cryogenic, monolithic differential GaAs preamplifier for bolometric detectors. *Nuclear Instruments and Methods in Physics Research*, A360:186–188, 1995. [255](#)
- [ABC⁺04] R.D. Abelson, T.S. Balint, K. Coste, J.O. Elliott, J.E. Randolph, G.R. Schmidt, T. Schriener, J.H. Shirley, and T.R. Spilker. Expanding Frontiers with Standard Radioisotope Power Systems. Technical Report NASA report: JPL D-28902, PP-266 0332, National Aeronautics and Space Administration, Nov 2004. [255](#)
- [ABE⁺05] R.D. Abelson, T.S. Balint, M. Evans, T. Schriener, J.H. Shirley, and T.R. Spilker. Extending Exploration with Advanced Radioisotope Power Systems. Technical Report NASA Report: JPL D-28903, PP-266 0333, National Aeronautics and Space Administration, Oct 2005. [255](#)
- [ABGO06] S.K. Atreya, S. Bolton, T. Guillot, and T.C. Owen. Multiprobe Exploration of the Giant Planets — Shallow Probes. *Proceedings of the 3rd International Probe Workshop — IPPW-3*, (WPP263), 2006. [255](#)
- [Ae71] W. Ackerman and et al. Magnetic properties of commercial soft magnetic alloys at cryogenic temperatures. *Advances in Cryogenic Engineering*, 16:46–50, 1971. [256](#)
- [AHRS04] E.F. Alberta, W.S. Hackenberger, C.A. Randall, and T.R. Shrout. High Temperature Ceramic Multilayer Capacitors. *Proceedings of the IMAPS International High Temperature Electronics Conference (HiTEC)*, May 2004. [255](#)
- [AKG⁺05] D.H. Atkinson, B. Kazeminejad, V. Gaborit, F. Ferri, and J.-P. Lebreton. Huygens Probe Entry and Descent Trajectory Analysis and Reconstruction Techniques. *Planetary and Space Science*, 53:586–593, 2005. [255](#)
- [AS85] C.M. Atkinson and R.G. Scurlock. Use of precision low noise monolithic instrumentation amplifiers at low temperatures. *Cryogenics*, 25(7):393–394, Jul 1985. [256](#)
- [AW05a] S.K. Atreya and A.S. Wong. Coupled Chemistry and Clouds of the Giant Planets — A Case for Multiprobes. *Space Science Review*, 116(1-2):121–136, 2005.
- [AW05b] S.K. Atreya and A.S. Wong. *The Outer Planets and their Moons*, chapter Coupled Chemistry and Clouds of the Giant Planets — A Case for Multiprobes, pages 121–136. Springer Publishers, New York - Heidelberg, 2005. [255](#)
- [BAC⁺06] K.H. Baines, S. Atreya, R.W. Carlson, A. Chutjian, D. Crisp, J.L. Hall, D.L. Jones, V.V. Kerzhanovich, S.S. Limaye, and S.K. Stephens. In-situ exploration of Venus on a global scale: Direct measurements of origins and evolution, meteorology, dynamics, and chemistry by a long-duration aerial science station. *Proceedings of the 3rd International Probe Workshop — IPPW-3*, (WPP263), 2006. [255](#)
- [Bal04] T.S. Balint. Europa Surface Science Package Feasibility Assessment. Technical Report JPL D-30050, National Aeronautics and Space Administration, Washington, D.C., USA, Sep 2004. [255](#)

- [Bal05] T.S. Balint. Exploring Triton with Multiple Landers. *56th International Astronautical Congress*, (IAC-05-A.3.2.A.09), Oct 2005. [255](#)
- [Ban01] D. Banerjee. Structural materials in aerospace systems. *Material Research Society Bulletin*, Mar 2001. [255](#)
- [BCe01] Y. Bar-Cohen and et al. Ultrasonic/Sonic Driller/Corer (USDC) as a Sampler for Planetary Exploration. *IEEE Aerospace Conference: Missions, Systems and Instruments for In-situ Sensing*, Mar 2001. [256](#)
- [BDS03] J.L. Barth, C.S. Dyer, and E.G. Stassinopoulos. Space, Atmospheric and Terrestrial Environments. *IEEE Transactions on Nuclear Science*, 50(3):466–482, 2003. [256](#)
- [Ben99] G.A. Bennett. Thermal protection methods for electronics in hot wells. *High-Temperature Electronics*, pages 111–124, 1999. [255](#)
- [Bie04] B. Bienstock. Pioneer Venus and Galileo entry probe heritage. *Proceedings of the International Workshop Planetary Probe Atmospheric Entry and Descent Trajectory Analysis and Science*, (ISBN 92-9092-855-7):37–45, Oct 2004. [255](#)
- [BJ05] T.S. Balint and J.F. Jordan. RPS Strategies to Enable NASA’s Next Decade Robotic Mars Missions. *56th International Astronautical Congress*, (IAC-05-A5.2.03), Oct 2005. [255](#)
- [BKM86] G. Burdick, E.H. Kopf, and D.D. Meyer. The Galileo single-event upset solution and risk assessment. In *Proceedings of the Annual Rocky Mountain Guidance and Control Conference*, pages 199–220, Feb 1986. [255](#)
- [BMJ02] H.N. Becker, T.F. Miyahira, and A.H. Johnston. Latent Damage in CMOS Devices from Single-Event Latchup. *IEEE Transactions on Nuclear Science*, 49(6):3009–3015, 2002. [256](#)
- [Bri91] A. Briggs. Characterization of some chip resistors at low temperatures. *Cryogenics*, 31(11):932–935, Nov 1991. [256](#)
- [BW81] T.J. Borden and J.W. Winslow. Packaging techniques for low-altitude Venus balloon beacon. *Proceedings of the Conference on High Temperature Electronics*, (NTIS PB82-114414, NSF/ECS-81007):117–121, Mar 1981. [255](#)
- [BWH⁺96] J.L. Bertaux, T. Wideman, A. Hauchecorne, V.I. Moroz, and A.P. Ekomonov. Vega1 and Vega 2 entry ptobes. *Journal of Geophysical Research*, 101:709–746, 1996. [255](#)
- [CHV⁺02] K.C. Clausen, H. Hassan, M. Verdant, P. Couzin, G. Huttin, M. Brisso, C. Sollazzo, and J.-P. Lebreton. The Huygens probe system design. *Space Science Review*, 104:155–189, 2002. [255](#)
- [CKRR96] M. Citterio, J. Kierstead, S. Rescia, and V. Radeka. Radiation effects on Si-JFET devices for front-end electronics. *IEEE Transactions on Nuclear Science*, 43(3):1576–1584, Jun 1996. [256](#)
- [Cla07] K.B. Clark. Europa Explorer An Exceptional Mission Using Existing Technology. *Proceeding of the 2007 IEEE Aerospace Conference*, (IEEEAC paper #1417; IEEE Catalog Number 07TH8903C; ISBN 1-4244-0525-4; ISS 1095-323X), Mar 2007. [189, 255](#)
- [CM02] L.-Y. Chen and P. McCluskey. Microsystem packaging for high temperature environments. *EEE Links*, 8(2), Aug 2002. [255](#)
- [Coe96] J. Coetzer. *Journal of Power Sources*, 18:277–380, 1996. [256](#)

- [Coh02] M.M. Cohen. Selected Precepts in Lunar Architecture. *53rd International Astronautical Congress*, (IAC-02-Q4.3.08), Oct 2002. [255](#)
- [Coo03] J. A. Cooper Jr. Development of a SiC-Based Electronics Technology for Extreme Environments. *Workshop on Extreme Environments Technologies for Space Exploration*, May 2003. [255](#)
- [Cra03] Ceramatec presentation. *Extreme environments workshop*, 2003. [256](#)
- [CRD86] L.M. Colonna-Romano and D.R. Deverell. Operation of a CMOS microprocessor while immersed in liquid nitrogen. *Journal of Solid-State Circuits*, SC-21(3):491–492, Jun 1986. [256](#)
- [Cre94] J.D. Cressler. Operation of SiGe bipolar technology at cryogenic temperatures. *Proc. First European Workshop on Low Temperature Electronics (WOLTE 1)*, *J. de Physique*, 4(Colloque C6):101, 1994. [256](#)
- [Cre03] J.D. Cressler. SiGe HBT BiCMOS technology for extreme environment applications. *Workshop on Extreme Environments Technologies for Space Exploration*, May 2003. [256](#)
- [DCF88] M.J. Deen, C.Y. Chan, and N. Fong. Operational characteristics of a CMOS microprocessor system at cryogenic temperatures. *Cryogenics*, 28(5):336–338, May 1988. [256](#)
- [De04] P.E. Dodd and et al. Production and Propagation of Single-Event Transients in High-Speed Digital Logic ICs. *IEEE Transactions on Nuclear Science*, 51(6):3278–3284, 2004. [256](#)
- [DG83] N. Divine and H. B. Garrett. Charged particle distributions in Jupiter’s magnetosphere. *Journal of Geophysics Research*, 88:6889–6903, Sep 1983. [255](#)
- [Div93] N. Divine. Five populations of interplanetary meteoroids. *Journal Geophysics Research*, 98:17029–17048, 1993. [255](#)
- [DJ84] J.G. Dooley and R.C. Jaeger. Temperature dependence of latchup in CMOS circuits. *IEEE Electron Device Letters*, EDL-5(2):41–43, Feb 1984. [256](#)
- [Dod96] P.E. Dodd. Device Simulation of Charge Collection and Single-Event Upset. *IEEE Transactions on Nuclear Science*, 43(2):561, 1996. [256](#)
- [DPK96] M.N. De Parolis and W. Pinter-Krainer. Current and future techniques for spacecraft thermal control — Design drivers and current technologies. ESTEC, Noordwijk, The Netherlands, ESA Bulletin Nr. 87, Website: <http://esapub.esrin.esa.it/bulletin/bullet87/paroli87.htm>, Aug 1996. [255](#)
- [Ee01] L.D. Edmonds and et al. Ion-Induced Stuck Bits in 1T/1C SDRAM Cells. *IEEE Transactions on Nuclear Science*, 48(6):1925–1930, 2001. [256](#)
- [EHG⁺02] M. Elbuluk, A. Hammoud, S. Gerber, R. Patterson, and A. Sharma. Evaluation of power electronic components and systems at cryogenic temperatures for space missions. *NEPP ’02 Workshop*, Apr 2002. [256](#)
- [FAF02] P.D. Fieseler, S.M. Ardalan, and A.R. Frederickson. The Radiation Effects on Galileo. *IEEE Transactions on Nuclear Science*, 49(6):2739–2758, 2002. [255](#)

- [Fe97] N. Fourches and et al. Thick film SOI technology: characteristics of devices and performance of circuits for high-energy physics at cryogenic temperatures; effects of ionizing radiation. *Nuclear Instruments and Methods in Physics Research A*, A401:229–237, 1997. [256](#)
- [Fe01] D.J. Frank and et al. Device Scaling Limits of Si MOSFETs and Their Application Dependencies. *Proc. IEEE*, 89(3):259–288, 2001. [256](#)
- [Fey88] International particle environment. Proceedings of a conference. Technical Report N-89-28454;NASA-CR-185461; JPL-PUBL-88-28; NAS-1.26:185461; CONF-8703326-, Jet Propulsion Laboratory, California Institute of Technology, Pasadena, CA, Apr 1988. [255](#)
- [Fie00] P. D. Fieseler. The Galileo star scanner as an instrument for measuring energetic electrons in the Jovian environment. Master's thesis, University of Southern California, Los Angeles, Dec 2000. [255](#)
- [Fri95] High Temperature Electronics. Technical Report ISBN: 0444821740, 1995. [255](#)
- [GDC01] E.A. Gutierrez, J. Deen, and C. Claeys, editors. *Low Temperature Electronics: Physics, Devices, Circuits and Applications*. Number ISBN: 0-12-310675-3. Academic Press, 2001. [256](#)
- [GGS92] T.L. Garrard, N. Gehrels, and E.C. Stone. The Galileo heavy element monitor. *Space Science Review*, 60(1-4):305–315, May 1992. [255](#)
- [GH00] H.B. Garrett and A.R. Hoffman. Comparison of spacecraft charging environments at the Earth, Jupiter, and Saturn. *IEEE Transactions on Plasma Science*, 28:2048–2057, Dec 2000. [255](#)
- [Gil02] D.G. Gilmore. *Spacecraft Thermal Control Handbook Volume I: Fundamental Technologies*, volume 1 of 1-8849889-11-X. The Aerospace Press and the American Institute of Aeronautics and Astronautics, second edition, 2002. [255](#)
- [GJR⁺03] H.B. Garrett, I. Jun, J.M. Ratliff, R.W. Evans, G.A. Clough, and R.W. McEntire. Galileo Interim Radiation Electron Model. Jet Propulsion Laboratory, Pasadena, Feb 2003. [255](#)
- [GPS96] S.S. Gerber, B. Patterson, R.L. Ray, and C. Stell. Performance of a spacecraft DC–DC converter breadboard modified for low temperature operation. *IEEE and ASME 31st Intersociety Energy Conversion Engineering Conference (IECEC '96)*, 1:592–598, Aug 1996. [256](#)
- [Gri97] D.H. Grinspoon. *Venus Revealed: A New Look Below the Clouds of Our Mysterious Twin Planet*. Perseus Publishing, 1997. [255](#)
- [Har99] G.G. Harman. Metallurgical bonding systems for high-temperature electronics. *High-Temperature Electronics*, pages 752–769, 1999. [255](#)
- [HAR⁺04] W.S. Hackenberger, E.F. Alberta, P. Rehrig, S. Zhang, C.A. Randall, R. Eitel, and T.R. Shrout. High Temperature Electrostrictive Ceramics for a Venus Rock Sampling Tool. *IEEE Ultrasonics Symposium*, Aug 2004. [256](#)
- [HB06] S. Hayati and T.S. Balint. The Potential Benefits of Nuclear Power on the Surface of Mars: The Robotic Exploration Perspective. *Space Technology and Applications International Forum, STAIF-2006, C.06. Special Session on Mars Exploration*, Feb 2006. [255](#)

- [He01] S. Hareland and et al. Impact of CMOS Process Scaling and SOI on the Soft Error Rates of Logic Processes. *Digest of Papers from the 2001 Symposium on VLSI Technology*, pages 73–74, 2001. [256](#)
- [HFF⁺06] J.L. Hall, D. Fairbrother, T. Frederickson, V.V. Kerzhanovich, M. Said, C. Sandy, C. Willey, and A.H. Yavrouian. Prototype design and testing of a Venus long duration, high altitude balloon. *36th COSPAR Scientific Assembly*, Jul 2006. [256](#)
- [HJK⁺06] J.L. Hall, J. A. Jones, T. Kerzhanovich, V.V. andn Lachenmeier, P. Mahr, J.M. Mennella, M. Pauken, G.A. Plett, L. Smith, M.L. Van Luvender, and A.H. Yavrouian. Experimental results for Titan aerobot thermo-mechanical subsystem development. *36th COSPAR Scientific Assembly*, Jul 2006. [256](#)
- [HKJ⁺98] G. Henriksen, . Kaun, A. Jansen, J. Prakash, and D. Vissers. *Electrochem. Soc. Proc.*, 98-11:302, 1998. [256](#)
- [HKY⁺06] J.L. Hall, V.V. Kerzhanovich, A.H. Yavrouian, J.A. Jones, C.V. White, B.A. Dudik, G.A. Plett, J. Mennella, and A. Elfes. An Aerobot for Global In Situ Exploration of Titan. *Advances in Space Research / Originally presented at the 35th COSPAR Scientific Assembly*, 37:2108–2119, Jul 2006. [256](#)
- [HMS⁺00] J.L. Hall, P.D. MacNeal, M.A. Salama, J.A. Jones, and M. Kuperus Heun. Thermal and Structural Test Results for a Venus Deep Atmosphere Instrument Enclosure. *AIAA Journal of Spacecraft and Rockets*, 37(1):142–144, 2000. [256](#)
- [HV78] L.A. Hennis and M.N. Varon. *Thermal Design and Development of Pioneer Venus Large Probe*, volume 65 of *Thermophysics and Thermal Control, Progress in Astronautics and Aeronautics*. 1978. [255](#)
- [Ie02] F. Irom and et al. Single-Event Upset in Commercial Silicon-on-Insulator PowerPC Microprocessors. *IEEE Transactions on Nuclear Science*, Dec 2002. [256](#)
- [IF04] F. Irom and F. Farmanesh. Frequency Dependence of Single-Event Upset in Advanced Commercial PowerPC Microprocessors. *IEEE Transactions on Nuclear Science*, 51(6):3505–3509, 2004. [256](#)
- [JKS⁺94] G.H. Johnson, W.T. Kemp, R.D. Schrimpf, K.F. Galloway, M.R. Ackermann, and R.D. Pugh. The effects of ionizing radiation on commercial power MOSFETs operated at cryogenic temperatures. *IEEE Transactions on Nuclear Science*, 41(6):2530–2535, Dec 1994. [256](#)
- [Joh96] A.H. Johnston. The Influence of VLSI Technology Scaling on Radiation-Induced Latchup. *IEEE Transactions on Nuclear Science*, 43(2):505–521, 1996. [256](#)
- [Jon93] J.A. Jones. Alternative cooling system for moderate duration Venus Lander. Technical Report JPL IOM # 3546/178/T&CTD/JJ/93, Jet Propulsion Laboratory, California Institute of Technology, Mar 1993. [151](#), [156](#), [255](#)
- [JPL07] JPL. Cassini-Huygens, Mission to Saturn and Titan. Website: <http://saturn.jpl.nasa.gov/mission/index.cfm>, Apr 2007. [255](#)
- [JRH⁺04] X. Jiang, P. Rehrig, W. Hackenberger, S. Dong, and D. Viehland. Single Crystal Ultrasonic Motor for Cryogenic Actuations. *Proc. 2004 IEEE UFFC Symposium*, 2004. [256](#)
- [Jur99] R.F. Jurgens. High temperature electronics applications in space exploration. *High-Temperature Electronics*, pages 172–176, 1999. [255](#)

- [KBB⁺96] A.K. Kalafala, J. Bascunan, D.D. Bell, L. Blecher, F.S. Murray, M.B. Parizh, M.W. Sampson, and R.E. Wilcox. *IEEE Transactions on Magnetics*, 32(4):2276, 1996. [256](#)
- [KBC⁺99] K.P. Klaasen, H.H. Breneman, W.F. Cunningham, J.M. Kaufman, J.E. Klemaszewski, K.P. Magee, A.S. McEwen, H.B. Mortensen, R.T. Pappalardo, D.A. Senske, and Sullivan. Calibration and performance of the Galileo solid-state imaging system in Jupiter orbit. *Optical Engineering*, 38:1178–1199, Jul 1999. [255](#)
- [KH80] R.G. Knollenberg and D.M. Hunten. The microphysics of the clouds of Venus: Results of the Pioneer Venus particle size spectrometer experiments. *Journal of Geophysical Research*, 85:8039–8058, 1980. [255](#)
- [KHGS07] H.J. Krokoszinski, J. Helfrich, D. Gilbers, and H.J. Schmutzler. Hybrid technology for high temperature applications. Website: <http://www.fernuni-hagen.de/LGBE/papers/Hybrid.html>, Apr 2007. [255](#)
- [KHY01] V.V. Kerzhanovich, J.L. Hall, and A.A. Yavrouian. Balloon Precursor Mission for Venus Surface Sample Return. *2001 IEEE Aerospace Conference*, (Paper No.48), Mar 2001. [256](#)
- [KHYC05] V. Kerzhanovich, J. Hall, A. Yavrouian, and J. Cutts. Two Balloon System to Lift Payloads for the Surface of Venus. *AIAA 5th ATIO and 16th Lighter-Than-Air Sys Tech. and Balloon Systems Conferences*, (AIAA-2005-7322), Sep 2005. [256](#)
- [Kir00] R. K. Kirschman. Interface electronics for smart sensors in low-temperature and high-temperature environments. *Proceedings of the Sensors Expo*, pages 341–347, May 2000. [255](#)
- [KJHV96] T.D. Kaun, A.N. Jansen, G.L. Henriksen, and D.R. Vissers. *Electrochemical Society Proceedings*, 96-97:342, 1996. [256](#)
- [Kra89] V.A. Kransnopolsky. Vega mission results and composition of Venusian clouds. *Icarus*, 80:202–210, 1989. [255](#)
- [Ksa83] L.V. Ksanfomaliti. Electrical activity of the atmosphere of Venus: Measurements on descending probes. *Kosmich. Issled.*, 21:279–296, 1983. [255](#)
- [Lan04] G.A. Landis. Robotic Exploration of the Surface and Atmosphere of Venus. *55th International Astronautical Congress*, (IAC-04-R.2.06), Oct 2004. [255](#)
- [Lau02] B. Laub. New TPS materials for aerocapture. *AIP Conference Proceedings*, 608:337–344, 2002. [255](#)
- [LBCC05] R. Lorenz, B. Bienstock, P. Couzin, and G. Cluzet. Thermal design and performance of probes in thick atmospheres: Experience of Pioneer Venus, Venera, Galileo, and Hughens. In *3rd International Planetary Probe Workshop, 27 June 2005 - 1 July 2005*, Anavyssos, Attiki, Greece, Jun 2005. [255](#)
- [LEApr] LEAG. Lunar Exploration Analysis Group. Website: <http://www.lpi.usra.edu/>, 2007 Apr. [255](#)
- [Len74] B. Lengeler. Semiconductor devices suitable for use in cryogenic environments. *Cryogenics*, 14(8):439–447, Aug 1974. [256](#)
- [LLC03] G.A. Landis, C. LaMarre, and A. Colozza. Atmospheric Flight on Venus: A Conceptual Design. *Journal of Spacecraft and Rockets*, 40(5):672–677, Sep 2003. [256](#)

- [LM02] R. Lorenz and J. Mitton. *Lifting Titan's Veil: Exploring the Giant Moon of Saturn.* Cambridge Press, 2002. [255](#)
- [LM04] G.A. Landis and K.C. Mellott. Venus Surface Power and Cooling System Design. *55th International Astronautical Congress*, Oct 2004. [255](#)
- [LR02] D. Linden and T. Redy. *Handbook of Batteries.* McGraw Hill, New York, 3rd edition edition, 2002. [256](#)
- [LV03] B. Laub and E. Venkatapathy. Thermal Protection System Technology and Facility Needs for Demanding Future Planetary Missions. *Proceedings of the International Workshop on Planetary Probe Atmospheric Entry and Descent Trajectory Analysis and Science*, Oct 2003. [255](#)
- [LW05] J.F. Liu and M.H. Walmer. Thermal stability and performance data for SmCo 2:17 high temperature magnets on PPM structures. *IEEE Transactions on Electron Devices*, 52(5):899–902, 2005. [256](#)
- [LWS⁺05] J-P. Lebreton, O. Witasse, C. Sollazzo, T. Blancquaert, P. Couzin, A-M. Schipper, J.B. Jones, D.L. Matson, L.I. Gurvits, D.H. Atkinson, B. Kazeminejad, and M. Pérez-Ayúcar. An overview of the descent and landing of the Huygens probe on Titan. *Nature*, 438:758–764, Dec 2005. [255](#)
- [Mal] M.C. Malin. Venus Geophysical Network Pathfinder: A Discovery Workshop Mission Proposal. M. C. Malin, Malin Space Science Systems, P. O. Box 910148, San Diego, CA 92191-0148 <http://www.msss.com/venus/vgnp/vgnp.txt.ht>. [255](#)
- [Mar78] M.Ya. Marov. Results of Venus missions. *Annual Review of Astronomy and Astrophysics*, 16:141–169, 1978. [255](#)
- [McC97] High Temperature Electronics. Technical Report ISBN: 0849396239, 1997. [255](#)
- [MCM⁺] M.S. Mazzola, J.B. Casady, N. Merrett, I. Sankin, W. Draper, D. Seale, V. Bondarenko, Y. Koshka, J. Gafford, and R. Kelley. Assessment of “Normally On” and “Quasi On” SiC VJFET’s in Half-Bridge Circuits. *Materials Science Forum*, 457- 460:1153–1156. [255](#)
- [Mee91] G.W. Meetham. High-temperature materials — a general review. *Journal of Materials Science*, 26:853–860, 1991. [255](#)
- [Mel04a] K.D. Mellott. Electronics and Sensor Cooling with a Stirling Cycle for Venus Surface Mission. *2nd International Energy Conversion Engineering Conference*, (AIAA 2004-5610), Aug 2004. [255](#)
- [Mel04b] K.D. Mellott. Power Conversion with a Stirling Cycle for Venus Surface. *2nd International Energy Conversion Engineering Conference*, (AIAA 2004-5622), Aug 2004. [255](#)
- [MEP07] MEPAG. Mars Scientific Goals, Objectives, Investigations, and Priorities (Active Version). Website: <http://mepag.jpl.nasa.gov/reports/index.html>, Mars Exploration Program Analysis Group, Apr 2007. [255](#)
- [MG98] M. Marov and D.H. Grinspoon. *The Planet Venus.* The Planetary Exploration Series. 1998. [255](#)
- [Mit07] D.P. Mitchell. The Venus-Halley Missions. Website: http://www.mentallandscape.com/V_Vega.htm, Apr 2007. [255](#)

- [MS82] J.N. Moss and A.L. Simmonds. Galileo Probe Forebody Flowfield Predictions During Jupiter Entry. *Proceedings of the AIAA/ASME 3rd joint Thermophysics, Fluids, Plasma and Heat Transfer Conference*, (AIAA-82-0874), Jun 1982. [256](#)
- [MSBE02] M. Mulvihill, R. Shawgo, R. Bagwell, and M. Ealey. Cryogenic Cofired Multilayer Actuator Development for a Deformable Mirror in the Next Generation Space Telescope. *Journal of Electroceramics*, 8:121–128, 2002. [256](#)
- [MV00] G.W. Meetham and M.H. Van de Voorde. *Materials for High Temperature Engineering Applications*. Springer, 2000. [256](#)
- [MVT04] E. Martinez, E. Venkatapathy, and O. Tomo. Current developments in future planetary probe sensors for TPS. *Proceedings of the International Workshop Planetary Probe Atmospheric Entry and Descent Trajectory Analysis and Science, Lisbon, Portugal, October 6-9, 2003*, (ISBN 92-9092-855-7):249–252, 2004. [255](#)
- [NAS70a] NASA. NASA Space Vehicle Design Criteria (Environment); Meteoroid Environment Model, Interplanetary and Planetary. Technical Report NASA SP-8038, National Aeronautics and Space Administration, Washington, D.C., USA, 1970. [255](#)
- [NAS70b] NASA. NASA Space Vehicle Design Criteria (Environment); Meteoroid Environment Model, Near Earth to Lunar Surface. Technical Report NASA SP-8038, National Aeronautics and Space Administration, Washington, D.C., USA, 1970. [255](#)
- [NAS05] NASA. NASA’s Exploration Systems Architecture Study. Final Report NASA-TM-2005-214032, National Aeronautics and Space Administration, Washington, D.C., USA, Nov 2005. [255](#)
- [NAS06] NASA. Solar System Exploration — The Solar System Roadmap for NASA’s Science Mission Directorate. Technical Report JPL D-35618, National Aeronautics and Space Administration, Washington, D.C., USA, Sep 2006. [255](#)
- [NAS07a] NASA. Deep Impact Mission. Website: http://www.nasa.gov/mission_pages/deepimpact/main/index.html, Apr 2007. [255](#)
- [NAS07b] NASA. SRM 3 — The Solar System Exploration Strategic Roadmap. Available from the Outer Planets Assessment Group (OPAG), Website: <http://www.lpi.usra.edu/opag/>, Oct 2007. [255](#)
- [NH96] T. Neilson and K. Hilbert. Extensions to the Galileo attitude control system for the Probe mission. *Adv. Astron. Sci.*, 92:647–665, 1996. [255](#)
- [NOC02] P.G. Neudeck, R.S. Okojie, and L.Y. Chen. High-temperature electronics - A role for wide bandgap semiconductors. *Proceedings of the IEEE*, 90(6):1065–1076, Jun 2002. [162](#), [255](#)
- [NRC03] NRC. New Frontiers in the Solar System, an integrated exploration strategy. Technical report Washington, D.C., Space Studies Board, National Research Council, 2003. [255](#)
- [OPA07] OPAG. Outer Planets Assessment Group. Website: <http://www.lpi.usra.edu/opag/>, Apr 2007. [255](#)
- [PGB⁺02] C. Poivey, G. Gee, J. Barth, K. LaBel, and H. Safren. Lessons learned from radiation induced effects on solid state recorders (SSR) and memories. Website: http://radhome.gsfc.nasa.gov/radhome/papers/2002_SSR.pdf, Dec 2002. [255](#)

- [PHD⁺00] R.L. Patterson, A. Hammoud, J.E. Dickman, S.S. Gerber, and E. Overton. Development of electronics for low temperature space missions. *Proceedings of WOLTE 4*, pages 115–119, Jun 2000. [256](#)
- [PHD⁺02] R.L. Patterson, A. Hammoud, J.E. Dickman, S.S. Gerber, M.E. Elbuluk, and E. Overton. Electronic components and systems for cryogenic space applications. *Proceedings of the Cryogenic Engineering Conference (CEC)*, 47B:1585–1591, Jul 2002. [256](#)
- [RCMR00] P.G. Russell, D. Carmen, C. Marsh, and T.B. Reddy. *Proceedings of the 39th Power Sources Conference*, pages 73–76, 2000. [256](#)
- [Ree83] Materials at Low Temperatures. *American Society for Metals*, 1983. [256](#)
- [RWR97] A.D. Robertson, A.R. West, and A.G. Ritchie. *Solid State Ionics*, 104:1–11, 1997. [256](#)
- [Sad03] L. Sadwick. Applications for high temperature semiconductor and other electronics. *Workshop on Extreme Environments Technologies for Space Exploration*, May 2003. [255](#)
- [SC68] H. Shimotake and E.J. Cairns. *3rd Annual Intersociety Energy Conversion Engineering Conference (IECEC) record*, page 76, 1968. [256](#)
- [Se93] G.J. Shaw and et al. Low temperature proton irradiation of GaAs MESFETs. *IEEE Transactions on Nuclear Science*, 40(6):1300–1306, Dec 1993. [256](#)
- [Se01] G.W. Swift and et al. Single-Event Upset in the Power PC750 Microprocessor. *IEEE Transactions on Nuclear Science*, 48(6):1822–1827, 2001. [256](#)
- [SHC⁺04] L.P. Sadwick, R.J. Hwu, J.H. Chern, C.H. Lin, L. del Castillo, and T. Johnson. 500 °C Electronics for Harsh Environments. *Proceedings of the IEEE Aerospace Conference*, 2004. [255](#)
- [SLRJ03] G. Swift, G. Levanas, M. Ratliff, and A. Johnston. In-flight annealing of displacement damage in GaAs LEDs: A Galileo story. *IEEE Transactions on Nuclear Science*, 50(6), 2003. [255](#)
- [SR98] E.G. Stassinopoulos and J.P. Raymond. The Space Radiation Environment for Electronics. *Proc. IEEE*, 76(11):1424–1442, 1998. [256](#)
- [Te73] Y. S. Touloukian and et al., editors. *Thermophysical Properties of Matter*, volume 1-13. Plenum Press, 1973. [255](#)
- [The04] The White House. A Renewed Spirit of Discovery, The President’s Vision for U.S. Space Exploration. Website: http://www.whitehouse.gov/space/renewed_spirit.html, Jan 2004. [255](#)
- [TYC85] J.J. Tzou, C. Yao, and H. Chan. Hot-Electron-Induced MOSFET Degradation at Low Temperatures. *IEEE Electron Device Letters*, EDL-6(9):450–452, Sep 1985. [256](#)
- [VEX07] VEXAG. Venus Exploration Analysis Group. Website: <http://www.lpi.usra.edu/vexag/>, Apr 2007. [255](#)
- [VLW06] E. Venkatapathy, B. Laub, and M. Wright. Enabling in-situ science: Engineering of Thermal Protection System for future Venus Entry Missions. *Chapman Conference: Exploring Venus as a Terrestrial Planet*, Feb 2006. [255](#)
- [Wig71] D.A. Wigley. *Mechanical Properties of Materials at Low Temperatures*. Plenum Press, 1971. [256](#)

- [WMJW92] D.J. Williams, R.W. McEntire, S. Jaskulek, and B. Wilken. The Galileo energetic particle detector. *Space Science Review*, 60(1-4):385–412, May 1992. [255](#)
- [Zak07] A. Zak. History of the Venera 75 project. Website: <http://www.russianspaceweb.com/venera75.html#history>, Apr 2007. [255](#)
- [ZLG⁺02] J.C. Zarnecki, M.R. Leese, J.R.C. Garry, N. Ghafoor, and B. Hathi. Huygens' surface science package. *Space Science Review*, 104:593–611, 2002. [255](#)

National Aeronautics and
Space Administration

Jet Propulsion Laboratory
California Institute of Technology
Pasadena, California

JPL D-32832